HIGHER-ORDER THICKNESS EXPANSIONS FOR CYLINDRICAL SHELLS

DISSERTATION

Randy A. Smith
Major, USAF

AFIT/DS/ENY/91-1

DEPARTMENT OF THE AIR FORCE
AIR UNIVERSITY
AIR FORCE INSTITUTE OF TECHNOLOGY
Wright-Patterson Air Force Base, Ohio

AFIT/DS/ENY/91-1

HIGHER-ORDER THICKNESS EXPANSIONS FOR CYLINDRICAL SHELLS

DISSERTATION

Randy A. Smith
Major, USAF

AFIT/DS/ENY/91-1

Approved for public release; distribution unlimited

REPORT DOCUMENTATION PAGE

Form Approved
OMB No. 0704-0188

1. AGENCY USE ONLY (Leave blank)	2. REPORT DATE	3. REPORT TYPE AND DATES COVERED
	September 1991	Doctoral Dissertation

4. TITLE AND SUBTITLE
HIGHER-ORDER THICKNESS EXPANSIONS FOR CYLINDRICAL SHELLS

5. FUNDING NUMBERS

6. AUTHOR(S)
Randy A. Smith, Major, USAF

7. PERFORMING ORGANIZATION NAME(S) AND ADDRESS(ES)
Air Force Institute of Technology, WPAFB OH 45433-6583

8. PERFORMING ORGANIZATION REPORT NUMBER
AFIT/DS/ENY/91-1

9. SPONSORING/MONITORING AGENCY NAME(S) AND ADDRESS(ES)

10. SPONSORING/MONITORING AGENCY REPORT NUMBER

11. SUPPLEMENTARY NOTES

12a. DISTRIBUTION/AVAILABILITY STATEMENT
Approved for public release; distribution unlimited.

12b. DISTRIBUTION CODE

13. ABSTRACT *(Maximum 200 words)*

Eight variations of higher-order transverse shear deformation (HTSD) theory were developed for composite shells. Three attributes were varied to produce the eight variations. These attributes included the order of the thickness expansions used to approximate the shell shape factors and the assumed linear displacement field and the nonlinearity of transverse shear strain. Several cylindrical shell problems were investigated using SHELL, a finite element code with a 36 degree of freedom cylindrical shell element. MACSYMA, a symbolic manipulation code, was used to formulate the element independent stiffness arrays for each variation of the theory.

When all nonlinear strain-displacement terms for transverse shear were included for thin shallow isotropic cylindrical shells, the theory predicted a more flexible response during collapse. Higher-order thickness expansions had negligible effect upon results for the shallow shell problems investigated. For deeper shells, the linear displacement assumption prohibited the use of nonlinear strain-displacement relations for transverse shear strains. Thus, for deep shells nonlinearity was limited to in-plane strain-displacement relations. This quasi-nonlinear HTSD theory produced a more flexible response during collapse when the order of approximation of shell shape factor terms was increased. The effects of quartic displacement were less significant than the effects of quadratic shape factor approximation.

14. SUBJECT TERMS	15. NUMBER OF PAGES
Transverse Shear Strain, Nonlinear Strain-Displacement, Finite Element Method, Symbolic Manipulation, MACSYMA, Green-Lagrange Strain, Numerical Analysis	257
	16. PRICE CODE

17. SECURITY CLASSIFICATION OF REPORT	18. SECURITY CLASSIFICATION OF THIS PAGE	19. SECURITY CLASSIFICATION OF ABSTRACT	20. LIMITATION OF ABSTRACT
Unclassified	Unclassified	Unclassified	UL

AFIT/DS/ENY/91-1

HIGHER-ORDER THICKNESS EXPANSIONS FOR CYLINDRICAL SHELLS

DISSERTATION

Presented to the Faculty of the School of Engineering

of the Air Force Institute of Technology

Air University

In Partial Fulfillment of the

Requirements for the Degree of

Doctor of Philosophy

Randy A. Smith, B.S., M.S.

Major, USAF

September, 1991

AFIT/DS/ENY/91-1

HIGHER-ORDER THICKNESS EXPANSIONS FOR CYLINDRICAL SHELLS

Randy A. Smith, B.S., M.S.

Major, USAF

Approved:

Anthony P. Palazotto — Aug 5, 1991

Randy A. Smith — 5 August 1991

John Jones Jr. — 5 August 1991

Mark S. Ewing — 6 AUG 1991

J. S. Przemieniecki — 6 Aug 1991

J. S. Przemieniecki

Institute Senior Dean

Acknowledgments

Dr. Anthony Palazotto, my committee chairman, guided me through this research and through my entire course of study. His advice, questions, and leadership have helped me to define and pursue this research effort to this end. Thank you Dr. Palazotto for all your help and confidence in me. Dr. Janusz S. Przemieniecki, Dr. Peter Torvik, Dr. John Jones, and Dr. Mark Ewing (Major USAF) served as members of my committee. I wish to thank these individuals for their guidance and suggestions regarding this research and the preparation of my dissertation. I am especially grateful to Dean Przemieniecki for personally reading my dissertation, in lieu of a Dean's reader, and for the many suggestions he offered.

Several other professionals have influenced this work. To Mr. Robert Bader, Mr. Nelson Wolf, and Dr. Narendra Khot of the AF Wright Laboratory Structures Division, I owe my gratitude for their willingness to sponsor this research by providing a portion of their computer budget for my research. Their assistance and the use of the Cray computer allowed me to accomplish research not possible using AFIT computers. Ms. Kristin Larsen, a UNIX computer systems consultant employed by AFIT, guided me, helped me, and saved me from self destruction on many of my encounters within the UNIX environment. I am deeply indebted to Ms. Larsen, without her help I could not have completed this dissertation within the time allowed. I also wish to thank Dr. Howard Gans (Captain USAF) for his suggestions on my draft dissertation.

This work would not have been possible without the strength, wisdom, perseverance, patience, and love the Lord Jesus Christ has given to me. He has also blessed me with a loving wife, Marisa, to whom I am forever grateful. She nurtured and cared for our children—almost single-handedly—during the past three years. She also typed the majority of this manuscript. My most sincere thanks, apologies, and love I extend to my family who have given me love and support while receiving so little of my time.

Randy A. Smith

Table of Contents

List of Figures

List of Tables

Abstract

Eight variations of higher-order transverse shear deformation (HTSD) theory were developed for laminated composite shells. The behavior and limitations of these variations were numerically evaluated for several cylindrical shell problems. All variations of the theory used linear kinematic assumptions and nonlinear strain-displacement relations for in-plane strain components. Three different higher-order attributes were included, or excluded, in various combinations to produce the eight variations. The first attribute defined the order of the series expansions, in the thickness direction, used to approximate the assumed displacement field. The second attribute defined the order of the series expansions used to approximate the geometric shape factors of the shell. The third attribute was the choice to include, or exclude, the nonlinear terms of the Green-Lagrange strain-displacement relations for the transverse shear strains. When nonlinear terms of transverse shear were excluded, the theory was called quasi-nonlinear.

Several problems were investigated using a finite element computer code (SHELL) with an element independent stiffness matrix formulation and a 36 degree of freedom cylindrical shell element. The original version of SHELL was written at AFIT in 1989. MACSYMA, a symbolic manipulation code, was used to formulate the element independent stiffness arrays for each variation of the theory. Thin shallow isotropic cylindrical shell panels exhibited a more flexible response during collapse when nonlinear transverse shear was included. The use of quartic, versus cubic, displacement and/or the use of quadratic, versus linear, shape factor approximations had no significant effect upon accuracy of the nonlinear HTSD theory. For deeper shells, the linear displacement assumption prohibited the use of nonlinear strain-displacement relations for transverse shear strains. Thus, for deep shells, the quasi-nonlinear HTSD theory produced a more flexible response during collapse when the order of shell shape factor approximations was increased. The effects of quartic displacement were much less significant than the effects of quadratic shape factor approximation.

HIGHER-ORDER THICKNESS EXPANSIONS FOR CYLINDRICAL SHELLS

I. Introduction

Recent increased interest in composite shell analysis has been generated by the use of fiber-reinforced composite materials for aerospace applications. A second factor in the proliferation of composite shell research is the use of modern digital computers. With computers, solutions can now be found for problems which before were impossible to solve analytically. In particular, problems involving geometric and material nonlinearities can be solved by numerical methods.

Composite shell structures are used in many US Air Force and defense-related equipment because of the inherently high strength-to-weight ratios of composite shells. Historically, thin isotropic shells have been analyzed for many years according to the linear elastic theory formulated by A. E. H. Love [47] in the late 1800's. Love's theory assumes normals to the shell's midsurface remain straight and normal during deformation. This assumption, like the Kirchhoff assumption for flat plates, implies transverse shear strain and stress are zero throughout the shell. Also, since the shell is assumed to be very thin compared to its other characteristic lengths, many terms in the equations are approximated (e.g., terms with radius in the denominator are assumed negligible). More recently, Donnell [23], Mushtari, and Vlasov [104] independently derived comparable theories for thin elastic shells that included nonlinear terms (functions of transverse displacement) for the in-plane strains. These theories, however, still ignored transverse shear and most terms with radius in the denominator.

In general, shell theories that ignore transverse shear effects will predict stiffer behavior than experimental data shows. Inclusion of transverse shear effects reduces this stiff behavior. Like Love theory, the newer Donnell, Mushtari, and Vlasov theories invoked the Kirchhoff hypothesis. Thus, they also ignored transverse shear strain and stress. For thick

shells, however, the transverse shear terms can not be ignored in all cases. Likewise, transverse shear terms become more significant with the introduction of non-isotropic composite materials. This is primarily due to the small transverse shear modulus of fiber-reinforced composite laminates.

During the last two decades, many composite shell problems with transverse shear-effects included have been solved using numerical solution techniques. Some investigators have solved these problems using fully three-dimensional models. These models, however, generally require excessive computational times. They may also exhibit singularities and other mathematical problems when used to analyze thin shells. Other investigators have solved these problems using shell theories, which require less computational effort, with either first-order or higher-order transverse shear deformation.

The "order" of transverse shear deformation theories refers to the highest order polynomial, in terms of the thickness coordinate, used to describe the assumed displacement field. This does not, in general, imply that higher-order shear theories have more independent degrees of freedom. The first-order transverse shear deformation (FTSD) theories use shear correction factors and reduced integration. These artifices compensate for the theoretically incorrect distribution of transverse shear strain. The higher-order transverse shear deformation (HTSD) theories allow normals to the shell's midsurface to rotate from normal and also to warp. This assumption results in a transverse shear strain distribution that is parabolic through the thickness of a flat plate. Most previous theories for geometrically nonlinear shell problems with HTSD theory have retained some nonlinear strain displacement terms for in-plane strain components. Most, however, have also ignored nonlinear strain displacement terms and the effect of higher-order thickness expansions for the transverse shear components. In this dissertation, transverse shear deformation theories which include nonlinear terms for in-plane strains but linear strain-displacement relations for transverse shear strains are generally called linear FTSD (or HTSD) theories. In some cases, when the distinction is important, particularly in the summary chapter, these theories are more precisely called *quasi-nonlinear* theories. Only HTSD theories including nonlinear terms of transverse shear are called *nonlinear* HTSD theories.

For this research, the full nonlinear strain displacement relations for laminated composite shells with nonlinear HTSD terms were developed. This was done without neglecting higher-order terms in the thickness expansions. These relations were then incorporated into a proven finite element formulation to investigate the accuracy of various geometric approximations of curvature and displacements and the effect of nonlinear HTSD.

A review of related research in the areas of composite shells and transverse shear deformation is included in Chapter II. Some theoretical concepts are presented in Chapter III. These concepts, common to most of the published literature addressing the subject area of this dissertation, were not independently developed by the author. They are included in the dissertation to assure a common understanding of the theoretical background of this research. The new theory, developed by the author for this research, is presented in Chapter IV. Since strain equations for this theory are very lengthy, abridged equations are used in Chapter IV; unabridged equations of strain components are listed in the appendices. Typical composite shell problems of interest to the USAF and some classical isotropic shell problems were investigated to determine the effects of higher-order thickness expansions and nonlinear HTSD theory. Results of these investigations are discussed in Chapters V and VI. A significant tool used in the development of this theory was a computerized symbolic manipulation code called MACSYMA [48]. Use of a symbolic code, like MACSYMA, allows the formulation of the full nonlinear HTSD theory without ignoring terms. The use of one "symbolic input program" to generate all variations of theory provided reliability and confidence that the Fortran codes were correctly generated. Part of the symbolic input program is included as an appendix since it played such a critical role in this research program.

II. Literature Review

The field of structural shell analysis is rich in history and significant accomplishments. Many textbooks, conference collections, and review articles have been published over the last century. These publications and the hundreds of related technical articles published over the last two decades present a comprehensive view of what has been accomplished in this field. One of the most recent review articles by Noor and Burton [56] comprehensively reviews 400 published works on computational models for multilayered composite shells. The cited works include those with analytic three-dimensional solutions, analytic solutions using two-dimensional shear deformation theories, and finite element or other numerical solutions [56]. Two other recent review articles cite many references related to this research. Kapania and Raciti reviewed recent advances in analysis of transverse shear effects and buckling of laminated beams and plates [38]. They cite 145 references. Wempner cited about 150 references on the mechanics and finite elements of shells [106].

For many years, the well-known Kirchhoff-Love assumptions were used as a starting point for shell theory derivations. These assumptions include a state of plane stress and inextensible normals which remain straight and normal during deformation. Koiter [40] estimated the relative error associated with Love's approximation to be less than h^2/L^2 or h/R, whichever was larger. Koiter defined h as thickness, L as the smallest "wave length" of the deformation pattern of the shell midsurface, and R as the smallest principal radius of curvature of the shell midsurface [40]. Koiter also estimated the magnitudes of the transverse strain components. He indicated transverse *shear* stresses are generally of the order h/L times the bending or direct stresses, but transverse *normal* stresses are of the order h^2/L^2 or h/R times the same stresses. Koiter concluded, "... a refinement of Love's approximation is indeed meaningless, in general, unless the effects of transverse shear and normal stresses are taken into account ..." [40]. Koiter used simplifications based upon small strain assumptions for isotropic materials. For large strain problems, or for non-isotropic material behavior, including transverse shear deformation may be even more necessary.

The simplicity and efficiency of the Donnell-Mushtari-Vlasov thin shell theory justifies its use for many thin isotropic shell problems. For problems undergoing large rotations or problems with significant radii of curvature a more general nonlinear theory is required. Reissner [83, 84] developed a nonlinear theory for shallow shells and symmetrically deforming shells of revolution with transverse shear deformation. Habir and Lock [87] developed a shell theory using a displacement field derived from "simple independent generalized strain functions." Their work was based upon plane stress assumptions and ignored transverse shear deformation. Their results for a 100-inch radius hinged-free isotropic shell with thicknesses of 0.75, 0.5, and 1.0 inches are often cited as comparisons.

Simmonds and Danielson [95] developed a general nonlinear theory for thin shells of arbitrary midsurface geometry. Their theory included compatibility equations, equilibrium equations and boundary conditions which were valid for shells undergoing arbitrarily large rotations and strains. In their work, they used a finite rotation vector defined by:

$$\vec{\Omega} = \vec{e} \sin\theta \tag{2.1}$$

where $\vec{e}(x^\alpha, t)$ is a unit vector, t is the shell thickness coordinate, x^α, $\alpha = 1, 2$ are the shell surface coordinates, and $\theta(x^\alpha, t)$ is the magnitude of rotation about an axis parallel to $\vec{e}$. When Eq (2.1) is included as part of the kinematic relations, one obtains highly nonlinear expressions for the shell extensional and bending strain components in terms of the shell curvature tensor and the components of Eq (2.1). These expressions, according to Simmonds and Danielson, can be simplified to the equations of Reissner's theory and to those of the Sanders-Koiter shell theory [95].

Other authors have separated rigid body rotations from rotations caused by deformations. Belytschko and Glaum [8] accounted for initial curvature and moderate variations of rigid body rotation. Their formulation was for shallow arch structures where, despite large rotations, deflections were less than two percent of the radius. They used Euler-Bernoulli beam theory which, like the Kirchhoff-Love theory, assumes normals to the midsurface remain straight and normal. Their results for an arch with a rise to thickness ratio of 6.835 were approximately 13 percent stiffer than experimental results [8]. Belytschko and

Glaum did not discuss the possible influence of transverse shear deformation.

Hughes and Liu [30] incorporated FTSD theory in a quasi-nonlinear, large-strain, large-rotation finite element model for general shells. In their development, they reduce the three-dimensional theory of nonlinear continuum mechanics to a two-dimensional shell theory simultaneously with the finite element discretization. This method of derivation is sometimes called the degenerated shell method. Their incorporation of shear correction factors, however, was unique. For the general nonlinear problem, the transverse shear terms in the equilibrium equations are coupled with the in-plane terms. Hughes and Liu modified their strain displacement relations to incorporate the shear correction factor, instead of incorporating the factor in the constitutive relations. This allowed extension of the selective integration procedure to the fully-coupled nonlinear case. Selective integration refers to using exact numerical integration for the finite element equations associated with in-plane strain terms, and less-than-exact numerical integration for the transverse shear strain terms. Hughes and Liu investigated shallow circular 100-inch radius arches and hinged-free shells under point load. Their results compared well with other studies up to the onset of instability [30]. Unfortunately, no results were shown for these problems beyond this initial point of instability.

Parisch presented a "layered" shell element model with large rotation capability and nonlinear material assumptions. His results for the 100-inch radius hinged-free cylindrical shell under point load also compared well to published works up to the point of instability [69]. Parisch's theory was intended for large displacement analysis, however, he neglected all quadratic nonlinear strain terms in the constitutive relations. Thus, transverse shear stresses were constant through the shell thickness [69]. Like Simmonds's formulation, Parisch's formulation has complicated nonlinear expressions of rotations within the strain components.

Surana also published a paper [98] on a curved shell theory incorporating higher-order nonlinear rotation terms. His shell theory employed five degrees of freedom at each node. Although Surana's eight-node isoparametric elements permitted large nonlinear rotations and linear elastic orthotropic material behavior, the effect of transverse shear was not discernible from the published results. This was apparently due to the small ratio of

thickness to radii of curvature for Surana's problems. The clamped-hinged circular arch, Surana studied, had a radius of 100 inches, thickness of 1 inch, and an included angle of 215 degrees. Surana's results for a 2-inch wide arch showed beam-like behavior, but a 24-inch wide arch behaved more like a shell strip. His results for hinged-free cylindrical shells, generally, compared well with other published results [87]. Surana concluded that linearizing the element displacement field with respect to nodal rotations limits the magnitude of rotations during the large deformation process [98]. According to Surana, his formulation includes many nonlinear terms of nodal rotation, and therefore, achieves good convergence rates for large load increments.

Koiter's estimates of error can be used to show the important role transverse shear can play in the behavior of shell structures. In the previously cited papers, the hinged-free cylindrical shell had an undeformed ratio of $h/R = 1/100$. As the panel deforms, however, the local radii of curvature at any point is no longer the undeformed radius of the shell. Curvature, where the point load is applied, may even change sign. The wave length of deformation will generally be less than the largest in-plane dimension of the shell. For the hinged-free shells Sabir and Lock studied, the longitudinal and circumferential arc lengths of the shell are both 20 inches. The effects of local changes in the shell shape are often ignored in shell theories. Morley [51] showed that thin shell finite elements which use quadratic polynomials (with Cartesian coordinates) to describe components of displacement cannot adequately represent inextensible bending. The well-known Semi-Loof shell finite element developed by Irons and Ahmad [32] is such an element. Morley indicates even isoparametric finite elements do not provide an acceptable description of inextensible bending of curved surfaces unless the element nodal interpolation functions are at least cubic in order [51].

The development of a shell model for large-rotation nonlinear problems is complicated by the introduction of laminated anisotropic materials or large changes in curvature of the surfaces. Noor, Peters, and Andersen [55] developed mixed finite element models for beams, and later for shells, which employed "reduction" techniques for large-rotation nonlinear problems. Their mixed finite element model assumes other nodal unknowns, such as stress, strain, etc., in addition to nodal displacements. Their results for the 100-

inch radius clamped-hinged deep arch showed excellent convergence. They also included Reissner's large deformation transverse shear approximations. Noor, Peters, and Andersen state, "The development of mixed models is simpler and more straight forward than those of the displacement models. This is particularly true for large-rotation and large strain problems in which the functional of the mixed variational principle is simpler than that of the minimum potential energy principle" [55].

Bathe and Dvorkin [5] also used a mixed finite element formulation to develop general shell elements. They suggested six "Requirements on shell elements" which they consider important for general shell elements. Three of these requirements are related to this research. Condition 1 implied no specific shell theory should be used. Condition 3 specified "[the element] must not—ever—contain any spurious zero energy nodes; it must not—ever—lock and must not be based on numerically adjusted factors." Condition 4 suggested five or six engineering degrees of freedom per node should be maximum for shell elements [5]. Condition 3 seems to suggest FTSD-based finite elements are not acceptable, since these models have shear correction factors and will shear lock if not numerically underintegrated. On the other hand, HTSD-based finite elements require at least seven degrees of freedom per node. Condition 1 seems to eliminate most two-dimensional shell-based theories, since these generally assume the transverse displacement w is constant through the thickness and the transverse normal stress σ_{33} is approximately equal to zero. Furthermore, even the use of orthogonal curvilinear coordinate systems (and strain definitions) based on lines of principal curvature seem forbidden.

Bathe and Dvorkin [5] developed their theory in terms of element-based isoparametric coordinates. They used this "convected" coordinate system to numerically interpolate the in-plane covariant components of the Green-Lagrange strain tensor and to determine contravariant components of the Second Piola-Kirchhoff stress tensor. Transverse shear strains were interpolated differently than in-plane strains. The values of transverse shear strain components ε_{13} and ε_{23} were interpolated numerically at two points of a four-noded rectangular element using the appropriate Green-Lagrange strain tensor equation [5]. These two values for a each transverse shear strain component were then linearly interpolated to determine approximate values of ε_{13} and ε_{23} at each node point. Their eight-noded

shell element used a higher-order interpolation, based on six points, of transverse shear strain. In-plane strain for this element were calculated using an eight–point interpolation scheme. Bathe and Dvorkin presented results of a 20–inch radius curved cantilever of 0.2–inch thickness subjected to constant bending moment. Their finite element results with undistorted elements were within 2 percent of analytical solutions. Results with distorted elements were within 8 percent of analytical results [5]. They also reported good comparison with analytic solutions for a pinched cylinder with $h/R = 1/100$ and $h/L = 1/200$, a Scordelis-Lo cylindrical roof and an isotropic cylindrical shell panel. Their shell panel was rigidly supported at the cylindrical ends and free along the longitudinal edge with $h/R = 1/100$ and $L/R = 1/200$. The only load on the shell was due to gravity. Again, based on Koiter's estimates, the transverse shear strains occurring in these problems were on the order of 1–2 percent of the in-plane strains. Thus, the results reported by Bathe and Dvorkin do not substantiate the transverse shear performance of their element.

With so many shell theories available, a method to assess the capability of a particular theory to represent large nonlinear rotations was needed. According to Nolte, Makowski, and Stumpf, Pietraszkiewicz [71, 70] suggested classifying "small strain shell theories according to the magnitude of rotation angle ω of the material elements as follows: small rotations $\omega \leq \mathcal{O}(\theta^2)$, moderate rotations $\omega = \mathcal{O}(\theta)$, large rotations $\omega = \mathcal{O}(\sqrt{\theta})$ and finite rotations $\omega \geq \mathcal{O}(1)$, where θ is a common small parameter ..." [53]. The term "material elements" includes a vector normal to the shell midsurface and two vectors tangent to the midsurface in the directions of principal curvature. The parameter θ was defined by Nolte et al., based upon the work of Koiter [40] and John [35], as follows:

$$\bar{\theta} = \max\left\{\frac{h}{d}, \frac{h}{L}, \frac{h}{L^*}, \sqrt{\frac{h}{R}}, \sqrt{\eta}\right\}, \quad \theta^2 \ll 1 \tag{2.2}$$

where R, h, L, L^*, η, d are "the minimum principal radius of curvature, the shell thickness, the wave length of deformation, the wave length of the curvature pattern, the maximum principal strain in the shell space and the distance of any point under consideration to the lateral shell boundary" [53]. The wave length of deformation is the distance between points where the derivatives of transverse displacement have the same values. The wave

length of the curvature pattern is the distance between counter-flexure points of the shell midsurface.

Nolte, Makowski, and Stumpf [53] evaluated error estimates derived for cylindrical bending of thin shells under the Kirchhoff-Love hypothesis for several shell theories. These theories included moderate rotation theories of Donnell, Koiter, Sanders, and Pietraszkiewicz; various nonlinear theories of Koiter, Basar, Chuyko, Shapavalov, Yaghmai, and Varpasuo; large rotation formulations of Nolte et al., Pietraszkiewicz, and Schmidt; and the finite rotation theory of Pietraszkiewicz and Szwabowicz [53]. Many of these theories were shown by Nolte to be inconsistent, because they ignored essential terms in the strain-displacement relations, the geometric boundary condition relations, or in the energy equations. Nolte et al. state that

> ... all nonlinear shell equations, widely used in theory and engineering practice, are valid only in restricted domaines [*sic.*] of applicability, whereas these domaines [*sic.*] are in general not well-defined ... the consistency of a geometrically nonlinear theory cannot be proved by proper estimates of the so called 'intrinsic' error bounded to the required range of applicability, or in other words that 'small' terms in the strain-displacement relations will lead to 'small' differences in the solution. [53]

The theories evaluated by Nolte, Makowski, and Stumpf were for thin shells assuming the Kirchhoff-Love hypothesis that normals remain straight and normal to the midsurface of the shell. Recall that Koiter indicated theories which ignore transverse normal stress cannot improve on the classical Kirchhoff-Love shell theory [40]. Thus, unless the shell is truly thin, one may need to include transverse shear deformation. Surana's nonlinear large rotation finite element formulation [98] discarded the Kirchhoff-Love assumptions. Surana generalized his theory to include "axisymmetric shells, two-dimensional isoparametric beams, curved shells, two-dimensional transition elements and solid-shell transition elements ..." [99].

Schmidt [90] revisited the general nonlinear theory of thin elastic shells undergoing small strains and arbitrary, unrestricted rotations. In this paper Schmidt develops, in detail, a consistent "first approximation" shell theory for small strains and unrestricted ro-

tations, where first approximation refers to Koiter's modified version of the Kirchhoff-Love hypotheses. Kirchhoff-Love theory is based upon the assumption that straight normals remain straight, normal and inextensible. This is equivalent to the assumption of plane strain. In the case of plane strain, transverse strains are assumed to be zero and transverse stresses are assumed to be nonzero. The classical Kirchhoff-Love theory assumes transverse normal stress is zero instead of normal strain being zero. Thus, the classical Kirchhoff-Love theory is inconsistent. Koiter's first approximation corrects this inconsistency by allowing transverse stresses to be nonzero. They are, however, restricted to magnitudes at least one order less than the in-plane stresses [92:613]. Schmidt's theory assumed plane stress and no transverse shear deformation. He then reduced this finite rotation theory to a large rotation theory. Next, he reduced it further by assuming rotations about the normal were small. Finally, a consistent small strain moderate rotation theory was derived by eliminating more terms in the governing equations. This paper shows the process of deriving what Schmidt calls a "variationally consistent" nonlinear shell theory.

Many other investigators have used finite element shell models to solve practical design-related problems. The development of general families of finite element models by Bathe and Dvorkin [5] and Surana [99] seem to support this trend. A general purpose finite element code called STAGSC-1 [1] was developed by Lockheed for aerospace research. This program also has a series of elements (all flat) used to simulate shell structures. Knight, Starnes, and Williams [39] investigated the post-buckling response and failure characteristics of graphite-epoxy cylindrical panels loaded in axial compression. They used experimental tests and the STAGSC-1 computer code to evaluate post-buckling response of cylindrical shells and curved panels. They found a severe reduction in load occurs at buckling and failures begin near regions with severe local bending gradients. Knight et al. point out that many previous studies of the post-buckling behavior of composite cylindrical panels were extensions of classical methods. These often ignored the effects of large rotations. They found that even low values of applied load can cause high values of local surface strains to develop near regions with severe local bending gradients. Failures occurred in regions of large radial displacements and severe bending gradients, which apparently caused large surface strains [39:146]. Knight et al. were able to predict responses

that correlated well with experiment up to buckling. They blamed the influence of local failures for deteriorating correlation after buckling. They noted STAGSC-1 assumes the composite material system remains linear elastic throughout the analysis. This assumption is inaccurate since many composites suffer severe reduction in local stiffness as a result of local failures. Furthermore, the local failures which occurred near regions of large changes in curvature can not be analytically modeled by STAGSC-1 [39]. (STAGSC-1 uses flat plate elements with a "corotational" scheme to model large rotations [76]. This program also ignores higher-order curvature terms in the kinematic assumptions [1].)

Palazotto, Tisler, and others [61, 62] have also used the STAGS computer code. These authors compared analytical predictions of buckling response to experimental work on graphite-epoxy cylindrical panels. Their work included the effects of rectangular, unreinforced cutouts. They also saw large radial displacements, large curvatures over small regions, and severe gradients of curvature for loads less than 10 percent of the critical buckling load. Again, the STAGSC-1 assumption of linear elastic material response was used. Under these small loads no permanent damage occurred.

Design also entails estimation of failure or, more importantly, assurance that failure will not occur. The STAGSC-1 computer code can provide stress distribution estimates for a composite laminate. The accuracy of these estimates is subject to the approximation of curved surfaces by flat elements. To improve stress estimates for shell models, some investigators have used the full three-dimensional equilibrium equations to derive transverse stress distributions. Chaudhuri [15] computed in-plane stresses using "assumed quadratic displacement triangular elements based on transverse inextensibility and layerwise [*sic.*] constant shear angle theory (LCST)." Transverse stresses were then computed using the equilibrium equations. Results for an infinitely-long fiber-reinforced [90/0/90]s strip loaded with sinusoidal pressure matched exact results for the transverse shear variation at the boundary [15]. Engblom and Ochoa [24] superimposed shear rotation on the midplane rotation, thus, relaxing the Kirchhoff hypothesis for a quadrilateral plate element. This method is actually a FTSD theory, but only midplane displacements and rotations are evaluated during the first step of the solution. Transverse shear and normal stresses are then calculated by integrating the three-dimensional equilibrium equations. This method

results in a parabolic distribution of transverse shear stress. According to Engblom and Ochoa, this distribution for a 3×3 quarter-plate model of a simply supported [0/90/0] square plate with sinusoidal load predicts a σ_{23} at the midplane that is 32 percent greater than theoretical. The stress is reduced to 27 percent greater than theoretical for a 6×6 quarter plate mesh [24].

Higher-order transverse shear deformation theory was used by Kwon and Akin [41] for the analysis of layered composite plates. Their mixed element formulation used six unknown variables u_o, v_o, w_o, M_x, M_y, and M_{xy} defined only at the midsurface of the shell. Through the thickness shear is parabolic in this method, and thus, correction factors are not needed. Kwon and Akin's transverse deflection results for several plate configurations with sinusoidal load matched Pagano's exact elasticity solutions much closer than previous finite element work by Mawenja (1974) and Panda (1979) [41]. Reddy's displacement-based HTSD finite element model for plates is referenced, but Reddy's results are not included in Kwon and Akin's comparison of results. In general, Reddy's results were closer to the exact elasticity solutions than the two finite element works cited by Kwon and Akin. Kwon and Akin's results, however, predicted defections much more accurately than Reddy's. For ratios of h/L exceeding 0.1, Kwon and Akin's results were actually more flexible than the exact elasticity solution. Apparently, Kwon and Akin's mixed formulation overcompensates for the flexural stiffness reductions caused by transverse shear deformation.

Reddy et al. published several technical reports and papers [42, 65, 66, 74, 80, 81, 77, 78, 79] addressing transverse shear deformation of plates and shells. Their research included analytical solutions of the linear theory with HTSD for various boundary conditions, moderate rotation theory of laminated composite plates, and development of finite element models for failure analysis using a mixed finite element method.

Liu in his dissertation, as reported by Reddy and Liu [80], formulated a "new" third-order theory of laminated shells that accounts for a parabolic distribution of transverse shear stresses and von Karman strains. Exact Navier solutions were derived for several simply-supported laminated composite shells. A mixed variational principal was developed, and from it, a mixed C° finite element was generated to study bending, vibration, and transient response of laminated composite shells. In this formulation, generalized

displacements u, v, w, ϕ_1, and ϕ_2 and generalized moments M_1, M_2, M_6, P_1, P_2, and P_6 are used as the dependent variables. The higher-order displacements ϕ_1, and ϕ_2, are actually rotations and must be included in a displacement-based transverse shear deformation theory. Recall, Kwon and Akin only used u, v, w, M_1, M_2, and M_6 as dependent variables in their mixed finite element model. According to Reddy and Liu [80], some higher-order displacement-based shear deformation theories have been developed using equilibrium equations of the first-order theory. Thus, the higher-order terms of the displacement field are included only in the strain calculation not in the governing differential equations or boundary conditions. Thus, they claim these theories are inconsistent [80].

The issues of variational consistency and theoretical accuracy have resulted in continued research in basic shell theory [3, 4, 46]. Axelrad and Emmerling were concerned with analysis of flexible shells instead of those designed for strength and stiffness [3, 4]. Thus, "Not any thinkable large displacements and rotations but preferably those actually *realizable* by small strain ..." were considered. The theory developed by Axelrad and Emmerling is strictly "intrinsic." This means the deformed shape and displacements are calculated in terms of strain resultants instead of solving for displacement parameters. These types of formulations, according to Axelrad and Emmerling, have their foundation in the fundamental works of Reissner, Goldenveizer, and others [3]. The flexible shell is, essentially, in a state of inextensible bending. For this case, the displacement form of the field equations may be ill-conditioned. Thus, according to Axelrad and Emmerling, "The intrinsic approach makes the problem involving finite, and in particular large, rotations immensely more tractable" [3]. Their analysis, however, used approximations of the assumed stress state, such that all substantial strain and stress resultants occur in one co ordinate direction. Thus, their theory is a one-dimensional theory like the one-dimensional beam-shell theories of Libai [43, 44].

Librescu and Schmidt [45, 46] also re-examined shell theory with transverse shear deformation and moderate rotations of the normal. Their theory was based upon the following assumptions:

"(a) that the strains are small everywhere in the shell,

"(b) that the in-surface rotations of the shell material elements about normals to the midsurface are small (and of the same order as the strains), and

"(c) that the rotations of the normal to the midsurface are moderate. [46]

With these assumptions, the order-of-magnitude estimates of the linearized components of the rotation vector $\hat{\Omega}$ are $\Omega_{\alpha 3} = \mathcal{O}(\theta)$ and $\Omega_{\alpha\beta} = (\theta^2)$, where only the linear part of the full nonlinear rotational components are used [46]. For the generally shaped shell described in an orthogonal curvilinear coordinate system based on lines of principal curvature, the transverse strain components include contravariant components of the rotation vector. The displacement vector $\vec{V}$ is written as a truncated power series of the shifted components of $\vec{V}$ across the shell thickness. Then, the transverse strains become an infinite series summation across the shell thickness. The in-plane strains are a finite sum with $2(n+1)$ terms, where n is the truncation order of $\vec{V}$. Librescu and Schmidt indicate that these infinite summations for transverse strains may only be reduced to finite sums under four conditions:

(a) in the case of shallow shells (and, as a limiting case for planar surfaces),

(b) within the linearized higher-order shell theories,

(c) when an appropriate "thinness" requirement of the form $(h/R)^n \ll 1$ is envoked, and finally,

(d) under Kirchhoff-Love constraints [46].

Librescu and Schmidt also showed that the infinite summations for transverse strains of an FTSD theory could be replaced by finite summations. The shell theory they developed was, thus, a variationally consistent "geometrically nonlinear theory of elastic anisotropic shells with transverse (normal and shear) deformations and higher-order effects and accounts for small strains and moderate rotations of the normal" [46].

Schmidt and Reddy [92] simplified the earlier works of Librescu and Schmidt [45, 46] by simplifying the strain displacement relations of the FTSD theory. This included deriving the governing equations in terms of displacements associated with the first-order expansion

in the thickness coordinate. They retained small strain moderate rotation restrictions, such that the strains $E_{ij} = \mathcal{O}(\theta^2)$, where $\theta^2 \ll 1$, and the rotation components $\omega_{\alpha 3} \approx \mathcal{O}(\theta)$ and $\omega_{\alpha\beta} \approx \mathcal{O}(\theta^2)$. To achieve a consistent moderate rotation theory, they retained terms in the strain-displacement equations of the order θ^3. Schmidt and Reddy stressed the desirability of consistent, variationally derived theories:

> ... introducing the moderate rotation order estimates for linearized strains and rotations and omitting those terms which are small when compared to the leading terms ... can lead to inadequate and inconsistent equations, because it can result in omission of such terms in the equilibrium equations which would correspond to important terms in associated variationally-consistent moderate rotation strain-displacement relations. [92]

Pandya and Kant [68] developed a C° continuous displacement isoparametric finite element for laminated composite plates using HTSD theory. Their element was a nine-noded quadrilateral with nine degrees of freedom per node. These degrees of freedom included higher-order deformation parameters resulting from a Taylor's series expansion of the primary variables (in-plane displacement and rotation) in the thickness direction. Pandya and Kant did not enforce the zero transverse shear stress conditions on the top and bottom of the plate. Their transverse normal displacement was assumed constant through the thickness. Using the total potential energy functional, they derived equilibrium equations for the eight common engineering stress-resultants N_x, N_y, N_{xy}, M_x, My,M_{xy}, Q_x, and Q_y and 10 higher-order stress resultants.

Using a displacement-based isoparametric finite element formulation, Pandya and Kant numerically solved several problems of laminated square plates with uniform and sinusoidal transverse loading. Their finite element solutions for the in-plane stress-resultants were then used in the full three-dimensional equilibrium equations to compute transverse shear strains. Interestingly, the *constitutive*-derived transverse shear strains were generally about 10 percent *greater* than those predicted by Pagano. In contrast, the *equilibrium*-derived values were 10 percent *less* than Pagano's [68]. This element may have suffered from the rather arbitrary choice of not satisfying zero transverse shear stress conditions on the surfaces of the plate.

Another paper by Pandya and Kant [67] used a novel method to force satisfaction of the zero transverse shear stress conditions. For a curved shell, where the transverse stress is of the order h/R times the in-plane bending stress [40], nonzero transverse stresses may cause generation of equilibrating surface tractions during the nonlinear solution process. Membrane and/or shear locking would, thus, seem possible despite the use of higher-order shear deformation theory.

Dennis [18] developed a large displacement, moderately large rotation finite element formulation for laminated composite shells with HTSD theory. His two-dimensional quasi-nonlinear theory assumed a state of modified plane stress. In this case, direct normal stress σ_{33} was assumed negligible and the transverse displacement w was assumed constant through the thickness [18]. These two assumptions implied direct normal strain ϵ_{33} would be zero, and hence, there would be no strain energy contribution resulting from normal strain. To more accurately account for all strain energy, ϵ_{33} was assumed to be a function of the direct strains in the element's 1- and 2-directions. This was equivalent to the Poisson's ratio effect for isotropic materials. Dennis assumed an orthogonal curvilinear coordinate system and a cubic-expansion of midsurface displacement parameters. This displacement field was similar to the cubic displacement field used for the HTSD theory of plates. Due to the curvature of the shell, however, a cubic displacement field will not satisfy the conditions of zero transverse shear at the top and bottom surfaces of the shell. Dennis ignored this inconsistency by eliminating linear terms of the order h^2/R^2 in his assumed displacement field. He also ignored linear terms of the order h/R in his transverse shear strain-displacement equations. Furthermore, Dennis assumed 26 higher-order nonlinear terms of the in-plane strain-displacement relations were negligible compared to other terms. This according to Schmidt and Reddy [92] can lead to inadequate and inconsistent equations.

Dennis's quasi-nonlinear HTSD formulation [18, 22] does accurately predict global responses of thin and moderately thick shells This theory reduces to the third-order HTSD theory of Reddy [81] for flat plates. Dennis showed good comparisons with exact solutions by Pagano and finite element solutions by others for many flat plate problems [18, 20]. Results for hinged-free cylindrical shells, deep cylindrical arches, and laminated cylindrical

pressure vessels showed results in good agreement with published works [18, 20]. Dennis later [21] compared linear results from his theory to exact solutions for laminated cylindrical shells under cylindrical bending published by Ren [85]. For the [90] and [90/0/90] laminates evaluated, Dennis's theory showed nearly exact results for transverse displacement at values of R/h in excess of 50, but for an R/h value of 10, his solution was too stiff by 6 percent for the [90] laminate and 11 percent for [90/0/90] laminate. At an R/h value of 4, Dennis's theory predicted 11 percent and 16 percent stiffer deflection response for the [90] and [90/0/90] laminates, respectively. Dennis did indicate in References [18, 22] that values of R/h less than 5 would make the assumptions of his theory inappropriate. The effect of σ_{33} being ignored is a significant factor for thick shells. Results of practical problems analyzed using Dennis's theory have shown excellent results [19, 93, 88, 102, 100]. The use of Dennis's theory for these studies was appropriate since R/h values were not less than 25.

For shell analysis, a higher-order finite element approximation can be used to model curvature with a minimum number of elements [106]. In this sense, "higher-order" relates to the order of nodal interpolation functions used in the finite element. Many papers have been published on various higher-order shell elements. The most common element is the degenerated isoparametric shell element [16, 68, 14, 11]. Chang, Saleeb, and Graf [14] developed a mixed formulation nine-node Lagrange shell element with independent assumptions for the displacement and strain fields. Their strain assumptions were based upon the following guidelines for a linear strain field:

> "(1) all kinematic modes must be suppressed,
>
> "(2) natural (or local) coordinates must be used to prevent invariant element properties, ...
>
> "(4) membrane and bending strains are interpolated separately in local coordinates,
>
> "(5) strain function have complete linear polynomial terms in r and s so that uniform convergence is ensured to the linear order, and
>
> "(6) the number of strain parameters is kept minimal [14].

Guidelines 4–6 eliminate membrane locking. The question of membrane locking for a finite element model is a difficult issue to deal with, according to Chang et al., who concluded "... a shell element (whether thick or thin) must have the same ability in representing the membrane as well as bending actions of a structure" [14]. Chang et al. used the Scordelis-Lo cylindrical roof, a pinched cylinder, and a hemispherical shell with opposing point loads to show the performance of their element. Their results converged to analytical solutions for each problem despite the lack of a nonlinear strain-displacement formulation. As indicated earlier, these particular problems are not a rigorous test of nonlinear theory.

Simple degenerated isoparametric shell elements have been used for problems exhibiting nonlinear geometric behavior and/or nonlinear material behavior[106, 16]. Yuan and Liang [109] used a three-noded axisymmetric shell element with the nonlinear finite rotation scheme introduced by Surana [98]. In their formulation only three nodal parameters were required—two translations and one rotational parameter (axisymmetric deformation was assumed). Yuan and Liang also incorporated nonconservative deformation-dependent loads and elastic-plastic constitutive relations. They did not, however, use a HTSD theory. Their rotational parameter represents the rotation of the normal at the node. Since this rotation is independent of the translational parameters, the normal is free to rotate. The normal is not, however, permitted to warp in this formulation. Hence, the transverse shear deformation is of first-order. No mention was made of the use of shear correction factors, but reduced integration was used to prevent shear locking. To achieve a satisfactory stress distribution through the shell, they resorted to a layered approach as used by Parisch [69]. This approach requires numerical integration through the shell's thickness. Their results compared well with similar published works.

Hsiao, Hung, and Chen also used degenerated isoparametric shell elements for nonlinear analysis [27, 28]. In the first of these papers, two new rotation strategies were proposed and evaluated along with four previously published strategies. In this paper, Hsiao and Hung used the Kirchhoff-Love hypothesis, thus, transverse shear deformation was not included in this analysis [27]. In the second paper, Hsiao and Chen [28] evaluate the four large rotation strategies of Ramm, Oliver and Onate, Parisch and Surana, and Bathe. The technique of Hughes and Liu [30, 31] is similar to that of Bathe. Hsiao and

Chen proposed a "finite rotation" method and a "mixed rotation" method. In the finite rotation method the rotational parameters are the incremental rotations of the shell normal during deformation. These are called α and β and are defined with respect to the x_1 and x_2 axes of a coordinate system fixed to the shell midsurface. The x_3 direction coincides with the shell normal and x_2 is aligned with one of the element's edges. In the mixed rotation method, the same parameters are used and the reference frame has x_3 aligned with the shell normal, but x_2 is aligned with the global X_2 direction. Hsiao and Chen used several problems, including the deep hinged-clamped circular arch and hinged-free cylindrical shells, to evaluate the various rotation strategies. They concluded that their two new rotation strategies and those of Ramm, Oliver and Onate, Parisch and Surana, and Bathe all gave similar performance. They also concluded that the choice of rotation axes has little effect on accuracy or convergence characteristics [27].

The large rotation strategies Hsiao and Chen evaluated were based upon the total rotation which includes rigid-body rotations. Many large rotation theories have been developed using corotational formulations which separate rigid-body rotations from strain rotations [76, 8]. Hsiao and Hung [27] used a corotational total Lagrangian formulation for a four-node linear isoparametric shell element and for a similar nine-node quadratic element. They showed good correlation with published results for a hinged-free cylindrical shell. This work according to Hsiao, was a "compromise between the total Lagrangian formulation for the degenerated shell element using large-displacement theory and the corotational formulation for the facet element using small-displacement theory" [27].

Neither of these papers by Hsiao and colleagues incorporated transverse shear deformation. For many problems of practical interest thin-shell theory is sufficient. Yang and Saigal [108] used a four-noded thin shell element with 12 degrees of freedom at each node to study rigid-body mode representation and locking mechanisms for nonlinear shell problems. They wanted to determine whether curvilinear coordinates or Cartesian coordinates were best suited for particular elements. They noted that rigid-body displacement of a curved member is curvilinear and can be exactly described by trigonometric functions of the element's arc angle. When polynomial functions are used to describe this curvilinear motion, the trigonometric functions will be reproduced only approximately. As the el-

ment's arc angle increases, the error in this approximation increases. Hence, for highly curved shell elements the rigid body mode representation will deteriorate [108]. Yang and Saigal used a displacement field defined in a Cartesian system, versus curvilinear, to obtain exact implicit modeling of the rigid-body modes. Their formulation included nonlinear extensional strains, but they used linearized bending strains. This effectively restricted their analysis to problems with moderate bending.

Yang and Saigal also discussed locking of thin shell models [108]. They explained that degenerate shell elements may suffer from membrane locking and shear locking when used to model curved thin structures such as arches and shells where bending is predominant. Yang and Saigal showed that their elements do not exhibit membrane locking by analyzing a pinched cylinder with several different finite element meshes. This analysis was performed using varying the order of the numerical integration (Gauss quadrature) from 3×3 to 5×5. Their results were identical for all meshes with the 4×4 and 5×5 integration rule, thus, "indicating that the element does not suffer from membrane locking" [108]. They also showed inconclusive results for hinged-free cylindrical shells. Their most interesting results were based on an analysis of a semitoroidal bellows under axisymmetric load (axial extension). The bellows have regions of positive, negative, and zero Gaussian curvature. Accurately modeling this shell with curvilinear coordinates based on lines of principal curvature is not a trivial problem due to the varying curvature. Yang and Saigal showed significant differences in converged curvilinear displacements u and v compared with Cartesian displacement parameters—the Cartesian parameters were better for this problem [108].

The classification scheme used by Nolte, Makowski, and Stumpf [53] may help explain why some of these problems don't provide a suitable test for nonlinear HTSD theories. For example, if one considers various values of thickness h and $\theta = \sqrt{h/R}$ for the hinged cylindrical shell of Sabir and Lock, then an approximate rotational limit can be estimated for each of Nolte's shell theory classifications. These limits are shown in Table 2.1. Despite large differences in thickness and significantly different load-displacement behavior for the shells of Table 2.1, the rotational limits for different shell theory classifications are the same. For example, if material rotations are on the order of 1/2 degree, then Nolte's

Table 2.1. Rotation Limits of Shell Theory Classifications

h	θ	classification [53]	rotation ω	
			radians	degrees
1.0	0.1	finite, $\omega \geq 1$	1.00	57
		large, $\omega = \sqrt{\theta}$	0.32	18
		moderate, $\omega = \theta$	0.10	6.0
		small, $\omega \leq \theta^2$	0.01	0.6
0.5	0.07	finite, $\omega \geq 1$	1.00	57
		large, $\omega = \sqrt{\theta}$	0.26	15
		moderate, $\omega = \theta$	0.07	4.0
		small, $\omega \leq \theta^2$	0.005	0.3
0.25	0.05	finite, $\omega \geq 1$	1.00	57
		large, $\omega = \sqrt{\theta}$	0.22	13
		moderate, $\omega = \theta$	0.05	3.0
		small, $\omega \leq \theta^2$	0.003	0.1

classification scheme suggests small rotation theory may be used for any thickness of the Sabir and Lock shell listed in Table 2.1. If rotations are on the order of 5 degrees, then moderate rotation theory should be used. Large rotation theory should supposedly be used for rotations on the order of 15 degrees. Finally, rotations in excess of 50 degrees will surely require finite rotation theory. All the theories discussed in this dissertation, according to their authors, have been small- to large-rotation theories. Also, these theories generally matched analytical results for problems where rotations were in excess of the Table 2.1 limits. Obviously, either this use of the classification scheme is not correct (i. e., it may ignore transverse shear deformation effects, anisotropic material effects, and large- or finite-strain effects), or the published results for these classical problems are in error. The author suspects the classification scheme of Nolte et al. is not appropriate for this use. Nonetheless, how does one determine what theory is appropriate for a given problem?

Simmonds [94] raised several questions regarding shell analysis. He indicated "The displacement form of the field equations is ill-conditioned in (near) inextensional [*sic.*] bending" [94]. This, according to Simmonds, is caused by relative errors of the order $\mathcal{O}(1)$ caused by approximating the term $1 + h^2/(12R^2)$ as unity [94]. This term is a result of the geometric approximation of the shell's shape. In this expression, h is thickness and

R is the radius of curvature of the shell. The theory developed by Donnell, for example, approximates this term as unity. Simmonds also raised a question about "non-experts in shell theory" [94] using finite element codes for general problem solving. Terms like ill-conditioning, spurious modes, stiffness locking, etc. are commonly used in the field of finite element analysis to describe numerical difficulties caused by inaccurate approximations. Many of these problems can be overcome, but before results should be used for design applications, the errors inherent in the theory and the element formulation must be estimated.

Yang and Wu [108] developed a geometrically nonlinear tensorial formulation of a skewed thin quadrilateral finite element. This element retained the coupling terms of the metric and curvature tensors since they no longer vanish in the non-orthogonal curvilinear coordinate system. The tensor form was used to develop the shell shape functions, geometric derivatives, stiffness matrix and finite element computer code. The element incorporates a small strain linear elastic isotropic material assumption and thickness is assumed to be small compared with the smallest radius of curvature of the shell's reference surface. In this theory, Yang and Wu retained only linear terms in the curvature-displacement relations. This decision was based upon observations by Bushnell [12] that nonlinear terms in the curvature-displacement relations can be neglected, provided the largest midsurface rotation is less than about 20 degrees; and upon experience gained in other investigations [108]. Yang and Wu showed excellent results for problems like the 1/2-inch thick hinged-free cylindrical shell, a pinched cylinder, rhombic plates, trapezoidal shells, and spherical shells. These problems included distortions of up to 16 degrees for the pinched cylinder, 8 degrees for the hinged-free cylindrical shell, and 60 degrees for the rhombic plate.

Simo, Fox, and Rifai [96] discussed the computational aspects of a geometrically-exact mixed finite element shell model. In this context, geometrically exact refers to not ignoring terms in the theoretical treatment of the shell geometry and the governing equations. Given a kinematic assumption (which may, or may not, exactly describe the physical problem), Simo et al. then treated the geometry and all equations exactly. The only numerical approximation was a result of the solution procedure used to solve the governing equations. Their model was based on the "theory of a one-director inextensible Cosserat surface, which

using the weak form of the momentum equations, can be parameterized in a way that avoids the use of Christoffel symbols or the second fundamental form" [96]. This provides a more simple formulation than most tensorial-based theories. Their formulation used the Hu-Washizu type of variational principle for mixed parameter problems [105]. Hence, the stress resultants and the (assumed) transverse shear strain field were included in the formulation. They showed results for a number of classical problems including hinged-free cylindrical shells, a pinched hemispherical shell, and other more complex problems. Problems such as the nonlinear buckling of a built-in right angle frame and the collapse analysis of an axially loaded cylinder showed good results with quadratic rates of convergence for all problems [96].

Several recent papers authored, or co-authored, by Reddy [78, 79] specifically addressed the issue of transverse shear deformation. Reddy [79] has reviewed all third-order two-dimensional technical theories of plates. He states in the abstract:

> *All* third-order theories published during the last two decades are shown to be based on the *same* displacement field, contrary to the claims by many authors. Consequently, all variationally derived plate theories are a special case of the third-order plate theory published by the author in 1984. [79]

In the paper, Reddy shows equivalence between kinematic assumptions used in over 20 published works of research and the third-order displacement field of Jemielite [34]. Reddy further clarifies that many of these works were based on equilibrium equations of the first-order theory of Reissner-Mindlin, and that he was the first to use consistent variational principles to derive a third-order theory of laminated composite plates [79]. In the other paper, Reddy [78] solves various linear and nonlinear bending, natural vibration, and stability problems using his refined computational model of composite laminates (the variationally consistent generalized third-order transverse shear deformation theory). Issues such as locking, symmetry considerations, boundary conditions, and geometric nonlinearity effects on displacements, buckling loads, and frequencies were discussed [78].

Fuehne and Engblom [25] developed a doubly-curved eight-noded isoparametric finite element with FTSD. Their element used three independently prescribed rotations and three

displacements per node in each layer. Evaluation of the stiffness matrix was performed numerically using reduced integration layer by layer. Fuehne's element included rotation about the normal as one of the six degrees of freedom. The stiffness terms related to this degree of freedom, according to Fuehne and Engblom [25:88] were "very minute." To overcome numerical difficulties caused by these small terms, they substituted "a fraction of the smallest rotational stiffness due to the θ_x or θ_y rotation for each element." These authors used the equilibrium equations to compute through the thickness stresses based on in-plane stresses calculated from the FTSD finite element solution. This process yields parabolic transverse shear stresses instead of the constant transverse shear stresses of the FTSD solution. This paper included results for a laminated composite cylinder with internal pressure. Compared with a previously published analytical solution, Fuehne and Engblom achieved "excellent" results for interlaminar shear stress [25:95].

Bhimaraddi, Carr, and Moss [9, 10] presented isoparametric finite element models for shear deformable shells of revolution and laminated curved (constant curvature) beams with HTSD. For the beam, they used nodal parameters called u_1 and v_1 defined as rotations about the element's axes. Their assumed displacement field included both of these parameters multiplied by "almost any function whose first derivative vanishes at ... [the surfaces of the element] and is non zero elsewhere ..." [10:312]. Thus, Bhimaraddi et al. achieved a parabolic distribution of transverse shear stress. The strain displacement relations chosen were the "exact" linear relations which included transverse normal strain and did not assume the shape function $1 + y_3/R$ was equal to unity. They indicated that ignoring the y_3/R factor would result in neglecting the variation of beam curvature across the cross-section which would lead to greater errors in predicted response.

Kant and Menon [37] investigated the effects of h/R for thick shells compared to thin shells using "higher-order" theories for composite laminates. They assumed the displacement field shown in Eq (2.3).

$$U_i = u_i + \theta_i z + u_i^* z^2 + \theta_i^* z^3, \quad (i = 1, 2) \tag{2.3}$$

$$U_3 = u_3 \tag{2.4}$$

where the u_i and θ_i are midsurface displacements and rotations, and the u_i^* and θ_i^* are the corresponding terms of the Taylor's series expansion. Kant and Menon discuss the use of "functions" of thickness coordinate z, similar to that used by Bhimaraddi [9], but do not define them, or discuss how they were used in this paper. Bhimaraddi's formulation included a cubic "function" with a parabolic first derivative as part of the displacement field. This assured zero transverse shear strain at the top and bottom surfaces of the element [10:312].

To arrive at their strains, Kant and Menon substituted the displacement field of Eq (2.3) into linear strain displacement relations and reduced these for a cylindrical shell. Their resulting strain components include 23 functions which form their generalized strain vector of the reference surface. Using standard constitutive relations for an orthotropic composite lamina, Kant and Menon formulated the potential energy of the system in terms of stress resultants and couples. They then discretized their problem domain using a C° formulation with selective integration to avoid membrane and shear locking. They used four-noded bilinear, eight-noded Lagrangian, and nine-noded Serendipity quadrilateral elements. Kant and Menon compared results for some interesting problems by assuming for thin shells $h/R = 0$, and for thick shells $h^2/R^2 = 0$. For the thick shells, the assumed loads acted at the top or bottom surface of the shell instead of at the shell midsurface. This, they concluded was the predominant factor in differences between their thin and thick shell results [37:1202].

The method of incorporating transverse shear into a shell model is not standard, even though FTSD and HTSD theories are both well accepted. These two theories are generally employed with the linearized transverse shear strain components of the Green-Lagrange strain tensor. They can, however, be used with nonlinear transverse shear strain terms. Singh, Rao, and Iyengar [97] used a FTSD theory with selected nonlinear terms included in the transverse strain components. Equation (2.5) shows these nonlinear terms in parentheses.

$$\begin{aligned} \varepsilon_4 &= \psi_x + \frac{\partial w}{\partial x} + \left(\frac{\partial u}{\partial x}\psi_x + \frac{\partial v}{\partial x}\psi_y\right) \\ \varepsilon_5 &= \psi_y + \frac{\partial w}{\partial y} + \left(\frac{\partial u}{\partial y}\psi_x + \frac{\partial v}{\partial y}\psi_y\right) \end{aligned} \tag{2.5}$$

where

$$\begin{aligned} u(x,y,z) &= u_o(x,y) + z\psi_x(x,y) \\ v(x,y,z) &= v_o(x,y) + z\psi_y(x,y) \\ w(x,y,z) &= w_o(x,y) \end{aligned}$$

Singh, Rao, and Iyengar studied the effects of anisotropy, transverse shear modulus, aspect ratio, and boundary conditions on the buckling behavior of thick laminated composite plates. They found transverse shear to be a significant factor in determining buckling load. Although this FTSD formulation included nonlinear $\varepsilon_4 = \varepsilon_{23}$ and $\varepsilon_5 = \varepsilon_{13}$, the authors did not mention of the effects of these nonlinear terms.

Palmerio, Reddy, and Schmidt published a series of two papers [65, 66] on a moderate rotation FTSD for laminated anisotropic shells. This theory was proposed by Schmidt and Reddy [92]. Their paper was reviewed earlier in this Chapter; see page 2-12. In their finite element formulation, Palmerio et al. separate transverse shear and transverse normal effects from in-plane extension and bending terms. This allows them to use reduced integration for the transverse stiffness terms to prevent shear locking. Interestingly, they retain transverse normal strain in their formulation. They add a sixth degree of freedom to the typical five used for a FTSD theory. This sixth parameter is the linear term in the transverse normal strain component ε_{33}. Having a nonzero ε_{33} normally requires use of the full three-dimensional constitutive relations. Palmerio et al. assume a state of plane stress and set $\nu_{13} = \nu_{23} = 0$ to achieve results similar to a five degree of freedom FTSD model. Their results are stiffer without this assumption.

Palmerio, Reddy, and Schmidt [66] investigated several problems including Sabir and Lock shells. For 1-inch and 1/2-inch shells this theory compared well with published solutions. A variation of this problem was also studied by substituting a 1-inch thick [0/90] composite material for the isotropic material of the Sabir and Lock shell. Results of these moderate rotation theory (MRT) models compared well with a "refined" von Karman (RVK) analysis, but none of the results compared favorably with a full continuum model by Liao and Reddy. Palmerio et al. suggested that, "One of the reasons for the discrepancy

could be due to not updating the geometry in the RVK and MRT formulations" [66]. In their discussion of the results, they indicated that the MRT has nonlinear transverse shear strain terms due to in-plane displacements which are not present in the RVK. Thus, if both theories give similar results then the additional terms in the MRT do not contribute significantly to the solution [66]. Based upon their comparison with Liao and Reddy's results, Palmerio et al. revised their MRT to include more nonlinear terms in their in-plane Green-Lagrange strain tensor components. Their first-order through the thickness expansion of displacements was retained. They noted that the resulting "non-linear transverse shear terms are exactly the same as the MRT, ...[if they neglect the transverse normal strain degree of freedom]" [66]. The major difference in this modification was that the bending components contained substantially more terms. With essentially the full Green-Lagrange strain tensor representation, the modified theory of Palmerio, Reddy and Schmidt gave results that were in close agreement with the continuum model of Liao and Reddy for a thin shallow isotropic spherical panel and a thin shallow isotropic arch. They concluded that including more nonlinear bending terms improved results for one problem and "elimination" of nonlinear transverse shear terms was necessary to reduce the overly stiff behavior of the MRT for some cases [66].

III. Theoretical Background

The primary goal of this research was to consider the ability of a higher-order transverse shear deformation (HTSD) theory to model deformation of a composite shell undergoing large displacements, rotations, and changes in curvature. In particular, more exact through-the-thickness approximations of displacement, more exact approximations of shell geometric parameters, and the incorporation of nonlinear transverse shear strain were considered in this research. Many HTSD models have been developed in recent years [18, 78]. These theories are suitable for linear or nonlinear problem solving by a number of numerical solution methods. This chapter of the dissertation includes some theoretical background material. The background material is necessary to assure a common understanding of the concepts underlying the nonlinear HTSD theory. A presentation of the nonlinear HTSD theory developed for this research is included as Chapter IV.

3.1 Surface Geometric Considerations

Components of particular physical quantities, such as displacement, stress, and strain, however, are more generally defined for arbitrary curvilinear coordinate systems as being either covariant or contravariant. These quantities are identified in the text as being covariant or contravariant when the tensorial nature of the quantity is generally accepted in the literature. Conventional tensor notation requires that contravariant quantities be identified by superscripts and covariant quantities be identified by subscripts. This practice is generally followed throughout this dissertation. For convenience, however, coordinates are always identified with subscripts. The basic assumptions of a two-dimensional shell theory are tied to the concepts of a reference surface, the midsurface of the shell, and a local curvilinear coordinate system associated with this surface. When this curvilinear coordinate system is based upon lines of principal curvature, which by definition are orthogonal, then the coordinate system is also orthogonal. In orthogonal system of coordinates, the components of the metric tensor form a diagonal matrix. Thus, contravariant and covariant components of tensors are identical. For this research, the author has decided to restrict the theoretical development to orthogonal coordinate systems based upon

lines of constant curvature. This is one of the most common coordinate systems used for analysis of shells [50, 57].

The development of nonlinear strain displacement relations generally begins with the mathematical description of the midsurface geometry. If one considers a surface in a three-dimensional space, then the positions of points on its surface can be defined by:

$$\vec{r} = \vec{r}(\theta_1, \theta_2) \tag{3.1}$$

where $\vec{r}$ is the position vector from the origin O to points on the surface [50]. The parameters $(\theta_1,\ \theta_2)$ are defined in a closed region S in the $(\theta_1,\ \theta_2)$ plane. Next, assume the unit normal vector to the surface is $\vec{a}_3(\theta_1,\ \theta_2)$ and the thickness of the shell is $h = h(\theta_1,\ \theta_2)$, where $h > 0$. The position vector of a point within the shell can be written in terms of $\vec{r}$ and $\vec{a}_3$. This position vector is given by:

$$\vec{r}(\theta_1, \theta_2) + z\vec{a}_3(\theta_1, \theta_2) \tag{3.2}$$

where $(\theta_1, \theta_2) \in S$ and $|z| = \frac{1}{2}h(\theta_1, \theta_2)$. The (θ_1, θ_2)-plane defined by the surface S is called the middle surface. The lines defined by $\theta_1 =$ constant and $\theta_2 =$ constant are called coordinate curves. These curves define a curvilinear coordinate system with covariant base vectors a_1 and a_2 given by:

$$\vec{a}_1 = \partial\vec{r}/\partial\theta_1, \quad \vec{a}_2 = \partial\vec{r}/\partial\theta_2 \tag{3.3}$$

or

$$\vec{a}_\alpha = \partial\vec{r}/\partial\theta_\alpha \tag{3.4}$$

where Greek subscripts have values 1 and 2. The covariant base vectors, $\vec{a}_1$ and $\vec{a}_2$, are parallel to the tangents to the θ_1 and θ_2 coordinate curves. This is shown in Figure 3.1.

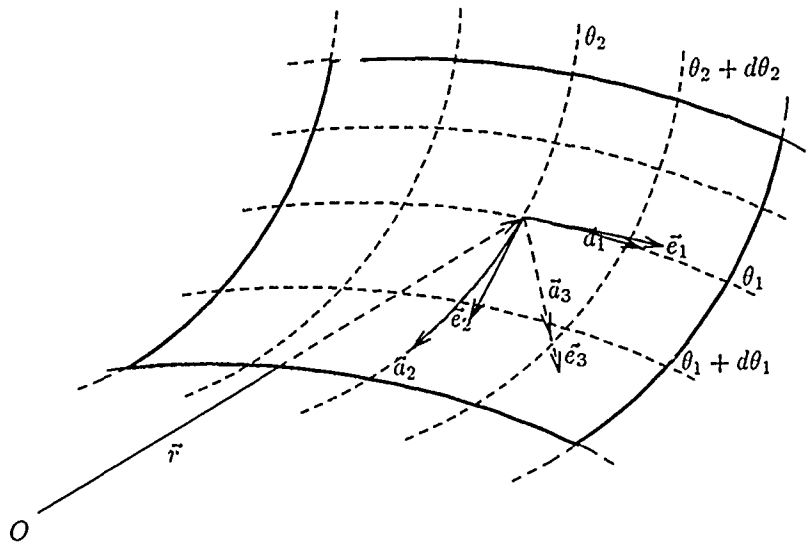

[105]

Figure 3.1. Base Vectors and Coordinate Curves

An infinitesimal vector connecting two points on the surface with coordinates (θ_1, θ_2) and $(\theta_1 + d\theta_1, \theta_2 + d\theta_2)$ is given by:

$$d\vec{r} = \frac{\partial \vec{r}}{\partial \theta_1} d\theta_1 + \frac{\partial \vec{r}}{\partial \theta_2} d\theta_2 = \sum_{\alpha=1}^{2} \vec{a}_\alpha d\theta_\alpha \equiv \vec{a}_\alpha d\theta_\alpha \tag{3.5}$$

where the repeated subscripts imply summation as shown in Eq (3.5). The length (ds) of this vector is given by:

$$(ds)^2 = d\vec{r} \cdot d\vec{r} = \vec{a}_\alpha \cdot \vec{a}_\beta d\theta_\alpha d\theta_\beta \tag{3.6}$$

Defining the covariant surface metric tensor as:

$$a_{\alpha\beta} = \vec{a}_\alpha \cdot \vec{a}_\beta = a_{\beta\alpha} \tag{3.7}$$

allows one to write $(ds)^2$ in terms of the covariant surface metric tensor as:

$$(ds)^2 = a_{\alpha\beta} d\theta_\alpha d\theta_\beta \tag{3.8}$$

Equation (3.8) is called the first fundamental form of the surface.

Next, consider a point on the middle surface with coordinates θ_α and a unit vector $\vec{t}$ in the tangent plane at this point. The normal curvature associated with the direction determined by $\vec{t}$ is given by:

$$\frac{1}{R}ds = -d\vec{a}_3 \cdot \vec{t} \tag{3.9}$$

or

$$\frac{1}{R} = -\frac{d\vec{a}_3}{ds} \cdot \vec{t} \tag{3.10}$$

If one substitutes Eqs (3.5) and (3.6) into Eq (3.10), then one finds:

$$\vec{t} = \frac{d\vec{r}}{ds} = \vec{a}_1 \frac{d\theta_1}{ds} + \vec{a}_2 \frac{d\theta_2}{ds} \tag{3.11}$$

and

$$\frac{d\vec{a}_3}{ds} = \vec{a}_{3,1} \frac{d\theta_1}{ds} + \vec{a}_{3,2} \frac{d\theta_2}{ds} \tag{3.12}$$

where a comma in the subscripts implies differentiation with respect to the coordinate following the comma. Substituting Eqs (3.11), (3.12), and (3.8) into Eq (3.10) gives:

$$\frac{1}{R} = \frac{-\sum_{\alpha,\beta} \vec{a}_{3,\beta} \cdot \vec{a}_\beta d\theta_\alpha d\theta_\beta}{\sum_{\alpha,\beta} a_{\alpha\beta} d\theta_\alpha d\theta_\beta} \tag{3.13}$$

The quantity $b_{\alpha\beta}$ can be defined, such that:

$$b_{\alpha\beta} = -\vec{a}_{3,\alpha} \cdot \vec{a}_\beta = \vec{a}_\beta \cdot \vec{a}_{\alpha,\beta} = \vec{a}_3 \cdot \vec{a}_{\alpha,\beta} = b_{\beta\alpha} \tag{3.14}$$

The curvature can now be defined as:

$$\frac{1}{R} = \frac{\sum_{\alpha,\beta} b_{\alpha\beta} d\theta_\alpha d\theta_\beta}{\sum_{\alpha,\beta} a_{\alpha\beta} d\theta_\alpha d\theta_\beta} \tag{3.15}$$

where $b_{\alpha\beta} d\theta_\alpha d\theta_\beta$ is called the second fundamental form of the surface. Thus, the normal curvature is given by the ratio between the first and second fundamental forms.

If one defines the coordinate curves of Figure (3.1) to be lines of principal curvature of the shell, then the θ_1 and θ_2 curves are mutually orthogonal families of curves [50, 57].

In this coordinate system, the lengths A_α of the basis vectors $\vec{a}_\alpha$ are given by:

$$A_\alpha = |\vec{a}_\alpha| = \sqrt{(\vec{a}_\alpha \cdot \vec{a}_\alpha)} \tag{3.16}$$

where the A_α are called the Lamé parameters of the surface.

Next, define mutually orthogonal unit vectors $\vec{e}_1$, $\vec{e}_2$, $\vec{e}_3$ in the directions of the base vectors $\vec{a}_1$, $\vec{a}_2$ and the normal vector $\vec{a}_3$, respectively. These unit vectors are given by:

$$\vec{e}_\alpha = \vec{a}_\alpha / A_\alpha, \quad (\alpha = 1,2); \qquad \vec{e}_3 = \vec{a}_3 \tag{3.17}$$

The derivatives of the orthonormal base vectors are given by [50:8]:

$$\begin{aligned}
\vec{e}_{1,1} &= -\tfrac{A_{1,2}}{A_2}\vec{e}_2 + \tfrac{A_1}{R_1}\vec{e}_3 & \vec{e}_{1,2} &= \tfrac{A_{2,1}}{A_1}\vec{e}_2 \\
\vec{e}_{2,1} &= \tfrac{A_{1,2}}{A_2}\vec{e}_1 & \vec{e}_{2,2} &= -\tfrac{A_{2,1}}{A_1}\vec{e}_1 + \tfrac{A_2}{R_2}\vec{e}_3 \\
\vec{e}_{3,1} &= \tfrac{A_1}{R_1}\vec{e}_1 & \vec{e}_{3,2} &= \tfrac{A_2}{R_2}\vec{e}_2
\end{aligned} \tag{3.18}$$

If one now considers a vector field $\vec{V}(\theta_1, \theta_2)$ on the middle surface of the shell, then one can resolve this field in the directions of the orthogonal base vectors $\vec{e}_1$, $\vec{e}_2$, $\vec{e}_3$ as follows:

$$\vec{V}(\theta_1, \theta_2) = V_1\vec{e}_1 + V_2\vec{e}_2 + V_3\vec{e}_3 \tag{3.19}$$

Differentiating Eq (3.19) with respect to θ_1 and θ_2 gives:

$$\vec{V}_{,\alpha} = V_{i,\alpha}\vec{e}_i + V_i\vec{e}_{i,\alpha} \tag{3.20}$$

where repeated indices imply summation and Latin subscripts have the values 1,2,3 and Greek subscripts have values 1,2. If one substitutes Eq (3.18) for the derivatives of the base vectors into Eq (3.19), then the derivatives of the vector $\vec{V}$ are given as follows:

$$\begin{aligned}
\vec{V}_{,1} &= \left(\vec{V}_{1,1} + \tfrac{A_{1,2}}{A_2}\vec{V}_2 - \tfrac{A_1}{R_1}\vec{V}_3\right)\vec{e}_1 + \left(\vec{V}_{2,1} - \tfrac{A_{1,2}}{A_2}\vec{V}_1\right)\vec{e}_2 + \left(\vec{V}_{3,1} + \tfrac{A_1}{R_1}\vec{V}_1\right)\vec{e}_3 \\
\vec{V}_{,2} &= \left(\vec{V}_{1,2} - \tfrac{A_{2,1}}{A_1}\vec{V}_2\right)\vec{e}_1 + \left(\vec{V}_{2,2} + \tfrac{A_{2,1}}{A_1}\vec{V}_1 - \tfrac{A_2}{R_2}\vec{V}_3\right)\vec{e}_2 + \left(\vec{V}_{3,2} + \tfrac{A_2}{R_2}\vec{V}_2\right)\vec{e}_3
\end{aligned} \tag{3.21}$$

One can show that certain relationships between A_1, A_2, R_1, and R_2 must be satisfied. These relationships are given by Codazzi's equations:

$$\left(\frac{A_1}{R_1}\right)_{,2} = \frac{A_{1,2}}{R_2}, \qquad \left(\frac{A_2}{R_1}\right)_{,1} = \frac{A_{2,1}}{R_1} \tag{3.22}$$

and Gauss's equation:

$$\left(\frac{A_{1,2}}{A_1}\right)_{,1} + \left(\frac{A_{1,2}}{A_2}\right)_{,2} = -\frac{A_1 A_2}{R_1 R_2} \tag{3.23}$$

3.2 Strain Tensor Definition

In Figure 3.2, consider the displacement of a body in a three-dimensional space from its original undeformed state to a new deformed state denoted by a superscript star. The coordinates y_1, y_2, and y_3 are chosen to form an orthogonal curvilinear coordinate system. This system is not the same coordinate system as the two-dimensional (θ_1, θ_2) system of the shell midsurface. In the (y_1, y_2, y_3) system, the original length (ds) of the line from M to N is given by:

$$(ds)^2 = g_{ij} dy_i dy_j \tag{3.24}$$

where g_{ij} is the metric tensor associated with the undeformed curvilinear coordinate system (y_1, y_2, y_3). The components of g_{ij} are given by the scalar product $\vec{g}_i \cdot \vec{g}_j$.

In the deformed system of coordinates, the distance (ds^*) from point M^* to N^* is given by:

$$(ds^*)^2 = g^*_{ij} dy^*_i dy^*_j \tag{3.25}$$

If we use a Lagrangian description of deformation, we attempt to express all variables in terms of conditions prior to deformation [86]. From Figure 3.2, the displacement $\vec{U}$ of point M and the derivatives of $\vec{U}$ are given by:

$$\vec{U} = \vec{r}^* - \vec{r} \tag{3.26}$$

$$\frac{\partial \vec{U}}{\partial y_i} = \frac{\partial \vec{r}^*}{\partial y_i} - \frac{\partial \vec{r}}{\partial y_i} = \vec{g}^*_i - \vec{g}_i \tag{3.27}$$

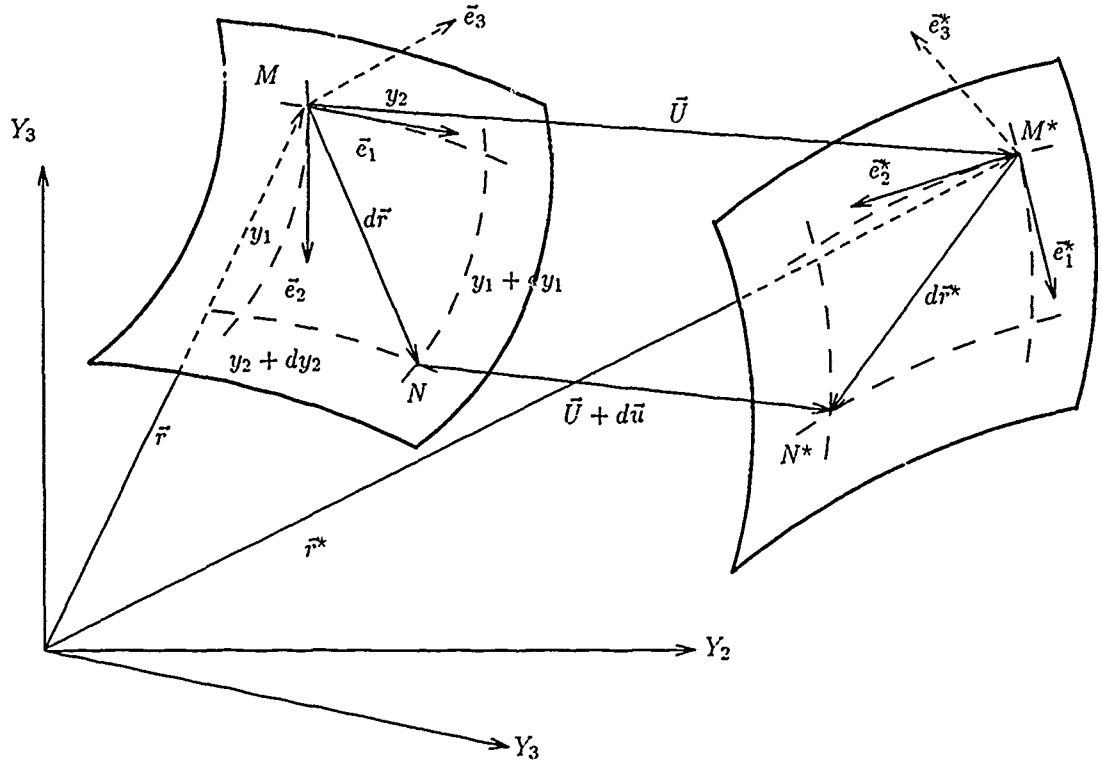

[86, 105]

Figure 3.2. Body Before and After Deformation

If one combines Eqs (3.24) and (3.25), then one can define the strain tensor γ_{ij} as:

$$2\gamma_{ij} = (g^*_{ij} - g_{ij}) \tag{3.28}$$

If one substitutes Eq (3.27) into Eq (3.28), then one can express the strain tensor γ_{ij} as follows:

$$2\gamma_{ij} = \vec{g}_i \cdot \frac{\partial \vec{U}}{\partial y_j} + \vec{g}_j \cdot \frac{\partial \vec{U}}{\partial y_i} + \frac{\partial \vec{U}}{\partial y_i} \cdot \frac{\partial \vec{U}}{\partial y_j} \tag{3.29}$$

The orthogonal base vectors $\vec{g}_i$ are related to a new set of orthonormal base vectors $\vec{e}_i$ by the following relationship:

$$\vec{e}_i = \frac{\vec{g}_i}{|\vec{g}_i|} = \frac{\vec{g}_i}{\sqrt{\vec{g}_i \cdot \vec{g}_i}} = \frac{\vec{g}_i}{h_i} \tag{3.30}$$

where the h_i are called scale factors [86:118]. The displacement vector $\vec{U}$ can be written in terms of $\vec{e}_1$, $\vec{e}_2$, $\vec{e}_3$ at point M as follows:

$$\vec{U} = u_1\vec{e}_1 + u_2\vec{e}_2 + u_3\vec{e}_3 \tag{3.31}$$

If one substitutes Eq (3.31) into Eq (3.29), then one obtains:

$$2\gamma_{ij} = \vec{g}_i \cdot \frac{\partial(u_k\vec{e}_k)}{\partial y_j} + \vec{g}_j \cdot \frac{\partial(u_l\vec{e}_l)}{\partial y_i} + \frac{\partial(u_m\vec{e}_m)}{\partial y_i} \cdot \frac{\partial(u_n\vec{e}_n)}{\partial y_j} \tag{3.32}$$

Next, if one expands the implied summations on k, l, m, and n over their values of 1, 2, and 3, the result becomes:

$$\begin{aligned} 2\gamma_{ij} \;=\; & \vec{g}_i \cdot \frac{\partial(\vec{e}_k)}{\partial y_j}(u_1\vec{e}_1 + u_2\vec{e}_2 + u_3\vec{e}_3) + \\ & \vec{g}_j \cdot \frac{\partial(\vec{e}_l)}{\partial y_i}(u_1\vec{e}_1 + u_2\vec{e}_2 + u_3\vec{e}_3) + \\ & \frac{\partial(\vec{e}_m)}{\partial y_i}(u_1\vec{e}_1 + u_2\vec{e}_2 + u_3\vec{e}_3) \cdot \frac{\partial(\vec{e}_n)}{\partial y_j}(u_1\vec{e}_1 + u_2\vec{e}_2 + u_3\vec{e}_3) \end{aligned} \tag{3.33}$$

If one uses the relationships of Eqs (3.17) and (3.18), the strain components γ_{ij} can be written in terms of the displacement components and Lamé parameters [86:136-137] as

follows:

$$\begin{aligned}\gamma_{11} &= h_1\frac{\partial u_1}{\partial y_1}+\frac{h_1u_2}{h_2}\frac{\partial h_1}{\partial y_2}+\frac{h_1u_3}{h_3}\frac{\partial h_1}{\partial y_3}\\ &+\frac{1}{2}\left(\frac{\partial u_1}{\partial y_1}+\frac{u_2}{h_2}\frac{\partial h_1}{\partial y_2}+\frac{u_3}{h_3}\frac{\partial h_1}{\partial y_3}\right)^2\\ &+\frac{1}{2}\left(\frac{\partial u_2}{\partial y_1}-\frac{u_1}{h_2}\frac{\partial h_2}{\partial y_2}\right)^2+\frac{1}{2}\left(\frac{\partial u_3}{\partial y_1}-\frac{u_1}{h_3}\frac{\partial h_1}{\partial y_3}\right)^2\end{aligned} \tag{3.34}$$

$$\begin{aligned}\gamma_{22} &= h_2\frac{\partial u_2}{\partial y_2}+\frac{h_2u_3}{h_3}\frac{\partial h_2}{\partial y_3}+\frac{h_2u_1}{h_1}\frac{\partial h_2}{\partial y_1}\\ &+\frac{1}{2}\left(\frac{\partial u_2}{\partial y_2}+\frac{u_3}{h_3}\frac{\partial h_2}{\partial y_3}+\frac{u_1}{h_1}\frac{\partial h_2}{\partial y_1}\right)^2\\ &+\frac{1}{2}\left(\frac{\partial u_3}{\partial y_2}-\frac{u_2}{h_3}\frac{\partial h_3}{\partial y_3}\right)^2+\frac{1}{2}\left(\frac{\partial u_1}{\partial y_2}-\frac{u_2}{h_1}\frac{\partial h_2}{\partial y_1}\right)^2\end{aligned} \tag{3.35}$$

$$\begin{aligned}\gamma_{33} &= h_3\frac{\partial u_3}{\partial y_3}+\frac{h_3u_1}{h_1}\frac{\partial h_3}{\partial y_1}+\frac{h_3u_2}{h_2}\frac{\partial h_2}{\partial y_2}\\ &+\frac{1}{2}\left(\frac{\partial u_3}{\partial y_3}+\frac{u_1}{h_1}\frac{\partial h_3}{\partial y_1}+\frac{u_2}{h_2}\frac{\partial h_3}{\partial y_2}\right)^2\\ &+\frac{1}{2}\left(\frac{\partial u_1}{\partial y_3}-\frac{u_1}{h_2}\frac{\partial h_1}{\partial y_1}\right)^2+\frac{1}{2}\left(\frac{\partial u_2}{\partial y_3}-\frac{u_3}{h_2}\frac{\partial h_3}{\partial y_2}\right)^2\end{aligned} \tag{3.36}$$

$$\begin{aligned}\gamma_{12} &= \frac{1}{2}\left(h_1\frac{\partial u_1}{\partial y_2}+h_2\frac{\partial u_2}{\partial y_1}-u_2\frac{\partial h_2}{\partial y_1}-u_1\frac{\partial h_1}{\partial y_2}\right)\\ &+\frac{1}{2}\left(\frac{\partial u_1}{\partial y_2}-\frac{u_2}{h_1}\frac{\partial h_2}{\partial y_1}\right)\left(\frac{\partial u_1}{\partial y_1}+\frac{u_2}{h_2}\frac{\partial h_1}{\partial y_2}+\frac{u_3}{h_3}\frac{\partial h_1}{\partial y_3}\right)\\ &+\frac{1}{2}\left(\frac{\partial u_2}{\partial y_1}-\frac{u_1}{h_2}\frac{\partial h_1}{\partial y_2}\right)\left(\frac{\partial u_2}{\partial y_2}+\frac{u_1}{h_1}\frac{\partial h_2}{\partial y_1}+\frac{u_3}{h_3}\frac{\partial h_2}{\partial y_3}\right)\\ &+\frac{1}{2}\left(\frac{\partial u_3}{\partial y_1}-\frac{u_1}{h_3}\frac{\partial h_1}{\partial y_3}\right)\left(\frac{\partial u_3}{\partial y_2}-\frac{u_2}{h_3}\frac{\partial h_2}{\partial y_3}\right)\end{aligned} \tag{3.37}$$

$$\begin{aligned}\gamma_{13} &= \frac{1}{2}\left(h_3\frac{\partial u_3}{\partial y_1}+h_1\frac{\partial u_1}{\partial y_3}-u_1\frac{\partial h_1}{\partial y_3}-u_3\frac{\partial h_3}{\partial y_1}\right)\\ &+\frac{1}{2}\left(\frac{\partial u_1}{\partial y_3}-\frac{u_3}{h_1}\frac{\partial h_3}{\partial y_1}\right)\left(\frac{\partial u_1}{\partial y_1}+\frac{u_3}{h_3}\frac{\partial h_1}{\partial y_3}+\frac{u_2}{h_2}\frac{\partial h_1}{\partial y_2}\right)\\ &+\frac{1}{2}\left(\frac{\partial u_3}{\partial y_1}-\frac{u_1}{h_3}\frac{\partial h_1}{\partial y_3}\right)\left(\frac{\partial u_3}{\partial y_3}+\frac{u_1}{h_3}\frac{\partial h_3}{\partial y_1}+\frac{u_2}{h_2}\frac{\partial h_3}{\partial y_2}\right)\\ &+\frac{1}{2}\left(\frac{\partial u_2}{\partial y_1}-\frac{u_1}{h_2}\frac{\partial h_1}{\partial y_2}\right)\left(\frac{\partial u_2}{\partial y_3}-\frac{u_3}{h_2}\frac{\partial h_2}{\partial y_2}\right)\end{aligned} \tag{3.38}$$

$$\begin{aligned}\gamma_{23} &= \frac{1}{2}\left(h_3\frac{\partial u_3}{\partial y_2}+h_2\frac{\partial u_2}{\partial y_3}-u_2\frac{\partial h_2}{\partial y_3}-u_3\frac{\partial h_3}{\partial y_2}\right)\\ &+\frac{1}{2}\left(\frac{\partial u_2}{\partial y_3}-\frac{u_3}{h_2}\frac{\partial h_3}{\partial y_2}\right)\left(\frac{\partial u_2}{\partial y_2}+\frac{u_3}{h_3}\frac{\partial h_2}{\partial y_3}+\frac{u_1}{h_1}\frac{\partial h_2}{\partial y_1}\right)\\ &+\frac{1}{2}\left(\frac{\partial u_3}{\partial y_2}-\frac{u_2}{h_3}\frac{\partial h_2}{\partial y_3}\right)\left(\frac{\partial u_3}{\partial y_3}+\frac{u_2}{h_2}\frac{\partial h_3}{\partial y_2}+\frac{u_1}{h_1}\frac{\partial h_3}{\partial y_1}\right)\\ &+\frac{1}{2}\left(\frac{\partial u_1}{\partial y_2}-\frac{u_2}{h_1}\frac{\partial h_2}{\partial y_1}\right)\left(\frac{\partial u_1}{\partial y_3}-\frac{u_3}{h_1}\frac{\partial h_3}{\partial y_1}\right)\end{aligned} \tag{3.39}$$

For the shell discussed earlier, the Lamé parameters A_α, $\alpha = 1,2$, describe the *two*-dimensional relationship between the orthogonal surface base vectors $\vec{a}_\alpha$ and their orthonormal counterparts $\vec{e}_\alpha$. For the strains of Eqs (3.34-3.39), the scale factors h_i, $i = 1,2,3$, describe the *three*-dimensional relationship between the orthogonal base vectors $\vec{g}_i$ of the three-dimensional orthogonal curvilinear coordinate system $\vec{y}_i$ and their orthonormal counterparts $\vec{e}_i$. For a two-dimensional orthogonal curvilinear coordinate system, the scale factors of Eqs (3.34-3.39) become:

$$h_1 = A_1(1 - y_3/R_1), \quad h_2 = A_2(1 - y_3/R_2), \quad h_3 = 1 \tag{3.40}$$

where recalling Eqs (3.4) and (3.16), we have:

$$A_1 = \left(\frac{\partial \vec{r}}{\partial \theta_1}\cdot\frac{\partial \vec{r}}{\partial \theta_1}\right)^{1/2}, \quad A_2 = \left(\frac{\partial \vec{r}}{\partial \theta_2}\cdot\frac{\partial \vec{r}}{\partial \theta_2}\right)^{1/2} \tag{3.41}$$

Thus, for the convenient case of a cylindrical shell with radius R_2 and local coordinates $\theta_1 = x$, $\theta_2 = s$, z described in an orthogonal space with global coordinates $y_1 = x$, $y_2 = s$, $y_3 = z$, the position vector $\vec{r}(y_1, y_2, y_3)$ would be given by:

$$\vec{r} = x\vec{e}_1 + s\vec{e}_2 + z\vec{e}_3 \tag{3.42}$$

and the Lamé parameters reduce to $A_1 = A_2 = 1$. For the same shell described in terms of an angle, say ϕ, the circumferential coordinate s would be given by $ds = R_2 d\phi$. In this case, $d\vec{r}(y_1, y_2, y_3)$ is given by:

$$d\vec{r} = dx\vec{e}_1 + R_2 d\phi\vec{e}_2 + dz\vec{e}_3 \tag{3.43}$$

and the Lamé parameters would be $A_1 = 1$ and $A_2 = R_2$.

At this point, it is important to realize the strain components of Eqs (3.34-3.39) are related to the orthogonal curvilinear basis vectors $\vec{a}_1$, $\vec{a}_2$, and $\vec{a}_3$, which change in magnitude and direction. This strain tensor is typically called the Green-Lagrange strain tensor [105]. These tensorial strain components must be converted to physical components in order to complete the analysis. For the infinitesimal linear problem, the linear parts of this strain tensor can be related to the physical strain of the line from point M to N [86:129]. The change in length of the line segment from M to N, shown in Figure 3.2, is given by:

$$\varepsilon_{MN} = \frac{1}{2}\frac{(ds^*)^2 - (ds)^2}{(ds)^2} \tag{3.44}$$

This equation can be written in terms of the curvilinear coordinates y_1, y_2, y_3 as follows:

$$\varepsilon_{MN} = \gamma_{ij}\frac{dy_i}{ds}\frac{dy_j}{ds} \tag{3.45}$$

The derivatives appearing in Eq (3.45) can be written in terms of the direction cosines l_1, l_2, l_3 of the line from M to N relative to the orthonormal base vectors $\vec{e}_1$, $\vec{e}_2$, $\vec{e}_3$. These direction cosines are given by:

$$l_1 = h_1\frac{dy_1}{ds}, \quad l_2 = h_2\frac{dy_2}{ds}, \quad l_3 = h_3\frac{dy_3}{ds} \tag{3.46}$$

If one substitutes Eq (3.46) into Eq (3.45) and expands the summations, then:

$$\begin{aligned} \varepsilon_{MN} \;=\; & \gamma_{11}\left(\frac{l_1}{h_1}\right)^2 + \gamma_{22}\left(\frac{l_2}{h_2}\right)^2 + \gamma_{33}\left(\frac{l_3}{h_3}\right)^2 \\ & + 2\gamma_{12}\left(\frac{l_1 l_2}{h_1 h_2}\right) + 2\gamma_{13}\left(\frac{l_1 l_3}{h_1 h_3}\right) + 2\gamma_{23}\left(\frac{l_2 l_3}{h_2 h_3}\right) \end{aligned} \tag{3.47}$$

This equation can be written in terms of physical strain components ε_{ij} as follows:

$$\begin{aligned} \varepsilon_{MN} \;=\; & \varepsilon_{11}l_1^2 + \varepsilon_{22}l_2^2 + \varepsilon_{33}l_3^2 \\ & + 2\varepsilon_{12}l_1 l_2 + 2\varepsilon_{13}l_1 l_3 + 2\varepsilon_{23}l_2 l_3 \end{aligned} \tag{3.48}$$

where

$$\varepsilon_{11} = \frac{\gamma_{11}}{h_1^2}, \quad \varepsilon_{22} = \frac{\gamma_{22}}{h_2^2}, \quad \varepsilon_{33} = \frac{\gamma_{33}}{h_3^2}$$
$$\varepsilon_{12} = \frac{\gamma_{12}}{h_1 h_2}, \quad \varepsilon_{13} = \frac{\gamma_{13}}{h_1 h_3}, \quad \varepsilon_{23} = \frac{\gamma_{23}}{h_2 h_3} \tag{3.49}$$

are the physical components of strain for the case of an infinitesimal displacement $\vec{U}$ defined by Eq (3.31) [86, 50].

3.3 Composite Material Analysis

In the previous sections of this dissertation, the concepts of strain for a shell in an orthogonal curvilinear coordinate system have been presented. Next, the subject of constitutive relations will be discussed. One can consider the material of a composite laminate from a microscopic viewpoint or from a macroscopic viewpoint [2, 13, 36, 107]. For this research, the macro-mechanical behavior of the laminate will be assumed sufficient provided stresses are small enough to assure no material failure occurs. Thus, the material of each lamina is treated as a homogeneous anisotropic material. More specifically, we shall assume the material is transversely isotropic. This means the material has properties which are symmetric about two material axes. An orthotropic material has properties that are different in three mutually orthogonal directions with three mutually perpendicular planes of material symmetry. The small strain constitutive relations for an orthotropic material are written in matrix form as follows [36:35]:

$$\begin{Bmatrix} \sigma_{11} \\ \sigma_{22} \\ \sigma_{33} \\ \tau_{23} \\ \tau_{13} \\ \tau_{12} \end{Bmatrix} = \begin{bmatrix} C_{11} & C_{12} & C_{13} & 0 & 0 & 0 \\ C_{12} & C_{22} & C_{23} & 0 & 0 & 0 \\ C_{13} & C_{23} & C_{33} & 0 & 0 & 0 \\ 0 & 0 & 0 & C_{44} & 0 & 0 \\ 0 & 0 & 0 & 0 & C_{55} & 0 \\ 0 & 0 & 0 & 0 & 0 & C_{66} \end{bmatrix} \begin{Bmatrix} \varepsilon_{11} \\ \varepsilon_{22} \\ \varepsilon_{33} \\ \gamma_{23} \\ \gamma_{13} \\ \gamma_{12} \end{Bmatrix} \tag{3.50}$$

where

$$
\begin{aligned}
C_{11} &= (1-\nu_{23}\nu_{32})E_1/\Delta \\
C_{22} &= (1-\nu_{13}\nu_{31})E_2/\Delta \\
C_{33} &= (1-\nu_{12}\nu_{21})E_3/\Delta \\
C_{12} &= (\nu_{21}+\nu_{31}\nu_{23})E_1/\Delta \\
&= (\nu_{12}+\nu_{32}\nu_{13})E_2/\Delta \\
C_{13} &= (\nu_{31}+\nu_{21}\nu_{32})E_1/\Delta \\
&= (\nu_{13}+\nu_{12}\nu_{23})E_3/\Delta \\
C_{23} &= (\nu_{32}+\nu_{12}\nu_{31})E_2/\Delta \\
&= (\nu_{23}+\nu_{21}\nu_{13})E_3/\Delta \\
C_{44} &= G_{23} \\
C_{55} &= G_{13} \\
C_{66} &= G_{12}
\end{aligned}
\tag{3.51}
$$

and

$$\Delta = 1-\nu_{12}\nu_{21}-\nu_{23}\nu_{32}-\nu_{31}\nu_{13}-2\nu_{21}\nu_{32}\nu_{13} \tag{3.52}$$

The terms of Eqs (3.51) and (3.52) are not all independent. The relationship between these terms are given by:

$$\frac{\nu_{ij}}{E_i} = \frac{\nu_{ji}}{E_j}, \qquad i,j = 1,2,3 \tag{3.53}$$

As a further simplification, if the material properties are the same in the 2-direction as in the 3-direction, shown in Figure 3.3, then the material is transversely isotropic [36]. For this type of material there is no distinction between properties in the 2- and 3-directions, thus, $E_2 = E_3$, $\nu_{21} = \nu_{31}$, $\nu_{12} = \nu_{13}$, and $\nu_{23} = \nu_{32}$. With this assumption, Eqs (3.51) and

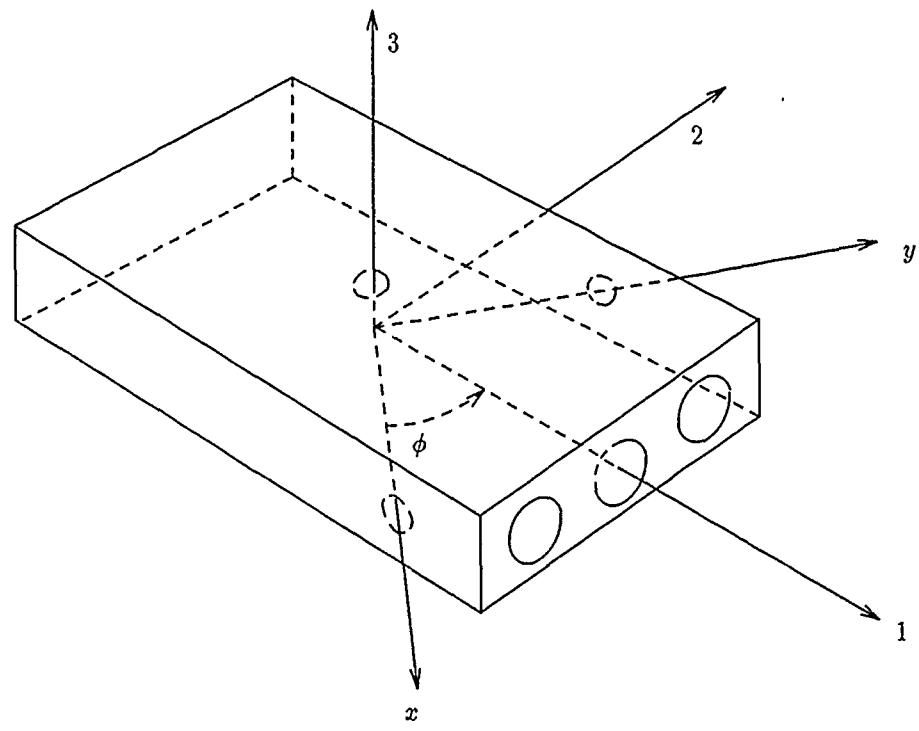

[2:20]

Figure 3.3. Material Axes for a Transversely Isotropic Lamina

(3.52) become:

$$\begin{aligned} C_{11} &= (1-\nu_{23}^2)E_1/\Delta^* \\ C_{22} &= C_{33} = (1-\nu_{12}\nu_{21})E_2/\Delta^* \\ C_{12} &= C_{13} = \nu_{11}(1+\nu_{23})E_1/\Delta^* \\ C_{23} &= (\nu_{23}+\nu_{12}\nu_{21})E_2/\Delta^* \\ C_{44} &= G_{23} \\ C_{55} &= G_{13} \\ C_{66} &= G_{12} \end{aligned} \tag{3.54}$$

where

$$\Delta^* = 1 - 2\nu_{12}\nu_{21} - \nu_{23}^2 - 2\nu_{12}\nu_{21}\nu_{23} \tag{3.55}$$

and the relationships of Eq (3.53) apply.

For a thin flat structural member, such as a plate, a state of plane stress is often assumed [16] where $\sigma_{13} = \sigma_{23} = \sigma_{33} = 0$. In this research, however, the effects of transverse shear deformation are to be considered. Thus, σ_{13} and σ_{23} are not assumed to be zero. The direct normal stress σ_{33}, however, is still assumed to be zero. This assumption is necessary to reduce the three-dimensional problem to a two-dimensional problem. If $\sigma_{33} = 0$ is substituted into Eq (3.50), the direct transverse normal strain can be found as:

$$\epsilon_{33} = -\frac{C_{13}}{C_{33}}\varepsilon_{11} - \frac{C_{23}}{C_{33}}\varepsilon_{22} \tag{3.56}$$

Thus, rewriting Eq (3.50) using Eq (3.56) to eliminate ε_{33} gives:

$$\begin{Bmatrix} \sigma_{11} \\ \sigma_{22} \\ \tau_{23} \\ \tau_{13} \\ \tau_{12} \end{Bmatrix} = \begin{bmatrix} Q_{11} & Q_{12} & 0 & 0 & 0 \\ Q_{12} & Q_{22} & 0 & 0 & 0 \\ 0 & 0 & Q_{44} & 0 & 0 \\ 0 & 0 & 0 & Q_{55} & 0 \\ 0 & 0 & 0 & 0 & Q_{55} \end{bmatrix} \begin{Bmatrix} \varepsilon_{11} \\ \varepsilon_{22} \\ \gamma_{23} \\ \gamma_{13} \\ \gamma_{12} \end{Bmatrix} \tag{3.57}$$

where

$$\begin{aligned} Q_{11} &= C_{11} - C_{13}^2/C_{33} = E_1/(1 - \nu_{12}\nu_{21}) \\ Q_{22} &= C_{22} - C_{23}^2/C_{33} = E_2/(1 - \nu_{12}\nu_{21}) \\ Q_{12} &= C_{12} - C_{13}C_{23}/C_{33} = \nu_{21}E_2/(1 - \nu_{12}\nu_{21}) \\ Q_{44} &= G_{23} \\ Q_{55} &= G_{12} \end{aligned} \tag{3.58}$$

To form a structural component, the lamina are assumed to be perfectly bonded together with their fibers oriented at a particular angle with respect to the structure's reference axis. The stiffness contribution of each lamina in the laminate can be determined. These stiffnesses must first be transformed to a common reference system of axes. If one assumes the kth lamina's fibers are all in the same direction (say, the 1-direction of Figure 3.3), and this direction is at an angle ϕ from the reference axis (say, the x axis)

then the constitutive relations in the reference system are given by:

$$\begin{Bmatrix} \sigma_x \\ \sigma_y \\ \tau_{yz} \\ \tau_{xz} \\ \tau_{xy} \end{Bmatrix}_k = \begin{bmatrix} \overline{Q}_{11} & \overline{Q}_{12} & 0 & 0 & \overline{Q}_{16} \\ \overline{Q}_{12} & \overline{Q}_{22} & 0 & 0 & \overline{Q}_{26} \\ 0 & 0 & \overline{Q}_{44} & \overline{Q}_{45} & 0 \\ 0 & 0 & \overline{Q}_{45} & \overline{Q}_{55} & 0 \\ \overline{Q}_{16} & \overline{Q}_{26} & 0 & 0 & \overline{Q}_{66} \end{bmatrix}_k \begin{Bmatrix} \varepsilon_x \\ \varepsilon_y \\ \gamma_{yz} \\ \gamma_{xz} \\ \gamma_{xy} \end{Bmatrix}_k \tag{3.59}$$

where

$$\begin{aligned}
\overline{Q}_{11} &= Q_{11}\cos^4\phi + 2(Q_{12}+2Q_{66})\sin^2\phi\cos^2\phi + Q_{22}\sin^4\phi \\
\overline{Q}_{12} &= (Q_{11}+Q_{22}-4Q_{66})\sin^2\phi\cos^2\phi + Q_{12}(\sin^4\phi+\cos^4\phi) \\
\overline{Q}_{22} &= Q_{11}\sin^4\phi + 2(Q_{12}+2Q_{66})\cos^2\phi\sin^2\phi + Q_{22}\cos^4\phi \\
\overline{Q}_{16} &= (Q_{11}-Q_{12}-2Q_{66})\sin\phi\cos^3\phi + (Q_{12}-Q_{22}+2Q_{66})\sin^3\phi\cos\phi \\
\overline{Q}_{26} &= (Q_{11}-Q_{12}-2Q_{66})\sin^3\phi\cos\phi + (Q_{12}-Q_{22}+2Q_{66})\sin\phi\cos^3\phi \\
\overline{Q}_{66} &= (Q_{11}+Q_{22}-2Q_{66})\sin^2\phi\cos^2\phi + Q_{66}(\sin^4\phi+\cos^4\phi) \\
\overline{Q}_{44} &= Q_{44}\cos^2\phi + Q_{55}\sin^2\phi \\
\overline{Q}_{45} &= (Q_{44}-Q_{55})\cos\phi\sin\phi \\
\overline{Q}_{55} &= Q_{44}\sin^2\phi + Q_{55}\cos^2\phi
\end{aligned} \tag{3.60}$$

In Eq (3.59) and (3.60), each lamina has a specific orientation of fibers. Thus, each lamina can have different values of Q_{ij} given by Eq (3.58). These constitutive relations are valid for small strains where the material behaves as a linear elastic solid. Equation (3.56) relates the direct normal strain ϵ_{33} to changes in the direct in-plane strains ϵ_{11} and ϵ_{22} for $\sigma_{33} = 0$. The assumption that Eq (3.56) is valid for an arbitrary laminated composite shell is important for composite shell analysis. Without this assumption, the stress state is fully three-dimensional and the reduced computational effort of the two-dimensional model is lost. With the assumption, however, the two-dimensional model will never accurately predict the stress distribution within the shell, since σ_{33} generally will not be zero in the real structure. Research in the 1960's and 1970's, by many investigators, has validated the

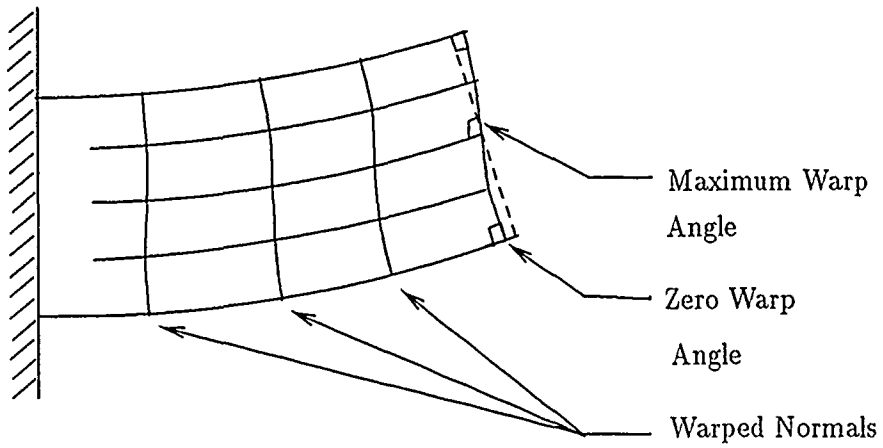

[72:234]

Figure 3.4. Shear Deformation of a Thin Elastic Body

acceptability of this assumption for certain problems.

3.4 Transverse Shear Deformation Theory

When a thin body undergoes a small (infinitesimal) deformation, material points on a line normal to the middle surface of the body will move relative to each other, as shown in Figure 3.4. This movement results in rotation and warping of the normal. The angle between the geometric normal to the midsurface and the warped normal is maximum at the midsurface and zero at the the upper and lower surface. For a linear elastic material undergoing infinitesimal displacement (i. e. , linear strain displacement relations hold), this angle of deviation is equal to the transverse shear strain. The distribution of transverse shear strain for the infinitesimal linear case is parabolic through the thickness of a flat plate. Under the classical Kirchhoff assumption, one assumes the normal (or cross-section of a beam) remains normal, straight, and inextensible. This assumption results in zero transverse shear strain. For thin shells, where $h/R \ll 1$, the Kirchhoff assumption allows accurate predictions of transverse deflection versus load for small displacements. For thick shells, where $h^2/R^2 \ll 1$, or when anisotropic material properties are assumed, transverse shear effects become more apparent. Thick shells and composite shells generally will show greater transverse deflection for a given load when the effect of transverse shear is included

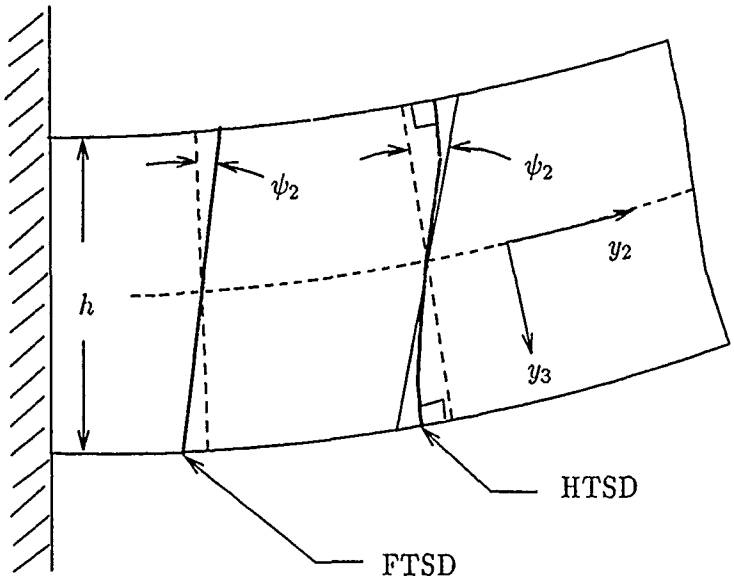

Figure 3.5. Deformation of Normals for FTSD and HTSD Theories

in the theoretical model.

3.4.1 First-Order Transverse Shear Deformation (FTSD) Theories. There are several ways to include transverse shear deformation. Transverse shear effects can be included using a first-order transverse shear deformation (FTSD) theory. In this case, material lines originally normal to the midsurface are allowed to deviate from the normal to the shell midsurface as shown in Figure 3.4.1. These lines remain straight and inextensible. Since the angle of deviation is constant, the displacement field varies linearly. The constant angle also implies transverse shear strain is constant, and thus, is not zero at the upper and lower surfaces of the shell. This inconsistent distribution results in an overly stiff model of the structure. This stiffening effect, called shear locking, becomes more pronounced as the shell thickness approaches zero. First-order transverse shear theories can be used, provided some artificial corrections are made. The excessive strain energy resulting from the constant shear strain assumption is usually reduced by multiplying the transverse strains by a constant factor of 5/6 for isotopic materials. Although 5/6 is often used for composite materials, there is no generally accepted method of determining shear correction factors for anisotropic materials. The predicted response of the FTSD model is sensitive to the

values of shear correction factors. Hence, some have suggested that theories of composite shells should not depend upon any numerical factors [5:698].

The derivation of transverse shear deformation theories is, generally, based on writing the displacement vector $\vec{U}$, of Eq (3.31), as a function of the thickness coordinate of the shell. According to Reddy [80], this approach was pioneered in 1890 by A. B. Bassett. According to literature cited by Dennis [18], Bassett expanded the displacement components u_i in an infinite power series as shown below:

$$u_i(y_1, y_2, y_3) = u_i(y_1, y_2, 0) + y_3 \frac{\partial u_i}{\partial y_3}\bigg|_{y_3=0} + y_3^2 \frac{\partial^2 u_i}{\partial y_3^2}\bigg|_{y_3=0} + \cdots \tag{3.61}$$

This displacement field, when substituted into Eqs (3.38) and (3.39), will give nonzero transverse shear strains γ_{13} and γ_{23}. Also, the u_3 component is a function of the thickness coordinate y_3. This will result in a nonzero σ_{33}.

Hildebrand, Reissner, and Thomas [26] examined the importance of the terms leading to the transverse strains for orthotropic shells. They truncated the expressions of Eq (3.61) for u_1 and u_2 at the second order terms. They also assumed, for the case of $\sigma_{33} \approx 0$ with ε_{33} given by Eq (3.56), that u_3 could be determined by intergrating Eq (3.56) though the thickness of the shell. Their investigations showed that the resulting linear and quadratic y_3 terms present in u_3 could be neglected. Thus, the displacement field of Hildebrand et al. has a u_3 displacement function that does not vary through the thickness of the shell. Theories based upon the assumptions of Hildebrand et al. are called first-order shear deformation theories. These types of theories were extensively studied by Reissner and Mindlin in the 1940's and 1950's [82, 49] for plates, and hence, are often called Reissner-Mindlin theories. For a shell, the FTSD theory is given by the following displacement field:

$$\begin{aligned} u_1 &= u(1 - y_3/R_1) + \psi_1 y_3 \\ u_2 &= v(1 - y_3/R_2) + \psi_2 y_3 \\ u_3 &= w \end{aligned} \tag{3.62}$$

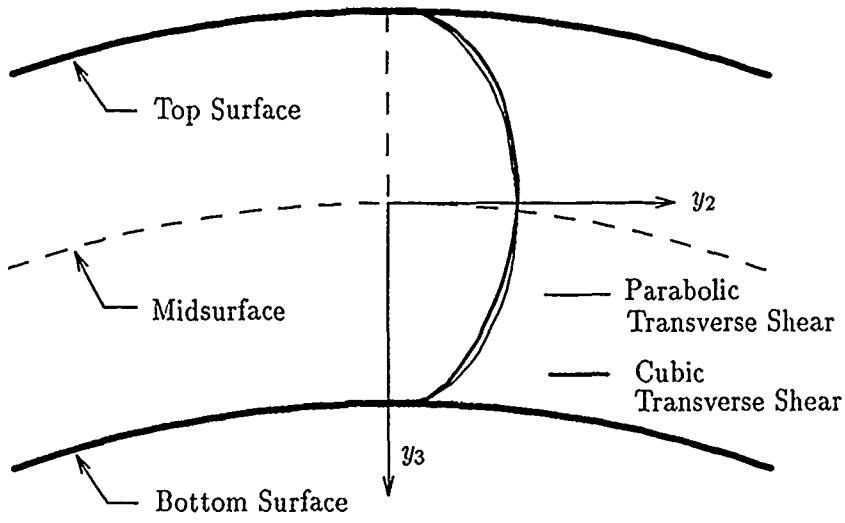

Figure 3.6. Parabolic and Cubic Transverse Shear Distributions for a Curved Shell

where the five degrees of freedom (dof), u, v, w, ψ_1 and ψ_2, are functions of the in-plane curvilinear coordinates y_1 and y_2.

3.4.2 Higher-Order Transverse Shear Deformation (HTSD) Theories. Higher-order transverse shear deformation (HTSD) theories generally eliminate the need for shear correction factors. The HTSD theory allows the normal to rotate and warp as shown in Figure 3.4.1. Some HTSD theories also allow the normal to change length. The HTSD theory for a flat plate produces a parabolic distribution of shear strain as shown in Figure 3.4.2. This distribution matches the exact distribution of shear strain for the linear infinitesimal case. The results for curved shells, however, are different because of the curvature of the shell. Due to curvature of the shell, the transverse shear strain is distorted as shown in Figure 3.4.2 by the heavier line labeled cubic transverse shear. Since the small-strain transverse shear distribution for a shell is a cubic function of the thickness coordinate, the displacement field should be at least quartic in the thickness coordinate. For a shell, the curvature generally creates coupling between in-plane extension and bending activity. To include this effect, one needs to include quartic terms in the displacement field or include nonlinear strain displacement terms. Assuming a general quartic displacement field, as

given in Eq (3.63), the derivation of a quasi-nonlinear HTSD theory for a shell follows:

$$\begin{aligned} u_1(y_1,y_2,y_3) &= u(1-y_3/R_1)+\psi_1 y_3+\phi_1 y_3^2+\gamma_1 y_3^3+\theta_1 y_3^4 \\ u_2(y_1,y_2,y_3) &= v(1-y_3/R_2)+\psi_2 y_3+\phi_2 y_3^2+\gamma_2 y_3^3+\theta_2 y_3^4 \\ u_3(y_1,y_2,y_3) &= w(y_1,y_2) \end{aligned} \tag{3.63}$$

where $u = u(y_1,y_2)$, $v = v(y_1,y_2)$, $w = w(y_1,y_2)$, $\psi_\alpha = \psi_\alpha(y_1,y_2)$, $\phi_\alpha = \phi_\alpha(y_1,y_2)$, $\gamma_\alpha = \gamma_\alpha(y_1,y_2)$, and $\theta_\alpha = \theta_\alpha(y_1,y_2)$ are degrees of freedom defined only at the midsurface of the shell. These degrees of freedom are functions of the in-plane coordinates y_1 and y_2 and will vary from point to point on the shell's midsurface. For the shell with $h_1 = (1-y_3/R_1)$, $h_2 = (1-y_3/R_2)$, and $h_3 = 1$ and the displacement field of Eq (3.63), the linear transverse shear strains (given by the first line of Eqs (3.38) and (3.39) are as follows:

$$\gamma_{13} = \frac{1}{(1-y_3/R_1)}\left[\frac{\partial u_3}{\partial y_1}+(1-y_3/R_1)\frac{\partial u_1}{\partial y_3}-u_1\frac{\partial(1-y_3/R_1)}{\partial y_3}\right] \tag{3.64}$$

$$\gamma_{23} = \frac{1}{(1-y_3/R_2)}\left[\frac{\partial u_3}{\partial y_2}+(1-y_3/R_2)\frac{\partial u_2}{\partial y_3}-u_2\frac{\partial(1-y_3/R_1)}{\partial y_3}\right] \tag{3.65}$$

Substituting Eq (3.63) into Eq (3.65) gives:

$$\begin{aligned} \gamma_{23} = \frac{1}{(1-y_3/R_2)}\Bigg[&\frac{\partial w}{\partial y_2}+\psi_2-2\phi_2 y_3+\left(\frac{\phi_2}{R_2}-3\gamma_2\right)y_3^2 \\ &+\left(\frac{2\gamma_2}{R_2}-4\theta_2\right)y_3^3+\frac{3\theta_2}{R_2}y_3^4\Bigg] \end{aligned} \tag{3.66}$$

For this equation to be zero at $y_3 = \pm h/2$ and yield a parabolic distribution of γ_{23}, the coefficients of odd powers of y_3 must cancel each other or be equal to zero. If one assumes $\phi_2 = 0$ and $\theta_2 = \gamma_2/R_2$, these coefficients vanish and γ_{23} is given by:

$$\gamma_{23} = \frac{1}{(1-y_3/R_2)}\left[\frac{\partial w}{\partial y_2}+\psi_2-3\gamma_2 y_3^2+\frac{3\gamma_2}{2R_2^2}y_3^4\right] \tag{3.67}$$

Evaluating Eq (3.67) at $y_3 = h/2$ and solving for γ_2 gives:

$$-\frac{3h^2}{4}\left(1-\frac{h^2}{8R_2^2}\right)\gamma_2 = \left(\frac{\partial w}{\partial y_2}+\psi_2\right) \tag{3.68}$$

For a shell with radius R_2 no smaller than five times the thickness h, the term $h^2/8R_2^2$ in Eq (3.68) is less than or equal to 1/400. If one ignores this term, then γ_2 is given by:

$$\gamma_2 = -\frac{4}{3h^2}\left(\frac{\partial w}{\partial y_2} + \psi_2\right) \tag{3.69}$$

Similarly, γ_1 can be found. If one substitutes Eq (3.69) and $\phi_2 = \theta_2 = 0$ amd similar relations for ϕ_1, γ_1, and θ_1 into Eq (3.63), the final form of the displacement field of a third-order quasi-nonlinear transverse shear deformation theory is obtained:

$$\begin{aligned} u_1(y_1, y_2, y_3) &= u\left(1 - \tfrac{y_3}{R_1}\right) + \psi_1 y_3 - \tfrac{4}{3h^2}\left(\tfrac{\partial w}{\partial y_1} + \psi_1\right) y_3^3 \\ u_2(y_1, y_2, y_3) &= v\left(1 - \tfrac{y_3}{R_2}\right) + \psi_2 y_3 - \tfrac{4}{3h^2}\left(\tfrac{\partial w}{\partial y_2} + \psi_2\right) y_3^3 \\ u_3(y_1, y_2, y_3) &= w \end{aligned} \tag{3.70}$$

This third-order displacement field has two additional degrees of freedom not present in the first-order theory. These two degrees of freedom are the differentials of transverse displacement w. The third-order theory, thus, allows the slopes of the elastic curve, $w_{,i}$, to be different from the bending angles, ψ_i. These differences are directly related to the transverse shear strains of the structure.

The third-order transverse shear theory can be generalized to represent all third-order theories of flat plates, including classical laminate theory or first-order shear theories [78] by assuming displacements of the form:

$$\begin{aligned} u_1 &= u + y_3\left(-\alpha\tfrac{\partial w_b}{\partial y_1} + \beta\psi_1\right) + \lambda y_3^2\left(\tfrac{\partial \psi_3}{\partial y_1}\right) + \tfrac{1}{3}y_3^3\left[-\beta\tfrac{4}{h^2}\left(\psi_1 + \tfrac{\partial w_s}{\partial y_1}\right) - \gamma\tfrac{\partial \phi_3}{\partial y_1}\right] \\ u_2 &= v + y_3\left(-\alpha\tfrac{\partial w_b}{\partial y_2} + \beta\psi_2\right) + \lambda y_3^2\left(\tfrac{\partial \psi_3}{\partial y_2}\right) + \tfrac{1}{3}y_3^3\left[-\beta\tfrac{4}{h^2}\left(\psi_2 + \tfrac{\partial w_s}{\partial y_2}\right) - \gamma\tfrac{\partial \phi_3}{\partial y_2}\right] \\ u_3 &= \alpha w_b + \beta w_s + \lambda y_3\psi_3 + \gamma y_3^2\phi_3 \end{aligned} \tag{3.71}$$

Here u, v are midsurface displacement functions in the y_1 and y_2 directions, respectively. The functions w_b and w_s are the transverse displacements due to bending and shear in the y_3 direction. The ψ_1 and ψ_2 are rotations of the transverse normal about the y_1- and y_2-axes, respectively. The choice of different values for α, β, and λ will lead to various theories. Classical shell theory is given by $\alpha = 1$, $\beta = 0$, and $\lambda = 0$. In this case, the

displacements are linearly dependent upon the slope of the midsurface and lines normal to the midsurface remain normal. Hence, there is no transverse shear deformation. The first-order quasi-nonlinear transverse shear theory is given by $\alpha = 0$, $\beta = 1$, and $\lambda = 0$. Thus, the displacement is a function only of the midsurface displacements (u, v, w) and the rotations (ψ_1, ψ_2) of the transverse normals. Since the displacements u_1 and u_2 vary linearly with changes in y_3, the effective transverse shear strain is constant through the thickness. The third-order quasi-nonlinear transverse shear theory is given by $\alpha = 0, \beta = 1$, and $\lambda = 1$. In this case, the displacement is a function of the midsurface displacements (u, v, w), the rotations (ψ_1, ψ_2) of the transverse normals, and the γ_1 and γ_2 of Eq (3.69). The γ_1 and γ_2 of Eq (3.69) are approximately equal to the transverse shear strain. Thus, the ψ_i represent rotations of the normal caused by bending activity and the γ_i represent rotations of the normal caused by transverse shear activity.

IV. Theoretical Development

The third-order quasi-nonlinear transverse shear deformation theory for a shell is suitable for many problems of practical interest. Two approximations of this theory, however, require further examination to assess their effects upon the accuracy of this theory for certain problems. Specific problems of interest are ones in which rotations and curvature within the element become very large. The first approximation, in question, is the neglect of some higher-order terms in the thickness-expansions of displacement and shell shape factors. The third-order displacement field of the quasi-nonlinear HTSD theory, as applied to flat plates, assures the linear terms of the transverse shear strain components have a parabolic distribution through the thickness and are zero at the top and bottom of the plate. The third-order kinematics of the quasi-nonlinear HTSD theory do not give zero linear transverse shear strain at the upper and lower surface of a shell—unless the shell is *flat* or some small terms of the transverse shear strain are ignored. The curvature of the shell is important, because the shell shape factors distort the distribution of strain through the thickness of the shell. Thus, the order of approximation of the shell shape factors affects the accuracy of the strain distributions. The second approximation, in question, is the neglect of nonlinear transverse shear strain terms. The quasi-nonlinear HTSD theory of Reference [18] ignores all nonlinear terms of both ε_{23} and ε_{13}. This linear restriction is not necessary physically, but satisfying the zero strain boundary conditions of the full nonlinear expressions is not a trivial problem.

According to Dennis [18] and Librescu [45, 46], the assumptions of quasi-nonlinear HTSD theories are accurate for problems where the in-plane strains and stresses are larger than the transverse quantities; these judgements are based upon Koiter's work [40] and the ratio of h/R. Dennis evaluated problems with various ratios of h/R, and concluded the quasi-nonlinear HTSD was acceptable provided h/R was less than 1/5. Some problems investigated using the quasi-nonlinear HTSD theory, however, would seem to have exhibited large stresses and strains despite small values of h/R. For example, a graphite-epoxy (AS4-350) cylindrical shell panel with clamped lateral edges and transverse point load was analyzed by Tsai et al. [103]. This shell had a 12-inch radius and was 0.04-inches thick, therefore, h/R was equal to 1/300. Transverse displacements for this problem exceeded 65

times the panel thickness (2.5–inch displacement). A deep circular arch problem Dennis investigated had transverse displacements of over 30 times the thickness[18:257–265]. The effects of ignoring nonlinear transverse shear terms and higher-order thickness expansion terms were not determined during these studies.

4.1 Higher-Order Thickness Expansions

The kinematics of Eq (3.70) can be corrected to yield exactly zero at the top and bottom surface of a curved shell by adding two correction factors to the last term as shown below:

$$\begin{aligned} u_1(y_1,y_2,y_3) &= u\left(1-\frac{y_3}{R_1}\right)+\psi_1 y_3+\left(\psi_1+\frac{\partial w}{\partial y_1}\right)\left[\underline{-\frac{y_3^2}{R_1}}+ky_3^3\underline{-\frac{k}{R_1}y_3^4}\right] \\ u_2(y_1,y_2,y_3) &= v\left(1-\frac{y_3}{R_2}\right)+\psi_2 y_3+\left(\psi_2+\frac{\partial w}{\partial y_2}\right)\left[\underline{-\frac{y_3^2}{R_2}}+ky_3^3\underline{-\frac{k}{R_2}y_3^4}\right] \\ u_3(y_1,y_2,y_3) &= w \end{aligned} \tag{4.1}$$

where $k=-4/(3h^2)$ and the underlined terms are the correction terms added to Eq (3.70). These kinematics will give zero linear transverse shear strains at the upper and lower surface of a curved shell where $y_3 \pm h/2$. The additional terms of Eq (4.1) also vanish for a flat plate, since each is divided by radius of curvature. Likewise, for a right circular cylinder with radius R_2 the first equation of Eq (4.1) reduces to the corresponding flat plate expression, since R_1 is equal to infinity. The comparison of results based upon the incomplete cubic kinematics of Eq (3.70) and results based upon the complete quartic kinematics of Eq(4.1) is a major aspect of this research. As stated earlier, the cubic displacement field of Eq (3.70) is the same as used by other authors [80, 18]. The complete quartic, however, is a unique displacement field not derivable from those of reference [80]. This quartic displacement field, thus, represents an exact solution for the linear traction free boundary conditions of a quasi-nonlinear HTSD theory for shells. Thus, satisfying the linear boundary condition for traction free surfaces involves four more terms in the displacement field.

4.2 Nonlinear Transverse Shear Deformation

The nonlinear transverse shear boundary conditions are not as easily solved as the linear versions of these conditions. If one substitutes the kinematics of Eq (3.63) into Eqs (3.38) and (3.39), the results are the two coupled nonlinear partial differential equations shown below:

$$
\begin{aligned}
\varepsilon_{23} \;=\; & (\psi_2 + w_{,2} - cuu_{,2} + c^2uw + u_{,2}\psi_1 + u_{,2}\psi_2 - cw\psi_2) \\
& + (cv + 2\phi_2 + cw_{,2} + c\psi_2 + 2\phi_1 u_{,2} + 2\phi_2 u_{,2} - 2\phi_2 cw \\
& + c^3uw + cu_{,2}\psi_1 + \psi_{1,2}\psi_1 - cu\psi_{2,2} - c^2w\psi_2 + \psi_{2,2}\psi_2)\, y_3 \\
& + (c^2v + 3\gamma_2 + \phi_2 c - c^3u + c^2\psi_2 + 3\gamma_1 u_{,2} + 3\gamma_2 u_{,2} + 2\phi_1 cu_{,2} + c^3uu_{,2} \\
& - 3\gamma_2 cw - 2\phi_2 c^2 w - cu\phi_{2,2} + 2\phi_1\psi_{1,2} + \phi_{1,2}\psi_1 + c\psi_{1,2}\psi_1 \\
& + 2\phi_2\psi_{2,2} - c^2u\psi_{2,2} - c^2u_{,2}\psi_2 + \phi_{2,2}\psi_2 + c\psi_{2,2}\psi_2)\, y_3^2 \\
& + (4\theta_2 + \gamma_2 c + \phi_2 c^2 + 4\theta_1 u_{,2} + 4\theta_2 u_{,2} + 3\gamma_1 cu_{,2} \\
& - 2\phi_2 c^2 u_{,2} - 4\theta_2 cw - 3\gamma_2 c^2 w - cu\gamma_{2,2} \\
& + 2\phi_1\phi_{1,2} + 2\phi_2\phi_{2,2} - c^2u\phi_{2,2} + 3\gamma_1\psi_{1,2} + 2\phi_1 c\psi_{1,2} + \gamma_{1,2}\psi_1 \\
& + c\phi_{1,2}\psi_1 + 3\gamma_2\psi_{2,2} + 2\phi_2 c\psi_{2,2} + \gamma_{2,2}\psi_2 + c\phi_{2,2}\psi_2)\, y_3^3 \\
& + (\theta_2 c + \gamma_2 c^2 + 4\theta_1 cu_{,2} - 3\gamma_2 c^2 u_{,2} - 4\theta_2 c^2 w + 2\phi_1\gamma_{1,2} \\
& + 2\phi_2\gamma_{2,2} - c^2u\gamma_{2,2} + 3\gamma_1\phi_{1,2} + 2\phi_1 c\phi_{1,2} + 3\gamma_2\phi_{2,2} \\
& + 2\phi_2 c\phi_{2,2} + 4\theta_1\psi_{1,2} + 3\gamma_1 c\psi_{1,2} + c\gamma_{1,2}\psi_1 + 4\theta_2\psi_{2,2} \\
& + 3\gamma_2 c\psi_{2,2} + c\gamma_{2,2}\psi_2 + \psi_1\theta_{1,2} - cu\theta_{2,2} + \psi_2\theta_{2,2})\, y_3^4 \\
& + (\theta_2 c^2 - 4\theta_2 c^2 u_{,2} + 3\gamma_1\gamma_{1,2} + 2\phi_1 c\gamma_{1,2} + 3\gamma_2\gamma_{2,2} \\
& + 2\phi_2 c\gamma_{2,2} + 4\theta_1\phi_{1,2} + 3\gamma_1 c\phi_{1,2} + 4\theta_2\phi_{2,2} + 3\gamma_2 c\phi_{2,2} + 4\theta_1 c\psi_{1,2} \\
& + 4\theta_2 c\psi_{2,2} + 2\phi_1\theta_{1,2} + c\psi_1\theta_{1,2} + 2\phi_2\theta_{2,2} - c^2u\theta_{2,2} + c\psi_2\theta_{2,2})\, y_3^5 \\
& + (4\theta_1\gamma_{1,2} + 3\gamma_1 c\gamma_{1,2} + 4\theta_2\gamma_{2,2} + 3\gamma_2 c\gamma_{2,2} + 4\theta_1 c\phi_{1,2} \\
& + 4\theta_2 c\phi_{2,2} + 3\gamma_1\theta_{1,2} + 2\phi_1 c\theta_{1,2} + 3\gamma_2\theta_{2.2} + 2\phi_2 c\theta_{2,2})\, y_3^6 \\
& + (4\theta_1 c\gamma_{1,2} + 4\theta_2 c\gamma_{2,2} + 4\theta_1\theta_{1,2} + 3\gamma_1 c\theta_{1,2} \\
& + 4\theta_2\theta_{2,2} + 3\gamma_2 c\theta_{2,2} + 4\theta_1 c\theta_{1,2} + 4\theta_2 c\theta_{2,2})\, y_3^7
\end{aligned}
\tag{4.2}
$$

$$
\begin{aligned}
\varepsilon_{13} \;=\; & (\psi_1 + w_{,1} - cvv_{,1} + u_{,1}\psi_1 + v_{,1}\psi_2) \\
& + (2\phi_1 + 2\phi_1 u_{,1} + 2\phi_2 u_{,1} + c^2 uu_{,1} + \psi_{1,1}\psi_1 - cu\psi_{2,1} \\
& - cu_{,1}\psi_2 + \psi_{2,1}\psi_2)\, y_3 \\
& + (3\gamma_1 + 3\gamma_1 u_{,1} + 3\gamma_2 u_{,1} - 2\phi_2 cu_{,1} - cu\phi_{2,1} + 2\phi_1\psi_{1,1} \\
& + \phi_{1,1}\psi_1 + 2\phi_2\psi_{2,1} + \phi_{2,1}\psi_2)\, y_3^2 \\
& + (4\theta_1 + 4\theta_1 u_{,1} + 4\theta_2 u_{,1} - 3\gamma_2 cu_{,1} - cu\gamma_{2,1} + 2\phi_1\phi_{1,1} + 2\phi_2\phi_{2,1} \\
& + 3\gamma_1\psi_{1,1} + \gamma_{1,1}\psi_1 + 3\gamma_2\psi_{2,1} + \gamma_{2,1}\psi_2)\, y_3^3 \\
& - (4\theta_2 cu_{,1} + 2\phi_1\gamma_{1,1} + 2\phi_2\gamma_{2,1} + 3\gamma_1\phi_{1,1} + 3\gamma_2\phi_{2,1} + 4\theta_1\psi_{1,1} \\
& + 4\theta_2\psi_{2,1} + \psi_1\theta_{1,1} - cu\theta_{2,1} + \psi_2\theta_{2,1})\, y_3^4 \\
& + (3\gamma_1\gamma_{1,1} + 3\gamma_2\gamma_{2,1} + 4\theta_1\phi_{1,1} + 4\theta_2\phi_{2,1} + 2\phi_1\theta_{1,1} + 2\phi_2\theta_{2,1})\, y_3^5 \\
& + (4\theta_1\gamma_{1,1} + 4\theta_2\gamma_{2,1} + 3\gamma_1\theta_{1,1} + 3\gamma_2\theta_{2,1})\, y_3^6 \\
& + (4\theta_1\theta_{1,1} + 4\theta_2\theta_{2,1})\, y_3^7
\end{aligned}
\tag{4.3}
$$

Recall ϕ_i, γ_i, and θ_i were undetermined functions of the in-plane coordinates defined only on the midsurface of the shell. In order to solve these two equations for all of the unknown functions (there are six unknowns), one must evaluate these two equations at $y_3 = \pm h/2$ and set each resulting equation equal to zero. This is required to satisfy the zero traction boundary condition on the surfaces of the shell. Although other authors have proposed the inclusion of nonlinear transverse shear and the use of linear kinematics [92, 97, 65, 66], none have done so within a HTSD theory.

Since no simple functions exist for ϕ_i, γ_i, and θ_i that are linear in terms of u, v, w and ψ_i, several options are available. One could choose to ignore the natural boundary conditions and use shear correction factors as done with the FTSD theory. Sing, Rao, and Iyengar [97] choose this approach. One could also simply ignore all nonlinear transverse shear strain terms. Palmerio and Reddy [65, 66], although intending to include nonlinear transverse shear, ultimately choose this approach for their quasi-nonlinear FTSD theory. These are the only two references, the author has located, which refer to nonlinear transverse shear terms in a FTSD or HTSD theory for shells. It should be noted that some thin shell theories include nonlinear transverse shear stress resultants. These, however, are not a result of explicit nonlinear transverse shear strain terms, but result from integration of the equilibrium equations with nonlinear in-plane stresses [46]. Thus, these nonlinear the-

ories are not suitable for thick or anisotropic shells where variation of parameters through the shell's thickness are important.

4.3 The Nonlinear Higher-Order Transverse Shear Deformation Theory

Some preliminary judgements of the relative importance of higher-order terms can be gained by examining the terms of ε_{23}. If one uses the third-order kinematic assumptions to compute strains for a shell with radius $R = 5h$, then the linear part of the γ_{23} component (first line of Eq (3.39)), when evaluated at the top ($y_3 = -h/2$) and bottom ($y_3 = +h/2$) surfaces of the shell, becomes:

$$\begin{aligned} \gamma_{23}(y_3 = -h/2) &= -\frac{1}{15}\left(\frac{\partial w}{\partial y_2} + \psi_2\right) \\ &= -0.0\overline{33}\left(\frac{\partial w}{\partial y_2} + \psi_2\right) \end{aligned} \tag{4.4}$$

$$\begin{aligned} \gamma_{23}(y_3 = +h/2) &= +\frac{1}{15}\left(\frac{\partial w}{\partial y_2} + \psi_2\right) \\ &= +0.0\overline{33}\left(\frac{\partial w}{\partial y_2} + \psi_2\right) \end{aligned} \tag{4.5}$$

When these quantities are divided by the shape factor $h_2 = 1 - y_3/R$ (evaluated at $y_3 = \pm h/2$), the ε_{23} values become:

$$\begin{aligned} \varepsilon_{23}(y_3 = -h/2) &= -\frac{10}{165}\left(\frac{\partial w}{\partial y_2} + \psi_2\right) \\ &= -0.0\overline{60}\left(\frac{\partial w}{\partial y_2} + \psi_2\right) \end{aligned} \tag{4.6}$$

$$\begin{aligned} \varepsilon_{23}(y_3 = +h/2) &= +\frac{10}{135}\left(\frac{\partial w}{\partial y_2} + \psi_2\right) \\ &= +0.0\overline{740}\left(\frac{\partial w}{\partial y_2} + \psi_2\right) \end{aligned} \tag{4.7}$$

If the term $(\partial w/\partial y_2 + \psi_2)$ is equal to 0.25, then $\varepsilon_{23}(y_3 = +h/2)$ would be equal to 0.0185 or about 2 percent strain. This magnitude of strain is significant for a small strain elastic material model where strains in excess of about 4 percent are considered too large for an elastic analysis. The use of the complete quartic kinematic assumptions of Eq (4.1) gives

exactly zero for these transverse shear strain quantities.

If nonlinear strain displacement terms are retained for the transverse shear strains, the equations for ε_{23} and ε_{13} become more involved. Using the kinematic assumptions of Eq (3.70) and evaluating Eq (3.39) with $y_3 = h/2$, $R_2 = 5h$, and $h = 1$, one has:

$$\begin{aligned}
\gamma_{23} \;=\; & \underline{0.0\overline{33}\left(\frac{\partial w}{\partial y_2} + \psi_2\right)} - 0.5\frac{\partial u}{\partial y_2}\frac{\partial w}{\partial y_1} - 0.45\frac{\partial v}{\partial y_2}\frac{\partial w}{\partial y_2} \\
& -0.1\overline{66}\left(\frac{\partial \psi_2}{\partial y_2}\frac{\partial w}{\partial y_2} + \frac{\partial \psi_1}{\partial y_2}\frac{\partial w}{\partial y_1}\right) + 0.1w\left(\frac{\partial w}{\partial y_2}\psi_2\right) \\
& +0.09v\frac{\partial v}{\partial y_2} + 0.08\overline{33}\left(\frac{\partial w}{\partial y_2}\frac{\partial^2 w}{\partial y_2^2} + \frac{\partial w}{\partial y_1}\frac{\partial^2 w}{\partial y_1 \partial y_2}\right) \\
& -0.0\overline{33}v\frac{\partial \psi_2}{\partial y_2} - 0.02vw + 0.01\overline{66}v\frac{\partial^2 w}{\partial y_2^2} \\
& +7.45 \times 10^{-9}\left(\psi_2\frac{\partial^2 w}{\partial y_2^2} + \psi_1\frac{\partial^2 w}{\partial y_1 \partial y_2} - 1.5\psi_2\frac{\partial v}{\partial y_2}\right) \qquad (4.8)
\end{aligned}$$

where the underlined terms are the linear terms of Eq (4.4). The last three terms of Eq (4.8) (those multiplied by 7.45×10^{-9}) are apparently negligible. For a cylindrical shell of radius R_2 undergoing large transverse displacement, say $[h \leq w \leq max\,(L, R_2)]$, if one assumes the shear-related term $\partial w/\partial y_2 + \psi_2$ is large, say $[0.5 \leq (\partial w/\partial y_2 + \psi_2) \leq 1.0]$, and all other quantities in Eq (4.8) are negligible, then:

$$\gamma_{23} \cong (0.0\overline{33} + 0.1w)\left(\frac{\partial w}{\partial y_2} + \psi_2\right) \qquad (4.9)$$

The types of shell problems of interest in this research will undergo large transverse displacement along with large bending rotations and shear angles. Thus, the $w\,(\partial w/\partial y_2 + \psi_2)$ term of Eq (4.9) may be of significance.

The author's approach to including nonlinear transverse shear terms in a HTSD theory includes several assumptions beyond those of the quasi-nonlinear HTSD theory. First, the author is primarily interested in problems involving large rotations and curvature changes for laminated shells. Thus, the new theory should reduce to the quasi-nonlinear HTSD theory for problems with smaller rotations or smaller curvatures. The kinematic

assumptions of Eq (4.1) reduce to those of [18] for small curvature problems, since each additional term includes the radius of curvature in the denominator. Secondly, the satisfaction of the nonlinear boundary conditions of Eqs (4.2) and (4.3) will not be achieved by the use of nonlinear kinematics. Although this seems feasible, one goal of this research was to extend the capability of HTSD theory to solve large-rotation large-curvature problems with transverse shear nonlinearity. The quasi-nonlinear HTSD of [18] is computationally quite expensive [18:278]. The incorporation of nonlinear kinematic terms and the corrective terms of Eq (3.62), therefore, seems prohibitive. There is also a practical problem associated with the ability of one researcher to numerically evaluate enough problems to determine the effects of each of these variables. Thus, the author has chosen to evaluate the kinematics of Eq (4.1) with the full nonlinear transverse shear relations of Eq (3.38) and (3.39) with an approximate approach to the nonlinear boundary conditions. This approximate approach assumes the nonlinear transverse shear strain should be zero at the upper and lower surfaces and that the strain energy of the nonlinear transverse shear strain terms is excessive. Recall the FTSD theory had excessive transverse shear strain energy which was approximately corrected by multiplying the transverse shear strain by 5/6. The author hopes to achieve similar results and also force the satisfaction of zero traction at the surface by multiplying the nonlinear transverse strain terms by a parabolic function of the thickness coordinate. Other researchers have used similar functions to provide the parabolic shear distribution of the quasi-nonlinear HTSD theory; see for example [9:300-301] and [37:1192].

Thus, the goal of this research is to evaluate the effects of two theoretical "attributes" not previously investigated for linear-elastic thick shells with large displacement, rotations, and curvatures using a higher-order transverse shear deformation theory. These two attributes are the exactness of traction-free surface boundary conditions and the inclusion of approximate nonlinear transverse shear strain terms. A third "attribute" will also be considered, and that is the exactness of the approximation of functions of the shell shape factors. These functions appear in the strain displacement relations of Eqs (3.34–3.39) as functions of the shape factors h_i and their derivatives. For a cylindrical shell, these geometric functions depend only on the thickness coordinate. For a FTSD or HTSD theory,

where displacements are expanded in terms of the thickness coordinate, these geometric functions are often expanded in terms of the thickness coordinate and arbitrarily truncated at a specific power of the thickness coordinate. Dennis [18:316–322] used Taylor's series expansions of 60 of these geometric functions that appear in the strain displacement relations for the quasi-nonlinear HTSD theory of a shell. These 60 functions are shown in Appendix A with their Taylor's series approximations. Dennis truncated these functions to the constant term for transverse shear strain components [18:65].

Although Dennis's quasi-nonlinear HTSD theory has been used for many problems [18, 22, 64, 88, 93, 100], Prathap and Naganarayana [52, 73] investigated the effect of inconsistently approximating the transverse shear strains for curved beam elements. An important aspect of their investigation was the consistency of approximation of the geometric terms involving curvature in the denominator. They found that inconsistent approximations of out-of-plane transverse shear strain resulted in force and stress oscillations which degraded convergence characteristics of numerical models. Although their geometric terms were not identical to the 60 shell geometry functions of the quasi-nonlinear HTSD theory for shells, the results of Prathap and Naganarayana suggest this "attribute" should also be considered in this research.

Thus, the full nonlinear higher-order transverse shear deformation theory of this research has been developed. This new theory incorporates, in its most complete form, a quartic displacement field, quadratic approximation of shell shape factor functions, and all nonlinear strain-displacement terms of the transverse shear strains. The surface boundary conditions of a shell are exactly satisfied for the linear case and approximately satisfied for the nonlinear case. The nonlinear boundary conditions are satisfied by forcing the transverse shear strains to zero at the upper and lower surfaces with a parabolic Other more common assumptions include the use of linear-elastic constitutive relations for laminated transversely isotropic composite material, transverse normal stress is assumed to be approximately zero, and transverse normal strain is assumed to be related to the direct strains in direction of the fiber and the direction transverse to the fiber. Several of these theoretical characteristics are shown in Tables 4.1 and 4.2 with the corresponding characteristics of the Kirchhoff-Love theory, Donnell's Theory, a typical FTSD theory and

Dennis's quasi-nonlinear HTSD Theory.

Table 4.1. Comparison of Shell Theories Without Transverse Shear Deformation

Kirchhoff-Love Theory
Shell Assumptions: Shell behavior is totally defined by the behavior of the midsurface. Shell has thickness. Assumes plane strain with $\sigma_{33} = 0$ and isotropic material.
Kinematic Assumptions: 3 primary dof: u, v, w. No variation through the thickness.
Transverse Shear Assumptions: Transverse shear strains are assumed to be zero.
Nonlinear Assumptions: None—linear strain-displacement relations typically used for all strain components.

Donnell-Mushtari-Vlasov Theory
Shell Assumptions: Shell behavior is totally defined by the behavior of the midsurface. Shell has thickness. Assumes $\sigma_{33} = 0$ and isotropic material.
Kinematic Assumptions: 3 primary dof: u, v, w. No variation through the thickness.
Transverse Shear Assumptions: Transverse shear strains are assumed to be zero.
Nonlinear Assumptions: Linear strain-displacement relations are used for transverse shear strain components. Some nonlinear strain displacement terms involving w and its derivatives are included for the in-plane strain components.

4.4 Element Independent Stiffness Formulation

The theory of the previous sections dealt with displacement fields, constitutive relations, and strain displacement relations for curved shells with a nonlinear HTSD theory. The next step required, to yield a suitable tool for the investigation of our three new "attributes", is the development and solution of the governing differential equations for shell problems. Since the author is specifically interested in the nonlinear phenomena of large displacements and rotations, no analytical or linear solutions are desired. Furthermore, to provide a suitable comparison to previously published methods, the author has chosen to develop the governing differential equations and solve these in a manner consistent with that of Dennis. In his development, Dennis used an "element independent" finite element formulation for an incremental/iterative solution based upon the principle of stationary potential energy of a linear-elastic laminated shell [18:78-95].

Table 4.2. Comparison of Shell Theories With Transverse Shear Deformation

Quasi-Nonlinear FTSD Theory
Shell Assumptions: Shell behavior is based on the behavior of the midsurface. Shell has thickness and linear variation of displacement. Assumes $\sigma_{33} = 0$ and isotropic material.
Kinematic Assumptions: 5 primary dof: u, v, w, ψ_1, ψ_2. Variation through the thickness described by $u_1 = u(1 - y_3/R1) + \psi_1 y_3$, $u_2 = v(1 - y_3/R2) + \psi_2 y_3$, and $u_3 = w$.
Transverse Shear Assumptions: Linear infinitesimal transverse shear strain varies linearly through the thickness of the shell.
Nonlinear Assumptions: Linear strain-displacement relations are used for transverse shear strain components. Some nonlinear strain displacement terms are typically used for in-plane strain components.

Dennis Quasi-Nonlinear HTSD Theory
Shell Assumptions: Shell behavior is based upon the behavior of the midsurface. Shell has thickness and incomplete cubic variation of displacements through the thickness. Assumes $\sigma_{33} = 0$ and laminated composite material.
Kinematic Assumptions: 7 primary dof: $u, v, w, \psi_1, \psi_2, w_{,1}, w_{,2}$. Variation through the thickness described by $u_1 = u(1 - y_3/R1) + \psi_1 y_3 - 4(\psi_1 + w_{,1})y_3^3/3h^2$, $u_2 = v(1 - y_3/R2) + \psi_2 y_3 - 4(\psi_2 + w_{,2})y_3^3/3h^2$, and $u_3 = w$.
Transverse Shear Assumptions: Linear infinitesimal transverse shear strain varies parabolically through the thickness of the shell.
Nonlinear Assumptions: Linear strain-displacement relations are used for transverse shear strain components. Most nonlinear strain displacement terms are included for in-plane strain components (10 higher-order terms of ε_{22} and 16 higher-order terms of ε_{12} are ignored).

Full Nonlinear HTSD Theory
Shell Assumptions: Shell behavior is based upon the behavior of the midsurface. Shell has thickness and complete quartic variation of u_1 and u_2 displacements through the thickness. Assumes $\sigma_{33} = 0$ and laminated composite material.
Kinematic Assumptions: 7 primary dof: $u, v, w, \psi_1, \psi_2, w_{,1}, w_{,2}$. Variation through the thickness described by $u_1 = u(1 - y_3/R1) + \psi_1 y_3 + (\psi_1 + w_{,1})[-1/R_1 - 4y_3/3h^2 + 4y_3^2/3h^2 R_1]y_3^2$, $u_2 = v(1 - y_3/R2) + \psi_2 y_3 + (\psi_2 + w_{,2})[-1/R_2 - 4y_3/3h^2 + 4y_3^2/3h^2 R_2]y_3^2$, and $u_3 = w$.
Transverse Shear Assumptions: Linear infinitesimal transverse shear strain distribution described by a complete quartic equation that exactly satisfies upper and lower surface zero-traction boundary conditions for a *curved* shell.
Nonlinear Assumptions: Nonlinear strain-displacement relations used for all strain components. Nonlinear transverse shear boundary conditions (zero-traction at surface) are approximated by forcing nonlinear transverse shear strain to zero at upper and lower surface using a parabolic function of thickness coordinate.

The finite element technique is a powerful numerical method capable of solving many coupled partial differential equations over a certain domain. In this research, the domain is a cylindrical shell, shown in Figure 4.1, and the equations are based upon the variation of the total potential energy Π_p of the elastic body. Specifically, the principle of stationary potential energy is used where $\delta\Pi_p = 0$. The potential energy expression is found by first examining the equilibrium state of the body. For a body of volume V with prescribed forces F^i on part of its surface S_1 and prescribed boundary conditions on the remaining part of the surface S_2, the equation of equilibrium for an infinitesimal virtual displacement $\delta\vec{u}$ is given by:

$$\int_V (\sigma^{ij}\delta\gamma_{ij} - P^k\delta u^k)dV - \int_{S_1} F^k\delta u^k dS = 0 \tag{4.10}$$

where

$\sigma^{ij} \equiv$ the components of the Second Piola Kirchhoff stress tensor (for the orthogonal coordinate system chosen, $\sigma^{ij} = \sigma_{ij}$)

$\gamma_{ij} \equiv$ the Green strain components expressed in the body's coordinate system

$P^k \equiv$ components of body forces, and

$F^k \equiv$ components of prescribed surface forces

For a conservative system, one where the forces $\vec{F}$ do not vary during virtual displacement, there exists a strain energy density function W^*, such that:

$$\sigma^{ij} = \frac{\partial W^*}{\partial \gamma_{ij}} \tag{4.11}$$

Assuming strains are small, then one can express the stress in terms of strain as:

$$\sigma^{ij} = C^{ijkl}\gamma_{ij} \tag{4.12}$$

where C^{ijkl} are constants of the elasticity tensor. Thus, the strain energy density becomes:

$$W^* = \frac{1}{2}C^{ijkl}\gamma_{ij}\gamma_{kl} \tag{4.13}$$

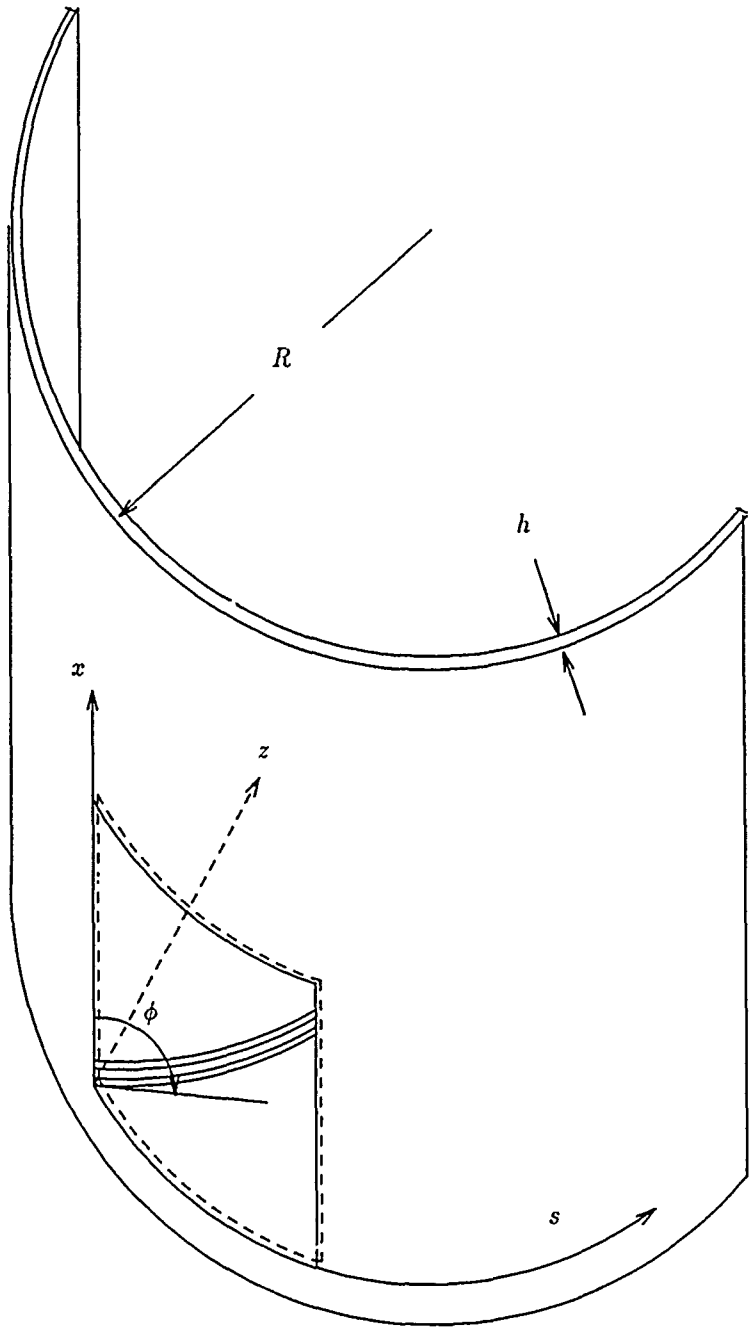

Figure 4.1. Cylindrical Shell Domain for Derivation of the HTSD Theory

The first variation of potential energy for the case with zero body forces is given by:

$$\delta\Pi_p = \delta \int_V W^*(u^k)dV - \int_{S_1} F^k \delta u^k dS = 0 \tag{4.14}$$

To evaluate Eq (4.14), a suitable reference frame must be chosen. A typical method is to assume a total Lagrangian approach where the strain tensor, elasticity tensor, and all other components are described in terms of coordinates of the original undeformed body.

For a laminated orthotropic material, the stress components can be written in terms of the reduced structural stiffness of the lamina as in Eq (3.59). Substituting Eq (3.59) into Eq (4.13) and integrating over the volume of the body, one obtains the strain energy as $U_1 + U_2$, where:

$$\begin{aligned} U_1 &= \tfrac{1}{2}\int_V \left(\overline{Q}_{11}\varepsilon_1^2 + \overline{Q}_{22}\varepsilon_2^2 + 2\overline{Q}_{12}\varepsilon_1\varepsilon_2 \right. \\ &\quad \left. + 2\overline{Q}_{16}\varepsilon_1\varepsilon_6 + 2\overline{Q}_{26}\varepsilon_2\varepsilon_6 + \overline{Q}_{66}\varepsilon_6^2\right) dV \\ U_2 &= \tfrac{1}{2}\int_V \left(\overline{Q}_{44}\varepsilon_4^2 + 2\overline{Q}_{45}\varepsilon_4\varepsilon_5 + \overline{Q}_{55}\varepsilon_5^2\right) dV \end{aligned} \tag{4.15}$$

The ε_i in Eq (4.15) depend on the thickness coordinate and the midsurface coordinates y_1 and y_2. The $\overline{Q}_{ij}$, defined by Eqs (3.58) and (3.60), however, depend only on the thickness coordinate. Thus, these equations can be reduced to an integral over the midsurface of the shell. This is done by first assuming displacement components u_1, u_2, and u_3 vary in the form of a series expansion with respect to the thickness coordinate. Then, one can directly integrate the $\overline{Q}_{ij}$ expressions through the thickness of the shell. The integral through the thickness of $\overline{Q}_{ij}y_3^r$ defines an elasticity array, say C_{ij_r}. These arrays are the familiar A_{ij}, B_{ij}, D_{ij}, ... associated with macro-mechanical behavior of laminated composite plates [36:154-155]. For the laminated composite, the integral is replaced by a summation over the number of plies as shown below:

$$\begin{aligned} C_{ij_0} &= A_{ij} = \sum_{k=1}^{N} \left(\overline{Q}_{ij}\right)_k \left(y_{3_k} - y_{3_{k-1}}\right) \\ C_{ij_1} &= B_{ij} = \frac{1}{2}\sum_{k=1}^{N} \left(\overline{Q}_{ij}\right)_k \left(y_{3_k}^2 - y_{3_{k-1}}^2\right) \end{aligned}$$

$$C_{ij_2} = D_{ij} = \frac{1}{3}\sum_{k=1}^{N}\left(\overline{Q}_{ij}\right)_k\left(y_{3_k}^3 - y_{3_{k-1}}^3\right) \tag{4.16}$$

$$\vdots$$

$$C_{ij_r} = X_{ij} = \frac{1}{r}\sum_{k=1}^{N}\left(\overline{Q}_{ij}\right)_k\left(y_{3_k}^r - y_{3_{k-1}}^r\right)$$

where r is determined by the order of the thickness expansion approximation for u_2 and for the shape factor approximations.

The previous expression for the variation of total potential energy Π_p gives five coupled nonlinear partial differential equations which govern the equilibrium of the system. These expressions contain 18 displacement parameters: u, $u_{,1}$, $u_{,2}$, v, $v_{,1}$, $v_{,2}$, w, $w_{,1}$, $w_{,2}$, $w_{,11}$, $w_{,22}$, $w_{,12}$, ψ_1, $\psi_{1,1}$, $\psi_{1,2}$, ψ_2, $\psi_{2,1}$, $\psi_{2,2}$. These parameters include the seven displacement parameters of Eq (4.1) and their derivatives. Since the equilibrium equations are nonlinear in terms of the displacement parameters, an incremental-iterative approach is typically used to solve a system of linearized equations which yields an equivalent solution. These linearized equations are found by differentiating the expression for Π_p with respect to the displacement functions. For simple theories, such as a Donnell theory or a linear FTSD theory where relatively few terms are included, the first variation of Π_p and its linearization, can be explicitly developed, term by term. For more complete theories, such as the quasi-nonlinear HTSD theory [18] or a fully nonlinear theory, the expression of Π_p has several hundred terms. Its first variation would include, perhaps, thousands of terms and the subsequent linear equilibrium equations would be quite lengthly.

Rajasekaran and Murray [75] developed a formal procedure for finite elements, which defines the total potential energy, its first variation, and the linear incremental equilibrium equations in terms of three stiffness matrices. Specifically, the total potential energy is given by:

$$\Pi_p = \{q\}^T\left[\frac{1}{2}[K] + \frac{1}{6}[N_1] + \frac{1}{12}[N_2]\right]\{q\} - \{q\}^T\{R\} \tag{4.17}$$

where

$\{q\} \equiv$ a column array of nodal displacement parameters

$\{R\} \equiv$ a column array of nodal loads

$[K] \equiv$ an array of constant stiffness coefficients

$[N_1] \equiv$ an array of nonlinear coefficients with each term dependent on one of the displacement parameters ($[N_1]$ is linear in terms of displacement)

$[N_2] \equiv$ an array of nonlinear coefficients with each term dependent on the product of two displacement parameters ($[N_2]$ is quadratic in terms of displacement)

The equilibrium equation, then is given by

$$\left[[K] + \frac{1}{2}[N_1] + \frac{1}{3}[N_2]\right]\{q\} - \{R\} = \{0\} \tag{4.18}$$

and the linear incremental equilibrium equation is given by:

$$[[K] + [N_1] + [N_2]]\{\Delta q\} - \{\Delta R\} = \{0\} \tag{4.19}$$

According to Rajasekaran and Murray, this notation was introduced by Mallett and Marcel in 1968 [75]. To assure the formalism of Eqs (4.17-4.19) holds, the stiffness matrices $[K]$, $[N_1]$, and $[N_2]$ must be derived in a specific way. Rajasekaran and Murray showed that by expressing strain components as follows:

$$\varepsilon_i = \{L_i\}^T\{d\} + \frac{1}{2}\{d\}^T[H_i]\{d\} \tag{4.20}$$

and then redefining the terms of $[K]$, $[N_1]$, and $[N_2]$, the formalism of Eqs (4.17-4.19) would always be valid for any finite element representation of elastic continuum. In Eq (4.20)

$\varepsilon_i \equiv$ a particular strain component

$\{d\} \equiv$ a column array of continuum displacement parameters

$\{L_i\} \equiv$ a column array of the constant coefficients of terms in ε_i containing only one displacement parameter (the terms linear in displacement)

$[H_i] \equiv$ a symmetric array of the constant coefficients of terms in ε_i containing the product of two displacement parameters (the terms quadratic in displacement)

Using Eq (4.20) and defining the terms for a specific ε_i as $\varepsilon_i = \varepsilon_i^L + \varepsilon_i^{NL}$, the expression for potential energy of an elastic material can be written as:

$$\Pi_p = \frac{1}{2}\int_V C_{ij}\left(\varepsilon_i^L\varepsilon_j^L + 2\varepsilon_i^L\varepsilon_j^{NL} + \varepsilon_i^{NL}\varepsilon_j^{NL}\right)dV - \{d\}^T\{P\} \tag{4.21}$$

where C_{ij} is the symmetric array of elasticity constants and summation on $i = 1,\ldots,6$ and $j = 1,\ldots,6$ is implied by the repeated subscripts. Introducing Eq (4.20) into Eq (4.21) gives:

$$\begin{aligned}\Pi_p \;=\; & \frac{1}{2}\int_V C_{ij}\{d\}^T\Big[\{L_i\}\{L_j\}^T + \{L_i\}\{d\}^T[H_j] \\ & + \frac{1}{4}[H_i]\{d\}\{d\}^T[H_j]\Big]\{d\}dV - \{d\}^T\{P\}\end{aligned} \tag{4.22}$$

Notice at this point, Eqs (4.20) and (4.21) are expressed in terms of $\{d\}$, the continuum displacement gradient vector; no finite element discretization has been used. Thus, these equations represent an element independent formulation. By defining a finite element approximation for the continuum displacements $\{d\}$ in terms of nodal displacements $\{q\}$, one defines a specific formulation. To provide the most general formulation, however, the stiffness matrices of Eqs (4.17–4.19) can be developed in terms of the element-independent formulation of Eqs (4.20) and (4.21). In this fashion, we seek definitions for $[K]$, $[N_1]$, and $[N_2]$, such that Eqs (4.17–4.19) will hold. Rajasekaran and Murray showed that the direct comparison of the terms of Eq (4.22) and those of Eq (4.17) will yield arrays $[K]$, $[N_1]$ and $[N_2]$ which satisfy Eq (4.17). Unfortunately, these arrays *will not* satisfy the formalism of Eq (4.19); in some cases, they will not even satisfy Eq (4.18). They showed that consistent representations of these arrays are given by the following expressions:

$$[\hat{K}] = C_{ij}\{L_i\}\{L_j\}^T \tag{4.23}$$

$$[\hat{N}_1] = \frac{1}{3}C_{ij}\left(\{L_i\}\{d\}^T[H_j] + \{d\}^T\{L_i\}[H_j] + [H_i]\{d\}\{L_j\}^T\right) \tag{4.24}$$

$$[\hat{N}_2] = \frac{2}{3}C_{ij}\left([H_i]\{d\}\{d\}^T[H_j] + \frac{1}{2}\{d\}^T[H_j]\{d\}[H_i]\right) \tag{4.25}$$

Rajasekaran and Murray's formulation was for finite elements where strains do not

vary through the thickness of the element. This formulation can be extended to account for variation of strain through the thickness [18:79-91]. To do this, one assumes strains at a point in the shell can be represented by the the following series expansion:

$$\varepsilon_i(y_1, y_2, y_3) = \varepsilon_i(y_1, y_2, 0) + \sum_{p=1}^{2d+g} \chi_i^p y_3^p \tag{4.26}$$

where

$y_3 \equiv$ the distance from the midsurface in the $\vec{e}_3$ direction

$\chi_i^p(y_1, y_2) \equiv$ the coefficients of y_3^p appearing in the strain expression

$d \equiv$ the degree of the displacement field expression

$g \equiv$ the degree of the series expansion approximation of shell shape factor functions appearing in the strain tensor

Rewriting Eq (4.26) consistent with Eq (4.20) gives:

$$\varepsilon_i = \sum_{p=0}^{n} \left(\{L_{i_p}\}^T \{d\} + \frac{1}{2} \{d\}^T [H_{i_p}] \{d\} \right) y_3^p \tag{4.27}$$

where

$\{L_{i_p}\} \equiv$ a row array of the constant coefficients of terms in ε_i containing only one displacement parameter and the thickness coordinate y_3 to the power p

$[H_{i_p}] \equiv$ a symmetric array of the coefficients of terms in ε_i containing products of displacement parameters and the thickness coordinate y_3 to the power p

With this power series expansion of strains, the terms of Eq (4.22) can be written as:

$$[\hat{K}] = \sum_{p=0}^{n} \sum_{r=0}^{n} \frac{1}{2} C_{ij(p+r)} \left(\{L_{i_p}\} \{L_{j_r}\}^T + \{L_{i_r}\} \{L_{j_p}\}^T \right) \tag{4.28}$$

$$[\hat{N}_1] = \frac{1}{3} \sum_{p=0}^{n} \sum_{r=0}^{n} \frac{1}{2} C_{ij(p+r)} \left(\{L_{i_p}\} \{d\}^T [H_{j_r}] + \{L_{i_r}\} \{d\}^T [H_{j_p}] \right) \tag{4.29}$$

$$[\hat{N}_2] = \frac{2}{3} \sum_{p=0}^{n} \sum_{r=0}^{n} \frac{1}{2} C_{ij(p+r)} \left([H_{i_p}] \{d\} \{d\}^T [H_{j_r}] + [H_{i_r}] \{d\} \{d\}^T [H_{j_p}] \right) \tag{4.30}$$

where

$$C_{ij_{(p+r)}} = \int_h \overline{Q}_{ij} y_3^{(p+r)} dy_3 \tag{4.31}$$

are the higher-order elasticity arrays and summation on $i = 1,2,4,5,6$ and $j = 1,2,4,5,6$ is implied. Notice that these equations are a result of directly substituting definitions of $\{L_{i_p}\}$ and $[H_{i_p}]$ into Eqs (4.24–4.25). These expressions will not satisfy the formalism of Eqs (4.17–4.19). In a fashion similar to Rajasekaran and Murray's formulation, Eqs (4.28–4.30) can be manipulated to yield new definitions for arrays $[\hat{K}]$, $[\hat{N}_1]$ and $[\hat{N}_2]$ that satisfy the formalism of Eqs (4.17–4.19) :

$$\left[\hat{K}\right] = \sum_{p=0}^{n}\sum_{r=0}^{n} \frac{1}{2} C_{ij_{(p+r)}} \left(\{L_{i_p}\}\{L_{j_r}\}^T + \{L_{i_r}\}\{L_{j_p}\}^T\right) \tag{4.32}$$

$$\begin{aligned}\left[\hat{N}_1\right] = {} & \frac{1}{3}\sum_{p=0}^{n}\sum_{r=0}^{n} \frac{1}{2} C_{ij_{(p+r)}} \left(\{L_{i_p}\}\{d\}^T[H_{j_r}] + \{L_{i_r}\}\{d\}^T[H_{j_p}] + \{d\}^T\{L_{i_p}\}[H_{j_r}]\right. \\ & \left. + \{d\}^T\{L_{i_r}\}[H_{j_p}] + [H_{i_p}]\{d\}\{L_{j_r}\}^T + [H_{i_r}]\{d\}\{L_{j_p}\}^T\right)\end{aligned} \tag{4.33}$$

$$\begin{aligned}\left[\hat{N}_2\right] = {} & \frac{2}{3}\sum_{p=0}^{n}\sum_{r=0}^{n} \frac{1}{2} C_{ij_{(p+r)}} \left[\left([H_{i_p}]\{d\}\{d\}^T[H_{j_r}] + [H_{i_r}]\{d\}\{d\}^T[H_{j_p}]\right)\right. \\ & \left. + \frac{1}{2}\left(\{d\}^T[H_{j_p}]\{d\}[H_{i_r}] + \{d\}^T[H_{j_r}]\{d\}[H_{i_p}]\right)\right]\end{aligned} \tag{4.34}$$

Equation (4.33) can be simplified and still retain the formalism of Eqs (4.17–4.19) [18:87-89]. The simplified version of Eq (4.33) is:

$$\begin{aligned}[\hat{N}_1] = {} & \frac{1}{3}\sum_{p=0}^{n}\sum_{r=0}^{n} C_{ij_{(p+r)}} \left(\{L_{i_p}\}\{d\}^T[H_{j_r}] + \{d\}^T\{L_{i_p}\}[H_{j_r}]\right. \\ & \left. + [H_{i_r}]\{d\}\{L_{j_p}\}^T\right)\end{aligned} \tag{4.35}$$

Thus, with the definitions of $\{L_{i_p}\}$, $[H_{i_p}]$, $[\hat{K}]$, $[\hat{N}_1]$, and$[\hat{N}_2]$, one can now form the element independent stiffness arrays given by Eqs (4.32), (4.35), and (4.34). This formulation requires literally hundreds of matrix multiplications to evaluate these equations. Thus, MACSYMA was used to accomplish this task.

4.5 Symbolic Generation of Elemental Codes

A significant accomplishment of this research was the development of a tool to generate comparable versions of "elemental code". The results comparing various theoretical attributes would be meaningless if undetected errors were present in some variations, or if different finite element models or discretization schemes were used. For this research, a reliable system of generating different, but comparable, versions of code was required. A MACSYMA routine was developed to symbolically generate the assumed displacement field, determine the strain components, determine the shell shape factor approximations, determine the elements of the strain definition arrays, and finally generate the Fortran code for elements of the $\left[\hat{K}\right]$, $\left[\hat{K}_s\right]$, $\left[\hat{N}_1\right]$, $\left[\hat{N}_{1s}\right]$, $\left[\hat{N}_2\right]$, and $\left[\hat{N}_{2s}\right]$ stiffness arrays. Development of this routine was a time consuming, but crucial aspect of this research. With elemental codes approaching 70,000 lines in length, the detection of errors caused by "hand generation" would have been virtually impossible. The symbolic generation of codes assured reliability and comparability not achievable by other means. By using these codes in an element independent formulation, the accuracy of each version of theory could be compared using the same finite element model and main program (SHELL). This further assured a fair comparison of the various theoretical attributes of each version. The only variables were the order of the assumed thickness expansion for the u_2 displacement, the order of the thickness expansion for the approximation of shell shape factor functions, and the choice to include or exclude nonlinear transverse shear strain terms. The theoretical attributes of the elemental codes used for this research are summarized in Table 4.3. The codes are identified by a symbol "GXYZ", where

G = C for cylindrical, S for spherical, or A for arbitrary shell geometry (Appendix A lists relations for arbitrary shells and Appendices B through E list relations for cylindrical shells. Complete relations for spherical shells were not generated for this research),

X = 0 for the incomplete cubic u_2 displacement of Eq (3.70), or 1 for the complete quartic u_2 displacement of Eq (4.1),

Y = 0 for linear shell shape function approximations, or 2 for quadratic approximations,

Z = 0 for linear transverse shear strain displacement relations, or 3 for nonlinear relations.

Table 4.3. Definition of Elemental Codes for Variations of Theory

Code Name	Displacement Assumption Order	Shape Factor Approximation Order	Transverse Shear Strains	Code Length (Lines)	Equations Given in Appendix
C000	cubic (1)	linear (2)	linear	13866	B
C003	cubic	linear	nonlinear	23176	B
C020	cubic	quadratic (3)	linear	24254	C
C023	cubic	quadratic	nonlinear	39322	C
C100	quartic (4)	linear	linear	29626	D
C103	quartic	linear	nonlinear	51637	D
C120	quartic	quadratic	linear	30777	E
C123	quartic	quadratic	nonlinear	67618	E

(1) u_i defined by Eq (3.70)
(2) See Appendix B for nonzero shell shape factor approximations.
(3) See Appendix C for nonzero shell shape factor approximations.
(4) u_i defined by Eq (4.1)

The MACSYMA routine for generating elemental codes is included as Appendix G. The routine includes comment statements to explain some special functions, called macros, and a few comments to explain the steps in the process. Significant examples and advice about using MACSYMA were garnered from References [54, 7] and from Dr. Mark Ewing, a member of the author's committee. The generation of every version of elemental code followed the same steps listed below:

PART 1 Generate Strain Definition Arrays

1. Specify choice of incomplete cubic u_2 thickness expansion or complete quartic thickness expansion.

2. Specify choice of linear shell shape factor approximation or quadratic approximation.

3. Specify choice of linear or nonlinear transverse shear strain.

4. Symbolically compute Green strain components for an arbitrary shell, where $h_1 = h_1(y_1, y_2, y_3)$, $h_2 = h_2(y_1, y_2, y_3)$ and $h_3 = 1$, by differentiating displacement field equations according to Eq (3.49).

5. Factor out all geometric shape factor functions, h_1, h_2 and derivatives of h_1 and h_2, appearing in the numerator and denominator of all terms in every strain component. There are 60 possible combinations of these functions for an arbitrary shell. These terms are shown in Appendix A as functions $\hat{H}_1$ through $\hat{H}_{60}$.

6. Specify the shell geometry by specifying h_1 and h_2 and symbolically compute the 60 shape factor approximations $\hat{H}_1, \ldots, \hat{H}_{60}$. Nonzero functions for each elemental code are listed in Appendices B–E.

7. Substitute shape factor function approximations into each strain component expression.

8. Identify coefficients of thickness coordinate y_3^p from each strain component expression. These are the χ_i^p expressions listed for each strain component in Appendices B–E.

9. From each χ_i^p, identify the coefficients of any terms containing two continuum displacement parameters. These are the 18 functions u, $u_{,1}$, $u_{,2}$, v, $v_{,1}$, $v_{,2}$, v', $w_{,1}$, $w_{,2}$, $w_{,11}$, $w_{,22}$, $w_{,12}$, ψ_1, $\psi_{1,1}$, $\psi_{1,2}$, ψ_2, $\psi_{2,1}$ and $\psi_{2,2}$. The coefficients of these quadratic nonlinear terms are stored as entries in an array $\mathcal{H}_{ijlm}$, where $i = 1, \ldots, 6$, $j = 0, \ldots, 12$, $l = 1, \ldots, 18$ and $m = 1, \ldots, 18$.

10. Similarly, identify the coefficients of each χ_i^p that depend on only one displacement parameter. These coefficients are stored as entries in an array $\mathcal{L}_{ijl}$, $i = 1,\ldots,6$, $j = 0,\ldots,7$ and $l = 1,\ldots,18$.

11. Form strain definition arrays $[L0],\ldots,[L7]$ and $[H0],\ldots,[H12]$ for strain components ε_1, ε_2 and ε_6, where

$$\begin{aligned} [Lj] &= [\{\mathcal{L}_{1jl}\}\,|\,\{\mathcal{L}_{2jl}\}\,|\,\{\mathcal{L}_{6jl}\}], \quad l = 1,\ldots,18 \\ [Hj] &= [[\mathcal{H}_{1jlm}]\,|\,[\mathcal{H}_{2jlm}]\,|\,[\mathcal{H}_{6jlm}]], \quad l,m = 1,\ldots,18 \end{aligned}$$

12. Form strain definition arrays $[S0],\ldots,[S7]$ and $[SS0],\ldots,[SS12]$ for strain components ε_4 and ε_5, where

$$\begin{aligned} [Sj] &= [\{\mathcal{L}_{4jl}\}\,|\,\{\mathcal{L}_{5jl}\}], \quad l = 1,\ldots,18 \\ [SSj] &= [[\mathcal{H}_{4jlm}]\,|\,[\mathcal{H}_{5jlm}]], \quad l,m = 1,\ldots,18 \end{aligned}$$

13. Store strain definition arrays for use in Part 2

PART 2 Generation of Elemental Stiffness Arrays and Fortran Code

1. Generate $\left[\hat{K}\right]$ and $\left[\hat{K}_s\right]$ matrices and Fortran code for each.

   (a) Combine Lp and Lr matrices with the elasticity arrays $C_{ij(p+r)}$ according to Eq (4.32) to form $\left[\hat{K}\right]$. (The elasticity arrays $C_{ij_{(p+r)}}$, where $p + r = 0,\ldots,12$ and $i,j = 1,2,6$, are labeled $A_{ij},\ldots,XR_{ij}$ and $AS_{ij},\ldots,XRS_{ij}$ in the MACSYMA Routine. This labeling corresponds to the Fortran variables used in the ELAST subroutine of the program SHELL [18]. ELAST was modified by the author to calculate the higher-order elasticity arrays needed for this research. Part 2 of the MACSYMA Routine uses only the even sums of $p + r$ which correspond to the elasticity arrays of a symmetric laminate.

   (b) Generate a Fortran program statement, using MACSYMA's *gentran* function, for computation of each nonzero upper right triangle entry of the $\left[\hat{K}\right]$ matrix. Repeat this step until all nonzero entries of $\left[\hat{K}\right]$ are coded

(c) If nonlinear transverse shear terms are desired, combine Sp and Sr matrices with the elasticity arrays $C_{ij(p+r)}$ where $p+r=0,\ldots,14$ and $i,j=4,5$ according to Eq (4.32), to form $\left[\hat{K}_s\right]$

(d) Generate a Fortran program statement, using MACSYMA's *gentran* function, for computation of each nonzero upper right triangle entry of the $\left[\hat{K}_s\right]$ matrix. Repeat this step until all nonzero entries of $\left[\hat{K}_s\right]$ are coded

2. Generate $\left[\hat{N}_1\right]$ and $\left[\hat{N}_{1s}\right]$ matrices and Fortran code for each

(a) Combine $[Lp]$, $[Lr]$, $[Hp]$, and $[Hr]$ arrays for the first elasticity array $C_{ij(p+r)}$ where $r+p=0$ and $i,j=1,2,6$, according to Eq (4.35) to form $\left[\hat{N}_1\right]_{C0}$

(b) Generate a Fortran program statement, using MACSYMA's *gentran* function, for computation of each nonzero upper right triangle entry of the $\left[\hat{N}_1\right]_{C0}$ matrix. Repeat this step until all nonzero entries of $\left[\hat{N}_1\right]_{C0}$ are coded

(c) If nonlinear transverse shear terms are desired, combine $[Sp]$, $[Sr]$, $[SSp]$, and $[SSr]$ arrays with the first elasticity array $C_{ij(p+r)}$ where $r+p=0$ and $i,j=4,5$, according to Eq (4.35) to form $\left[\hat{N}_{1s}\right]_{C0}$

(d) Generate a Fortran program statement, using MACSYMA's *gentran* function, for computation of each nonzero upper right triangle entry of the $\left[\hat{N}_{1s}\right]_{C0}$ matrix. Repeat this step until all nonzero entries of $\left[\hat{N}_{1s}\right]_{C0}$ are coded

(e) Repeat the four previous steps for $\left[\hat{N}_1\right]_{C1}$ and $\left[\hat{N}_{1s}\right]_{C1}$ through $\left[\hat{N}_1\right]_{C19}$ and $\left[\hat{N}_{1s}\right]_{C19}$

3. Generate $\left[\hat{N}_2\right]$ and $\left[\hat{N}_{2s}\right]$ matrices and Fortran code for each

(a) Combine $[Hp]$ and $[Hr]$ arrays for the first elasticity array $C_{ij(p+r)}$ where $r+p=0$ and $i,j=1,2,6$, according to Eq (4.34) to form $\left[\hat{N}_2\right]_{C0}$

(b) Generate a Fortran program statement, using MACSYMA's *gentran* function, for computation of each nonzero upper right triangle entry of the

$\left[\hat{N}_2\right]_{C0}$ matrix. Repeat this step until all nonzero entries of $\left[\hat{N}_2\right]_{C0}$ are coded

(c) If nonlinear transverse shear terms are desired, combine $[SSp]$ and $[SSr]$ arrays with the first elasticity array $C_{ij(p+r)}$ where $r+p=0$ and $i,j=4,5$, according to Eq (4.34) to form $\left[\hat{N}_{2s}\right]_{C0}$

(d) Generate a Fortran program statement, using MACSYMA's *gentran* function, for computation of each nonzero upper right triangle entry of the $\left[\hat{N}_{2s}\right]_{C0}$ matrix. Repeat this step until all nonzero entries of $\left[\hat{N}_{2s}\right]_{C0}$ are coded

(e) Repeat the four previous steps for $\left[\hat{N}_2\right]_{C1}$ and $\left[\hat{N}_{2s}\right]_{C1}$ through $\left[\hat{N}_2\right]_{C24}$ and $\left[\hat{N}_{2s}\right]_{C24}$

4.6 Verification of the MACSYMA Routine

Verification of the MACSYMA routine was accomplished by several methods. First, each segment of the program was developed independent of the others. Then each was thoroughly tested in an interactive mode to assure results corresponded to those expected. Segments were then combined to form larger blocks and finally, a full version of the routine was developed. This final version of the MACSYMA program was run in batch mode on a Digital Equipment Corporation VAX8550 with 64 megabytes of main memory. The first part of this program, generation of stain terms and strain definition arrays, generally took about 5 CPU hours depending on machine usage and the version of elemental code chosen. The second part of the program, generation of stiffness matrices and corresponding Fortran code, was accomplished also in batch mode. This last part of the program took about 5 CPU hours for the C003 code and up to 30 CPU hours for the C123 code.

Verification of this work was quite difficult. The output of Part 1 was compared with the strain components and strain definition arrays of Dennis [18:67-70,333-336,338-341]. Although some differences were noted, these were due to Dennis ignoring 26 terms of the in-plane strain components and significantly simplifying the transverse shear strain relations [18:67-70]. Once discrepancies were resolved, Part 2 of the program was executed. The

output of Part 2 was 45 files containing the Fortran statements for each element of $\left[\hat{K}\right]$, $\left[\hat{K}_s\right]$, $\left[\hat{N}_1\right]$, $\left[\hat{N}_{1s}\right]$, $\left[\hat{N}_2\right]$, and $\left[\hat{N}_{2s}\right]$ stiffness arrays. The C003 elemental code output files for the $\left[\hat{K}\right]$, $\left[\hat{K}_s\right]$, $\left[\hat{N}_1\right]$, and $\left[\hat{N}_2\right]$ stiffness arrays were compared, virtually term-by-term, with the Fortran subroutines generated by Dennis. Finally, all output files for the nonlinear arrays were compiled and assembled into four separate subroutine libraries. Each library contained the Fortran object files for the $\left[\hat{N}_1\right]$, $\left[\hat{N}_{1s}\right]$, $\left[\hat{N}_2\right]$, and $\left[\hat{N}_{2s}\right]$ stiffness array subroutines of either the C00X, the C02X, the C10X or the C12X elemental codes. The finite element program SHELL written by Dennis [18] was then modified to call element independent stiffness array subroutines needed to give either a modified Donnell solution, a CXX0 linear transverse shear solution, or a CXX3 nonlinear transverse shear solution.

4.7 Finite Element Solution

The element independent stiffness matrices of Eqs (4.32), (4.34), and (4.35) depend upon the continuum displacement gradient vector $\{d\}$. This vector includes the following functions: u, $u_{,1}$, $u_{,2}$, v, $v_{,1}$, $v_{,2}$, w, $w_{,1}$, $w_{,2}$, $w_{,11}$, $w_{,22}$, $w_{,12}$, ψ_1, $\psi_{1,1}$, $\psi_{1,2}$, ψ_2, $\psi_{2,1}$ and $\psi_{2,2}$. Likewise, the potential energy expression of Eqs (4.21) and (4.22) also depend upon these functions. Using a standard displacement-based finite element method, the 18 two-dimensional functions of the continuum displacement gradient vector $\{d(y_1, y_2)\}$ are approximated by interpolation from discrete values of nodal displacement parameters. These nodal parameters or degrees of freedom (dof), are defined only at a finite number of points or nodes and are denoted by $\{q\}$ in Eq (4.36)

$$\{d(y_1, y_2)\} = [\mathcal{D}(x, s)]\{q\} \tag{4.36}$$

where $[\mathcal{D}(x, s)]$ is an array of nodal interpolation functions and (x, s) are the local coordinates of a two-dimensional rectangular finite element. If one substitutes Eq (4.36) into Eq (4.22) and rewrites the expression in terms of $\{q\}$, then one obtains for the potential energy:

$$\Pi_p = \frac{\{q\}^T}{2}\left[[K] + \frac{1}{3}[N_1] + \frac{1}{6}[N_2]\right]\{q\} - \{q\}^T\{R\} \tag{4.37}$$

where

$$[K] = \int_V [\mathcal{D}]^T \left[\hat{K}\right] [\mathcal{D}]\, dV \tag{4.38}$$

$$[N_1] = \int_V [\mathcal{D}]^T \left[\hat{N}_1\right] [\mathcal{D}]\, dV \tag{4.39}$$

$$[N_2] = \int_V [\mathcal{D}]^T \left[\hat{N}_2\right] [\mathcal{D}]\, dV \tag{4.40}$$

The finite element method generally requires the computation of the stiffness matrices of Eqs (4.38–4.40) for each element independently. These elemental stiffnesses are then assembled according to their relationship to global nodes of the structure. In this manner, Eq (4.37) represents the potential energy of a single element. The total energy of the system is then found by summing the energies of each element.

4.8 The 36 Degree of Freedom Cylindrical Shell Finite Element

Defining the terms of Eq (4.37) requires definition of the specific element, since the nodal parameters $\{q\}$ and the associated nodal interpolation array $[\mathcal{D}]$ are element specific. Recall, the three stiffness arrays $\left[\hat{K}\right]$, $\left[\hat{N}_1\right]$, and $\left[\hat{N}_2\right]$ of Eqs (4.38–4.40) were element independent. The choices of the number of nodes per element and the nodal degrees of freedom at each node have not been specified at this point. In fact, virtually any two-dimensional element that will provide values for the 18 functions of the continuum displacement gradient vector $\{d\}$ could be used.

The author's research objective was to investigate structural phenomena. Thus, an existing, proven finite element model for laminated cylindrical shells was used for this research. The element chosen was the 36 degree of freedom (DOF) quadrilateral curved shell element described in Reference [18:95-111]. This element has been used for many investigations of static and dynamic response of plates arches and cylindrical shells undergoing large displacements with quasi-nonlinear HTSD theory [22, 61, 19, 64, 88, 93, 102]. In addition to these investigations, many linear problems were used to validate the element's performance. These problems included typical flat plate and patch tests used to show convergence as the number of elements in a mesh is increased [59]. These patch test problems were based upon a linear analysis, not a nonlinear analysis. This is because the

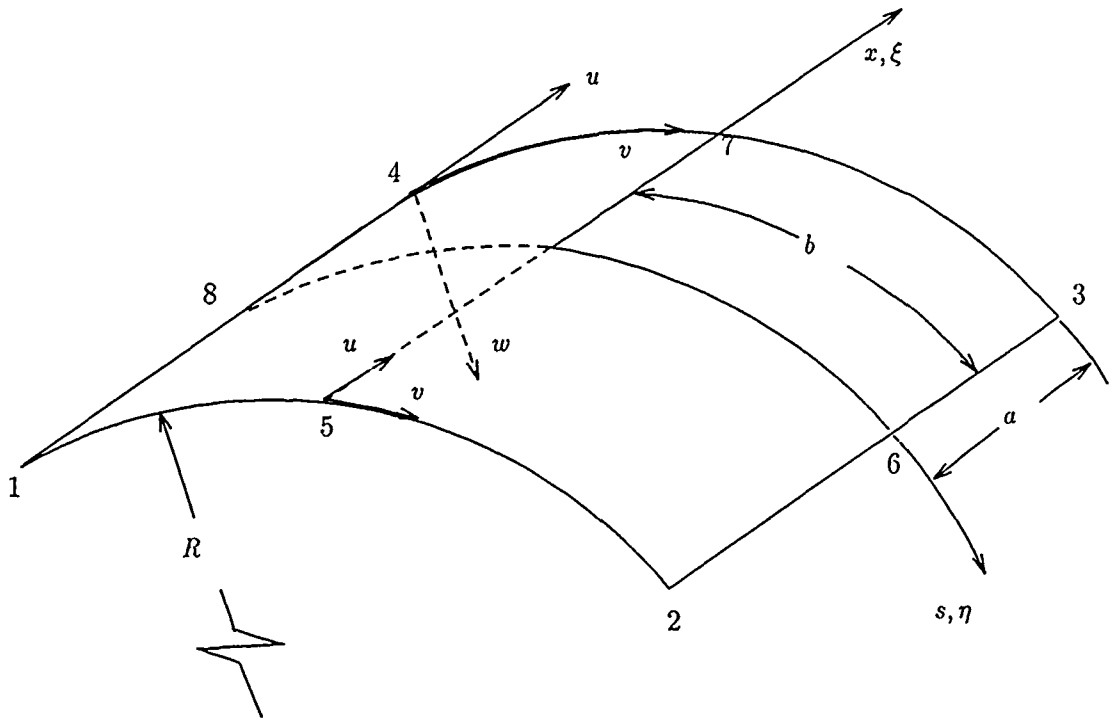

Figure 4.2. Translational DOF Definitions for the 36–DOF Cylindrical Shell Finite Element

patch test is based upon the mathematical theory of *linear* partial differential equations. Since the element stiffness array includes nonlinear terms, the element will not pass the usual definition of the of the patch test unless the nonlinear terms are eliminated. For the nonlinear problem, convergence cannot be proven by a simple patch test. Convergence must be demonstrated. The 36 DOF element is shown in Figure 4.2. This element has eight nodes with seven degrees of freedom, u, v, w, w_1, w_2, ψ_1, and ψ_2, at each of the four corner nodes and two degrees of freedom, u and v, at the four midside nodes. The two degrees of freedom at the midside nodes allow for quadratic interpolation of in-plane displacements u and v. This is important for shells due to the curvature-induced coupling of bending and membrane activity in shells.

The continuum values of u and v are interpolated from the nodal values u_k and v_k, using Eq (4.41) where Q_k are quadratic Lagrangian interpolation functions given in

Eq (4.42) [18:110]

$$u = \sum_{k=1}^{8} Q_k u_k \qquad v = \sum_{k=1}^{8} Q_k v_k \tag{4.41}$$

$$\begin{aligned} Q_k &= \frac{1}{4}(1+\xi_k\xi)(1+\eta_k\eta)(\xi_k\xi+\eta_k\eta-1), \quad k=1,2,3,4 \\ Q_k &= \frac{1}{2}\left(1-\xi^2\right)(1+\eta_k\eta), \quad k=6,8 \\ Q_k &= \frac{1}{2}\left(1-\eta^2\right)(1+\xi_k\xi), \quad k=5,7 \end{aligned} \tag{4.42}$$

where the kth node has natural coordinates $\xi_k = x_k/a$ and $\eta_k = s_k/b$. The natural coordinates correspond to local coordinates (x, s) in the longitudinal and circumferential directions shown in Figure 4.2. These translational degrees of freedom are also shown in Figure 4.3.

The continuum displacement gradient vector $\{d\}$ includes rotational degrees of freedom ψ_1 and ψ_2 and the first derivatives of these parameters. The parameters ψ_1 and ψ_2 are shown in Figure 4.3. Linear interpolation can be used for these parameters, since only C° continuity is required. The interpolations of ψ_1 and ψ_2 are given by Eqs (4.43) with the linear Lagrangian interpolation functions of Eq (4.44) [18:103]

$$\psi_1 = \sum_{k=1}^{4} \mathcal{N}_k \psi_{1_k} \qquad \psi_2 = \sum_{k=1}^{4} \mathcal{N}_k \psi_{2_k} \tag{4.43}$$

$$\mathcal{N}_k = \frac{1}{4}(1+\xi_k\xi)(1+\eta_k\eta) \tag{4.44}$$

The continuum displacement gradient variables associated with transverse displacement w, include w and it's first and second derivatives. Figure 4.3 shows w, $w_{,1}$, and $w_{,2}$. Nodal parameters associated with transverse displacement include only the values w_k, $w_{,1_k}$, and $w_{,2_k}$ at the four corner nodes where $k = 1,2,3,4$. Interpolation of w is accomplished using Eq (4.45) and the Hermitian shape functions of Eq (4.46) [18:103].

$$w(x,n) = \sum_{k=1}^{4} (\mathcal{H}1_k w_k + \mathcal{H}2_k w_k + \mathcal{H}3_k w_k) \tag{4.45}$$

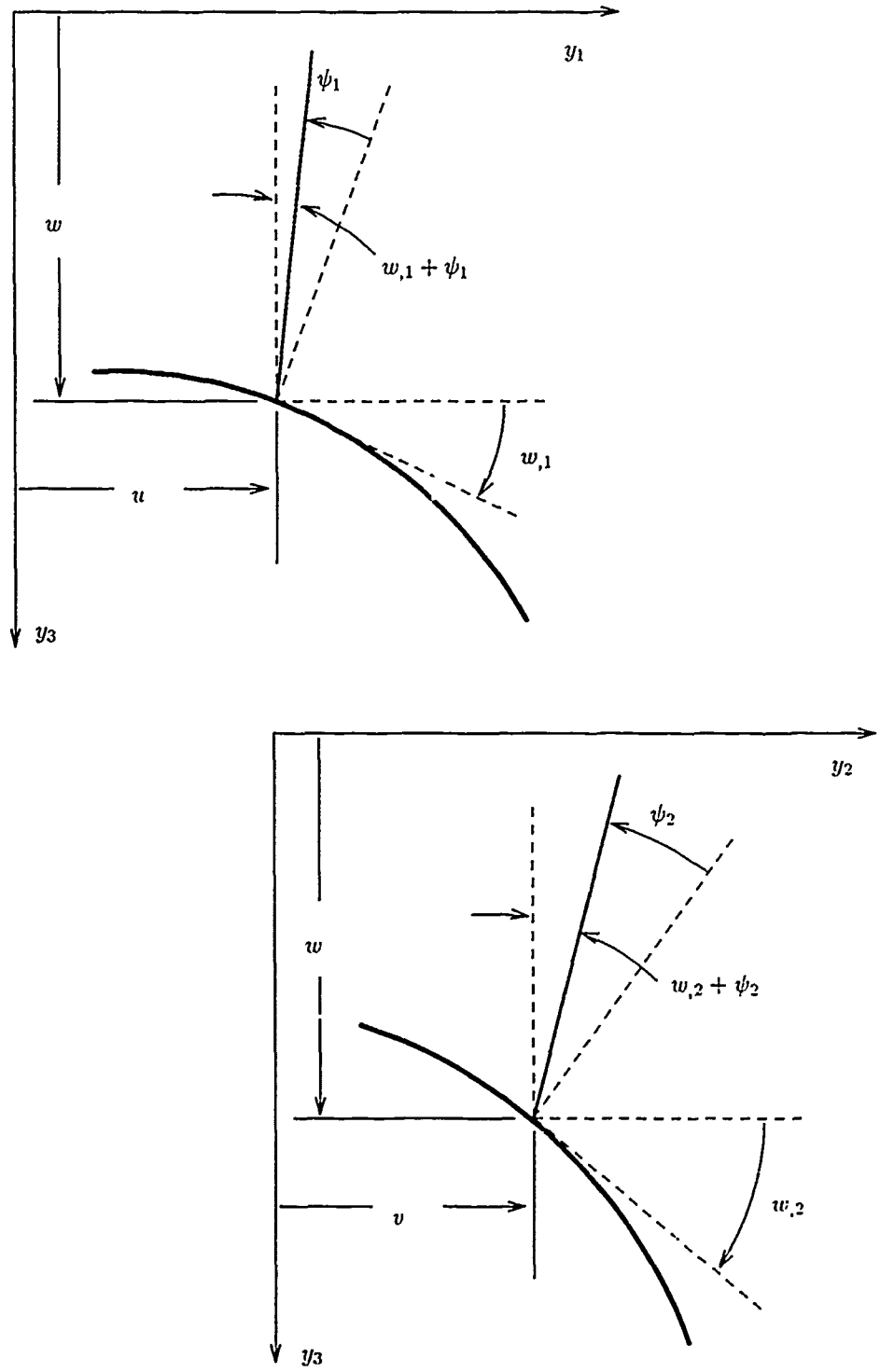

Figure 4.3. Rotational DOF Definitions for the 36-DOF Cylindrical Shell Finite Element

$$
\begin{aligned}
\mathcal{H}1_k &= \frac{1}{8}(1+\xi_k\xi)(1+\eta_k\eta)\left(2+\xi_k\xi+\eta_k\eta-\xi^2-\eta^2\right) \\
\mathcal{H}2_k &= \frac{a}{8}(1+\xi_k\xi)^2(\xi_k\xi-1)(1+\eta_k\eta)\xi_k \\
\mathcal{H}3_k &= \frac{b}{8}(1+\xi_k\xi)(\eta_k\eta-1)(1+\eta_k\eta)^2\eta_k
\end{aligned}
\tag{4.46}
$$

The approximate continuum values for derivatives of u, v, ψ_1, ψ_2, and w, at any point (ξ,η) in the element, are also found by interpolation. This is accomplished by using the corresponding derivatives of the interpolation functions. Thus, the approximate continuum displacement gradient vector is related to the array of discrete nodal degrees of freedom as shown below:

$$
\{d(\xi,\eta)\} = [\mathcal{D}(\xi,\eta)]\{q\} \tag{4.47}
$$

where

$$
[\mathcal{D}(\xi,\eta)] = \begin{bmatrix}
[\mathcal{Q}_1] & 0 & 0 & \cdots & [\mathcal{Q}_4] & 0 & 0 & [\mathcal{Q}_5] & \cdots & [\mathcal{Q}_8] \\
0 & [\mathcal{H}_1] & 0 & \cdots & 0 & [\mathcal{H}_4] & 0 & 0 & \cdots & 0 \\
0 & 0 & [\mathcal{N}_1] & \cdots & 0 & 0 & [\mathcal{N}_4] & 0 & \cdots & 0
\end{bmatrix} \tag{4.48}
$$

and

$$
[\mathcal{Q}_k] = \begin{bmatrix}
\mathcal{Q} & 0 \\
\mathcal{Q}_\xi & 0 \\
\mathcal{Q}_\eta & 0 \\
0 & \mathcal{Q} \\
0 & \mathcal{Q}_\xi \\
0 & \mathcal{Q}_\eta
\end{bmatrix}_k
\qquad
[\mathcal{N}_k] = \begin{bmatrix}
\mathcal{N} & 0 \\
\mathcal{N}_\xi & 0 \\
\mathcal{N}_\eta & 0 \\
0 & \mathcal{N} \\
0 & \mathcal{N}_\xi \\
0 & \mathcal{N}_\eta
\end{bmatrix}_k \tag{4.49}
$$

$$
[\mathcal{H}_k] = \begin{bmatrix}
\mathcal{H}1 & \mathcal{H}2 & \mathcal{H}3 \\
\mathcal{H}1_\xi & \mathcal{H}2_\xi & \mathcal{H}3_\xi \\
\mathcal{H}1_\eta & \mathcal{H}2_\eta & \mathcal{H}3_\eta \\
\mathcal{H}1_{\xi\xi} & \mathcal{H}2_{\xi\xi} & \mathcal{H}3_{\xi\xi} \\
\mathcal{H}1_{\eta\eta} & \mathcal{H}2_{\eta\eta} & \mathcal{H}3_{\eta\eta} \\
\mathcal{H}1_{\xi\eta} & \mathcal{H}2_{\xi\eta} & \mathcal{H}3_{\xi\eta}
\end{bmatrix}_k \tag{4.50}
$$

In Eq (4.48) the numerical subscripts refer to node numbers. In Eqs (4.49) and (4.50) the Greek subscripts imply differentiation with respect to the indicated natural coordinate variable. The k subscript implies that natural coordinates ξ_k and η_k appearing in each of the interpolation functions are to be assigned values corresponding to the natural coordinate of the kth node.

In Eq (4.47), notice that $\{q\}$ is a 36×1 array of nodal displacements, $[\mathcal{D}]$ is an 18×36 array, and the resulting array $\{d(\xi,\eta)\}$ is an 18×1 array as expected. Transformation of coordinates using the inverse of the Jacobian matrix J, as shown in Eq (4.51), completes the definition of the element interpolation scheme:

$$[\mathcal{D}(x,s)] = \left[J^{-1}\right][\mathcal{D}(\xi,\eta)] \tag{4.51}$$

where $[J^{-1}]$ is a diagonal matrix for the transformation of coordinates used in this research.

$$\begin{aligned}[J^{-1}] = \lceil \quad & 1, \quad 1/a, \quad 1/b, \quad 1, \quad 1/a, \quad 1/b, \quad 1, \quad 1/a, \quad 1/b, \\ & 1/a^2, \quad 1/b^2 \quad 1/ab, \quad 1, \quad 1/a, \quad 1/b, \quad 1, \quad 1/a, \quad 1/b \quad \rfloor\end{aligned} \tag{4.52}$$

With this finite element discretization, Eq (4.19) can be written as

$$\left[\sum_{n=1}^{m}\left[\int_{dA_n}[\mathcal{D}]^T\left[\left[\hat{K}\right]+\left[\hat{N}_1\right]+\left[\hat{N}_2\right]\right][\mathcal{D}]\,dA_n\right]_n\right]\{\Delta q\}$$

$$= \{R\} - \left[\sum_{n=1}^{m}\left[\int_{dA_n}[\mathcal{D}]^T\left[\left[\hat{K}\right]+\frac{1}{2}\left[\hat{N}_1\right]+\frac{1}{3}\left[\hat{N}_2\right]\right][\mathcal{D}]\,dA_n\right]_n\right]\{q\} \tag{4.53}$$

where

$dA_n \equiv$ the two-dimensional domain of an individual element n

$m \equiv$ the total number of elements in the mesh

$\{\Delta q\} \equiv$ the global column array of nodal displacement parameters assembled from elemental array $\{\Delta q\}_n$

$\{q\} \equiv$ the global column array of nodal displacement parameters assembled from elemental array $\{q\}_n$

$\{q\}_n \equiv$ a 36×1 nodal displacement array for element n, and

$\{R\} \equiv$ the global load array which has the same dimension as the global displacement arrays $\{\Delta q\}$ and $\{q\}$

The integrations of Eq (4.53) are approximated by numerical integration using Gaussian quadrature. Using one of the terms of the first summation of Eq (4.53) as an example, the integral I_n shown in Eq (4.54), can be transformed to natural coordinates as shown in Eq (4.55). Next, the integrations of Eq (4.55) are approximated numerically by a double summation of weighting factors at the corresponding Gaussian integration points. This is shown in Eq (4.56)

$$I_n = \int_{dA_n} [\mathcal{D}]^T \left[\left[\hat{K}\right] + \left[\hat{N}_1\right] + \left[\hat{N}_2\right]\right] [\mathcal{D}]\, dA_n \tag{4.54}$$

$$I_n = \int_{-1}^{1}\int_{-1}^{1} [\mathcal{D}]^T \left[\left[\hat{K}\right] + \left[\hat{N}_1\right] + \left[\hat{N}_2\right]\right] [\mathcal{D}] \det J \; d\xi d\eta \tag{4.55}$$

$$I_n = \sum_{i=1}^{m}\sum_{i=1}^{n} W_i W_j I(\xi_i, \eta_j) \tag{4.56}$$

where

$\det J \equiv$ the determinant of the Jacobian matrix

$I(\xi_i, \eta_j) \equiv [\mathcal{D}]^T \left[\left[\hat{K}\right] + \left[\hat{N}_1\right] + \left[\hat{N}_2\right]\right] [\mathcal{D}] \det J$ evaluated at Gauss integration points (ξ_i, η_j)

$W_i, W_i \equiv$ the weighting factors

The range of indices i and j define the order of the numerical integration. When $m = n$ the integration is called uniform; $n \times n$ integration will exactly integrate a polynomial integrand of order $2n - 1$ [16:172].

The solution of Eq (4.53) is accomplished by an incremental-iterative technique commonly called the Newton-Raphson method [18:115-127]. The parameters to be incremented are the elements of the array $\{q\}$ containing global degrees of freedom. For the first iteration of the first increment, all elements of $\{q\}$ are assumed to be zero and a linear solution of Eq (4.53), one involving only $[\hat{K}]$, is found by Gauss elimination. This solution, call it $\{q\}_1$, is used during the next iteration to compute $[\hat{N}_1]$ and $[\hat{N}_2]$. Eq (4.53) is then solved

using $[\hat{K}]$, $[\hat{N}_1]$ and $[\hat{N}_2]$ to generate a new solution, call it $\{q\}_2$. This process continues until the solution for $\{q\}$ has converged. The following criterion is used to determine convergence:

$$\frac{\left(\sum_i (q_{i_r})^2\right)^{1/2} - \left(\sum_i (q_{i_{r-1}})^2\right)^{1/2}}{\left(\sum_i (q_{i_1})^2\right)^{1/2}} \times 100\% \leq \nabla \tag{4.57}$$

where q_{i_r}, $q_{i_{r-1}}$ and q_{i_1} are the elements of $\{q\}$ for the r th, $(r-1)$th, and first iterations, respectively, for a given increment. The criterion is satisfied when the left hand side of Eq (4.57) is less than or equal to ∇, a user specified percentage tolerance. Values of ∇ ranging from 0.01 to 0.5 percent were chosen for the problems investigated.

V. Discussion of Shallow Shell Results with Nonlinear HTSD Theory

Chapters III and IV presented the development of eight variations of a nonlinear higher-order transverse shear deformation (HTSD) theory for a cylindrical shell. This chapter discusses the results for shallow shell structures using the full nonlinear HTSD theory developed for this research. Results for deep shell structures are discussed in Chapter VI. The depth criterion chosen was the ratio of the shell height (from the supports to the crown of the shell) versus one-half the distance between the supports. One objective of this research was to evaluate the accuracy of the HTSD variations shown in Table 4.3, another objective was to assess their limitations. The first step in achieving these objectives was verification of the computational tools used to achieve results. This verification process included verification of the MACSYMA routines used to generate the elemental codes (this process was discussed in Section 4.6), verification of the finite element program, and finally verification of numerical results.

Several test problems were solved to verify the MACSYMA generated Fortran codes. These test problems were classical flat plate and thin shell problems with known solutions. In all of these test problems, the higher-order elemental codes C020, C100 and C120 should give results equivalent to the C000 code. This result is expected since the additional terms of the higher-order thickness expansions include radius in the denominator. Thus, these terms are zero for the flat plate and should be negligible for the classical thin shell. In addition, these results should match those produced by Dennis [18]. Investigations of the limitations of quasi-nonlinear and nonlinear HTSD theories were based on shallow isotropic shell panel problems and a deep isotropic arch problem. The shallow shell problems were thin 100–inch-radius hinged-free shell panels with transverse point load. The 20×20–inch shell panels studied were 0.25–inch and 1–inch thick.

To study the limitations of the quasi-nonlinear and nonlinear HTSD theories with composite materials, two composite material problems were selected. A thin shallow axially-loaded 12–inch-radius quasi-isotropic 11×8–inch cylindrical shell panel exhibits large transverse deflection, large rotation, and large curvature. The 0.05–inch-thick quasi-isotropic material also has a large ratio of in-plane modulus to shear modulus. This large

ratio implies transverse shear deformation may be significant for this problem. The second problem was a deep clamped-free cylindrical shell with transverse point load. This problem is also discussed in Chapter VI. These composite shell problems required excessive computational times, because of the small mesh sizes required to achieve converged results. Therefore, results were calculated for the axially-loaded panel using codes C120 and C123 only.

5.1 Flat Quasi-Isotropic Panel with Uniform Transverse Pressure Load

A transversely-loaded flat plate problem was used to test the MACSYMA generated elemental codes and the modified finite element program. The plate chosen was an 8-ply quasi-isotropic laminated square plate with simple boundary conditions along each of its 16-inch long sides. The plate was loaded with a uniform transverse pressure load. The plate thickness was 1.6 inches, which being 1/10 of the edge length, should indicate transverse shear may be important. The plate was analyzed by discretizing one quadrant into a 4×4 mesh of uniform elements. Only one quadrant was analyzed because symmetric response is known to occur [18:221]. The problem was solved by incrementing load in five equal increments of 7500 pounds per square inch. Material properties and boundary conditions are:

$$
\begin{aligned}
&x = 0: \quad v = w_{,2} = \psi_2 = 0 \text{ (symmetry)} \\
&s = 0: \quad u = w_{,1} = \psi_1 = 0 \text{ (symmetry)} \\
&x = \pm a/2: \quad v = w = \psi_2 = 0 \text{ (simple)} \\
&s = \pm b/2: \quad u = w = \psi_1 = 0 \text{ (simple)} \\
&a = b = 8 \text{ in}, \qquad h = 1.6 \text{ in}
\end{aligned}
$$

$$
\begin{aligned}
&E_1 = 60 \times 10^6 \text{ psi} \qquad E_2 = 1.5 \times 10^6 \text{ psi} \\
&G_{23} = 0.75 \times 10^6 \text{ psi} \qquad G_{12} = G_{13} = 0.9 \times 10^6 \text{ psi} \\
&\nu_{12} = 0.25
\end{aligned}
$$

Transverse displacements at the center of the plate, as predicted by the CXXX codes and several other references, are shown in Table 5.1. The results shown on the first line of the table were those reported by Dennis in 1988 [18:236]. The second line of results, labeled

CDON, was produced using a modified Donnell theory. This theory includes transverse shear deformation; details of this theory are given in Appendix F. The third line of Table 5.1, labeled CSTD, was produced using the unmodified SHELL program (the 8JAN double precision version which Dennis wrote). The results Dennis previously reported were slightly stiffer than the CSTD results the author obtained using the same code. The most likely reason for these differences was the increased precision of the CRAY X-MP used for the author's computations versus the VAX 8550 used by Dennis. Line four, labeled CRAS, was obtained using the author's modified SHELL program with Dennis's stiffness routines. This version tests the modification of the SHELL program. Several changes were required to calculate the additional higher-order elasticity arrays and call the subroutines for the nonlinear HTSD stiffness arrays. The lines labeled C000 through C123 were results of the eight variations of the theory developed for this research. From Table 5.1, one can see that the six quasi-nonlinear HTSD codes (CSTD, CRAS, C000, C020, C100, and C120) produce identical results. This close agreement shows that the author's theories correctly degenerate to flat plate solutions when curvature is not a factor in the problem. Similarly, the four nonlinear HTSD codes (C003, C023, C103, and C123) predict identical results. The fully-nonlinear codes, however, predict a slightly greater transverse displacement than the quasi-nonlinear codes. The final line of the table includes the results reported by Putcha and Reddy [74]. They used a mixed finite element model with parabolic transverse shear deformation to solve the von Karman plate equations. Graphical results are also shown in Figure 5.1 for three of the theories given in Table 5.1.

5.2 Hinged-Free Isotropic Shell Panel, 0.25-Inch Thick, with Transverse Point load

The second class of problems investigated was thin hinged-free isotropic cylindrical shells with transverse point load. The first problem was a 1/4-inch-thick shell. The second problem was a 1-inch-thick shell of the same configuration. The 1/4-inch shell is shown in Figure 5.2. Geometric and material properties are also given for this problem in the same figure.

Solutions were computed using a 4×6 mesh of elements to model one quadrant of the shell. Convergence studies by Dennis [18:247] showed little difference in results between

Table 5.1. Comparison of Flat Plate Displacement Results for Variations of Geometrically Nonlinear HTSD Theory with Linear and Nonlinear Transverse Shear Strain Displacement

Total Load (psi)	7500	15000	22500	30000	37500
Ref. [18:236]	0.4414	0.7797	1.036	1.240	1.412
CDON (1)	0.4446	0.7939	1.065	1.288	1.479
CSTD (2)	0.4454	0.7982	1.076	1.308	1.513
CRAS (3)	0.4454	0.7982	1.076	1.308	1.513
C000	0.4454	0.7982	1.076	1.308	1.513
C020	0.4454	0.7982	1.076	1.308	1.513
C100	0.4454	0.7982	1.076	1.308	1.513
C120	0.4454	0.7982	1.076	1.308	1.513
C003	0.4457	0.8001	1.081	1.317	1.527
C023	0.4457	0.8001	1.081	1.317	1.527
C103	0.4457	0.8001	1.081	1.317	1.527
C123	0.4457	0.8001	1.081	1.317	1.527
Ref. [74:537]	0.45	0.80	1.1	1.3	1.5

(1) CDON refers to results obtained using program SHELL with stiffness arrays corresponding to a modified Donnell theory with transverse shear (see Appendix F for details)

(2) CSTD refers to results obtained using program SHELL, as written by Dennis [18], with Dennis's $\left[\hat{K}\right]$, $\left[\hat{N}_1\right]$, and $\left[\hat{N}_2\right]$ stiffness array subroutines

(3) CRAS refers to results obtained using program SHELL as modified to incorporate COOX subroutines, but calling Dennis's stiffness array subroutines to test the modifications made to SHELL.

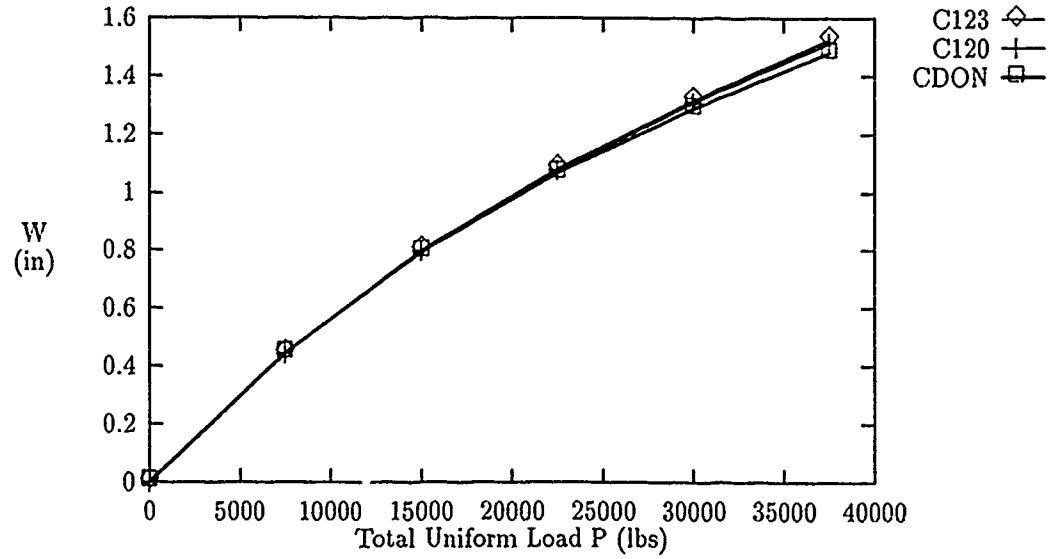

Figure 5.1. Comparison of Flat Plate Displacement Results for Variations of Geometrically Nonlinear HTSD Theory with Linear and Nonlinear Transverse Shear Strain Displacement

4 × 6 and 8 × 8 meshes. Significant computational savings result when the 24 element mesh is used instead of the 64 element mesh. Table 5.2 shows the results of equilibrium load predictions, for increments of transverse displacement from 0.1 to 1.0 inches, for the eight elemental codes and the modified-Donnell theory with transverse shear included (CDON). The values of load shown are four times the equilibrium load of the quarter shell; this load represents the total load on the entire shell panel. Values were computed using 10 increments of center point transverse displacement. One quadrant of the shell was modeled using a 24 element mesh with 4 elements in the lateral direction and 6 elements in the circumferential direction. From this table one observes the quasi-nonlinear HTSD codes (CXX0) all produce the same results, and the nonlinear HTSD codes (CXX3) all produce the same results. The results of the CDON, C120, and C123 codes were selected for more detailed analysis, since they represent the three variations with different results.

Figures 5.3 and 5.4 show the equilibrium paths of transverse load versus center-point displacement for the 1/4-inch shell predicted by the CDON and C120 codes, and by the CDON and C123 codes, respectively. As in the flat plate case, the results for the quasi-nonlinear HTSD codes are all the same. In contrast, the nonlinear HTSD codes all show

Boundary Conditions:
$x = 0$: $u, w_{,1}, \psi_1 = 0$ (symmetry)
$s = 0$: $v, w_{,2}, \psi_2 = 0$ (symmetry)
$s = \pm 10$: $u = v = w = \psi_1 = 0$ (hinged)
$x = \pm 10$: (free)

Other Data:
$E = 4.5 \times 10^5$ psi
$\theta = 0.1$ radians
$h = 0.25$ in.
$R = 100$ in.
$L = 20$ in.
$\nu = 0.3$

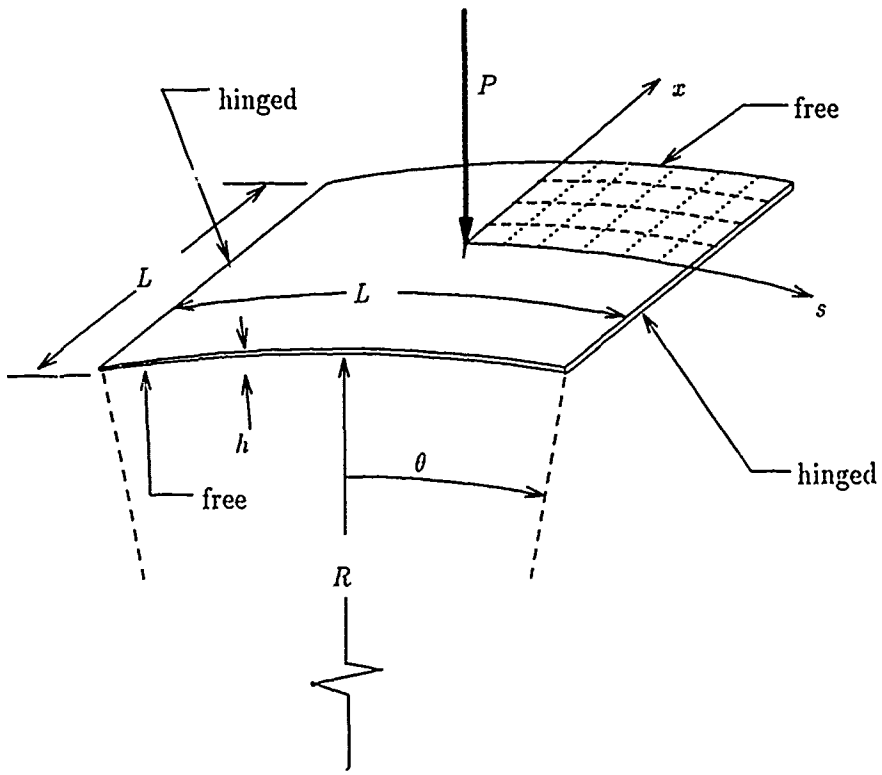

Figure 5.2. 1/4-Inch Hinged-Free Point-Loaded Isotropic Cylindrical Shell

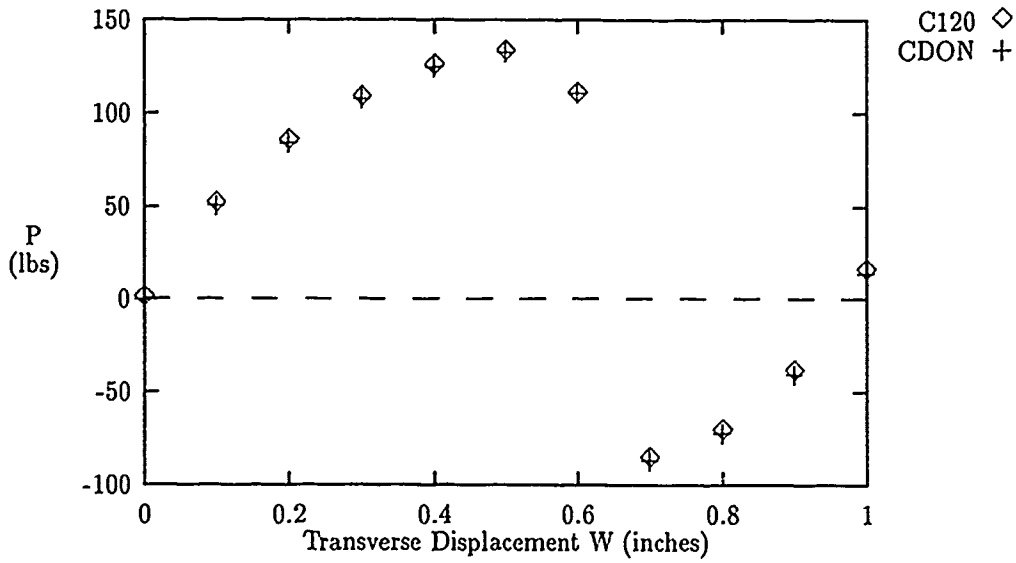

Figure 5.3. Equilibrium Path Comparisons for 1/4-inch Hinged-Free Cylindrical Shell — CDON and C120 Theories

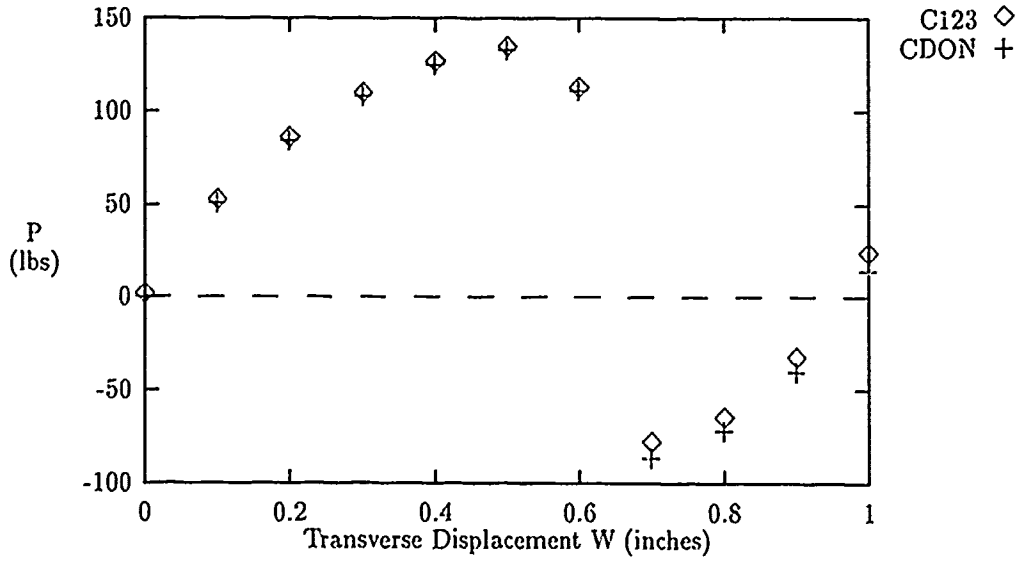

Figure 5.4. Equilibrium Path Comparisons for 1/4-inch Hinged-Free Cylindrical Shell — CDON and C123 Theories

Table 5.2. Predicted Transverse Point For Center Transverse Displacement of 1/4-inch Hinged-Free Isotropic Cylindrical Shell Panel

Disp.	CDON	C000	C020	C100	C120	C003	C023	C103	C123
0.1	50.6	50.6	50.6	50.6	50.6	50.6	50.6	50.6	50.6
0.2	84.2	84.2	84.2	84.2	84.2	84.2	84.2	84.2	84.2
0.3	107.7	107.7	107.7	107.7	107.7	107.7	107.7	107.7	107.7
0.4	125.0	124.6	124.6	124.6	124.6	124.9	124.9	124.9	124.9
0.5	133.0	132.4	132.4	132.4	132.4	133.0	133.0	133.0	133.0
0.6	111.2	109.6	109.6	109.6	109.6	111.1	111.1	111.1	111.1
0.7	-86.6	-86.6	-86.6	-86.6	-86.6	-79.5	-79.5	-79.5	-79.5
0.8	-72.0	-71.5	-71.5	-71.5	-71.5	-66.3	-66.3	-66.3	-66.3
0.9	-40.3	-39.6	-39.6	-39.6	-39.6	-33.9	-33.9	-33.9	-33.9
1.0	13.9	14.7	14.7	14.7	14.7	22.2	22.2	22.2	22.2

slightly greater flexibility (a smaller magnitude of load) during the collapse phase (from $w = 0.7$–0.9) than the quasi-nonlinear HTSD variants. This trend is shown in Figures 5.5 and 5.6 where the difference between loads predicted by the CDON and C120, and CDON and C123 theories are plotted versus transverse displacement. Values plotted in these figures are the relative difference (in percent) between the values of load predicted by the C120, or C123, and CDON theories. A negative value is given for data points where the new theory (C120 or C123) codes predict a more flexible structure (less transverse load required to achieve the same displacement) than the CDON code. Similarly, a positive value indicates a stiffer prediction for the C120, or C123, code than the CDON code. From Figure 5.5, one can see the C120 theory predicts a slightly more flexible structure at points, but this difference is negligible. From Figure 5.6, one can see the C123 theory predicts a load about 8 percent less in magnitude than the CDON theory in the range $0.7 \leq w \leq 0.8$ and about 15 percent less at $w = 0.9$. Once the shell has reached the point where it is fully snapped though, around $w = 1.0$, the C123 theory predicts a significantly stiffer structure than either the CDON or C120 theories. This is caused by the increased coupling of transverse terms with in-plane terms.

This result is interesting, since this phase of the collapse is characterized by the most extreme displacements and rotations occurring in the problem. The inclusion of nonlinear

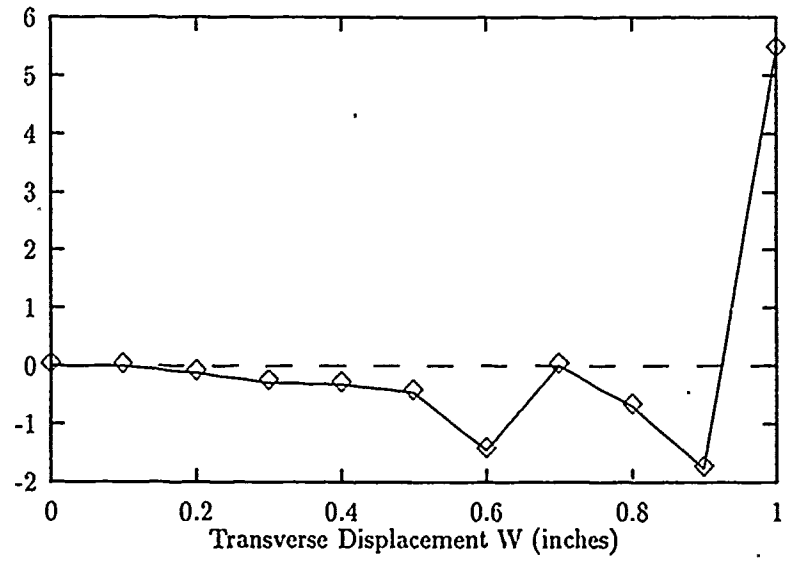

Figure 5.5. Percent Relative Load Difference Comparisons for Transversely Loaded 1/4-inch Shell — CDON and C120 Theories

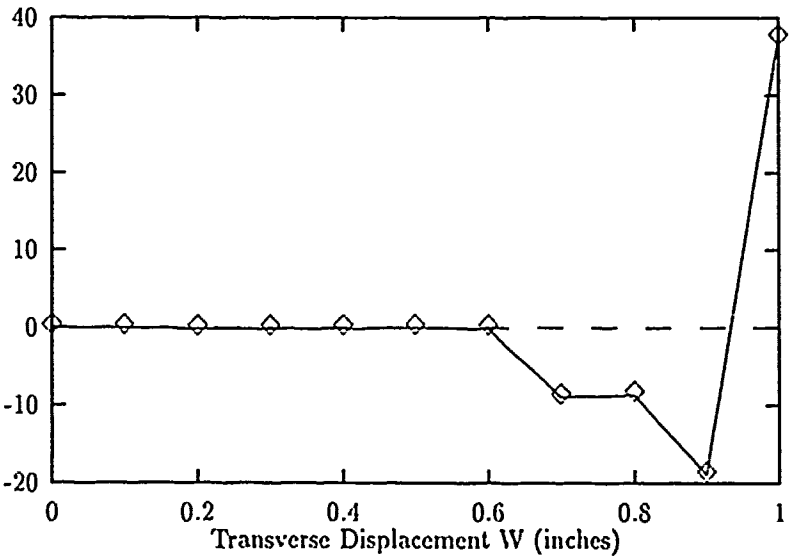

Figure 5.6. Percent Relative Load Difference Comparisons for Transversely Loaded 1/4-inch Shell — CDON and C123 Theories

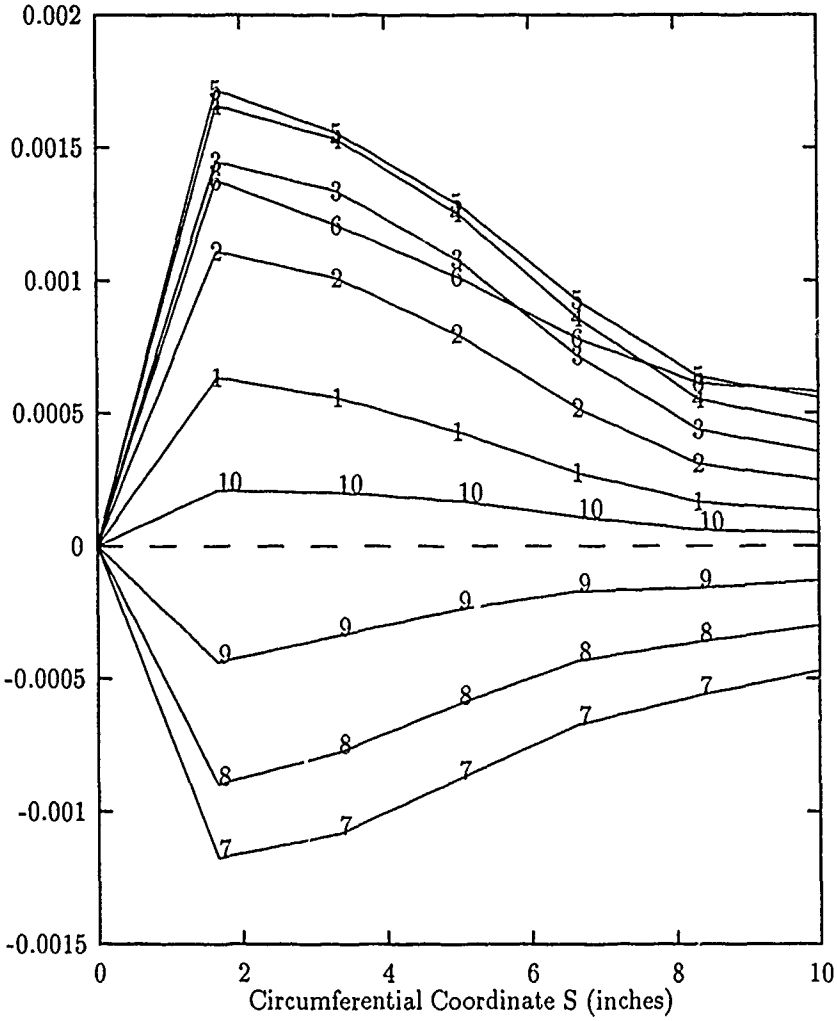

Figure 5.7. Meridian Values of $\psi_2 + w_{,2}$ for 10 Increments, 0.1-inch each, of Transverse Displacement of 1/4-inch Hinged-Free Cylindrical Shell — CDON Theory

transverse shear terms for this problem had a noticeable effect upon load-displacement results. Figures 5.7 and 5.8 show values of the linear χ_4^0 transverse shear term, $\psi_2 + w_{,2}$, for ten increments for transverse displacement w for the CDON and C123 theories, respectively. Values plotted are the values of $\psi_2 + w_{,2}$ at nodes along the $x = 0$ line from the center of the panel ($s = 0$) out to the hinge line ($s = 10$). The labels 1,...,10 indicate the 1st through 10th increments of transverse displacement w. These results are virtually identical for increments 1–6, before the shell snaps through. After the shell snaps, however, the values of $\psi_2 + w_{,2}$ are about 20–25 percent less in magnitude over the majority of the

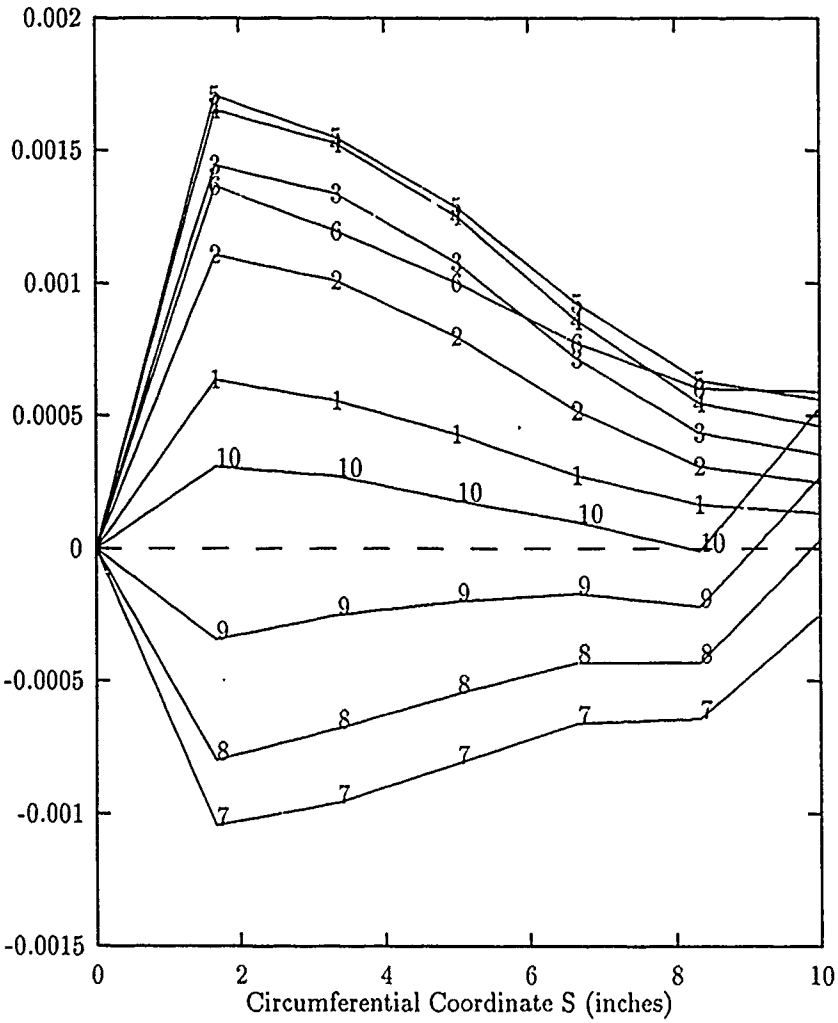

Figure 5.8. Meridian Values of $\psi_2 + w_{,2}$ for 10 Increments, 0.1-inch each, of Transverse Displacement of 1/4-inch Hinged-Free Cylindrical Shell — C123 Theory

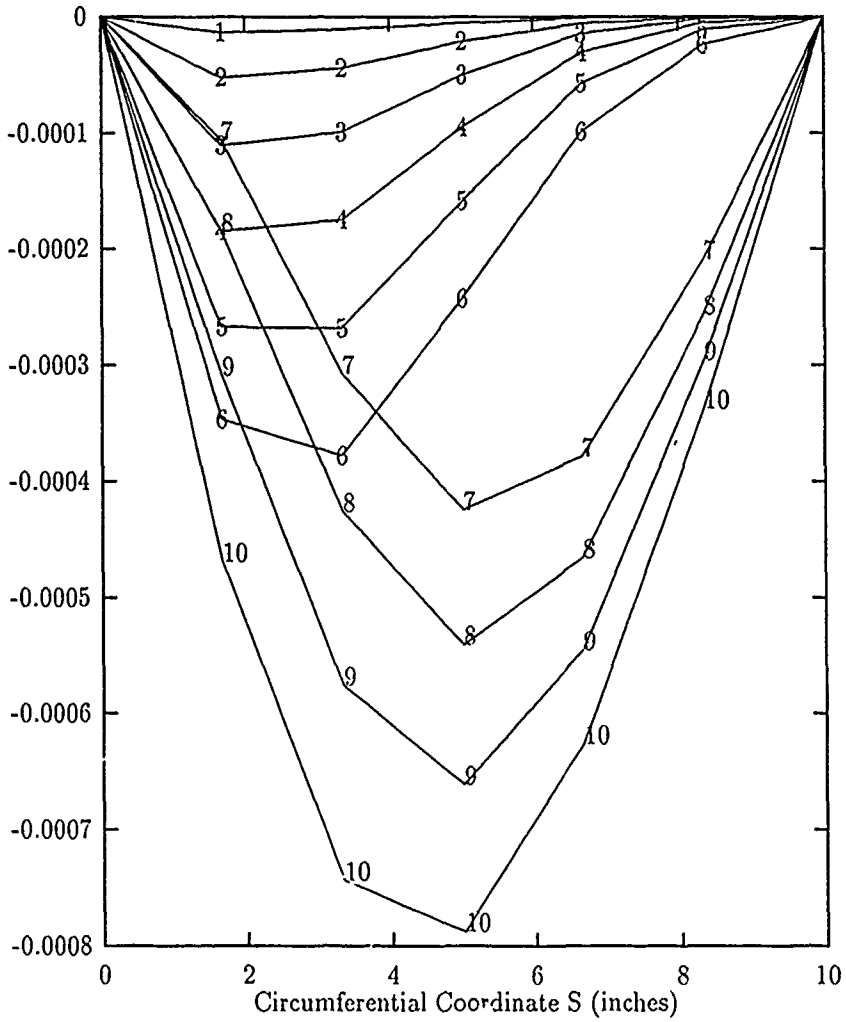

Figure 5.9. Meridian Values of $-w\psi_2/R_2$ for 10 Increments, 0.1-inch each, of Transverse Displacement of 1/4-inch Hinged-Free Cylindrical Shell — C123 Theory

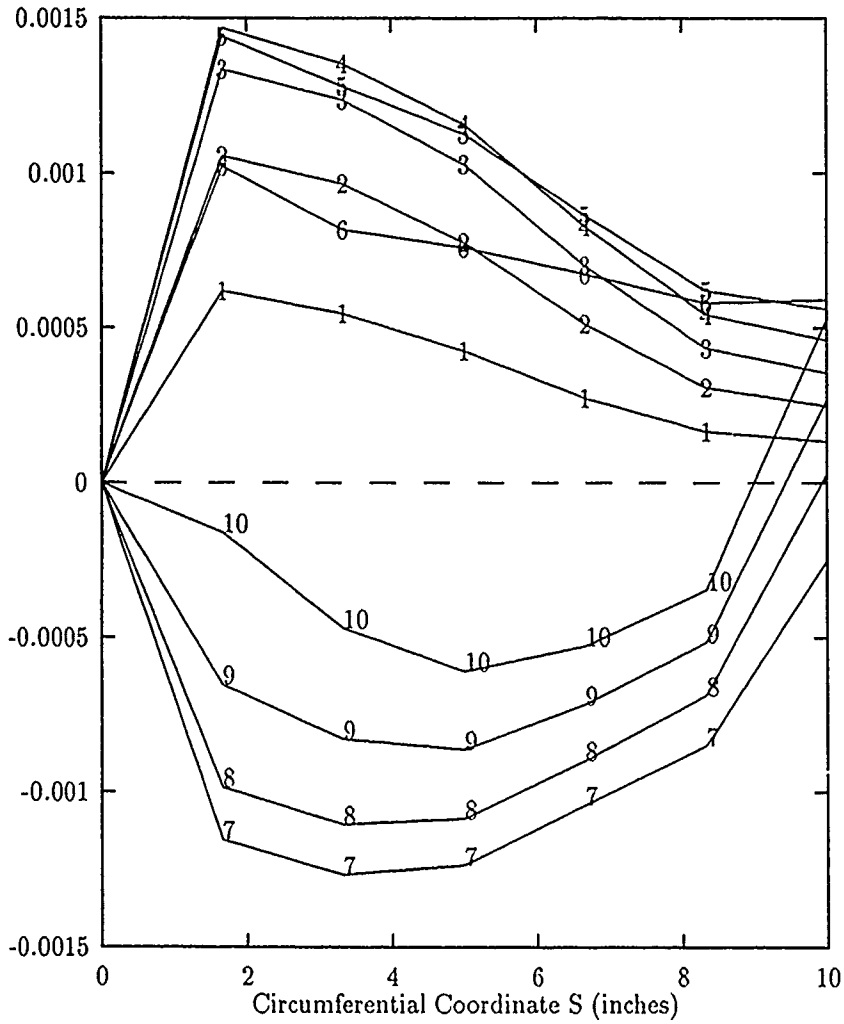

Figure 5.10. Meridian Values of $\psi_2 + w_{,2} - w\psi_2/R_2$ for 10 Increments, 0.1-inch each, of Transverse Displacement of 1/4-inch Hinged-Free Cylindrical Shell — C123 Theory

panel, where $1 \leq s \leq 8$, for the C123 theory as compared to the CDON quasi-nonlinear theory. In Figure 5.8, the value of $\psi_2 + w_{,2}$ is dramatically more positive at the hinge line ($s = 10$) during increments 7–10 for the C123 theory than for the CDON theory.

These figures show the values of only the linear term of the χ_4^0 term of the ε_{23} strain at the midsurface of the shell. For the nonlinear HTSD theory, the ε_{23} and ε_{13} strain components include many more nonlinear terms. These terms are shown for the C003, C023, C103 and C123 theories in Appendices B–E as $\chi^p_{4_{NL}}$ and $\chi^p_{5_{NL}}$. The distribution of shear strain is significantly affected by including the nonlinear transverse shear terms. Figure 5.9 shows the largest nonlinear term of the χ_4^0 term of the transverse shear strain component for the C123 theory. This term, $-w\psi_2/R_2$, and the linear term, $\psi_2 + w_{,2}$, are the predominant terms of the χ_4^0 strain component. Table 5.3 shows a comparison of these terms for the three theories. From Table 5.3, for increment 5 when the largest

Table 5.3. Comparison of Maximum Values of Linear and Nonlinear Terms of χ_4^0 for the 1/4—inch Cylindrical Shell

Code Name	χ_4^0 Term	Increment 1	5	7	8	9	10
CDON	$\psi_2 + w_{,2}$	.0006	.0017	-.0012	-.0009	-.0004	.0002
C123	$\psi_2 + w_{,2}$	.0006	.0017	-.0010	-.0007	-.0003	.0003
C123	$-w\psi_2/R_2$	.0000	-.0002	-.0004	-.0005	-.0006	-.0008
C123	$\psi_2 + w_{,2} - w\psi_2/R_2$	.0006	.0015	-.0014	-.0012	-.0009	-.0005

magnitude of $\psi_2 + w_{,2}$ occurs, the maximum values of $\psi_2 + w_{,2}$ and $-w\psi_2/R_2$ are 0.0017 and -0.0002, respectively. Thus, the largest nonlinear term of C123 is less than 20 percent of the linear term. With each increment from 7 to 9 (after the shell has snapped through), the nonlinear term becomes more significant compared with the linear terms. This nonlinear term, while it is of comparable magnitude with the linear terms, creates a softening effect. It effectively increases the magnitude of the transverse shear strain over a large area of the shell's midsurface.

Figure 5.10 shows the value of of $\psi_2 + w_{,2} - w\psi_2/R_2$ for the C123 theory. Comparing this figure with Figures 5.7 and 5.8 reveals the significant difference in the transverse shear terms for the nonlinear theory, as compared to the quasi-nonlinear HTSD theories. This

difference is large enough to affect the strain energy of the shell and subsequently results in slightly different equilibrium values of the nodal displacements for the C123 theory as compared to the CDON or C120 theories. At increment 10 when the largest magnitude of $-w\psi_2/R_2$ occurs, the magnitude of this nonlinear term exceeds that of the linear terms by some 800 percent. Thus, the beneficial effect of transverse shear has been totally obliterated by the nonlinear terms of this formulation. Palmerio and Reddy [66] reported an overstiff response for similar shells when nonlinear transverse shear was included in their formulation (See Chapter II, page 2-24, for more details on their work).

5.3 Hinged-Free Isotropic Shell Panel, 1.0-Inch Thick, with Transverse Point load

Table 5.4. Predicted Transverse Point Load for Center Transverse Displacement of 1-inch Hinged-Free Isotropic Cylindrical Shell Panel

Disp.	CDON	C123
0.1	830.3	826.5
0.2	1476.4	1467.6
0.3	1948.1	1933.6
0.4	2263.0	2242.7
0.5	2454.6	2430.0
0.6	2579.7	2554.7
0.7	2716.1	2697.5
0.8	2944.2	2940.2
0.9	3326.8	3345.3
1.0	3902.7	3950.4

A 1-inch thick isotropic shell exhibits a significantly different equilibrium path than the 1/4-inch shell. For this case, the shell never "snaps"; load always increases monotonically for all values of transverse displacement. The effects of nonlinear HTSD should be different in this case. The data of Figure 5.11 applies for this case. As shown in Figure 5.12, the increase in thickness significantly affects the equilibrium path of this shell. Data from the various theories are given in Table 5.4 Although the curvature of the shell, initially and finally, compares with that of the thin shell, the thicker shell never snaps through to the concave position. Figure 5.13 shows the relative differences between the CDON and

Boundary Conditions:
$x = 0: \quad u, w_{,1}, \psi_1 = 0$ (symmetry)
$s = 0: \quad v, w_{,2}, \psi_2 = 0$ (symmetry)
$s = \pm 10: \quad u = v = w = \psi_1 = 0$ (hinged)
$x = \pm 10: \quad$ (free)

Other Data:
$E = 4.5 \times 10^5$ psi
$\theta = 0.1$ radians
$h = 1$ in.
$R = 100$ in.
$L = 20$ in.
$\nu = 0.3$

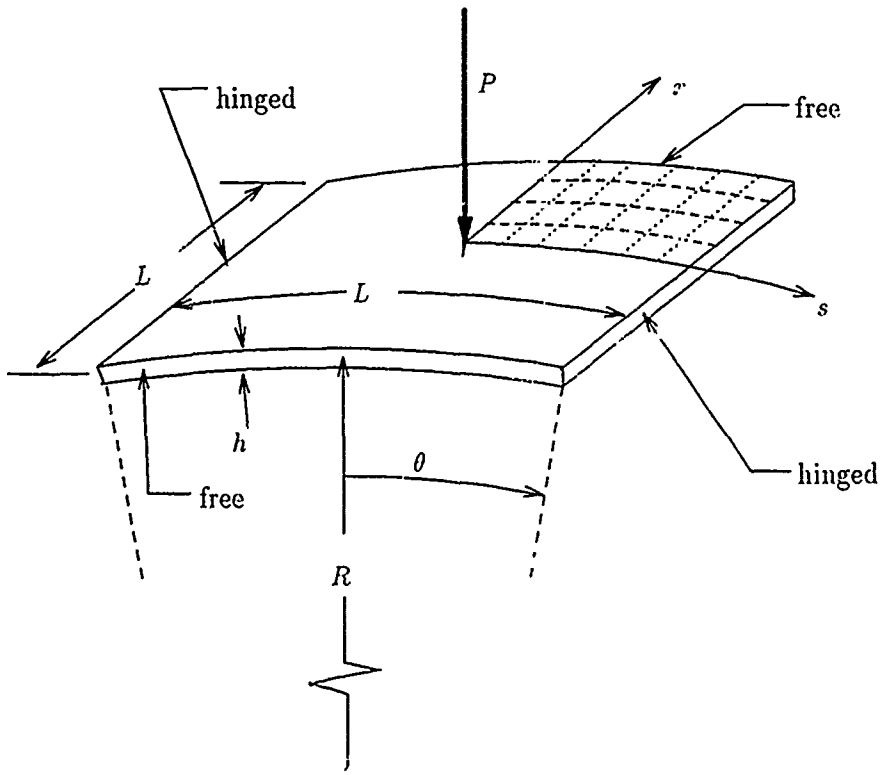

Figure 5.11. 1-Inch Hinged-Free Point-Loaded Isotropic Cylindrical Shell

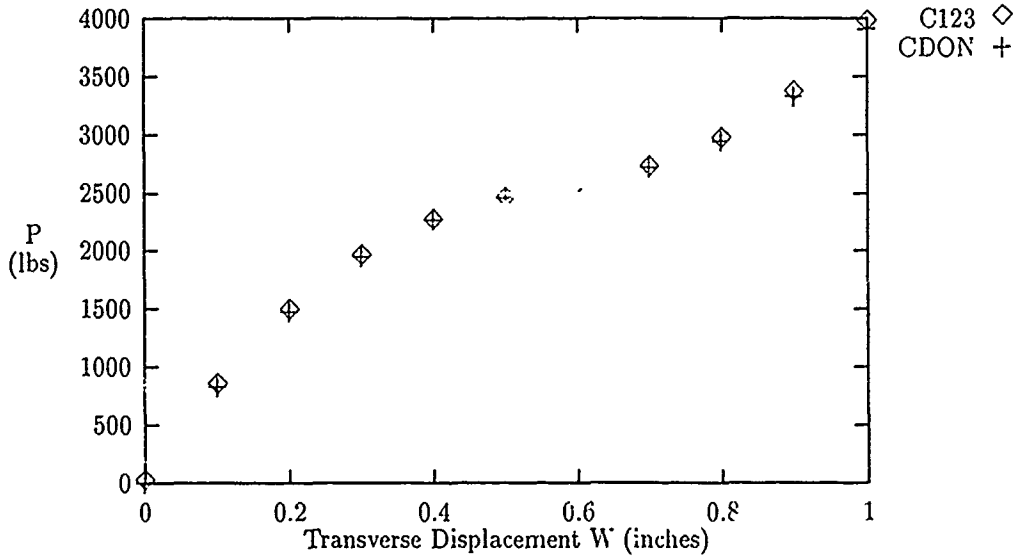

Figure 5.12. Equilibrium Path Comparisons for 1-Inch Hinged-Free Cylindrical Shell — CDON and C123 Theories

C123 theory. In this case there is less than about 1 percent difference over most of the graph.

Figures 5.14–5.17 show the linear χ_4^0 term $\psi_2 + w_{,2}$ and the largest nonlinear term $-w\psi_2/R_2$ for this shell with the CDON and C123 theories. Comparing the maximum value of Figure 5.17 with that of Figure 5.15, we can clearly see the significantly different character of the nonlinear transverse shear terms. Despite this difference, the in-plane extensional and bending terms in the strain energy expression for this shell are predominant. Thus, the equilibrium path is little affected by these changes in transverse shear strain.

5.4 Clamped-Free Quasi-Isotropic Shell Panel with 4-Inch Square Cut-Out and Axial Compression Load

The earlier quasi-isotropic flat panel results indicated the nonlinear HTSD codes predicted a slightly more flexible response than their quasi-nonlinear HTSD variants. Similarly, for the collapse phase of the thin isotropic cylindrical shell, the nonlinear HTSD codes also predicted a slightly more flexible response than their quasi-nonlinear HTSD variants. In both cases, the more exact geometric approximations predicted responses vir-

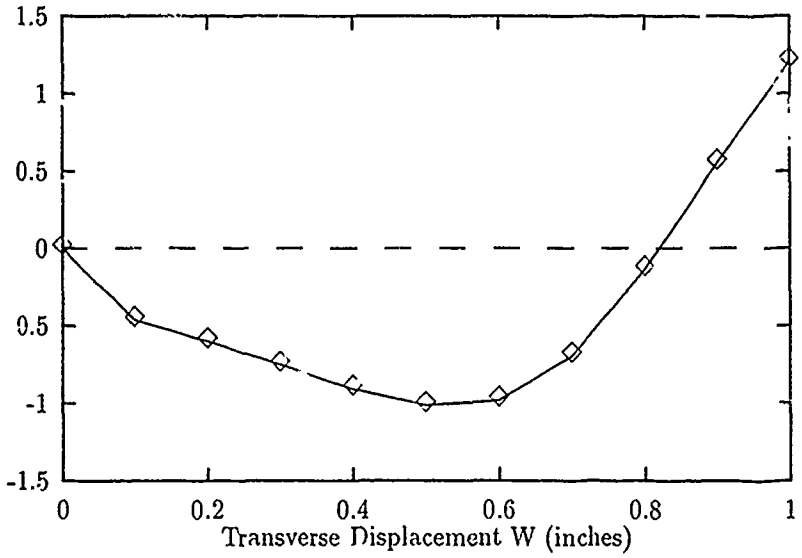

Figure 5.13. Relative Load Difference Comparisons for Transversely Loaded 1–Inch Shell — CDON and C123 Theories

tually identical to the simplest elemental codes. Problems combining the quasi-isotropic material and a smaller radius of curvature with large displacements and rotations should provide more interesting comparisc

The first problem selected was an axially-loaded quasi-isotropic cylindrical shell panel with a centrally-located cut-out. Figure 5.18 shows the shell configuration and gives boundary conditions and material data. Panels of this general configuration have been the subject of many AFIT research projects, conducted in cooperation with the Wright Laboratory at Wright-Patterson AFB, Ohio. Panels of this material and configuration were recently tested experimentally, as part of a Master's thesis by Schimmels [88]. The experimental procedures used for these experiments were similar to experimental procedures used by Becker [6], Janisse [33], and Tisler [60, 61, 58, 101] at Wright-Patterson AFB. Results of Tisler were used by Dennis for his comparisons of the linear HTSD theory he developed [18, 22]. According to Palazotto and Dennis, Tisler had problems with the experimental measurements and with the panels not being properly seated in the test fixtures [22:1087]. These particular problems were avoided during the latest series of experiments [88].

Table 5.5 shows results for total-applied compression load versus axial displacement

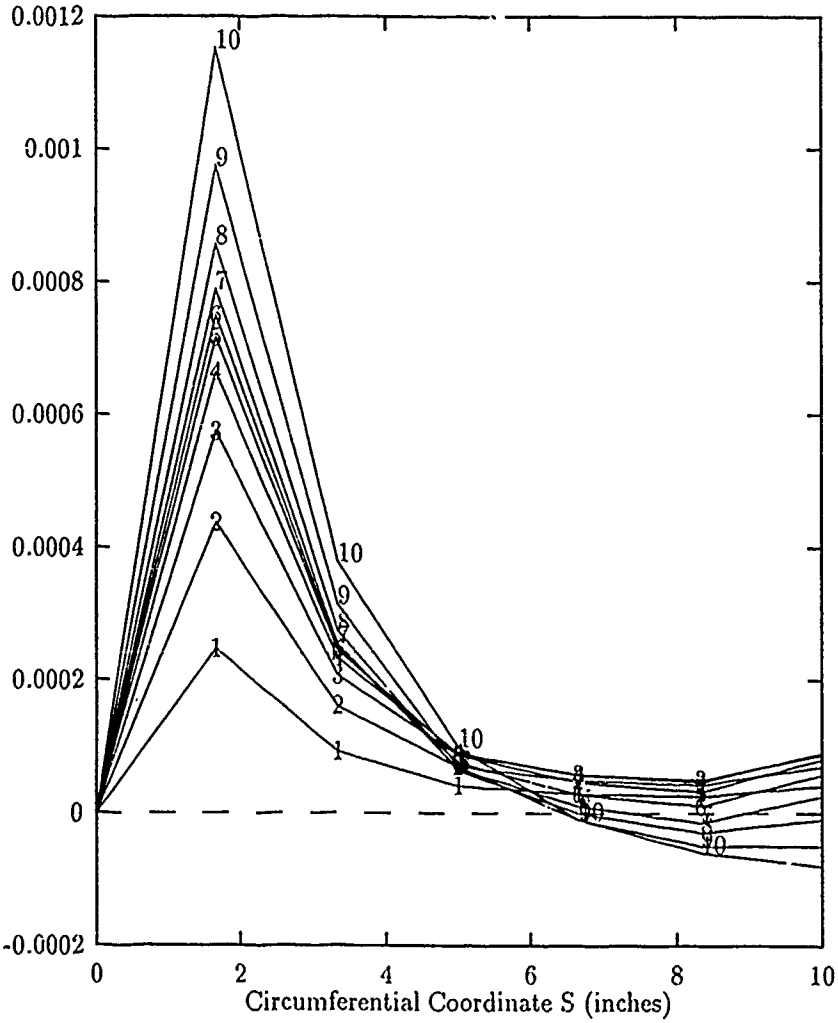

Figure 5.14. Meridian Values of $\psi_2 + w_{,2}$ for 10 Increments, 0.1-Inch each, of Transverse Displacement of 1-Inch Hinged-Free Cylindrical Shell — CDON Theory

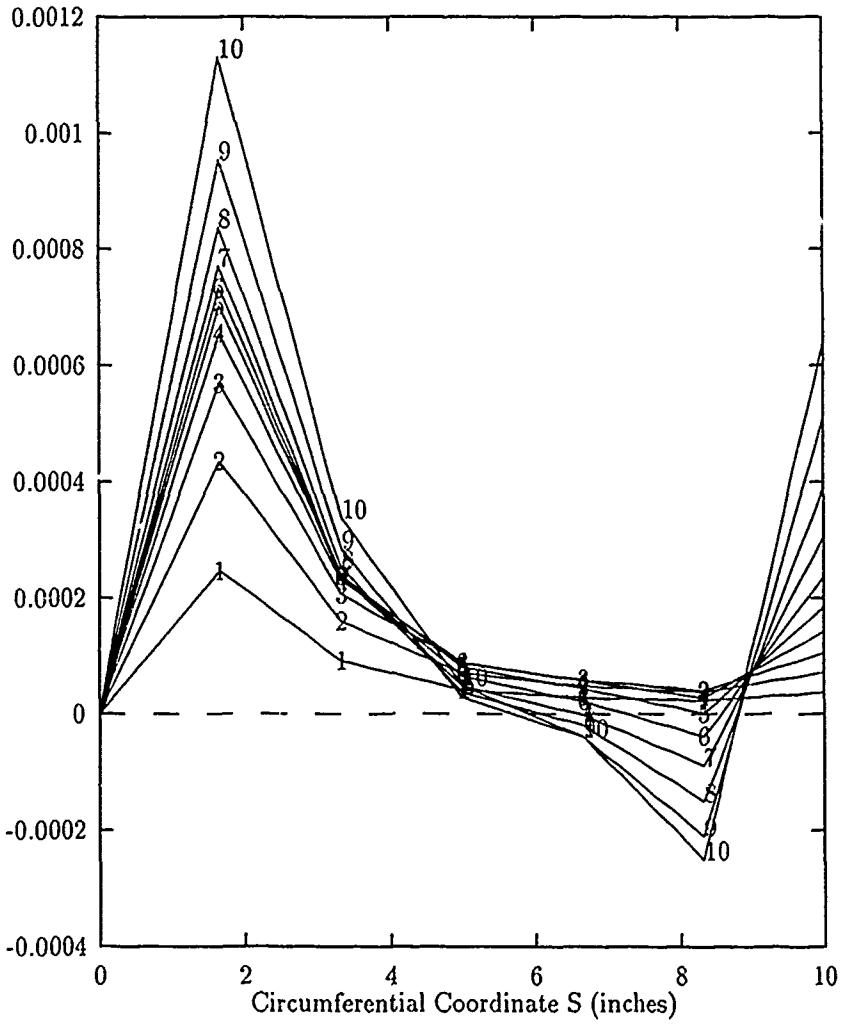

Figure 5.15. Meridian Values of $\psi_2 + w_{,2}$ for 10 Increments, 0.1-Inch each, of Transverse Displacement of 1-Inch Hinged-Free Cylindrical Shell — C123 Theory

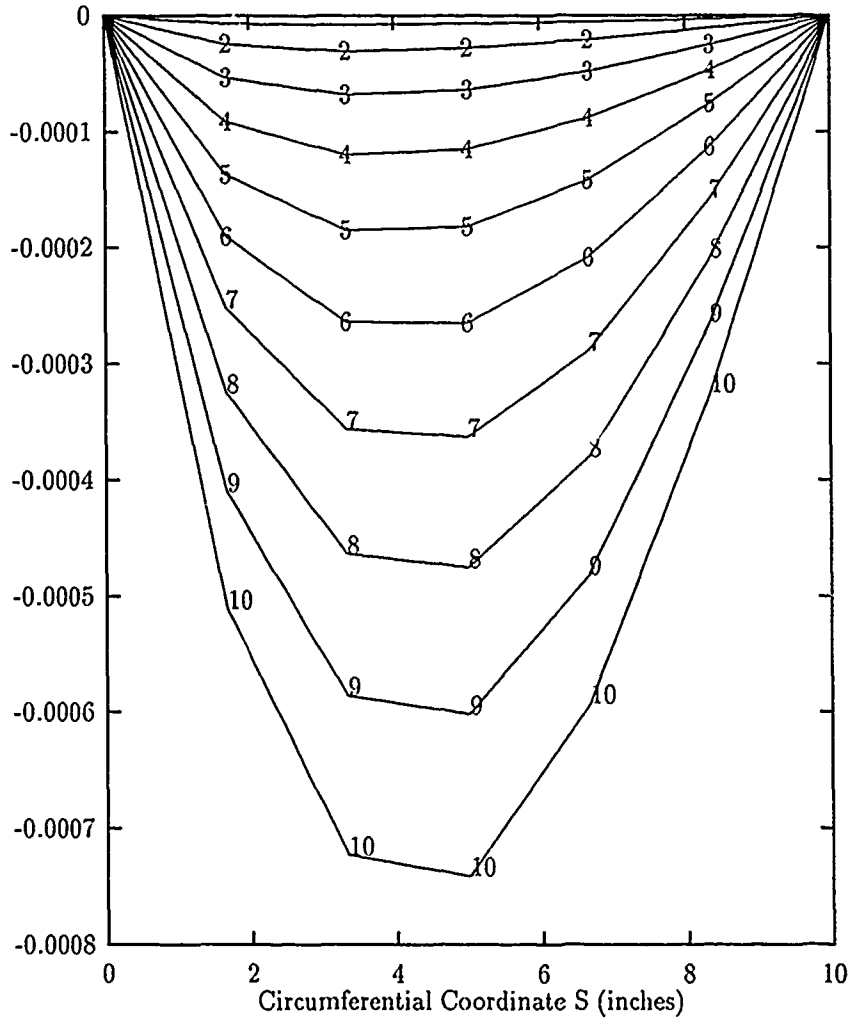

Figure 5.16. Meridian Values of $-w\psi_2/R_2$ for 10 Increments, 0.1-Inch each, of Transverse Displacement of 1-Inch Hinged-Free Cylindrical Shell — C123 Theory

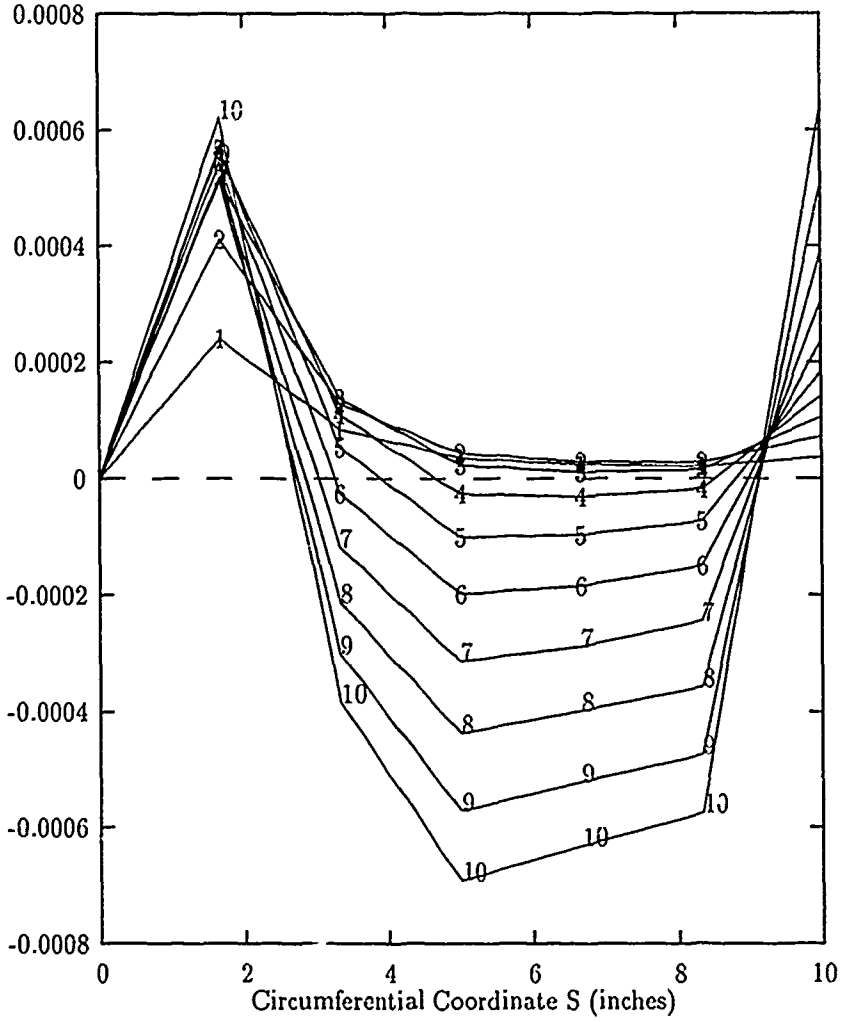

Figure 5.17. Meridian Values of $\psi_2 + w_{,2} - w\psi_2/R_2$ for 10 Increments, 0.1-Inch each, of Transverse Displacement of 1-Inch Hinged-Free Cylindrical Shell — C123 Theory

Boundary Conditions: $x = +11 : v, w, w_{,1}, w_{,2}, \psi_1, \psi_2 = 0$, (clamped, u controlled)
$x = 0 : u, v, w, w_{,1}, w_{,2}, \psi_1, \psi_2 = 0$, (clamped)
$s = 0$: (free)
$s = 8$: (free)
Cut-out: 4 in centered

Other Data: [88:4-2]
Material: AS4-3501 Graphite Epoxy
$E_1 = 20.461 \times 10^6$ psi
$E_2 = 1.3404 \times 10^6$ psi
$G_{12} = 0.8638 \times 10^6$ psi
$\nu_{12} = 0.301$
Ply Layup:
[0/-45/+45/90]s
$\theta = 0.75$ radians
$h = 0.05$ in.
$R = 12$ in.
$A = 11$ in.
$B = 8$ in.

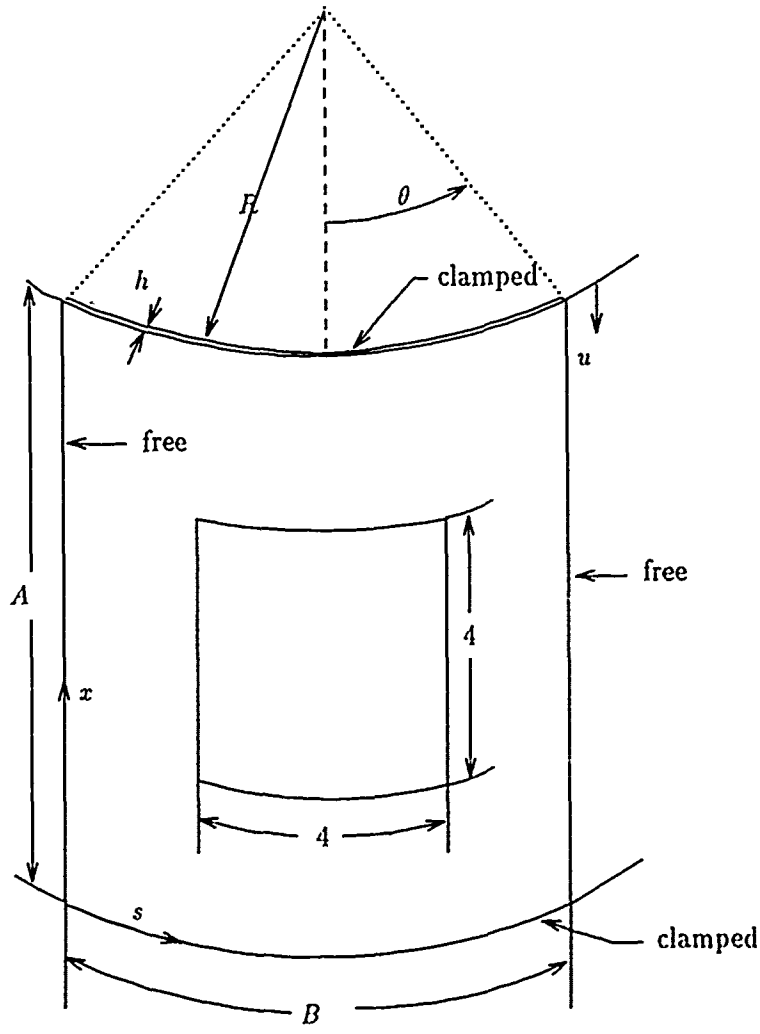

Figure 5.18. Quasi-Isotropic 12-Inch Radius Cylindrical Composite Shell with Centered 4-Inch Cut-Out and Free Edges Loaded in Axial Compression

u computed with the C120 and C123 theories. Values of transverse displacement w are also shown in this table. As shown in the table, the nonlinear HTSD theory gives virtually identical results to those of the quasi-nonlinear theory. Figure 5.19 shows predicted transverse displacement of a point, located at the shell's lateral center line ($x = 5.5$) and 1.5-inches in from the lateral edge ($s = 1.5$), versus axial displacement u for the C120 and C123 theories. Figure 5.20 shows the difference between the two theories as axial displacement is increased.

Table 5.5. Axial Displacement vs Transverse Displacement and Load for a 12-inch Radius 11 × 8-inch Quasi-Isotropic Cylindrical Shell Panel with Centered 4-inch Cutout under Axial Compressive Load — C120 and C123 Theories and Experimental

Axial	C120		C123	
Disp (in)	W† (in)	Load (lbs)	W† (in)	Load (lbs)
0.001	.002741	133.1	.002741	133.1
0.002	.008689	260.1	.008689	260.1
0.003	.002400	354.1	.002398	354.2
0.004	.04472	392.7	.04467	393.0
0.005	.06300	411.5	.06293	412.3
0.010	.1282	430.6	.1281	434.4
0.015	.1712	422.4	.1710	430.2
0.020	⋆	⋆	.2045	410.8

† W is measured at $(x, s) = (5.5, 1.5)$
⋆ Datum point not computed

Figures 5.21–5.24 show the linear χ_4^0 term $\psi_2 + w_{,2}$ and the largest nonlinear term $-w\psi_2/R_2$ for this shell with the C120 and C123 theories. Comparing the maximum values of Figure 5.24 with those of Figure 5.22, we can see for this case, the nonlinear χ_4^0 terms of the C123 theory are virtually identical to the linear χ_4^0 terms of the C120 theory. This could be attributed to many characteristics of this problem. The most significant difference between this panel and panels reported earlier is the ratio of thickness to characteristic length. The plate was 1.6-inches thick with an edge length of 16 inches. The isotropic shells had thicknesses of 1/4 and 1 inch with edge lengths of 20 inches. The axial panel

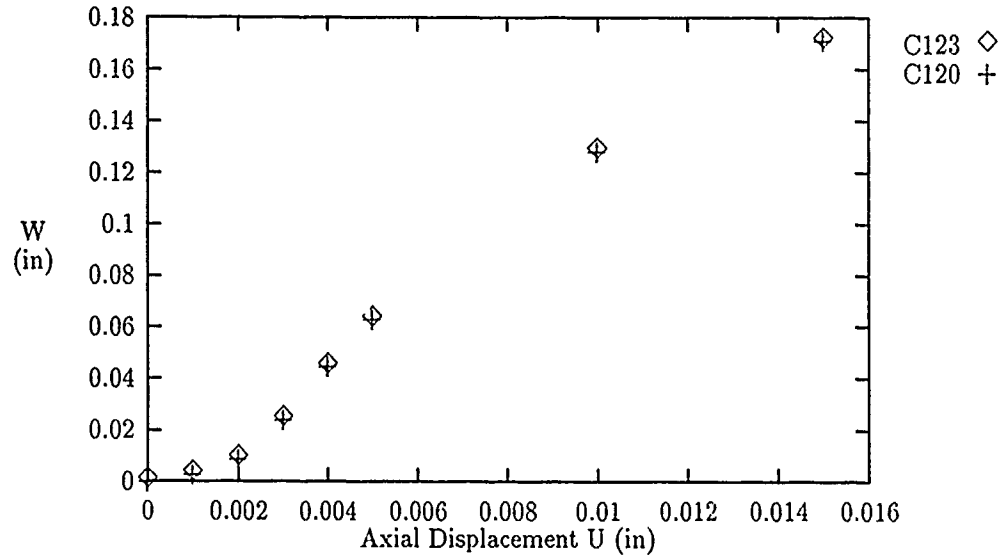

Figure 5.19. Transverse Displacement vs Axial Displacement at $(x, s) = (5.5, 1.5)$ — C120 and C123 Results for 11×8-inch Axially-Compressed Composite Panel with Centered 4-inch Cutout

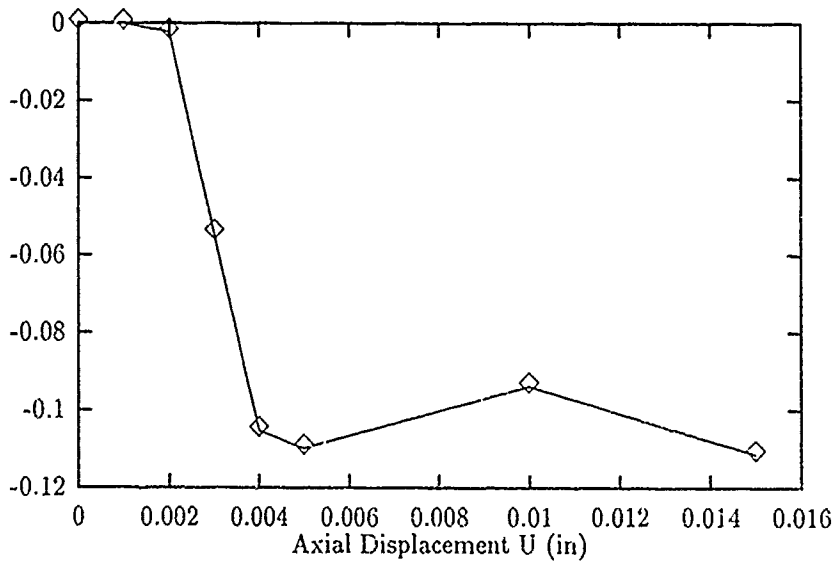

Figure 5.20. Difference in Transverse Displacement vs Axial Displacement at $(x, s) = (5.5, 1.5)$ — C120 and C123 Results for 11×8-inch Axially-Compressed Composite Panel with Centered 4-inch Cutout

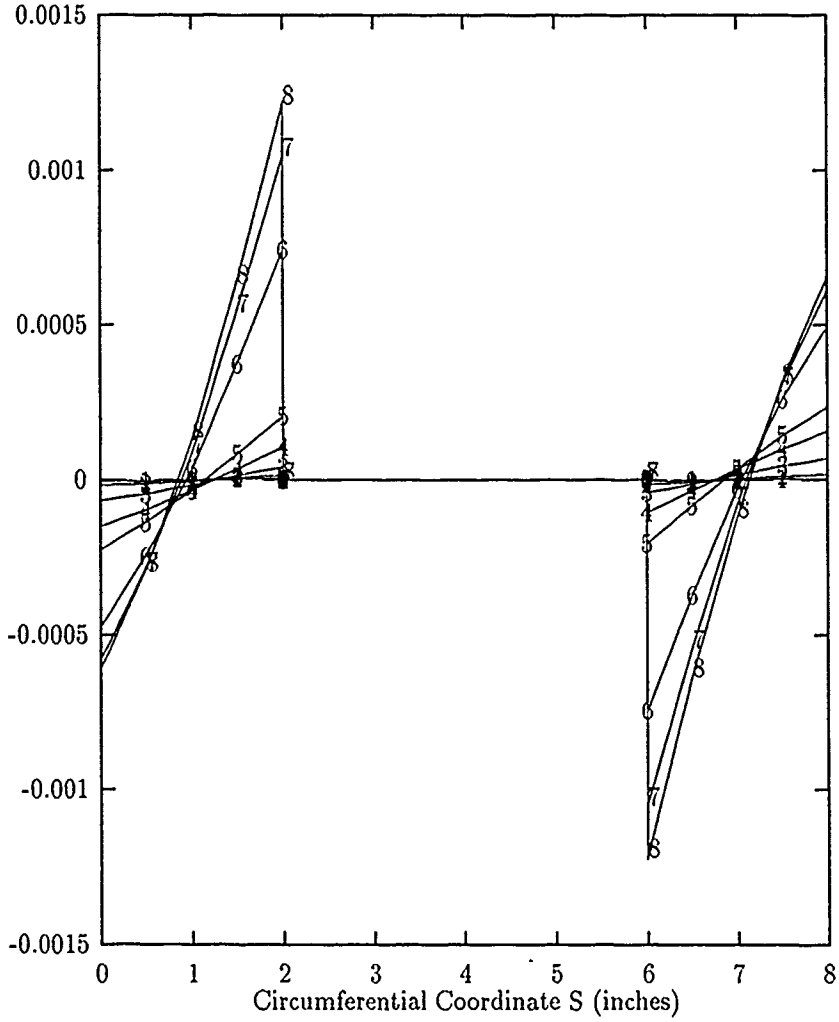

Figure 5.21. Meridian Values of $\psi_2 + w_{,2}$ for Increments of Axial Displacement of 12-inch Radius Composite Shell with Centered Cutout — C120 Theory

is 0.05-inches thick with radius and minimum edge length of 8 inches, respectively. Based on Koiter's work the transverse shear strains for these problems would be of the order h/L times the in-plane strains. Thus, for the plate the transverse shear strains would be about 1/10th the in-plane strains. For the isotropic shells the transverse shear strains would be 1/80th of the in plane strains. Finally, for the axial panel these strains are about 1/160th of the in-plane strains. Considering the relative magnitudes of transverse deflection, the axial panel represents a rather mild test of transverse shear behavior compared to the other two problems.

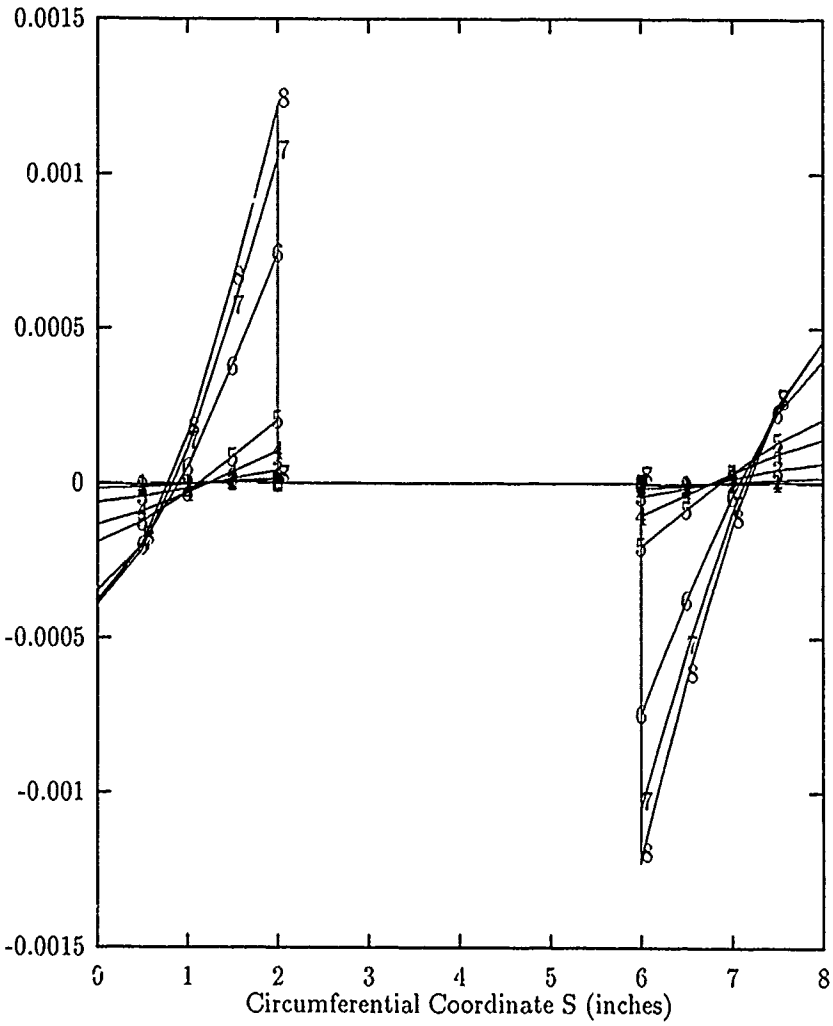

Figure 5.22. Meridian Values of $\psi_2 + w_{,2}$ for Increments of Axial Displacement of 12-inch Radius Composite Shell with Centered Cutout — C123 Theory

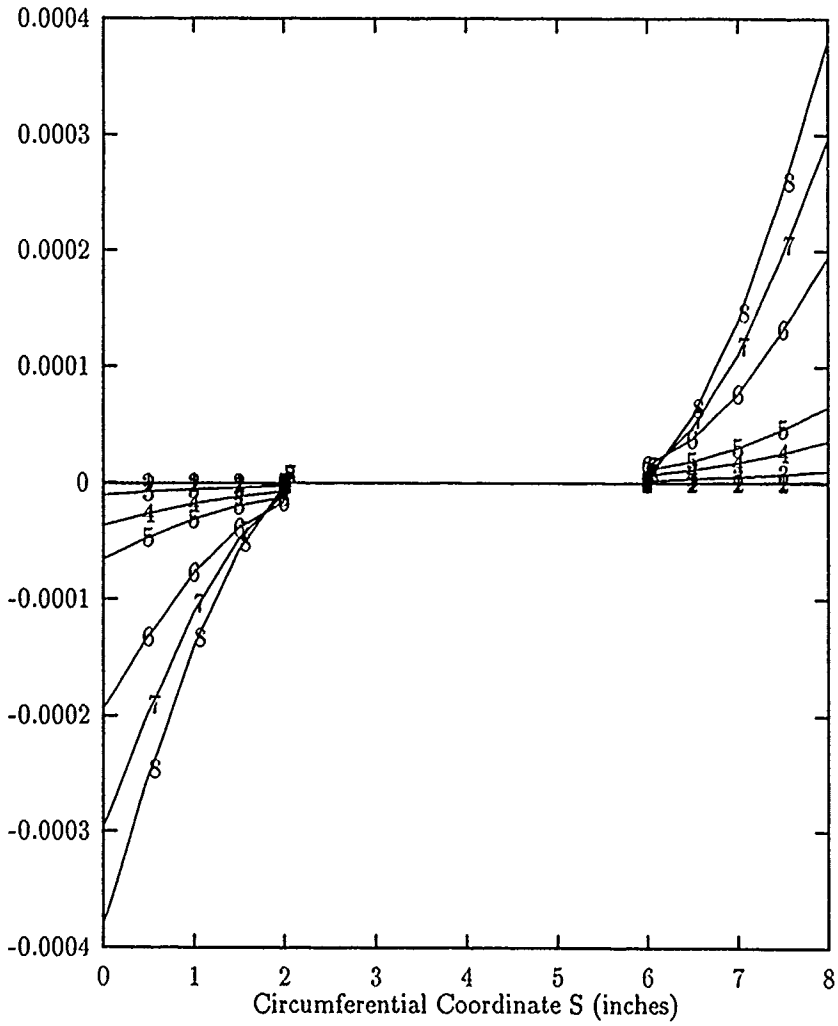

Figure 5.23. Meridian Values of $-w\psi_2/R_2$ for Increments of Axial Displacement of 12-inch Radius Composite Shell with Centered Cutout — C123 Theory

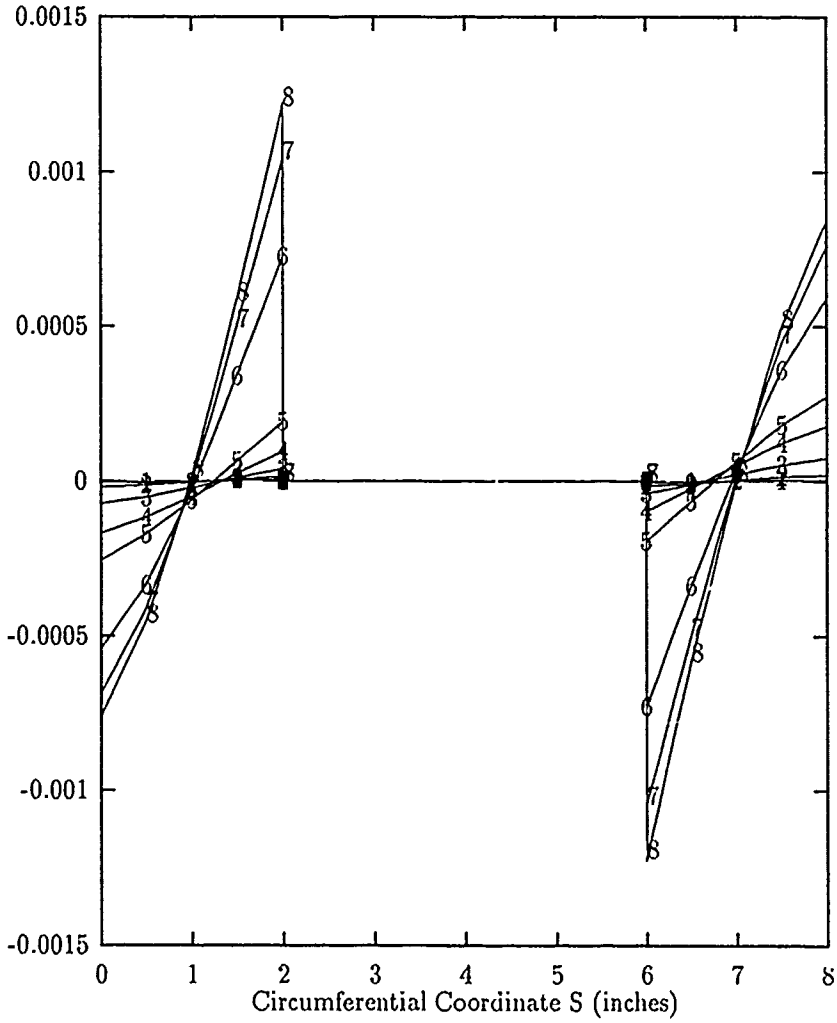

Figure 5.24. Meridian Values of $\psi_2 + w_{,2} - w\psi_2/R_2$ for Increments of Axial Displacement of 12-inch Radius Composite Shell with Centered Cutout — C123 Theory

VI. Discussion of Deep Shell Results with quasi-nonlinear HTSD Theory

6.1 Clamped-Free Quasi-Isotropic Shell Panel with Transverse Point Load

The first deep shell problem, chosen for this research, was a deep composite shell panel with transverse point load. This problem demonstrates a severe test of an HTSD theory because of the shell's depth, thickness, and quasi-isotropic properties. A deep 12-inch-radius quasi-isotropic 11×12-inch cylindrical shell panel was clamped at its lateral boundaries and free on the circumferential boundaries. The shell configuration is shown in Figure 6.1; geometric and material properties are also listed in the figure. A transverse point load was applied at the center of the 0.4-inch-thick panel until the panel center displaced over 2.5 inches. This distance is significantly greater than the 1.9-inch depth of the shell. Results for the transversely-loaded panel were compared with the computational results of Tsai [103]. Palazotto and others investigated shells of this configuration and compared static and dynamic results for different material properties and ply layups [63, 64, 102, 103]. Their work was typically based on a 96 element model of a quadrant of the shell. This mesh was chosen based on the results of their convergence studies summarized in Table 6.1. Tsai et al. concluded the 8×12 mesh results were acceptable considering

Table 6.1. Convergence Study for Quasi-Isotropic Shell Panel

Mesh	Load at Onset of Instability (lbs)
4×6	116
8×12	56
11×16	53

[103:69]

the CPU consumption was about 70 percent less than the 11×16 mesh [103:69]. Another recent study by Silva, however, revealed that the quasi-isotropic panel with transverse load does not deform in a symmetric manner [93:3-6]. Figures 6.2 and 6.3 show results taken from Reference [93] for a 24-ply quasi-isotropic $[0/-45/45/90]$s panel with $h = 0.12$ inches and $R = 100$ inches. Figure 6.2 shows the unsymmetric transverse displacement of the full

Boundary Conditions:
$s = \pm 6$: $u, v, w, w_{,1}, w_{,2}, \psi_1, \psi_2 = 0$, (clamped)
$x = \pm 5.5$: (free)

Other Data:
Material: AS4-3501 Graphite Epoxy
$E_1 = 20.461 \times 10^6$ psi
$E_2 = 1.3404 \times 10^6$ psi
$G_{12} = 0.8638 \times 10^6$ psi
$\nu_{12} = 0.301$
Ply Layup: [0/-45/+45/90]s
$\theta = 1.0$ radians
$h = 0.04$ in.
$\delta = 1.9$ in.
$R = 12$ in.
$A = 11$ in.
$B = 12$ in.

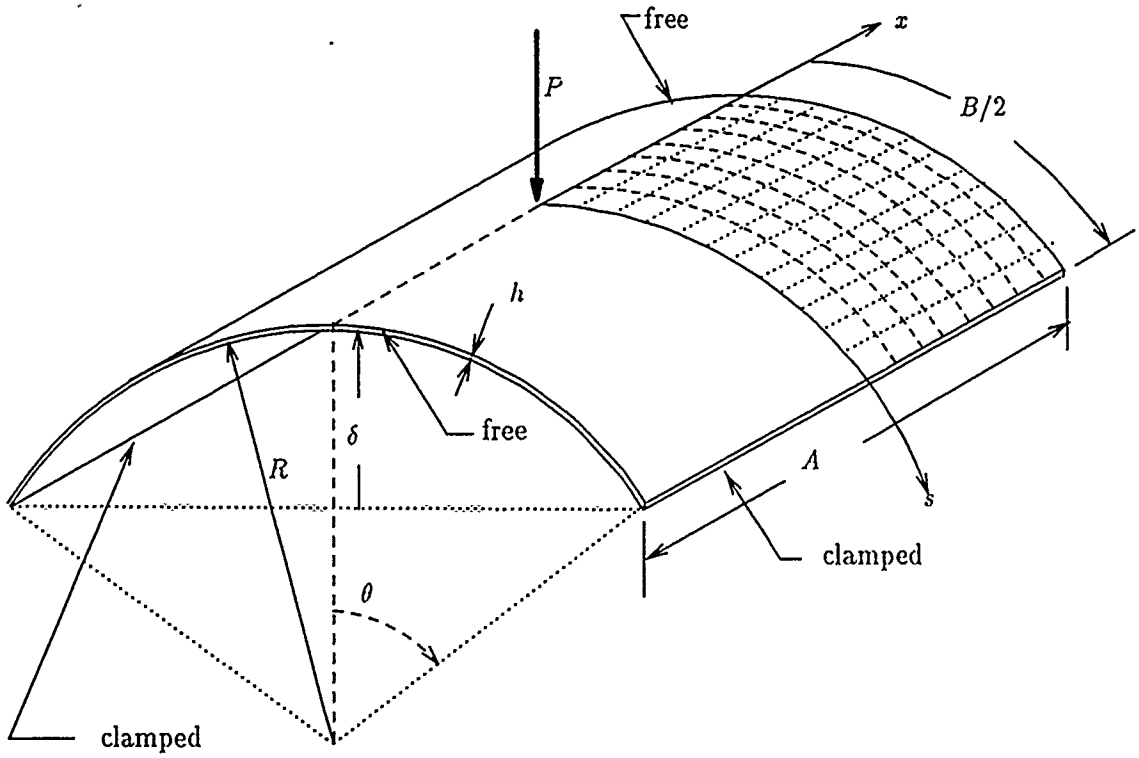

Figure 6.1. Clamped-Free Composite Shell with Transverse Point Load

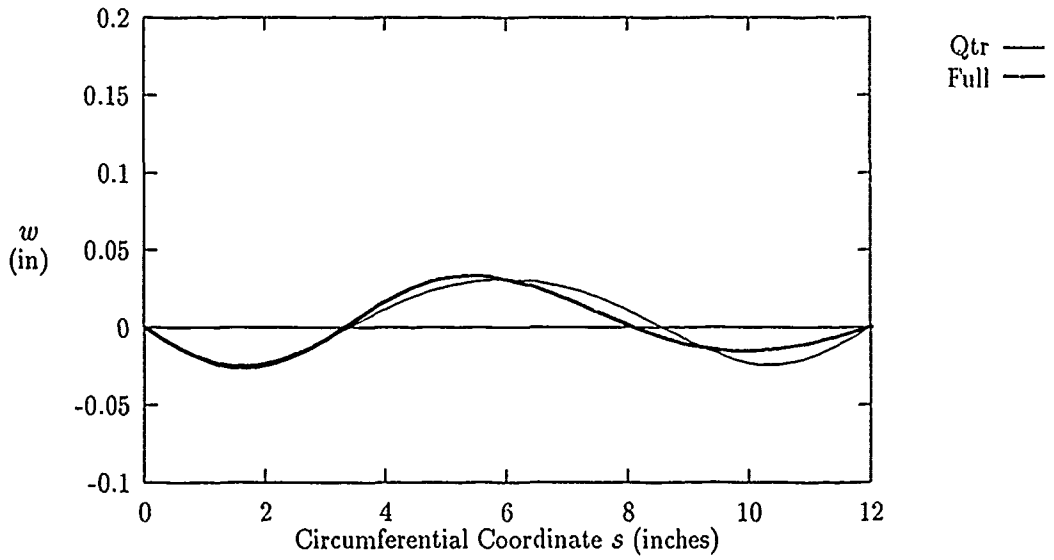

[93:3-6]

Figure 6.2. Quarter Panel vs Full Panel End Profile

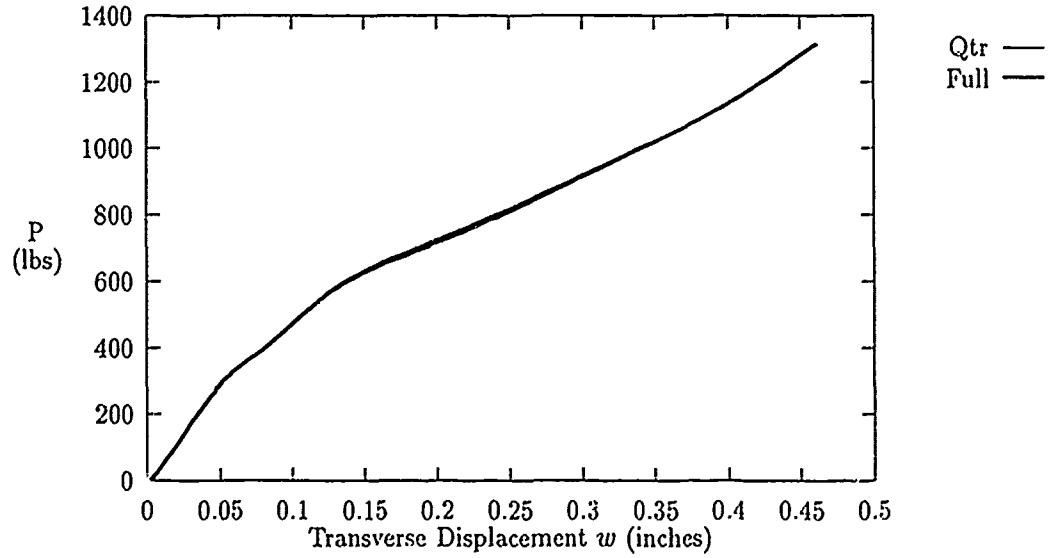

[93:3-5]

Figure 6.3. Load vs Transverse Displacement, Angle Ply Quarter Panel Test

panel (labeled as Full) versus the symmetric distribution of a quarter panel model (labeled as Qtr). Figure 6.3, however, shows little if any deviation in load versus displacement predictions for the two models. Thus, since this research was primarily concerned with load displacement behavior, a quarter shell 8 x 12 mesh was chosen for this problem.

Transverse load values versus displacements were computed for a [0/-45/+45/90]s ply layup, using the modified-Donnell, all quasi-nonlinear HTSD, and all nonlinear HTSD theories. Table 6.2 shows values of transverse load predicted by the various theories. The quasi-nonlinear HTSD elemental codes all predicted identical results, comparable to those of Tsai. Figure 6.4 shows the equilibrium values of transverse load for the quasi-nonlinear CDON and C100 HTSD theories. The fully-nonlinear HTSD theories predicted a significantly more flexible structure at the onset of loading, as shown in Figure 6.5. As w increased, however, the nonlinear codes predicted an increasingly stiffer structure. Figures 6.6 and 6.7 show relative differences in equilibrium loads predicted by these three theories. The differences are plotted as a percentage difference from the CDON values. A negative value would indicate a more flexible result for the HTSD theory as compared to the CDON theory. The deviation in the CDON results for displacement equal to 0.625 inches is caused by the use of two few elements in the mesh for this theory. The shell at this point of deflection is very unstable; its midsurface has severe local bending with large gradients of curvature. The CDON theory with only transverse nonlinear terms, w and its derivatives, can not achieve satisfactory equilibrium predictions at this point. If the number of elements are increased, the CDON code performs as expected. See the next section on deep arches for a comparison showing the use of more elements.

The quasi-nonlinear HTSD theory predicted snapping occurs at about $w = 0.5$. Palazotto et al. [63, 102] used the quasi-nonlinear HTSD developed by Dennis [18]. Their results showed snapping for many variations of material and geometric parameters [63:703-705]. The ratio of thickness to characteristic length of this problem is even smaller than any of the problems analyzed earlier. This ratio is equal to 1/300. Therefore, we would expect transverse shear strain to be totally insignificant, yet the results of the nonlinear variants for this problem deviate considerably from all the previous results. Several reasons for this behavior are apparent. The most obvious reason is the excessive strain energy caused by

Table 6.2. Transverse Center Point Load Predicted for Prescribed transverse Displacement of a 0.04–inch Clamped-Free Quasi-Isotropic Cylindrical Shell Panel

Disp.	CDON	C000	C020	C100	C120	C003	C023	C103	C123
0.250	35.5	34.6	34.6	34.6	34.6	9.1	9.1	9.1	9.1
0.375	53.7	56.6	56.6	56.6	56.6	16.0	16.0	16.0	16.0
0.500	53.3	52.1	52.0	52.1	52.0	25.2	25.2	25.2	25.2
0.625	29.6	47.3	47.2	47.3	47.2	35.3	35.3	35.3	35.3
0.750	38.5	36.7	36.6	36.7	36.6	49.4	49.4	49.4	49.4
1.000	11.0	7.6	7.4	7.6	7.4	88.0	88.0	88.0	88.0
1.250	15.4	12.5	12.3	12.5	12.3	160.8	160.8	160.8	160.8
1.500	21.9	21.3	21.0	21.3	21.0	252.1	252.0	252.1	252.0
1.750	32.7	38.4	38.1	38.4	38.1	361.7	361.6	361.7	361.6
2.000	54.0	70.4	70.1	70.4	70.1	488.7	488.7	488.7	*
2.250	100.8	132.6	132.2	132.6	132.2	629.7	629.6	629.7	*

* Datum point not computed

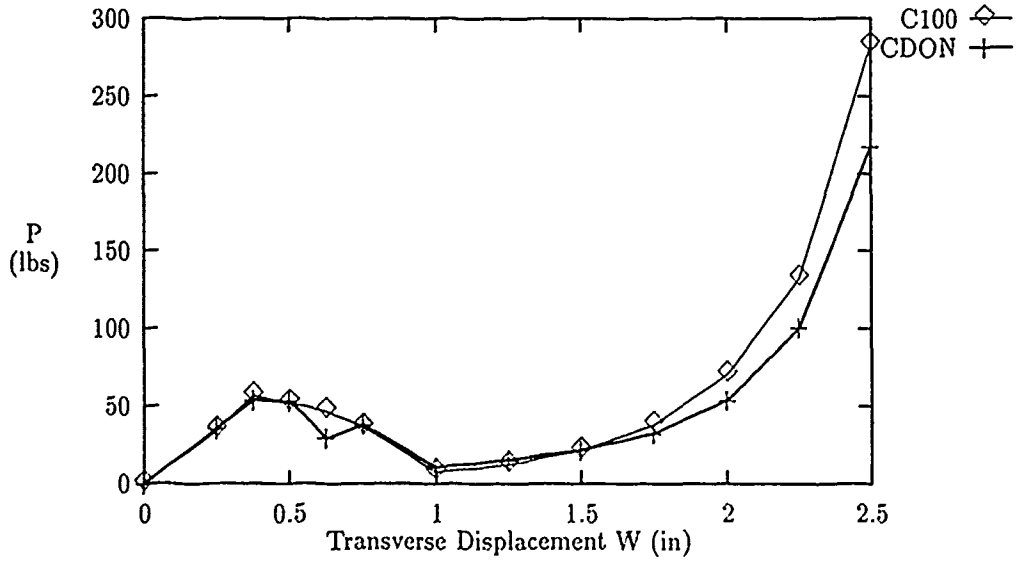

Figure 6.4. Equilibrium Path Comparisons for Transverse Point Loaded 0.04–inch Clamped-Free Quasi-Isotropic Cylindrical Shell — CDON and C100 Theories

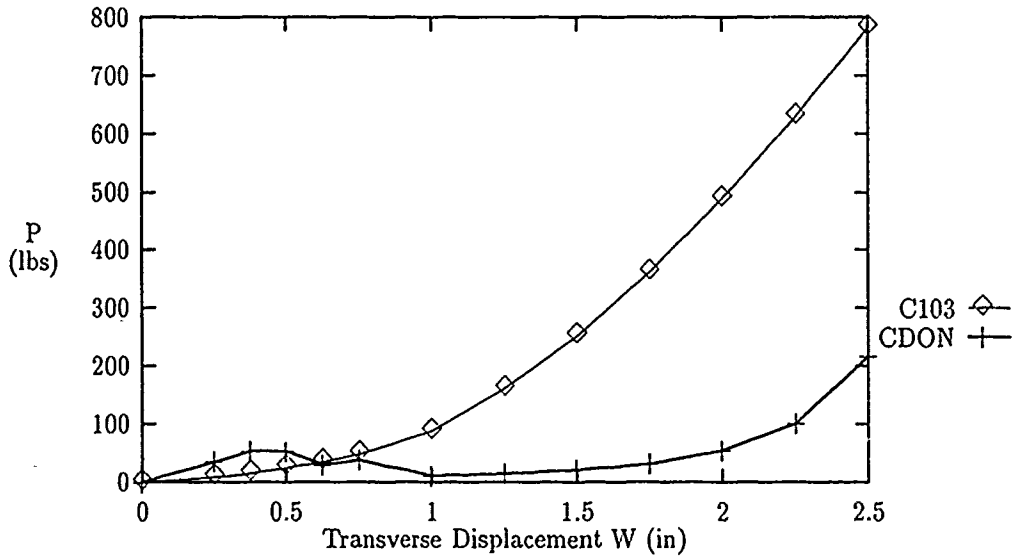

Figure 6.5. Equilibrium Path Comparisons for Transverse Point Loaded 0.04-inch Clamped-Free Cylindrical Shell — CDON and C103 Theories

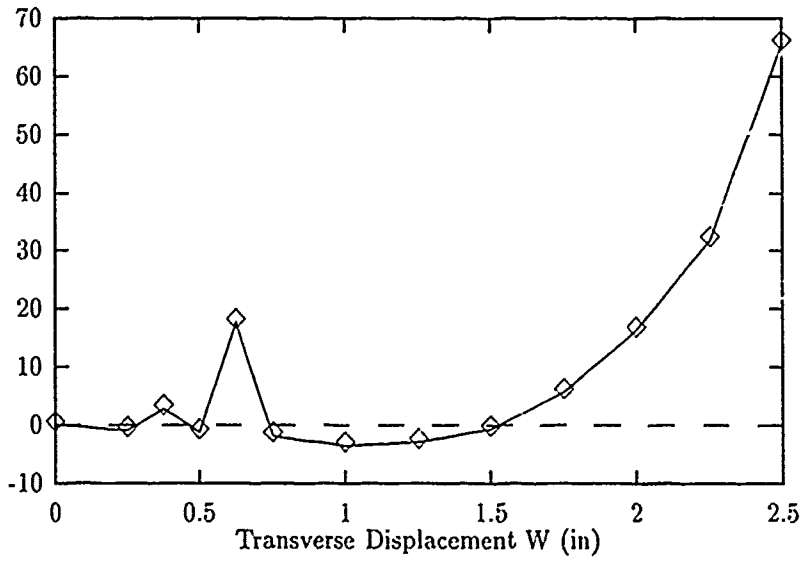

Figure 6.6. Relative Load Difference Comparisons for Transverse Point Loaded 0.04-inch Clamped-Free Cylindrical Shell — CDON and C100 Theories

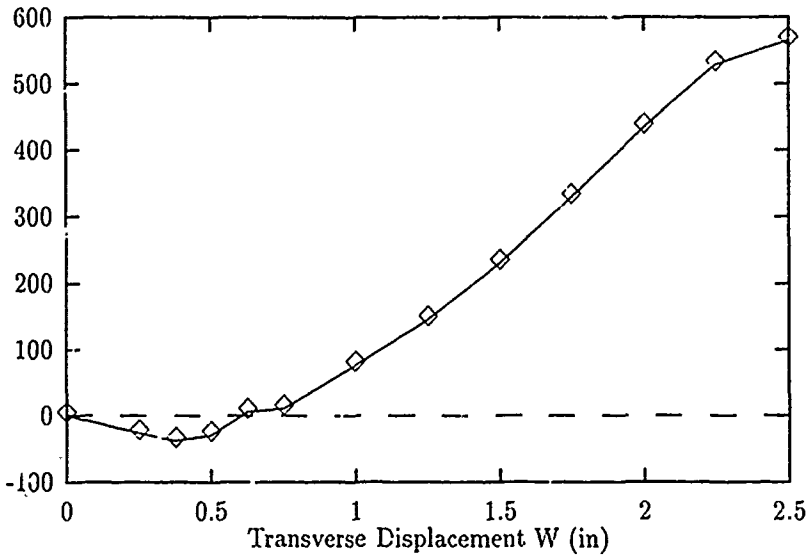

Figure 6.7. Relative Load Difference Comparisons for Transverse Point Loaded 0.04-inch Clamped-Free Cylindrical Shell — CDON and C103 Theories

the nonlinear terms of transverse shear. Figure 6.8 shows values for the linear terms of χ_4^0 for the CDON theory. Values plotted are the values of $\psi_2 + w_{,2}$ at nodes along the $x = 0$ line from the center of the panel ($s = 0$) out to the hinge line ($s = 6$). The labels 1,...,9 indicate the 1st through ninth increments of transverse displacement w. These can be compared with the linear terms of χ_4^0 for the C100 theory, shown in Figure 6.9, and the linear and nonlinear terms of χ_4^0 for the C103 theory, shown in Figures 6.10–6.12. From these graphs, we again see a significantly different behavior for the χ_4^0 terms of the C100 theory and the C103 theory. The C103 nonlinear term, shown in Figure 6.11, clearly dominates its linear counterpart, shown in Figure 6.10. This is caused by increased coupling of transverse shear and circumferential membrane activity. This problem is further compounded by the predominance of relatively weak material in the circumferential direction, compared to the lateral direction. The quasi-isotropic shell has a [0/-45/+45/90]s ply layup with a ratio of $E_1/E_2 = 15$ and transverse shear moduli less than E_2. The primary cause of deformation for this problem is bending activity. The outer plies of this laminated panel are the only plies oriented in the transverse direction. This implies that 75 percent of the material of this shell has a stiffness in the circumferential direction that is significantly less than the outer plies. This panel is only 0.04-inches thick, thus, the outer plies may

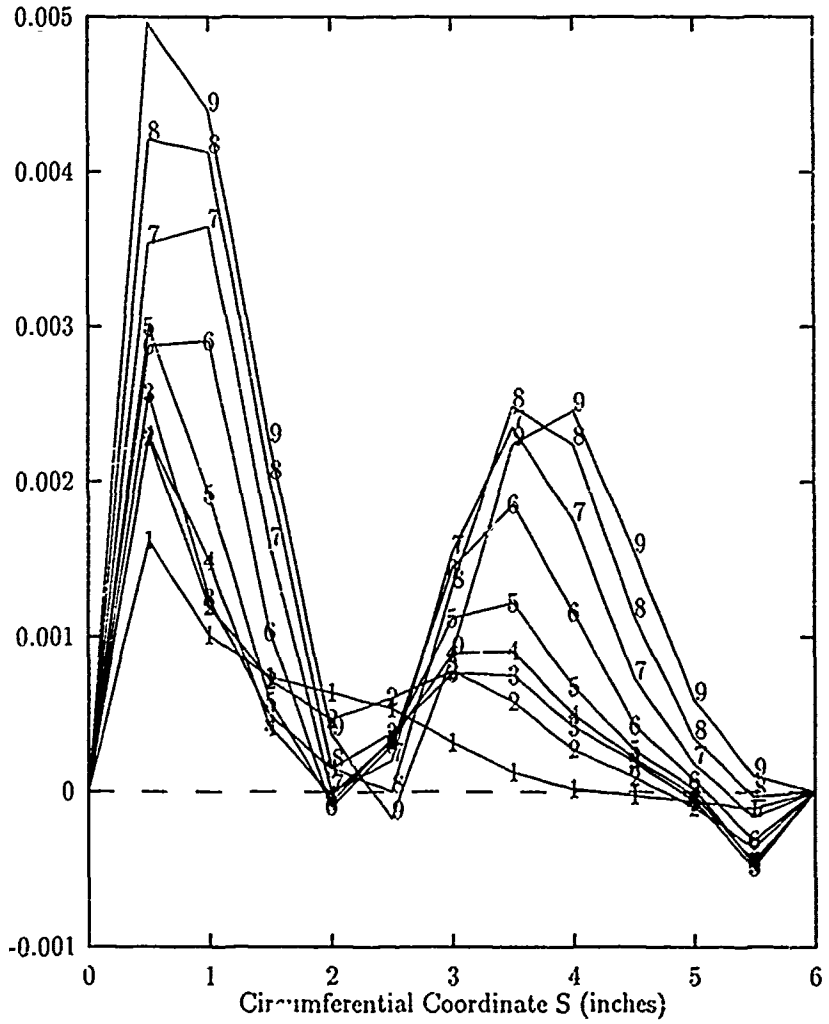

Figure 6.8. Meridian Values of $\psi_2 + w_{,2}$ for 11 Increments of Transverse Displacement of 0.04-inch Clamped-Free Quasi-Isotropic Cylindrical Shell — CDON Theory

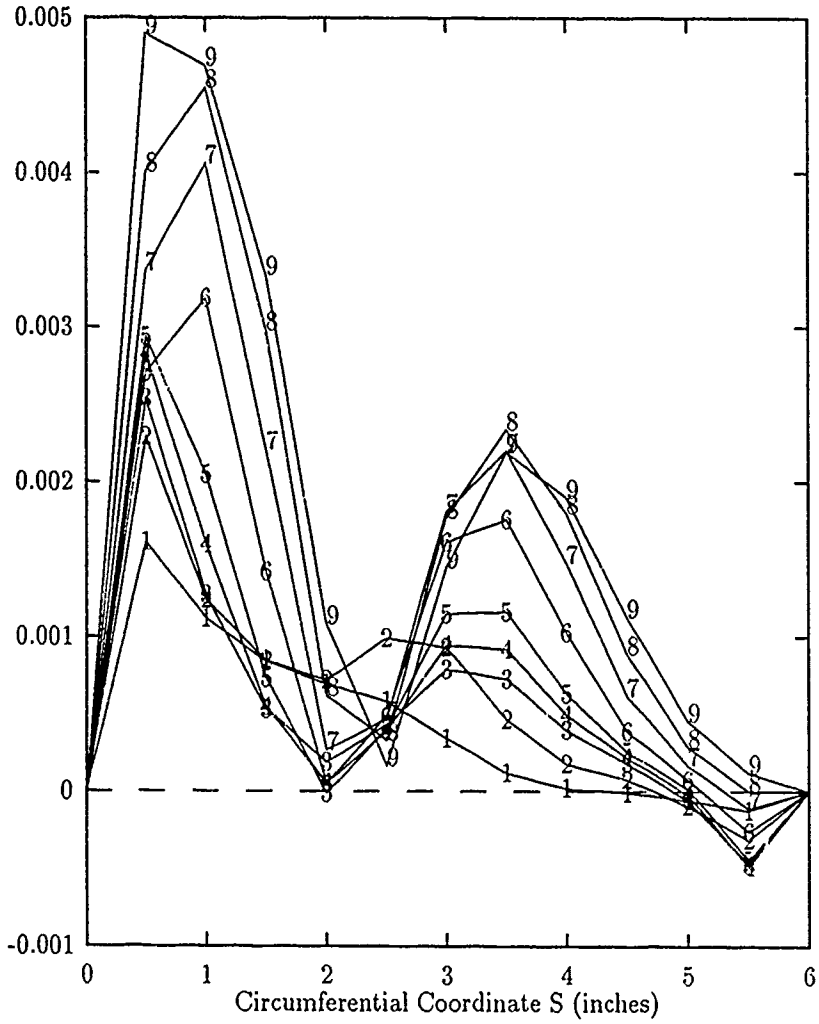

Figure 6.9. Meridian Values of $\psi_2 + w_{,2}$ for 11 Increments of Transverse Displacement of 0.04-inch Clamped-Free Quasi-Isotropic Cylindrical Shell — C100 Theory

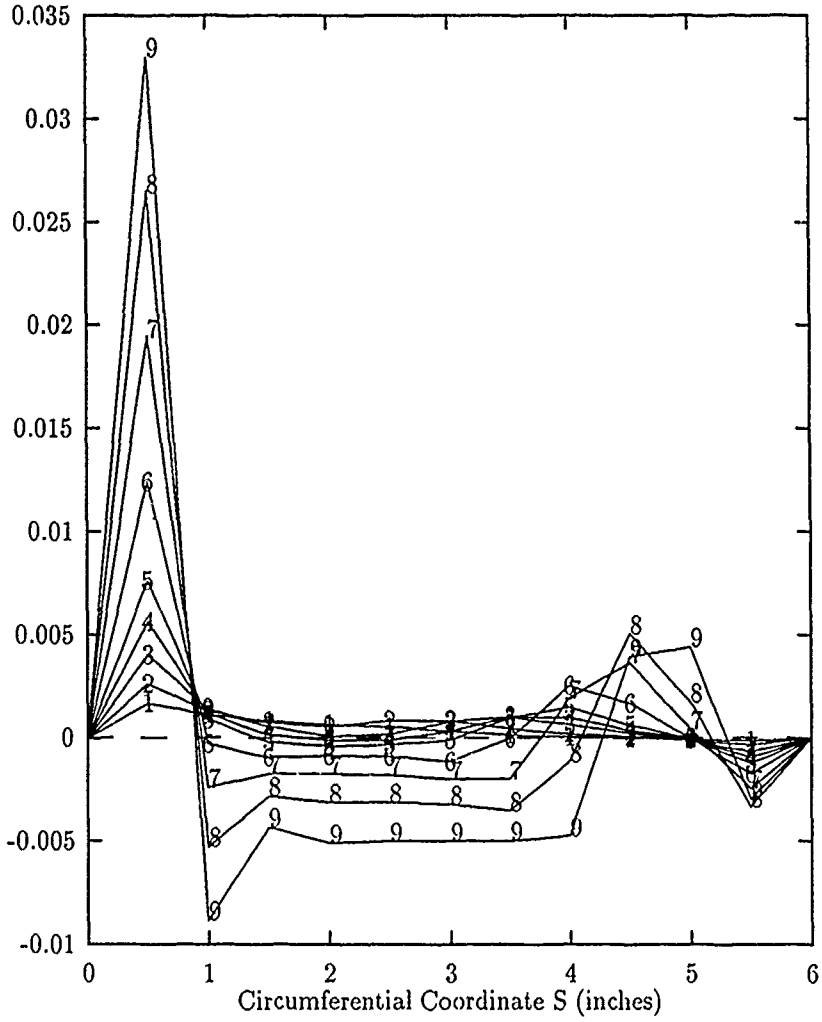

Figure 6.10. Meridian Values of $\psi_2 + w_{,2}$ for 11 Increments of Transverse Displacement of 0.04-inch Clamped-Free Quasi-Isotropic Cylindrical Shell — C103 Theory

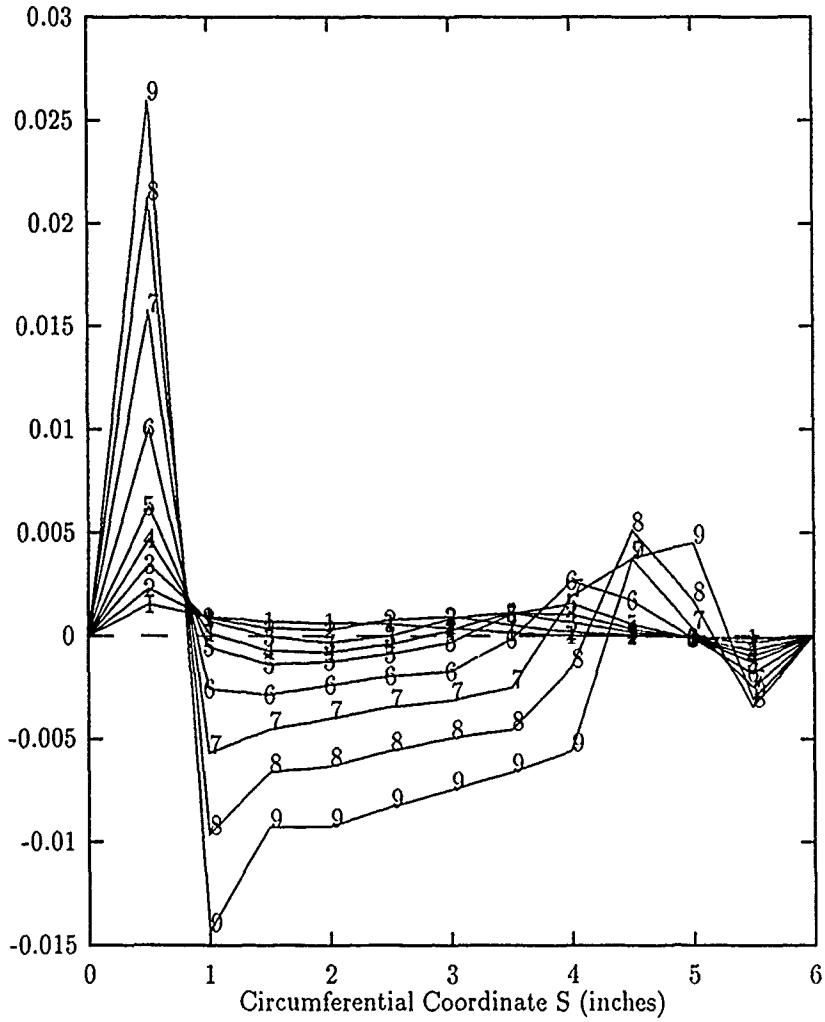

Figure 6.11. Meridian Values of $-w\psi_2/R_2$ for 11 Increments of Transverse Displacement of 0.04–inch Clamped-Free Quasi-Isotropic Cylindrical Shell — C103 Theory

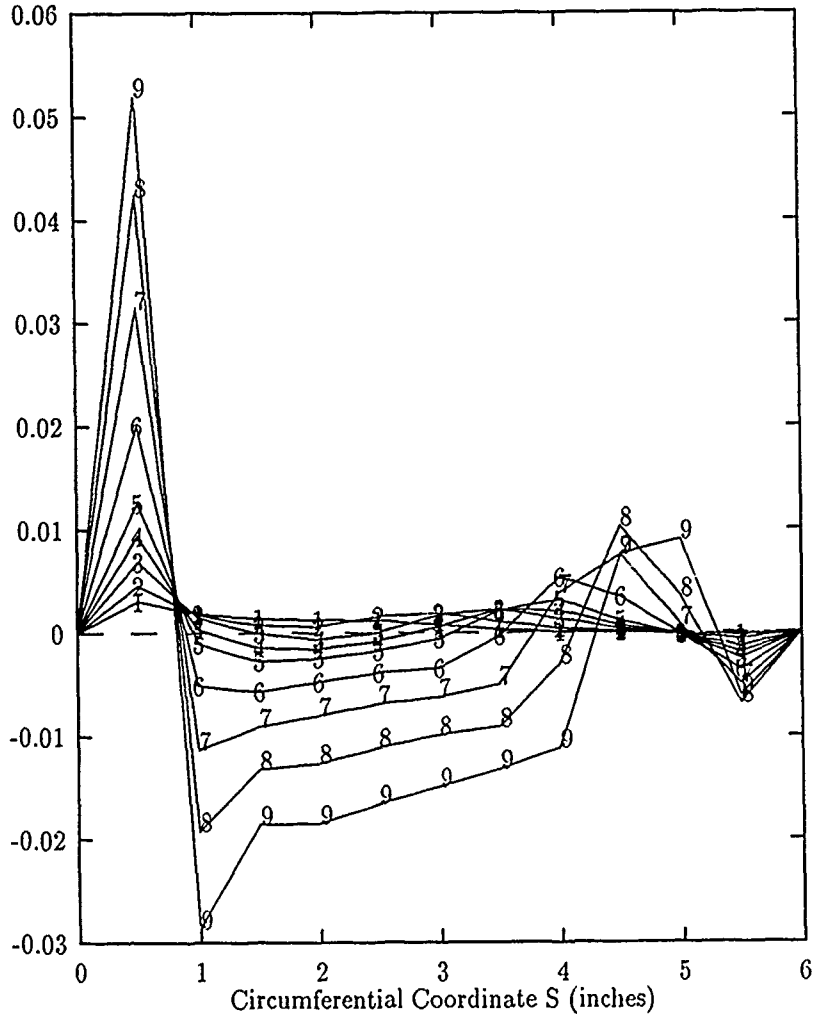

Figure 6.12. Meridian Values of $\psi_2 + w_{,2} - w\psi_2/R_2$ for 11 Increments of Transverse Displacement of 0.04–inch Clamped-Free Quasi-Isotropic Cylindrical Shell — C103 Theory

not be very effective in resisting bending, since they are so close to the midsurface of the shell. With the lateral supports of this shell clamped the final deformed shape of the shell exhibits both positive and negative curvatures. Thus, severity of bending is characterized by the distance between counterflexure points of the final deformed shape; a distance of about 2 inches. The bending activity of the clamped composite shell is more severe than that of the hinged isotropic shell. Since transverse shear stress is roughly equal to h/L times the bending stress, the clamped quasi-isotropic shell is a more severe test of nonlinear HTSD theory.

6.2 Deep Isotropic Cylindrical Arch with Transverse Point Load

Deep circular arches can be used to demonstrate a theory's ability to predict large displacements and rotations. Many variations of transversely-loaded deep arch problems have been reported in the literature [17, 29, 91, 98]. The problem chosen here is a 100–inch radius arch with a 1–inch square cross section and an opening angle of 106 degrees. The arch configuration is shown in Figure 6.13 along with geometric and material data. Solutions for this problem were computed using all eight elemental codes and a 1×16 mesh of elements to represent one quadrant of the arch. Data from the quasi-nonlinear theories are shown in Table 6.3. The higher-order quasi-nonlinear transverse shear deformation theories in this case predict a more dramatic collapse of the arch than the Donnell-type solution. Dennis explained this difference was due to the "many nonlinear in-plane displacement terms in the strain definitions that are not included in the Donnell equations " [18:260]. He reasoned that these additional terms become more important as displacements become large. A more exact representation of these terms, therefore, should produce more flexible results. Figure 6.14 shows load versus crown displacement values predicted by the C100 and C120 theories. Both the C000 and C100 theories predicted the same results. The C100 theory however does not give any more flexible results than the C000 theory despite the more exact u_2 displacement assumptions. The C020 and C120 theories both predict a more flexible response after collapse than the C000 and C100 theories. This difference is shown as a percentage reduction in load versus the transverse displacement in Figure 6.15. Values plotted are the relative difference (in percent) between the values of load

Boundary Conditions for one Quadrant:
$x = 0:\quad u, w_{,1}, \psi_1 = 0$ (symmetry)
$s = 0:\quad v, w_{,2}, \psi_2 = 0$ (symmetry)
$s = \pm 92.5:\quad u = v = w = \psi_1 = 0$ (hinged)
$x = \pm 0.5:\quad$ (free)

Other Data:
$E = 4.5 \times 10^5$ psi
$\theta = .92$ radians
width = 1 in.
$R = 100$ in.
$h = 1.0$ in.
$L = 160$ in.
$\delta = 40$ in.
$\nu = 0.0$

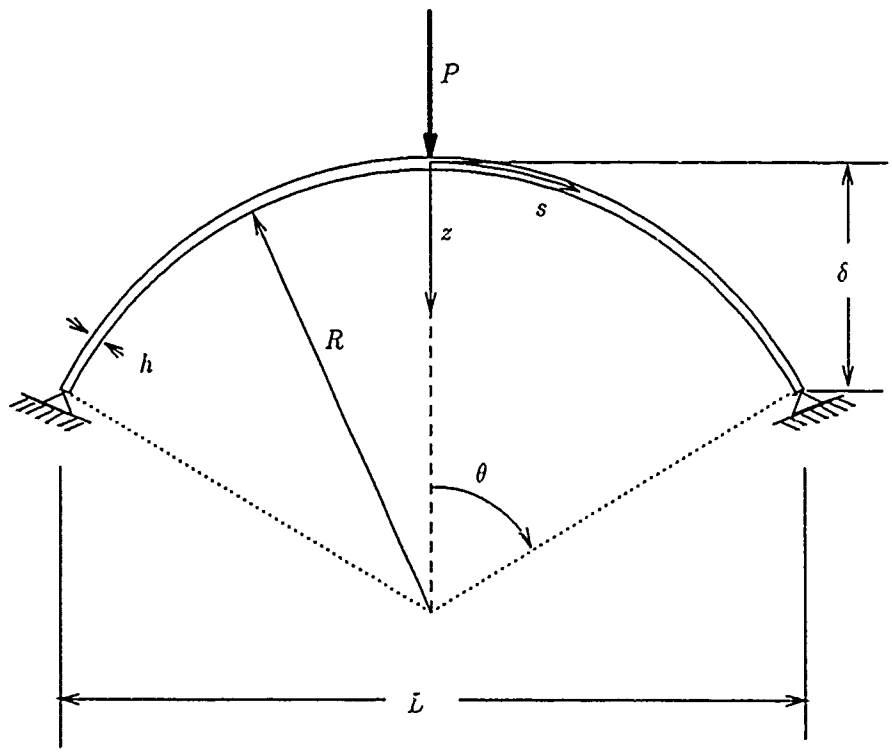

Figure 6.13. Hinged Point-Loaded Isotropic Cylindrical Arch

Table 6.3. Transverse Center Point Load Predicted for Prescribed transverse Displacement of a 100–Inch Radius Hinged-Free Deep Isotropic Cylindrical Arch

Disp.	CDON‡	C000	C020	C100	C120	C120†
4	621.24	640.6	640.0	640.6	640.0	632.5
8	893.66	914.8	911.6	914.8	911.6	899.1
12	1028.2	1018.6	1010.2	1018.6	1010.2	993.9
16	1088.3	929.5	914.0	929.5	914.0	978.7
20	1100.5	898.7	872.7	898.7	872.7	879.3
24	1078.4	775.3	728.7	775.3	728.7	705.2
28	1029.5	548.5	471.9	548.5	471.9	440.3
32	958.56	52.9	-232.3	52.0	-232.1	*

‡ Values taken from Reference [18:259]
† Computed with a 1×48 element mesh
* Datum point not computed

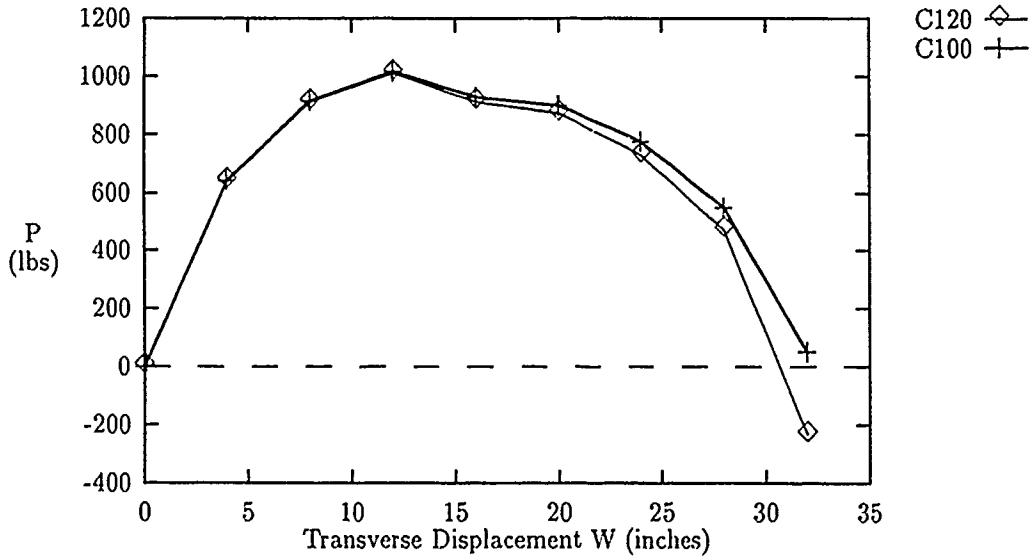

Figure 6.14. Deep Arch Crown Displacement vs Load — C100 and C120 Theories

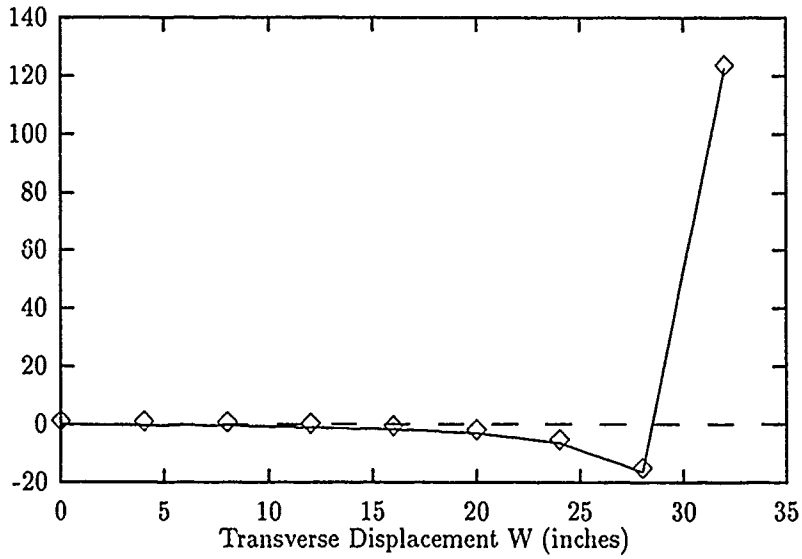

Figure 6.15. Percent Relative Load Difference vs Displacement for Deep Isotropic Arch — C120-C100 Theories

predicted by the C120 and C100 codes. A negative value is given for data points where the C120 code predicts a more flexible structure (less load required to achieve the same displacement) than the C100 code. Similarly, a positive value indicates a stiffer prediction for the C120 code than for the C100 code.

Comparison for Figure 6.15 with Figure 5.6 (the difference figure of the shallow 1/4-inch-thick isotropic shell panel) reveals that the shapes of these "difference" plots are similar. Recall, however, the differences for the shallow shell were due to the nonlinear transverse shear terms of the nonlinear HTSD theories. The differences of Figure 6.15 are due only to more exact kinematic and geometric approximations.

For the thin shallow cylindrical shell, the nonlinear HTSD variants produced promising results, an 8–14 percent reduction in loads during the collapse phase of the equilibrium path. For the deep circular arch, however, the nonlinear HTSD variants predicted stiff results, as shown in Figure 6.16. This stiff response was very similar to responses obtained for thin shallow shells when too few elements were used. The deep circular arch has characteristics similar to the cylindrical shells previously analyzed. With appropriate boundary conditions, one can even consider the arch as a small segment of a cylindrical shell. The

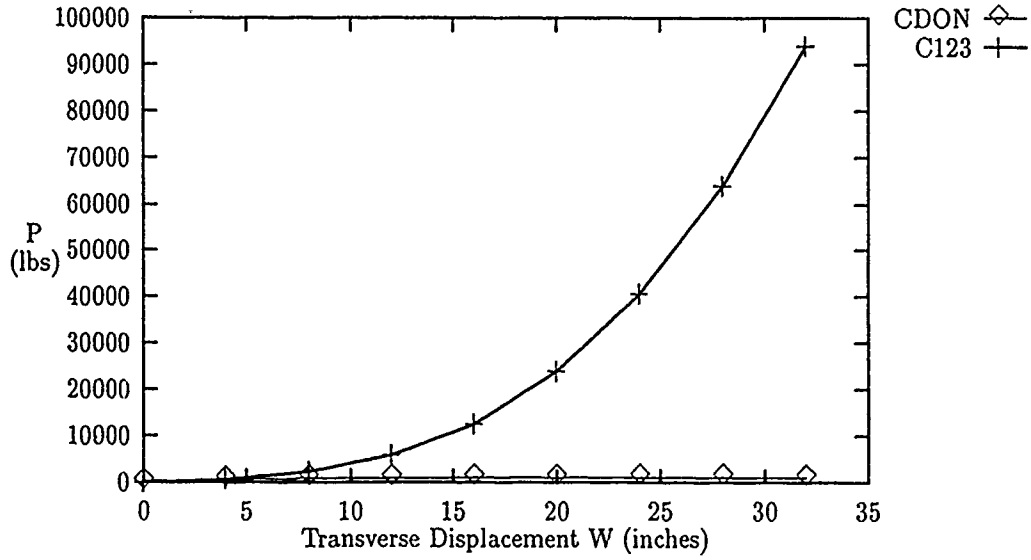

Figure 6.16. Deep Arch Crown Displacement vs Load — CDON and C123 Theories

arch is, however, very narrow. Because of this, the finite element discretization becomes more difficult, due to excessive aspect ratios when small numbers of elements are used. The isotropic shells discussed earlier were discretized with six elements in the meridian direction from the crown to the lateral edge. The lateral dimension was discretized with four elements. Since both dimensions from the crown to the edges in the x and s directions are 10 inches, the aspect ratio of each element is 1.5. Cook [16:558] defines a rough indicator of relative error caused by discretization as:

$$e_r \approx \rho_1 \rho_2 \left(\frac{1}{N^{1/n}} \right)^{q-r} \tag{6.1}$$

where

$\rho_1 \equiv$ largest element aspect ratio

$\rho_2 \equiv$ ratio of characteristic length of the largest element to characteristic length of the smallest element

$N \equiv$ number of elements in the mesh

$n \equiv$ spatial dimension (n =1, 2, or 3 for line, plane, and solid problems, respectively)

$q \equiv$ one plus the degree of the highest complete polynomial in the element displacement field, $r = 0$ for displacement error, $r = 1$ for stress or strain error

For the cylindrical shell with a 4×6 mesh of plane elements, the aspect ratio $\rho_1 = 1.5$, $n = 2$, and since all elements are of the same size $\rho_2 = 1$. The highest order complete polynomial in the element displacement field is cubic in order, therefore, $q = 3 + 1 = 4$. Thus, with 4×6 mesh of elements the relative errors estimated by Eq (6.1) are:

$$e_{r_{disp}} \approx 1.5 \left(\frac{1}{\sqrt{24}}\right)^3 = 0.0128 \tag{6.2}$$

$$e_{r_{\sigma,\epsilon}} \approx 1.5 \left(\frac{1}{\sqrt{24}}\right)^2 = 0.0625 \tag{6.3}$$

According to Cook, these values can be used to estimate total errors versus relative errors by multiplying these values by a factor of 10 [16:358]. Thus, we can pessimistically expect errors in displacements of up to 1.3 percent relative or 13 percent total for the shell panel. Stress and strain may be in error up to 6.3 percent relative, or about 63 percent total. For a 100-inch radius arch with 1-inch square cross section and an opening angle of 53 degrees, Eq (6.1) suggests at least 48 elements are needed to effectively model half the arch. In this case, the aspect ratio $\rho_1 = 3.85$ and the relative error estimates would be:

$$e_{r_{disp}} \approx 3.85 \left(\frac{1}{\sqrt{48}}\right)^3 = 0.0116 \tag{6.4}$$

$$e_{r_{\sigma,\epsilon}} \approx 3.85 \left(\frac{1}{\sqrt{48}}\right)^2 = 0.080 \tag{6.5}$$

Thus, despite the arch being a simple 1-dimensional problem, modeling it with 2-dimensional shell elements may create discretization errors which should be avoided. Even with twice as many elements as the cylindrical shell, the stress and strain estimates for the arch may be in error by up to 80 percent. Cook, however, points out that these estimates are "rough" and may be very pessimistic [16:559]. Nonetheless, the arch shown in Figure 6.13 was analyzed with more elements. Figure 6.17 shows results for a 1×48 element discretization using the quasi-nonlinear HTSD variants and the Donnell-type theory. These results show an even greater reduction in load after collapse with the C020 and C120 theories. Unfor-

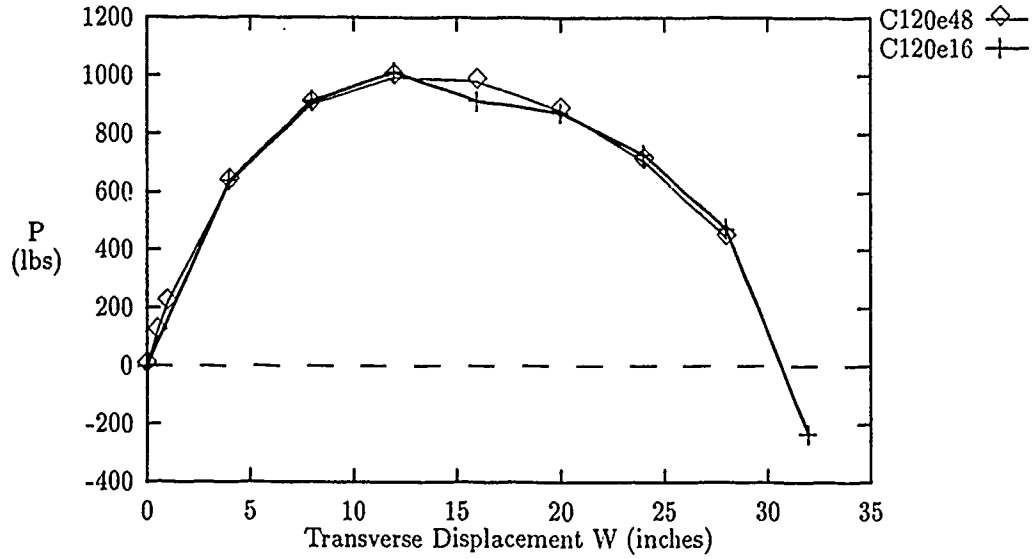

Figure 6.17. Comparison of 16 and 48 Element Meshs — Deep Arch Crown Displacement vs Load — C120 Theory

tunately, the nonlinear HTSD variants still diverged to overly stiff solutions beyond crown displacements of about 4 inches as shown in Figure 6.18.

At this point we have examined two "shells" with thickness of 1 inch and radius of 100 inches. The nonlinear HTSD theory predicts a slightly more flexible structure for the shallow shell panel, but it predicts a grossly overstiff response for the deep shell arch. The only differences between these problems are the width and the circumferential length. The arch has a width of one inch and a circumferential length of 185 inches. The shell panel has a width of 20 inches and a circumferential length of 20 inches. Correction of discretization errors due to large aspect ratios did not correct the overly stiff behavior of the nonlinear HTSD codes, therefore, there must be another explanation. Surana investigated similar 100-inch radius arches of varying width [98]. He found a 2-inch wide arch behaved like a beam, where as a 24-inch wide arch behaved more like a shell strip. The 24-inch wide arch generally was less stiff than the 2-inch arch despite equal values of bending stiffness EI. This implies the membrane activity of the shell panel must cause the shell to be less stiff.

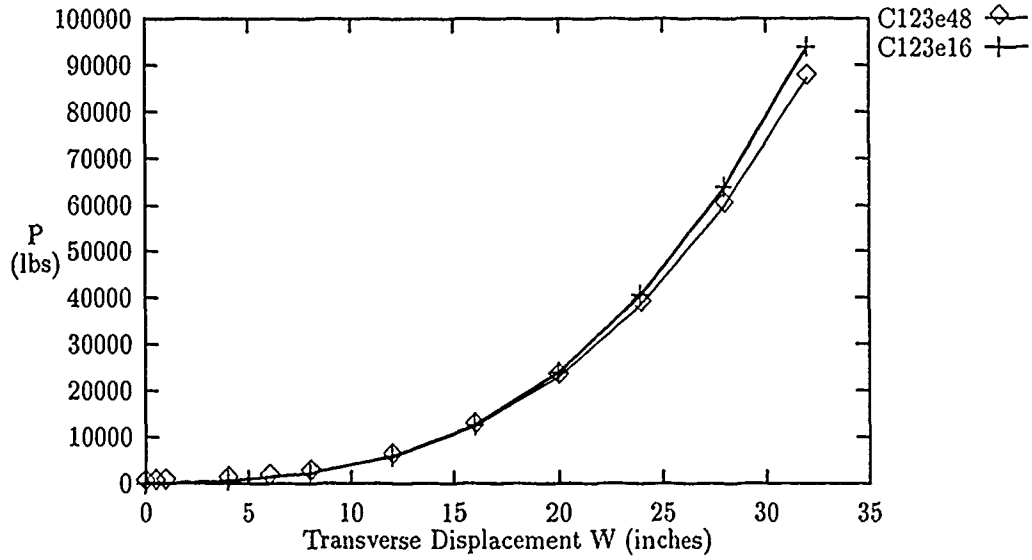

Figure 6.18. Comparison of 16 and 48 Element Meshs — Deep Arch Crown Displacement vs Load — C123 Theory

Huddleston [29] published a closed form solution for an arch with an extensible midsurface. Extensibility was characterized by a factor c relating bending stiffness EI to axial stiffness EA, as given below:

$$c = \frac{I}{AL^2} \tag{6.6}$$

where

$I \equiv$ area moment of inertia

$A \equiv$ cross sectional area

$L \equiv$ distance from centerline to supports

Inextensible behavior occurs when the bending stiffness EI is very small compared to the axial stiffness EA and c approaches zero. For the arch of Figure 6.13, $c = 3.3 \times 10^{-6}$ so the behavior is expected to be inextensible based upon Huddleston's factor. The shell panel of Figure 5.2, however, has a value of $c = 2 \times 10^{-4}$ which would also indicate an inextensible behavior. Clearly, the shell panel has significant membrane, or extensional, strain. Thus, it appears that Huddleston's factor does not fully explain the behavior of "wide" arches. Figure 6.19 shows Huddleston's results for an inextensible ($c = 0$) solution and an extensible

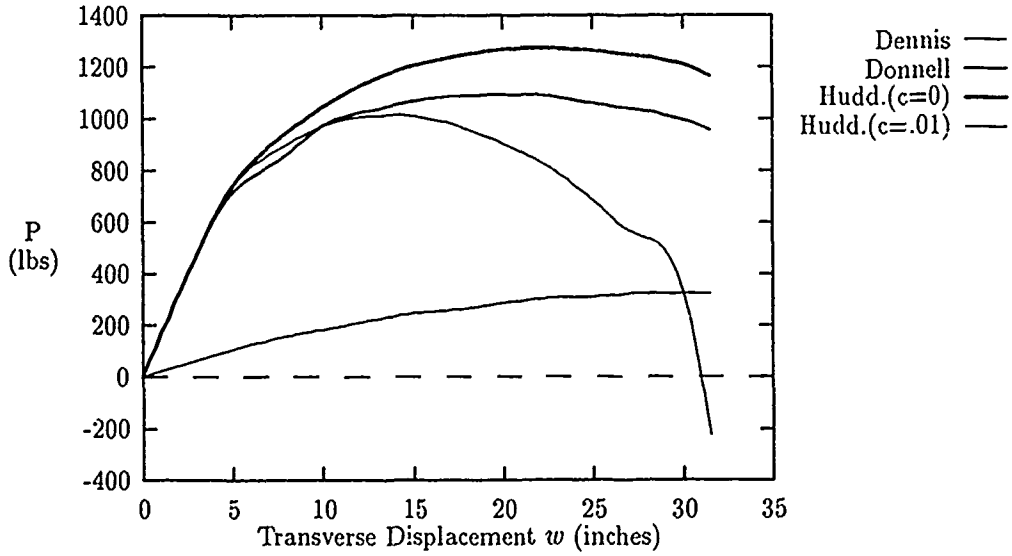

[18:261]

Figure 6.19. Deep Arch Results of Others

($c = 0.\dot{0}1$) solution. Interestingly, the two solutions have different behavior from the onset of deformation. Also shown in Figure 6.19 are results of Dennis's large displacement and rotational formulation with linear HTSD [18:258-265]. Dennis's solution was found to deviate considerably from the inextensible results of Huddleston for crown transverse displacement in excess of 5 inches. In fact, Dennis's formulation predicts a snapping phenomena where the transverse load must be negative to prevent displacements in excess of about 32 inches [18:261].

Based upon these observations, it seems feasible that nonlinear terms of the transverse shear strain components may have a more significant effect than expected for these deep arch problems. As discussed in Chapter IV, the nonlinear HTSD used for this research was not exact. The author has used linear kinematics that exactly satisfied the zero traction boundary conditions of the linear transverse shear strain of a curved shell. These kinematics, given in Eq (4.1), do not satisfy this boundary condition when the full nonlinear ε_{13} and ε_{23} of Eqs (3.38) and (3.39) are used. A parabolic function of thickness coordinate was included in the nonlinear transverse shear strain definitions of Eqs (3.38) and (3.39) to assure a traction free surface.

This approximate formulation has nonlinear transverse shear strain terms at the midsurface of the shell. The presence of these terms explains why the arch, which should behave in an inextensible fashion, exhibits a stiff response for the nonlinear theories. The linear and nonlinear midsurface terms for ε_{23} and ε_{13} of the C003 theory are given as χ_4^0 and χ_5^0 of Appendix B on page B-3 and page B-4, respectively. These terms are shown in the following two equations; the underlined terms are the linear terms and $c = 1/R$.

$$\varepsilon_{23}^0 = \chi_4^0 = \underline{w_{,2} + \psi_2} - cvv_{,2} + c^2vw + u_{,2}\psi_1 + v_{,2}\psi_2 - cw\psi_2 \tag{6.7}$$

$$\varepsilon_{13}^0 = \chi_5^0 = \underline{w_{,1} + \psi_1} - cvv_{,1} + u_{,1}\psi_1 + v_{,1}\psi_2 \tag{6.8}$$

The values of the linear term $\psi_2 + w_{,2}$ of Eq (6.7) for the C120 and C123 theories are shown in Figures 6.20 and 6.21, respectively. The largest nonlinear term $-w\psi_2/R_2$ of χ_4^0 is shown in Figure 6.22 for the C123 theory. The C120 theory has only linear terms for the transverse shear strains. Figure 6.23 shows the sum of the largest linear and nonlinear terms of Eq (6.7) for the C123 theory. From these figures, it is clear that the largest nonlinear term of χ_4^0 of the C123 theory deviates significantly from the linear χ_4^0 terms of the quasi-nonlinear C120 theory. Similar data for the shell panel was shown earlier in Figures 5.14 through 5.17. For the arch, the nonlinear transverse shear χ_4^0 term is heavily dominated by the last nonlinear term of Eq (6.7). This term effectively cancels out all positive terms of χ_4^0. This causes χ_4^0 to change sign, and ultimately the negative transverse shear strain becomes so dominant it causes stiff response instead of the more flexible response expected.

The deep arch revealed two significant findings. First, a more exact approximation of the shell's geometric shape factor functions will predict a more flexible structure during the collapse phase. Secondly, the linear kinematic assumptions of Eq (4.1) result in coupling of nonlinear transverse shear terms with transverse displacement w. This coupling can cause ε_{23} to vanish or dramatically vary from its expected behavior when transverse displacement increases beyond certain bounds. These bounds are dictated by the assumption that transverse shear strains should be of the order h/L times the bending or direct strains. This was one of the basic assumptions used to justify the use of a two-dimensional model

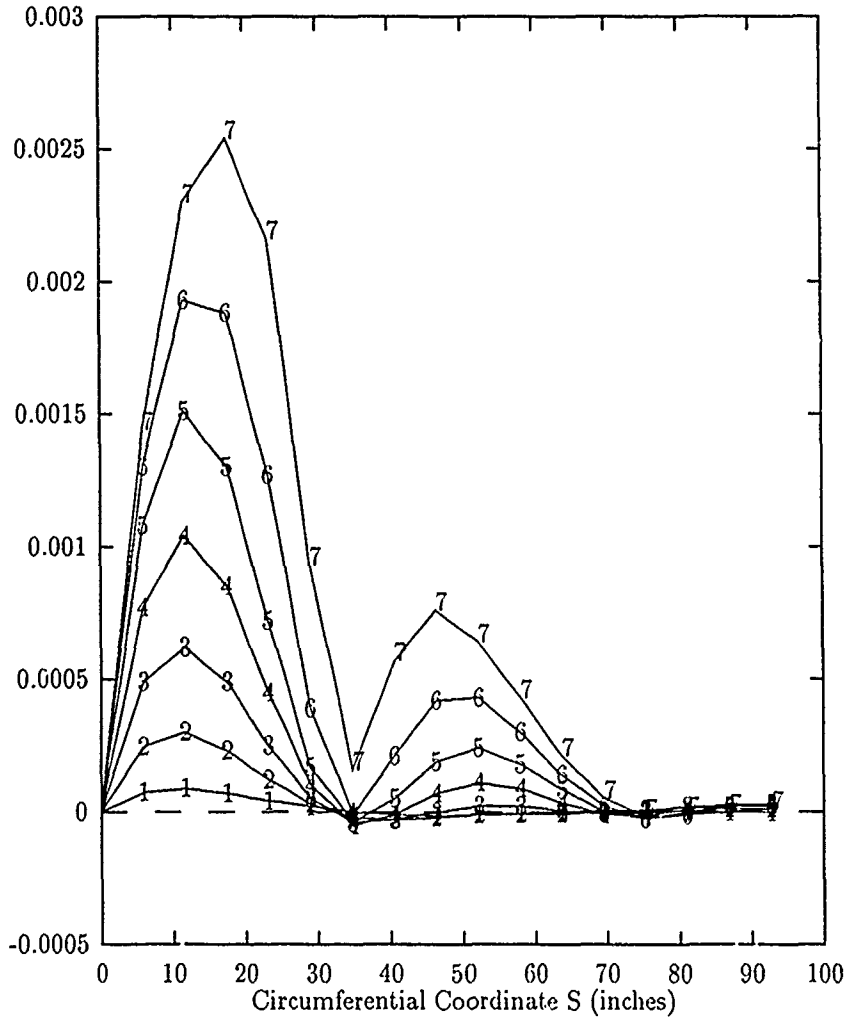

Figure 6.20. Meridian Values of $\psi_2 + w_{,2}$ for 10 Increments, 4 inches each, of Transverse Displacement of 1-inch Hinged Cylindrical Deep Arch — C120 Theory

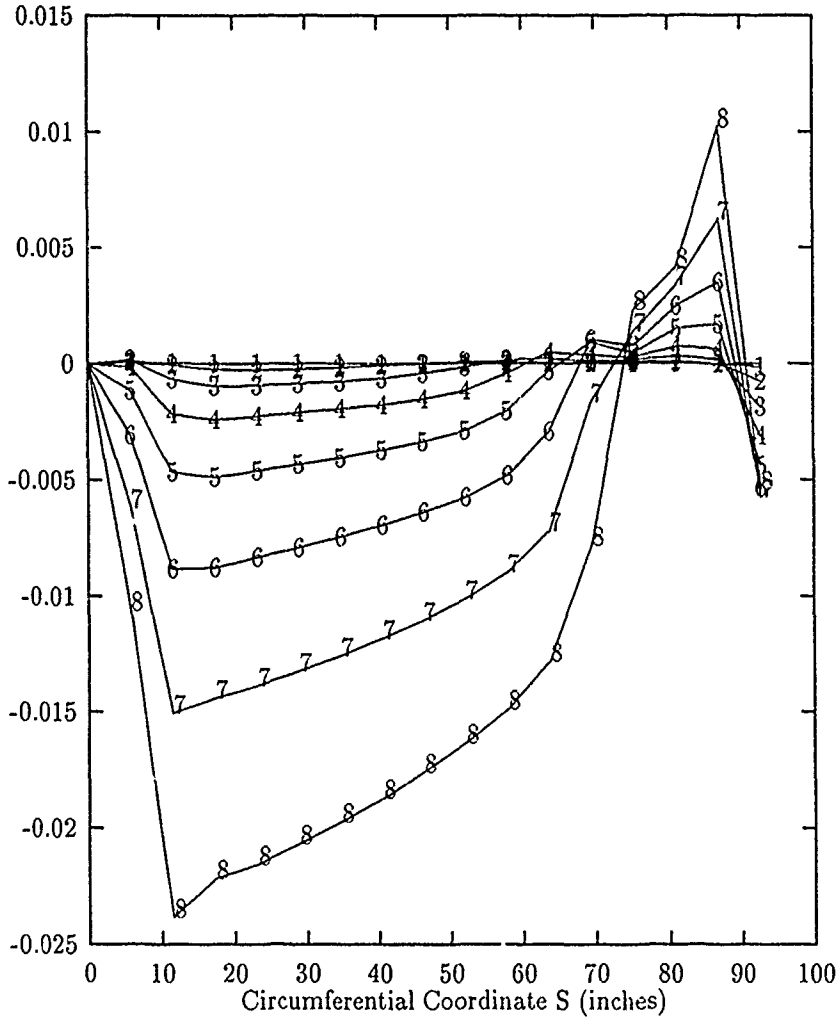

Figure 6.21. Meridian Values of $\psi_2 + w_{,2}$ for 10 Increments, 4 inches each, of Transverse Displacement of 1-inch Hinged Cylindrical Deep Arch — C123 Theory

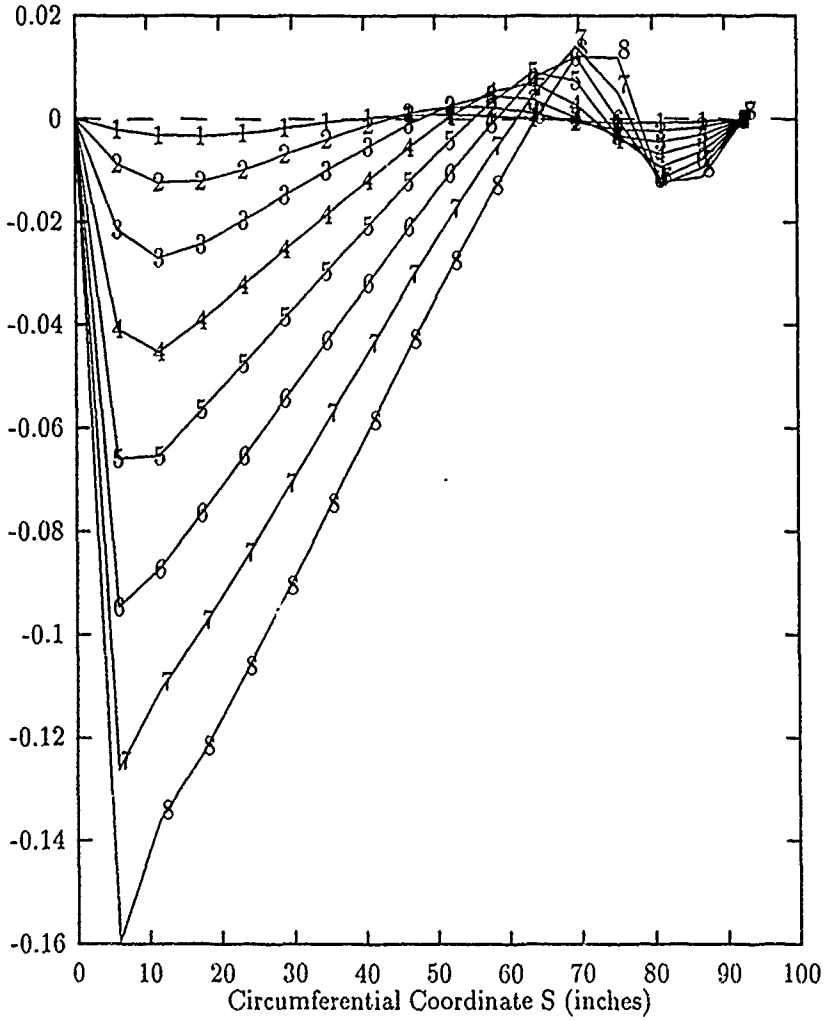

Figure 6.22. Meridian Values of $-w\psi_2/R_2$ for 10 Increments, 4 inches each, of Transverse Displacement of 1-inch Hinged Cylindrical Deep Arch — C123 Theory

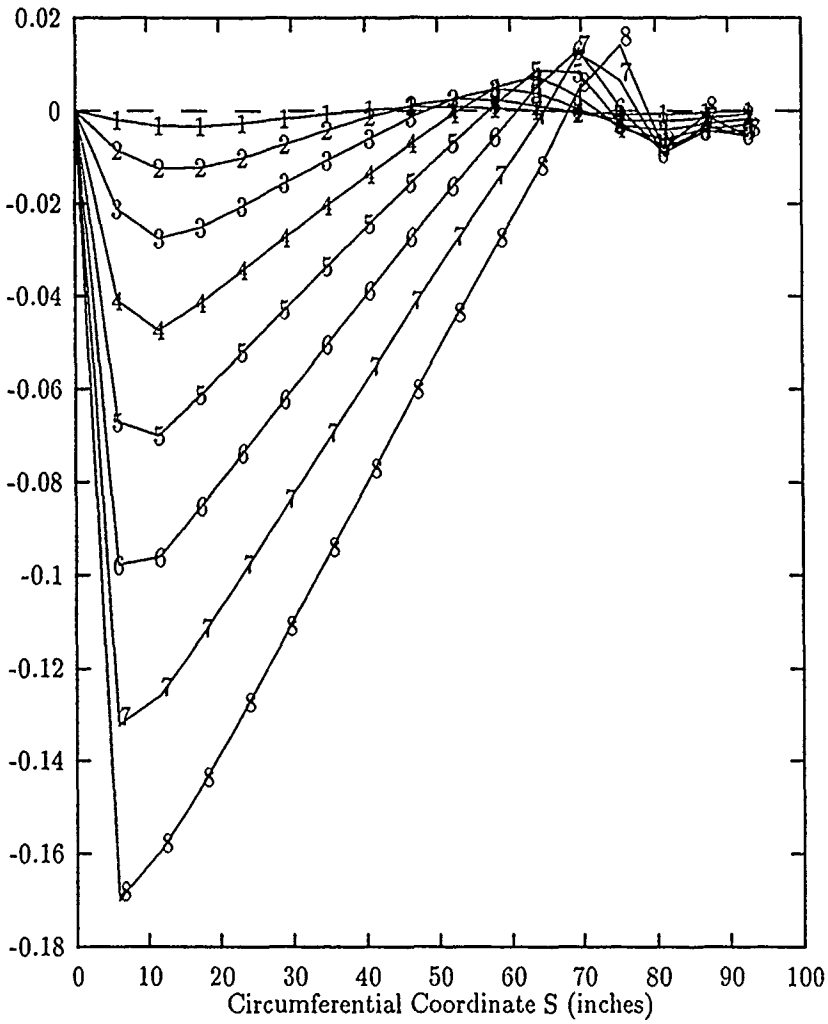

Figure 6.23. Meridian Values of $\psi_2 + w_{,2} - w\psi_2/R_2$ for 10 Increments, 4 inches each, of Transverse Displacement of 1-inch Hinged Cylindrical Deep Arch — C123 Theory

with $\sigma_{33} = 0$. This bound implies that the nonlinear terms of ε_{23} must also be of the order h/L times the in-plane strains. In Figure 6.16, we observe that the nonlinear variants predict the same behavior until transverse displacement exceeds about 5 inches, or about 5 times the thickness of the shell.

VII. Summary and Conclusions

The goal of this research was to develop a *nonlinear* higher-order transverse shear deformation (HTSD) theory with more-exact higher-order thickness expansions than used by previous researchers. In this case, the term *nonlinear* refers to using the full nonlinear Green-Lagrange strain tensor representation for the transverse shear strain components and for the in-plane strain components. Transverse shear deformation theories that use nonlinear terms for in-plane strains, but only linear terms for transverse shear strains, are referred to, in this dissertation, as *quasi-nonlinear* HTSD theories. In the past, *nonlinear* transverse shear deformation theories have been limited to kinematic assumptions based upon first-order polynomials in terms of the thickness coordinate. Similarly, most researchers truncated geometric shell shape factor approximations at the first-order terms of the corresponding thickness expansions. The theory developed for this research incorporated polynomial kinematic assumptions, for the u_1 and u_2 displacements, that were complete fourth-order polynomials in the thickness coordinate. These assumed displacements, however, were *linear* in terms of the unknown degrees of freedom of the system. These kinematic displacement assumptions assured that the linear parts of the transverse shear strain components were exactly zero when evaluated at the upper and lower surfaces of a curved shell. Furthermore, as a result of these kinematic assumptions, the distribution of transverse shear strain through the thickness of the shell was a complete third-order polynomial in the thickness coordinate. This distribution correctly modeled the nonsymmetric distribution of transverse shear stress caused by the effect of shell curvature.

7.1 Literature Review

A brief summary of the author's literature review follows. The complete literature review is included as Chapter II of the dissertation. For many years, the well-known Kirchhoff-Love assumptions were used as a starting point for shell theory derivations. These assumptions included a state of plane stress and inextensible normals that remained straight and normal during deformation. Koiter (1960) estimated the magnitudes of the transverse strain components. He indicated transverse *shear* stresses were generally of the

order h/L times the bending or direct stresses, but transverse *normal* stresses were of the order h^2/L^2 or h/R times the bending or direct stresses. (Koiter referred to h as the thickness, R as the minimum principal radius of curvature, and L as the distance between counter-flexure points of the deformed shell's midsurface.) Koiter used simplifications based upon small strain assumptions for isotropic materials; for problems with large strains or non-isotropic material behavior, including transverse shear deformation is even more necessary.

The development of a shell model for large-rotation nonlinear problems is complicated by the introduction of laminated anisotropic materials, changes in curvature of the surfaces, and geometric nonlinearity. Palazotto and Tisler (1987) compared computational predictions of buckling response to experimental work on graphite-epoxy cylindrical panels. Their work included the effects of rectangular unreinforced cutouts. They saw large radial displacements, large curvatures over small regions, and severe gradients of curvature for loads less than 10 percent of the critical buckling load. Many investigators have used finite element shell models to solve practical design-related problems that include these complications. Material nonlinearity could also be included in a nonlinear HTSD theory, but this was beyond the scope of this research project.

Dennis (1988) developed a large displacement, moderately large rotation, finite element formulation for laminated composite shells with a quasi-nonlinear HTSD theory. His theory assumed a state of modified plane stress. Direct normal stress, σ_{33}, was assumed negligible and the transverse displacement, w, was assumed constant through the thickness. Dennis assumed an orthogonal curvilinear coordinate system and an incomplete cubic-expansion of midsurface displacement parameters. This displacement field was similar to the cubic displacement field used for the linear HTSD theory of plates. Due to the curvature of the shell, however, a cubic displacement field will not exactly satisfy the conditions of zero transverse shear at the top and bottom surfaces of the shell. Dennis ignored this inconsistency by eliminating linear terms of the order h^2/R^2 in his assumed displacement field. He also ignored linear terms of the order h/R in his transverse shear strain-displacement equations. Furthermore, Dennis assumed 26 higher-order nonlinear terms of the in-plane strain-displacement relations were negligible compared to

other terms. Dennis's quasi-nonlinear HTSD formulation accurately predicted global responses of thin and moderately thick shells; practical problems, with h/R not greater than 1/25, compared well with known solutions.

Bhimaraddi, Carr, and Moss (1989) presented finite element models for shear deformable shells of revolution and laminated curved (constant curvature) beams with HTSD. For the beam, they used rotations about the element's axes as nodal parameters. Their assumed displacement field included these rotation parameters multiplied by a function whose first derivative vanished at the surfaces of the element and was non zero elsewhere. This resulted in a parabolic distribution of linear transverse shear strain. The strain displacement relations chosen were the "exact" linear relations which included transverse normal strain and did not assume the shape function $1 + y_3/R$ was equal to unity. They indicated that ignoring the y_3/R factor would result in neglecting the variation of beam curvature across the cross-section which would lead to greater errors in predicted response. Kant and Menon (1989) investigated the effects of h/R for thick shells compared to thin shells using "higher-order" theories for composite laminates. Kant and Menon discussed the use of "functions" of thickness coordinate z, similar to that used by Bhimaraddi, Carr, and Moss, but did not define them, or discuss how they were used in their paper.

The method of incorporating transverse shear into a shell model is not standard, even though FTSD and HTSD theories are both well accepted. These two theories are generally employed with the linearized transverse shear strain components of the Green-Lagrange strain tensor. They can, however, be used with nonlinear transverse shear strain terms. Singh, Rao and Iyengar (1989) used a FTSD theory with selected nonlinear terms included in the transverse strain components. They found transverse shear to be a significant factor in determining buckling load. Although this FTSD formulation included nonlinear transverse shear strains, the authors did not specifically evaluate the effects of the nonlinear terms.

Palmerio, Reddy, and Schmidt (1990) published two papers on a moderate rotation nonlinear FTSD theory for laminated anisotropic shells. This theory was proposed by Schmidt and Reddy in 1984. They indicated that their theory had nonlinear transverse shear strain terms, due to in-plane displacements, which were not present in a von Karman-

type theory. Based upon a poor comparison with the results of a continuum model by Liao and Reddy (1989), Palmerio et al. revised their new theory to include more nonlinear terms for their in-plane strain components. Their first-order through-the-thickness expansion of displacements was retained. They noted that the bending components, thus, contained substantially more terms. With essentially the full Green-Lagrange strain tensor representation, the modified FTSD theory of Palmerio, Reddy, and Schmidt gave results that were in close agreement with the continuum model of Liao and Reddy for a thin shallow isotropic spherical panel and a thin shallow isotropic arch. They concluded that including more nonlinear bending terms improved results. Interestingly, they had to eliminate nonlinear transverse shear terms to reduce an over-stiff behavior of the theory for a laminated composite cylindrical shell with transverse load.

Based upon the author's review of the published literature on transverse shear deformation of composite shell's, the author proposed the research project reported in this dissertation.

7.2 Theory

A summary of the theory developed for this research follows. Complete details are included in Chapters III and IV of the dissertation. The distribution of transverse shear through the thickness of a curved shell is distorted by the shell shape factors and their derivatives that appear in the representation of the strain components. (These shape factors are linear functions with respect to the thickness coordinate.) Thus, the exact distribution of transverse shear strain through the thickness of a curved shell is not parabolic, but is at least cubic in terms of the thickness coordinate. The theory of this research incorporated linear fourth-order u_1 and u_2 displacement assumptions. These assumptions exactly satisfied the linear transverse shear strain boundary conditions at the upper and lower surfaces of the shell. The exact satisfaction of these boundary conditions was accomplished by adding second-order and fourth-order correction terms to the assumed u_1 and u_2 displacement functions of the third-order linear HTSD theory. The theory also incorporated quadratic approximations of all geometric shape factor terms appearing in the strain displacement relations. The nonlinear transverse shear boundary conditions were

approximated by multiplying all nonlinear ε_{23} and ε_{13} terms by a parabolic function of the thickness coordinate. This assured the nonlinear transverse shear terms did not violate the zero transverse shear boundary condition at the upper and lower surfaces of the shell. Other more common assumptions of HTSD shell theories, such as the assumption that direct normal stress was equal to zero and that direct normal strain was a function of ε_{11} and ε_{22}, were also applied to this theory.

The basic assumptions of a two-dimensional shell theory are tied to the concepts of a reference surface (the midsurface of the shell) and a local curvilinear coordinate system associated with this surface. When this curvilinear coordinate system is based upon lines of principal curvature, which by definition are orthogonal, then the coordinate system is also orthogonal. For this research, the theoretical development was restricted to orthogonal coordinate systems based upon lines of constant curvature. This is one of the most common coordinate systems used for analysis of shells.

If one uses a Lagrangian description of deformation, all variables are expressed in terms of conditions prior to deformation. In this system, the displacement vector can be written in terms of orthonormal base vectors, $\vec{e}_i$, $(i = 1,2,3)$. For the shell, the Lamé parameters A_α, $(\alpha = 1,2)$, describe the *two*-dimensional relationship between the orthogonal surface base vectors $\vec{a}_\alpha$ and their orthonormal counterparts $\vec{e}_\alpha$. The shell shape factors, h_i, $(i = 1,2,3)$, describe the *three*-dimensional relationship between the orthogonal base vectors $\vec{g}_i$ of the three-dimensional orthogonal curvilinear coordinate system $\vec{y}_i$ and their orthonormal counterparts $\vec{e}_i$. For an orthogonal curvilinear coordinate system based upon the lines of principal curvature of a shell, the shape factors are:

$$h_1 = A_1(1 - y_3/R_1), \quad h_2 = A_2(1 - y_3/R_2), \quad h_3 = 1 \tag{3.40}$$

where

$$A_1 = \left(\frac{\partial \vec{r}}{\partial \theta_1} \cdot \frac{\partial \vec{r}}{\partial \theta_1}\right)^{1/2}, \quad A_2 = \left(\frac{\partial \vec{r}}{\partial \theta_2} \cdot \frac{\partial \vec{r}}{\partial \theta_2}\right)^{1/2} \tag{3.41}$$

Thus, for the convenient case of a cylindrical shell with radius R_2 and local coordinates $\theta_1 = x$, $\theta_2 = s$, z described in an orthogonal space with global coordinates $y_1 = x$, $y_2 = s$, $y_3 = z$, the position vector $\vec{r}(y_1, y_2, y_3)$ is given by:

$$\vec{r} = x\vec{e}_1 + s\vec{e}_2 + z\vec{e}_3 \tag{3.42}$$

and the Lamé parameters reduce to $A_1 = A_2 = 1$.

For this research, the macro-mechanical behavior of a composite lamina was assumed sufficient provided stresses were small enough to assure no material failure occurs. Thus, the material of each lamina was treated as a homogeneous anisotropic material. More specifically, the material was assumed to be transversely isotropic. This means the material has properties which are symmetric about two material axes. For a thin flat structural member, such as a plate, a state of plane stress is often assumed where σ_{13}, σ_{23}, and σ_{33} are all assumed to be equal to zero. In this research, however, the effects of transverse shear deformation were to be considered. Thus, σ_{13} and σ_{23} were not assumed to be zero. The direct normal stress, σ_{33}, however, was still assumed to be zero. This assumption was necessary to reduce the three-dimensional problem to a two-dimensional problem. The direct transverse normal strain was assumed to be given by:

$$\epsilon_{33} = -\frac{C_{13}}{C_{33}}\epsilon_{11} - \frac{C_{23}}{C_{33}}\epsilon_{22} \tag{3.56}$$

where the C_{ij} were functions of material properties and ply lay-up.

To form a structural component, the lamina were assumed to be perfectly bonded together with their fibers oriented at a particular angle with respect to the structure's reference axis. The stiffness contribution of each lamina in the laminate was transformed to a common reference system of axes. The constitutive relations used for this research were valid for small strains where the material behaved as a linear elastic solid. Eq (3.56) related the direct normal strain ϵ_{33} to changes in the direct in-plane strains ϵ_{11} and ϵ_{22} for the case where σ_{33} is equal to zero. The assumption that Eq (3.56) was valid for an arbitrary laminated composite shell was important. Without this assumption, the stress state would be fully three-dimensional and the two-dimensional model's reduced computational effort would be lost. With the assumption, however, the two-dimensional model will not accurately predict the stress distribution within the shell, since σ_{33} generally will not be zero in the real structure and ϵ_{33} may vary considerably from that predicted by Eq (3.56). Research in the 1960's and 1970's by many investigators, however, has validated

the acceptability of this assumption.

When a thin body undergoes a small (infinitesimal) deformation, material points on a line normal to the middle surface of the body move relative to each other. This movement results in rotation and warping of the normal. The angle between the geometric normal to the midsurface and the warped normal is maximum at the midsurface and zero at the the upper and lower surface. For a linear elastic material undergoing infinitesimal displacement, this angle of deviation is proportional to the transverse shear strain. The distribution of transverse shear strain in a flat plate, for the infinitesimal linear case, is parabolic through the thickness of the plate. Under the classical Kirchhoff assumption, one assumes the cross-section remains normal, straight, and inextensible. This assumption results in zero transverse shear strain throughout the body. Thick shells and composite shells generally will show greater transverse deflection for a given load when the effect of transverse shear is included in the theoretical model.

There are several ways to include transverse shear deformation. Transverse shear effects can be included using a first-order transverse shear deformation (FTSD) theory. In this case, material lines originally normal to the midsurface are allowed to deviate from the normal to the shell midsurface. These lines remain straight and inextensible. Since the angle of deviation is constant, the displacement field varies linearly through the thickness of the shell. The constant angle also implies transverse shear strain is constant, and thus, is not zero at the upper and lower surfaces of the shell. This inconsistent distribution results in a stiff model of the structure. This stiffening effect, called shear locking, becomes more pronounced as the shell thickness approaches zero. The higher-order transverse shear deformation (HTSD) theory allows the normal to rotate and warp. The HTSD theory for a flat plate produces a parabolic distribution of shear strain. This distribution matches the exact distribution of shear strain for the linear infinitesimal case. The results for curved shells, however, are different because of the curvature of the shell. These differences, due to curvature, were a primary concern of this research.

For a shell, the FTSD theory is given by the following displacement field:

$$\begin{aligned} u_1 &= u(1 - y_3/R_1) + \psi_1 y_3 \\ u_2 &= v(1 - y_3/R_2) + \psi_2 y_3 \\ u_3 &= w \end{aligned} \tag{3.62}$$

where the five degrees of freedom, u, v, w, ψ_1, and ψ_2, are functions of the in-plane curvilinear coordinates (y_1, y_2). The displacement field of a third-order linear transverse shear deformation theory is given by the following equations:

$$\begin{aligned} u_1(y_1, y_2, y_3) &= u\left(1 - \frac{y_3}{R_1}\right) + \psi_1 y_3 - \frac{4}{3h^2}\left(\frac{\partial w}{\partial y_1} + \psi_1\right) y_3^3 \\ u_2(y_1, y_2, y_3) &= v\left(1 - \frac{y_3}{R_2}\right) + \psi_2 y_3 - \frac{4}{3h^2}\left(\frac{\partial w}{\partial y_2} + \psi_2\right) y_3^3 \\ u_3(y_1, y_2, y_3) &= w \end{aligned} \tag{3.70}$$

This third-order displacement field has two additional degrees of freedom not present in the first-order theory. These two degrees of freedom are the derivatives of transverse displacement, w. These derivatives are independent degrees of freedom that represent the slope of the elastic curve. The third-order theory, thus, allows the slopes of the elastic curve to deviate from the bending angles. This deviation is directly related to the transverse shear strains of the structure.

The third-order linear transverse shear deformation theory for a shell is suitable for many problems of practical interest. Two approximations of this theory, however, required further examination to assess their effects upon the accuracy of this theory for certain problems. Specific problems of interest were ones in which rotations and curvature within the element become very large. The first approximation, in question, was the neglect of some higher-order terms in the thickness-expansions of displacement field and the shell shape factor functions. For a shell, the third-order kinematics of the linear HTSD theory do not give zero linear transverse shear strains at the upper and lower surface; unless, the shell is *flat* or some small terms of the transverse shear strains are ignored. The curvature of the shell is important, because the shell shape factors distort the distribution of strain through the thickness of the shell. Thus, the order of approximation of the shell shape factors affects the accuracy of the strain distributions. The second approximation, in

question, was the neglect of nonlinear transverse shear strain terms. The quasi-nonlinear HTSD theory ignores all nonlinear terms of both ε_{23} and ε_{13}. This linear restriction on ε_{23} and ε_{13} is not necessary physically, but satisfying the zero strain boundary conditions of the full nonlinear expressions is not a trivial problem.

The kinematics of Eq (3.70) were modified to yield exactly zero at the top and bottom surface of a curved shell by adding two correction factors to the last term as shown below:

$$\begin{aligned} u_1(y_1,y_2,y_3) &= u\left(1-\frac{y_3}{R_1}\right)+\psi_1 y_3+\left(\psi_1+\frac{\partial w}{\partial y_1}\right)\left[\underline{-\frac{y_3^2}{R_1}}+ky_3^3\underline{-\frac{k}{R_1}y_3^4}\right] \\ u_2(y_1,y_2,y_3) &= v\left(1-\frac{y_3}{R_2}\right)+\psi_2 y_3+\left(\psi_2+\frac{\partial w}{\partial y_2}\right)\left[\underline{-\frac{y_3^2}{R_2}}+ky_3^3\underline{-\frac{k}{R_2}y_3^4}\right] \qquad (4.1) \\ u_3(y_1,y_2,y_3) &= w \end{aligned}$$

where $k=-4/(3h^2)$ and the underlined terms were the correction terms added to Eq (3.70). These kinematics gave zero linear transverse shear strains at the upper and lower surface of a curved shell. The additional terms of Eq (4.1) also vanished for a flat plate, since each term was divided by radius of curvature. Likewise, for a right circular cylinder, with radius $R_2=R$ and $R_1=\infty$, the first equation of Eq (4.1) reduced to the corresponding flat plate expression, since R_1 was infinite. The comparison of results from the incomplete cubic kinematics of Eq (3.70) and results from the complete quartic kinematics of Eq (4.1) was a major aspect of this research. As stated earlier, the cubic displacement field of Eq (3.70) was the same as used by other authors. The complete quartic, however, was a unique displacement field not derivable from those of other authors. This quartic displacement field, thus, was an exact solution for the linear traction free boundary conditions of a quasi-nonlinear HTSD theory for shells.

The nonlinear transverse shear boundary conditions are not as easily solved as the linear version of these conditions. The general fourth order kinematic assumptions, when substituted into the full nonlinear Green-Lagrange strain-displacement relations for ε_{13} and ε_{23}, gave two coupled nonlinear partial differential equations that were seventh-order in the thickness coordinate. In order to solve these two equations for the six unknown functions of displacement, one must evaluate the equations at $y_3=\pm h/2$ and set each

resulting equation equal to zero. This is required to satisfy the zero traction boundary condition on the surfaces of the shell. Solving four coupled nonlinear partial differential equations with six unknowns was beyond the scope of this research project. Although other authors have proposed the use of nonlinear transverse shear strain-displacement relations with linear kinematics, none have done so within the context of a HTSD theory.

Since no linear kinematic assumption exactly satisfies the zero traction boundary conditions, several options were available. One could choose to ignore the natural boundary conditions and use shear correction factors as done with the FTSD theory. Singh, Rao, and Iyengar (1989) chose this approach. One could also simply ignore all nonlinear transverse shear strain terms. Palmerio, Reddy, and Schmidt (1990), although intending to include nonlinear transverse shear, ultimately chose this approach for their FTSD theory. These were the only two references which referred to nonlinear transverse shear terms in a FTSD or HTSD theory for shells.

The author's approach to including nonlinear transverse shear terms in the theory included several assumptions beyond those of the quasi-nonlinear HTSD theory. First, the author was primarily interested in problems involving large rotations and curvature changes for laminated shells. Thus, the displacement field of the new theory should reduce to the displacement field of the linear HTSD theory for problems with smaller rotations or smaller curvatures. The kinematic assumptions of Eq (4.1) reduce to the kinematics of the linear HTSD theories for small curvature problems. Secondly, nonlinear kinematic assumptions were not used to satisfy the nonlinear boundary conditions for ε_{13} and ε_{23}. The incorporation of nonlinear kinematic terms and the corrective terms of Eq (4.1) was prohibitive. Thus, the author chose to use the linear kinematics of Eq (4.1) with the full nonlinear transverse shear relations and an approximate approach to the nonlinear boundary conditions. This approximate approach assumed the nonlinear transverse shear strain should be zero at the upper and lower surfaces and that the strain energy of the nonlinear transverse shear strain terms was excessive. The author achieved a slight reduction in transverse shear strain energy and forced the satisfaction of zero traction, at the shell's surfaces, by multiplying the nonlinear transverse strain terms by a parabolic function of the thickness coordinate. Other researchers have used similar functions to provide the

parabolic transverse shear distribution of the linear HTSD theory.

Thus, the goal of this research was to evaluate the effects of two theoretical "attributes" not previously investigated for linear-elastic shells with large displacement, rotations, and curvatures using a higher-order transverse shear deformation theory. These two attributes were the accuracy of the displacement field assumption and the incorporation of nonlinear strain-displacement terms for the transverse shear strains. A third "attribute" was also considered, and that was the order of the approximation of functions of the shell shape factors. These functions appear in the strain displacement relations as functions of the shape factors and their derivatives. For a cylindrical shell, these geometric functions depend only on the thickness coordinate. For a FTSD or HTSD theory, where displacements are expanded in terms of the thickness coordinate, these geometric functions are often expanded in terms of the thickness coordinate and arbitrarily truncated at a specific power of the thickness coordinate.

The previous discussion of theory dealt with the development of the displacement field assumptions, the strain-displacement relations, and the constitutive relations for laminated composite shells. The next phase in the research was the development and solution of the governing differential equations for shell problems. Since the author was specifically interested in the nonlinear phenomena of large displacements and rotations, no analytical or linear solutions were desired. The finite element technique was used to obtain numerical solutions for cylindrical shells. The finite element equations were based upon the total potential energy of the elastic body. Specifically, the principle of stationary potential energy was used where the first variation of potential energy of the system is set equal to zero. The potential energy expression was found by first examining the equilibrium state of the body. For a body with prescribed forces on part of its surface and prescribed boundary conditions on the remaining part of the surface, the equations of equilibrium for an infinitesimal virtual displacement were developed in terms of the Second Piola Kirchhoff stress tensor and the Green strain components expressed in the body's coordinate system. Assuming strains were small, then the stresses could be written in terms of the strains. For a laminated orthotropic material, the stress components could be written in terms of the reduced structural stiffness of the lamina. These quantities depended only on the thickness

coordinate. Thus, they could be written in terms of an integral over the midsurface of the shell, with the integration in the thickness direction performed analytically.

The variation of total potential energy gave five coupled nonlinear partial differential equations which governed the equilibrium of the system. These expressions contained 18 displacement parameters: u, $u_{,1}$, $u_{,2}$, v, $v_{,1}$, $v_{,2}$, w, $w_{,1}$, $w_{,2}$, $w_{,11}$, $w_{,22}$, $w_{,12}$, ψ_1, $\psi_{1,1}$, $\psi_{1,2}$, ψ_2, $\psi_{2,1}$, and $\psi_{2,2}$. These parameters included the seven displacement parameters of Eq (4.1) and their derivatives. Since the equilibrium equations were nonlinear in terms of the displacement parameters, an incremental-iterative approach was used to solve a system of linearized equations which yields an equivalent solution. For simple theories, such as Donnell's theory or a linear FTSD theory where relatively few terms are included, the first variation of potential energy and its linearization, can be explicitly developed, term by term. For more complete theories, such as a linear HTSD theory or the fully nonlinear theory, the potential energy expression has several hundred terms. Its first variation would include, perhaps, thousands of terms, and the subsequent linear equilibrium equations would be quite lengthly.

Rajasekaran and Murray (1973) developed a formal procedure for finite elements, which defined the total potential energy, its first variation, and the linear incremental equilibrium equations in terms of three stiffness matrices. Specifically, the total potential energy was given by:

$$\Pi_p = \{q\}^T \left[\frac{1}{2}[K] + \frac{1}{6}[N_1] + \frac{1}{12}[N_2]\right] \{q\} - \{q\}^T\{R\} \tag{4.17}$$

where

$\{q\} \equiv$ a column array of nodal displacement parameters

$\{R\} \equiv$ a column array of nodal loads

$[K] \equiv$ an array of constant stiffness coefficients

$[N_1] \equiv$ an array of nonlinear coefficients with each term dependent on one of the displacement parameters ($[N_1]$ is linear in terms of displacement)

$[N_2] \equiv$ an array of nonlinear coefficients with each term dependent on the product of two displacement parameters ($[N_2]$ is quadratic in terms of displacement)

The first variation of potential energy, then was given by

$$\left[[K] + \frac{1}{2}[N_1] + \frac{1}{3}[N_2]\right]\{q\} - \{R\} = \{0\} \tag{4.18}$$

and the linear incremental equilibrium equation was given by:

$$[[K] + [N_1] + [N_2]]\{\Delta q\} - \{\Delta R\} = \{0\} \tag{4.19}$$

To assure the formalism of Eqs (4.17)-(4.19) held, the stiffness arrays $[K]$, $[N_1]$, and $[N_2]$ had to be derived in a specific fashion. This derivation is discussed in Chapter IV of the dissertation.

Rajasekaran and Murray's formulation was for finite elements in which strains did not vary through the thickness of the element. This formulation was extended to account for variation of strain through the thickness of the curved shell. To do this, strain at a point in the shell, was in terms of a series expansion in the thickness coordinate, and new definitions of $[\hat{K}]$, $[\hat{N}_1]$, and$[\hat{N}_2]$ were developed for the theory with transverse shear deformation. This formulation required literally hundreds of matrix multiplications to evaluate these equations. A MACSYMA routine was developed to symbolically generate the assumed displacement field, determine the strain components, determine the shell shape factor approximations, determine the elements of the strain definition arrays, form the stiffness arrays, and finally generate the Fortran code for elements of the $\left[\hat{K}\right]$, $\left[\hat{K}_s\right]$, $\left[\hat{N}_1\right]$, $\left[\hat{N}_{1s}\right]$, $\left[\hat{N}_2\right]$, and $\left[\hat{N}_{2s}\right]$ stiffness arrays. Development of this routine was a time consuming, but crucial aspect of this research. The symbolic generation of codes assured reliability and comparability, not achievable by other means. By using these codes in an element independent formulation, the accuracy of each version of theory could be compared using the same finite element model and main program (SHELL). This further assured a fair comparison of the various theoretical attributes of each version.

The element independent stiffness matrices of this theory depended upon the continuum displacement gradient vector $\{d\}$. Using a standard displacement-based finite element method, the 18 two-dimensional functions of the continuum displacement gradient vector were approximated by interpolation from discrete values of nodal displacement parameters. These nodal parameters, or degrees of freedom, were defined only at a finite number of points or nodes. The finite element method required the computation of the stiffness

matrices for each element independently. These elemental stiffnesses were then assembled according to their relationship to global nodes of the structure.

Defining the nodal degrees of freedom required definition of the specific element, since the nodal parameters of $\{q\}$ and the associated nodal interpolation array are element specific. The element chosen was the 36 degree of freedom quadrilateral curved shell element developed by Dennis (1988). This element has been used for many investigations of static and dynamic response of plates, arches, and cylindrical shells undergoing large displacements with linear HTSD theory. The element has eight nodes with seven degrees of freedom, u, v, w, w_1, w_2, ψ_1, and ψ_2, at each of the four corner nodes and two degrees of freedom, u and v, at the four midside nodes. The two degrees of freedom at the midside nodes allow for quadratic interpolation of in-plane displacements u and v. This is important for shells, due to the curvature-induced coupling of bending and membrane activity in shells. The continuum values of u and v were interpolated from the nodal values u_k and v_k, using quadratic Lagrangian interpolation functions. The continuum displacement gradient vector $\{d\}$ included ψ_1 and ψ_2 and the first derivatives of these parameters. Thus, linear interpolation could be used for these parameters, since only C^0 continuity was required. The interpolations of ψ_1 and ψ_2 were given by linear Lagrangian interpolation functions. Nodal parameters associated with transverse displacement included the values w, $w_{,1}$, and $w_{,2}$ at each of the four corner nodes. Thus, interpolation of w was accomplished using quadratic Hermitian shape functions.

The two-dimensional integration of the finite element equations, in the plane of the finite element, was accomplished by numerical integration using Gaussian quadrature. Solution of the resulting equations was accomplished by an incremental-iterative technique commonly called the Newton-Raphson method. The parameters to be incremented were the elements of the array $\{q\}$, containing global degrees of freedom. A global criterion, written in terms of the norms of all displacement parameters, was used to determine convergence.

7.3 Shallow Shell Results with Nonlinear HTSD Theory

One objective of this research was to evaluate the accuracy of the new HTSD theories; another objective was to assess their limitations. Shallow shell problems included a thick flat quasi-isotropic plate with uniform transverse pressure load, two thin isotropic cylindrical shell panels with a transverse point load, and a thin quasi-isotropic cylindrical shell panel with a large cut-out and uniform axial compression load.

The transversely-loaded flat plate problem was used to test the MACSYMA generated codes. The plate chosen was an 8-ply quasi-isotropic laminated square plate with total length of each side equal to 16 inches. Load was a uniform transverse pressure load. The plate thickness was 1.6-inches which indicated transverse shear may be important. For this problem, the eight HTSD theories all gave results that agreed within 1 percent of each other. Although the difference was negligible, all the nonlinear HTSD codes predicted a more flexible response than the linear HTSD codes predicted. In addition, the theories with the highest-order thickness expansions, and most floating point computer operations, gave identical results to the lower-order theories. This problem validated the computational algorithms used to develop and solve the linear and nonlinear HTSD finite element equations for laminated composite shells.

The second class of problems investigated was thin shallow hinged-free isotropic cylindrical shells with a transverse point load acting at the center of the panel. The first problem was a 1/4-inch-thick shell. The second problem was a 1-inch-thick shell of the same configuration. Solutions were computed using a 4×6 mesh of elements to model one quadrant of the shell. For this problem, the linear HTSD codes all produced the same results, and the nonlinear HTSD codes all produced the same results. In comparison with the flat plate problem, the nonlinear HTSD codes for this problem showed greater flexibility than the linear HTSD variants, but only during the collapse phase. The most sophisticated nonlinear HTSD theory predicted a load about 8 percent less in magnitude than a modified Donnell theory (with HTSD included) in the range $0.7 \leq w \leq 0.8$ and about 15 percent less at $w = 0.9$. This was due to the increased coupling of membrane, bending and transverse shear activity in the full nonlinear HTSD theory. Interestingly, this phase of the collapse was characterized by the most extreme displacements and rotations occurring

in the problem. Thus, including nonlinear transverse shear terms had a noticeable effect upon load-displacement predictions for this problem.

Values of the largest linear ε_{23} transverse shear term, $\psi_2 + w_{,2}$, for ten increments of transverse displacement, were compared for the full nonlinear HTSD theory and the modified Donnell theory. These results were virtually identical for increments 1–6, (before the shell snaps through). After the shell snaps, however, the values of $\psi_2 + w_{,2}$ were about 20–25 percent less in magnitude over the majority of the panel for the full nonlinear theory, as compared to the modified Donnell theory. The value of $\psi_2 + w_{,2}$ was dramatically more positive at the hinge line during increments 7–10 for the full nonlinear HTSD theory than for the modified-Donnell theory. For the nonlinear HTSD theory, the ε_{23} and ε_{13} strain components included many more nonlinear terms. The distribution of shear strain was significantly affected by including the nonlinear transverse shear terms. The largest nonlinear term of the ε_{23} transverse shear strain component for the full nonlinear HTSD theory was the term $-w\psi_2/R_2$. This term and the linear term, $\psi_2 + w_{,2}$, were the predominant terms of the ε_{23} transverse shear strain component. For increment 5, when the largest magnitude of $\psi_2 + w_{,2}$ occurs, the maximum values of $\psi_2 + w_{,2}$ and $-w\psi_2/R_2$ were 0.0017 and -0.0003, respectively. Thus, the largest nonlinear term of the full nonlinear HTSD theory was less than 20 percent of the linear term. With each increment from 7 to 9, after the shell has snapped through, the nonlinear term became more significant compared with the linear terms. This nonlinear term created a softening effect while it was of comparable magnitude with the linear terms. It effectively reduced the magnitude of the transverse shear strain over a large area of the shell's midsurface. This softening effect was large enough to affect the strain energy of the shell and subsequently resulted in slightly different equilibrium values of the nodal displacements for the full nonlinear HTSD theory, as compared to the theories with linear transverse shear strain-displacement relations.

A 1-inch thick isotropic shell exhibited a significantly different equilibrium path than the 1/4-inch shell. For this case, the shell never "snaps"; load always increased monotonically for all values of transverse displacement. Comparing results for the full nonlinear HTSD theory with results of the modified-Donnell theory revealed there was virtually no difference in load versus displacement results for this problem. Because of its

thickness, the in-plane extensional and bending terms in the strain energy expression for this shell were predominant. Thus, the equilibrium path was little affected by including nonlinear transverse shear strain terms.

The quasi-isotropic flat panel results indicated the nonlinear HTSD codes predicted a slightly more flexible response than their quasi-nonlinear HTSD variants. Similarly, for the collapse phase of the thin isotropic cylindrical shell, the nonlinear HTSD codes also predicted a more flexible response than the quasi-nonlinear HTSD variants. In both cases, the more exact geometric approximations predicted responses virtually identical to the simplest elemental codes for these shallow shell problems.

A problem with quasi-isotropic material and a smaller radius of curvature was chosen next. This problem was an axially-loaded quasi-isotropic cylindrical shell panel with a cut-out. This panel had a radius of 12-inches, a thickness of 0.04-inches, and dimensions of 12-inches (lateral) by 8-inches (circumferential). The cut-out was square, with 4-inch sides, and was centrally located. Due to the possibility of nonsymmetric deformation, the entire panel was discretized into 360 elements. Only the full nonlinear HTSD theory and the most sophisticated quasi-nonlinear HTSD theory were evaluated. For this case, the ε_{23} of the full nonlinear HTSD theory was virtually identical to the ε_{23} of the quasi-nonlinear HTSD theory. This was attributed to several characteristics of the problem. The most significant difference, between this panel and panels reported earlier, was the ratio of thickness to characteristic length. The plate was 1.6-inches thick with an edge length of 16 inches. The isotropic shells had thicknesses of 1/4 inch and 1 inch with edge lengths of 20 inches. The axial panel was 0.04-inches thick with a 12-inch radius and a minimum edge length of 8 inches. Based on Koiter's work, the transverse shear strains for these problems would be of the order h/L times the in-plane strains. Thus, for the plate the transverse shear strains would be about 1/10th of the in-plane strains. For the isotropic shells the transverse shear strains would be 1/80th and 1/20th of the in-plane strains. Finally, for the axial panel these strains were about 1/160th of the in-plane strains. Thus, this axial panel problem was a mild test of transverse shear behavior compared to the flat plate problem and the 1/4-inch-thick shell problem.

7.4 *Deep Shell Results with Quasi-Nonlinear HTSD Theory*

A deep clamped-free quasi-isotropic cylindrical shell panel, with a transverse point load at the center, was chosen to study the effects of nonlinear transverse shear for deep composite shell panels. This panel, like the axially-loaded panel, was a laminated quasi-isotropic panel with a radius of 12–inches, but the thickness was only 0.04–inches and the dimensions were 12-inches (lateral) by 12–inches (circumferential). Because of the larger circumferential dimension, this shell was significantly deeper than the axially-loaded panel. Tsai and others (1990) investigated shells of this configuration and compared static and dynamic results for different material properties and ply layups. A one quadrant 96 element mesh was chosen for this problem. The quasi-nonlinear HTSD theories all predicted identical results, comparable to those of Tsai. The nonlinear HTSD theories, however, predicted a significantly more flexible structure at the onset of loading. As transverse displacement increased, the nonlinear HTSD theories predicted an increasingly stiffer structure. This response was much stiffer than the quasi-nonlinear HTSD theories predicted. The ratio of thickness to characteristic length of this problem was even smaller than any of the problems analyzed earlier. This ratio was equal to 1/300, thus, nonlinear transverse shear strain was expected to be insignificant. However, The nonlinear HTSD results of this problem deviated considerably from the results of previous problems.

Comparing three of the linear and nonlinear terms of ε_{23}, as done for other problems, revealed a significantly different behavior for the ε_{23} of the fullly-nonlinear HTSD theory as compared to the modified-Donnell theory. This explained the stiff response as w increased, but did not explain the increased flexibility at the onset of loading. Although the depth of this shell was an important factor, the magnitude of transverse displacement did not cause the increased flexibility.

The 1/4–inch-thick isotropic panel had properties that did not vary with orientation of the material. Shear modulus for the isotropic material was assumed to be one-half the Young's Modulus. Since the shell behaved in a flexible manner and snapped through with relatively low transverse load, the primary cause of deformation was bending activity. Since the panel was hinged, the initial severity of bending was characterized by the distance between the lateral supports and the depth of the shell. The quasi-isotropic shell had a [0/-

45/+45/90]s ply layup with a ratio of $E_1/E_2 = 15$ and transverse shear moduli less than E_2. For the composite shell, the primary cause of deformation was also bending activity. The outer plies of this laminated panel were the only plies oriented in the transverse direction. This implied that 75 percent of the material of this shell had a stiffness in the circumferential direction that was significantly less than the outer plies. This panel was only 0.04–inches thick, thus, the outer plies may not have been very effective in resisting bending, since they were so close to the midsurface of the shell. With the lateral supports of this shell clamped the final deformed shape of the shell exhibited both positive and negative curvatures. Thus, severity of bending was characterized by the distance between counterflexure points of the final deformed shape; a distance of about 2 inches. The bending activity of the clamped composite shell was more severe than that of the hinged isotropic shell. Since transverse shear stress is roughly equal to h/L times the bending stress, the clamped quasi-isotropic shell was a more severe test of nonlinear HTSD theory.

This problem demonstrated that nonisotropic material properties could have a significant effect upon the predicted behavior of shell structures. Because of the reduced stiffness in the circumferential direction, the increased coupling of transverse shear activity with in-plane strains, and the significantly lower transverse shear properties of this panel, the incorporation of nonlinear terms for transverse shear strain significantly affected the strain energy of the composite shell. This resulted in a more flexible structure at the onset of loading.

Deep circular arches can be used to demonstrate a theory's ability to predict large displacements and rotations. Many variations of transversely-loaded deep arch problems have been reported in the literature. The problem chosen for this research was a 100–inch radius isotropic arch with a 1–inch square cross section and an opening angle of 106 degrees. Solutions for this problem were computed using all variations of the HTSD theory. A 1×16 mesh of elements was used to represent one quadrant of the arch. The quasi-nonlinear HTSD theories, in this case, predicted a more dramatic collapse of the arch than the Donnell-type solution (even though the Donnell theory was modified to include transverse shear deformation). This difference in predicted response was due to the many nonlinear in-plane displacement terms in the strain definitions that are not included

in the Donnell equations. A more exact representation of these terms, therefore, should produce more flexible results. The quasi-nonlinear HTSD theory with quartic u_2 displacement assumption, however, did not give a more flexible result than the quasi-nonlinear HTSD theory with the incomplete cubic u_2 displacement assumption. In contrast, the two quasi-nonlinear HTSD theories with quadratic shape function approximations both predicted a more flexible response after collapse than the theories with linear shape function approximations. This difference in results was 10–15 percent.

For the thin shallow isotropic cylindrical shell, the nonlinear HTSD variants produced promising results; the nonlinear HTSD variants predicted an 8–15 percent reduction in loads during the collapse phase of the equilibrium path. For the deep circular arch, however, the nonlinear HTSD variants predicted results that were too stiff when 16 elements were used to model a quadrant of the structure. The stiff response was similar to responses obtained for thin shallow shells when too few elements were used. A rough analysis of relative error, caused by discretization, revealed that more elements were needed for this arch to assure the accuracy of results was comparable with that of the shell panel. Thus, despite the arch being a simple 1–dimensional problem, modeling it with 2–dimensional shell elements created discretization errors which should be avoided. Results for a 1×48 element discretization, using the quasi-nonlinear HTSD variants and the modified Donnell theory, showed an even greater reduction in load after collapse with quadratic shape factor approximations. Unfortunately, the nonlinear HTSD variants still diverged to stiff solutions beyond crown displacements of about 4–inches.

At this point, two "shells" with thickness of 1 inch and radius of 100 inches had been analyzed with dramatically different results. For one, a shallow panel, the nonlinear HTSD theory predicted a more flexible structure. For the other, a deep arch, the same theory predicted a grossly over-stiff response. The only differences between these problems were the width, depth, and circumferential length. Correction of discretization errors due to large aspect ratios did not correct the over-stiff behavior of the nonlinear HTSD codes. Therefore, there must be another explanation. Surana (1986) investigated similar 100-inch radius arches of varying width. He found a 2-inch wide arch behaved like a beam, but a 24-inch wide arch behaved more like a shell. The 2-inch wide arch was stiffer than the

24–inch arch despite equal values of bending stiffness EI. This implies the membrane activity of the shell panel must cause it to be less stiff than the arch.

Based upon these observations, it seems feasible that nonlinear terms of the transverse shear strain components may have a more significant effect than expected. The nonlinear HTSD theory used for this research was not exact. The author used linear kinematics based upon exactly satisfying the zero traction boundary conditions of the linear transverse shear terms of a curved shell. These kinematics, given in Eq (4.1), did not satisfy this boundary condition when the full nonlinear ε_{13} and ε_{23} strain-displacement relations were used. A parabolic function of thickness coordinate was included in the nonlinear transverse shear strain definition to assure a traction free surface. The possibility of nonlinear transverse shear strain terms exceeding the allowable estimates of transverse shear stress (from Koiter's shell research), still existed with this approximate nonlinear HTSD theory. Comparing values for the linear and nonlinear terms of ε_{23} revealed a behavior very similar to the shell panel, but of much greater magnitude. The largest nonlinear term, $-w\psi_2/R_2$, deviated significantly from the linear terms of transverse shear strain. The nonlinear term effectively eliminated all positive terms of ε_{23}. This caused the transverse shear strain to change sign, and ultimately, the nonlinear transverse shear strain terms became so dominant, they caused an over-stiff response instead of the more flexible response expected.

The deep arch revealed two significant findings. First, a more-exact approximation of the shell geometric shape factors predicted a more flexible structure during the collapse phase. Secondly, the linear kinematic assumptions of Eq (4.1) resulted in coupling of nonlinear transverse shear ε_{23} and transverse displacement, w. This coupling caused ε_{23} to vary, dramatically, from its expected behavior when w increased beyond certain bounds. These bounds were dictated by the assumption that transverse shear strains be of the order h/L times the bending or direct strains. This was one of the basic assumptions used to justify the use of a two-dimensional shell model. Thus, the nonlinear HTSD theory (with linear kinematics) was suitable only for shallow shell problems which undergo small rotations.

7.5 Conclusions

This research revealed several unique findings related to the limitations of a nonlinear HTSD shell theory employing higher-order thickness expansions and linear kinematic assumptions. The ratio of thickness to wave length of curvature (distance between counter-flexure points of the deformed midsurface) and the ratio of transverse displacement to depth of the shell were found to be important factors in predicting the applicability of the nonlinear HTSD theory. If these ratios were negligible, nonlinear transverse shear strain terms had no impact on predicted response. If these ratios were small (on the order of 10^{-3} to 10^{-1}), the incorporation of nonlinear HTSD theory produced a more flexible response. A shallow 1/4–inch-thick hinged-free isotropic shell panel exhibited this more flexible response with nonlinear strain-displacement terms in the transverse shear strain formulation. If the ratios were large, the nonlinear terms of the transverse shear strain components could possibly exceed the magnitudes of the corresponding linear transverse shear strain terms. This resulted in a stiff response prediction. Both deep shell problems exhibited stiff response predictions with nonlinear transverse shear strain-displacement relations.

The additional computational burden of the nonlinear strain-displacement relations is significant. Table 4.3, on page 4-20, shows the number of lines of Fortran code required for each variation of theory. The most simple nonlinear HTSD theory is C003. This theory has 23176 lines of code compared to 13866 lines for the C000 quasi-nonlinear HTSD theory. The resulting computational burden of this additional code was significant in terms of CPU consumption and memory requirement. The elemental independent formulation of stiffness arrays, with Gauss integration in the plane of the element, requires execution of all 23176 lines of code at each Guass point of every element (for the 36 degree of freedom element chosen, 49 Guass points are calculated per element for exact integration) on every iteration of every load increment of the nonlinear problem. Clearly, this formulation of a higher-order theory is practical only for specialized research of this nature, not for routine engineering use. Since the element independent formulation is based upon arrays of strain coefficients, the possibility of "vectorizing" the formulation exists. In this manner, perhaps, a more efficient higher-order theory may be of practical use.

Koiter showed that typical shell theory assumptions resulted in transverse shear strains that were of the order h/L times the bending or direct strain components. For his work, strain and stress were directly related by the constitutive relations for linear elastic isotropic materials. For composite materials, however, the material properties can vary significantly in different directions. A quasi-isotropic composite shell panel with relatively few fibers oriented circumferentially exhibited a more flexible response from the onset of loading when nonlinear transverse shear terms were included. This was a direct result of the increased coupling of membrane and transverse shear activity with the nonlinear HTSD formulation. Thus, for composites, one must be careful to apply Koiter's estimates to stress instead of strain. Thus, provided one assures the nonlinear transverse shear terms of the nonlinear HTSD theory do not result in transverse shear *stresses* exceeding h/L times the bending or direct *stresses*, this theory can be used for the prediction of nonlinear HTSD responses of curved shells. For the six problems the author investigated, the nonlinear HTSD theory was suitable for the four shallow shell problems, but not for the deep composite shell problem or the deep isotropic arch.

Another objective of this research was to determine the effect of using higher-order thickness expansions for the displacement field assumptions and for the geometric shell shape factor approximations. The use of the complete quartic displacement assumption made no noticeable difference in static equilibrium load-displacement results, as compared to the incomplete third-order HTSD kinematic assumptions. The author believes the higher-order kinematic assumption would be important for shells with larger ratios of thickness to radii of curvature. The additional terms of the quartic displacement field are multiplied by factors of y_3/R, thus, large values of h/R will make these additional terms more significant. For the problems the author investigated, h/R was not less than 1/25. The quartic displacement assumption increased the number of lines for the quasi-nonlinear C100 theory to 29626, compared to 15806 lines for the incomplete cubic displacement assumption (C000). Since this additional computational effort had no significant effect upon results, one could conclude that practical problems, of the type investigated by the author, can be accurately and efficiently solved with incomplete cubic kinematic assumptions.

The use of quadratic approximations for the shell geometric shape factor functions consistently provided more flexible response predictions for the deep circular arch during the collapse phase. For the shallow shell panels analyzed, the quadratic shape factor approximations gave results identical to the linear shape factor approximations. The quadratic shape factor approximations, like the quartic displacement, significantly increased the number of lines of Fortran code required. From Table 4.3, the quasi-nonlinear HTSD theory with quadratic shape factor approximations (C020) had 24254 lines of code. For the deep shell problems investigated the ratio of h/R was never less than 1/100, thus, the effect of the higher-order shape factor approximations was not apparent until the deformation was significant. The deep arch required displacements of at least $R/4$ before the higher-order effect was recognizable. As with the quartic displacement, the higher-order shape factor approximations required significantly more computational resources. Thus, the author believes quasi-nonlinear HTSD theories based upon the assumption that $h^2/R^2 \ll 1$ are sufficiently accurate and economical for practical engineering analyses.

Thus, including higher-order thickness expansions in a *quasi-nonlinear* HTSD theory resulted in a more flexible response prediction for deep shell problems during the collapse phase. Similarly, the *nonlinear* HTSD theory provided a more flexible response prediction for shallow shell problems during the collapse phase. The incorporation of these theoretical characteristics required a significant increase in the amount of Fortran code with a proportional increase in the computational memory and time required for problem solution. The simplest nonlinear HTSD theory, developed for this research, incorporated incomplete third-order kinematics and a linear approximation of the shell geometric shape factor functions. This theory resulted in Fortran code about twice the length of the comparable quasi-nonlinear HTSD variant. Further investigations could be accomplished with this version of the theory, in lieu of the most complete nonlinear theory used for this research. The use of nonlinear kinematics was beyond the scope of this investigation. Their use, however, may allow nonlinear HTSD theories with nonlinear transverse shear strain terms which will not exceed the basic theoretical limitations of two-dimensional shell theory.

Appendix A. *Arbitrary Shell Strain Displacement Relations*

The arbitrary shell is described in terms of a curvilinear orthogonal coordinate system aligned with lines of principal curvature. Displacement within the shell is assumed to be of the form

$$\vec{U} = u_1\vec{e}_1 + u_2\vec{e}_2 + u_3\vec{e}_3 \tag{A.1}$$

where the orthonormal vectors $\vec{e}_1$ and $\vec{e}_2$ are aligned with principal lines of curvature. The direction of $\vec{e}_3$ is determined by the cross product of $\vec{e}_1$ and $\vec{e}_2$. The components of displacement in the 1–, 2–, and 3–direction are assumed to be unspecified functions of the curvilinear coordinates y_1, y_2 and y_3. The shell shape factors h_1 and h_2 are general arbitrary functions, specifically: $h_1 = h_1(y_1, y_2, y_3)$ and $h_2 = h_2(y_1, y_2, y_3)$ and $h_3 = 1$.

A.1 Midsurface Strain Components for the Arbitrary Shell

The strain equations listed below are the linear and nonlinear parts of the strain components for the case of an arbitrary shell. The ε_{33} component is assumed to be zero for this shell formulation. Contracted notation is used, where $\varepsilon_1 = \varepsilon_{11}$, $\varepsilon_2 = \varepsilon_{22}$, $\varepsilon_4 = \varepsilon_{23}$, $\varepsilon_5 = \varepsilon_{13}$, and $\varepsilon_6 = \varepsilon_{12}$.

$$\varepsilon_{1_L} = u_{1,1}/h_1 + h_{1,2}u_2/(h_1h_2) + h_{1,3}u_3/h_1$$

$$\varepsilon_{2_L} = h_{2,1}u_1/(h_1h_2) + u_{2,2}/h_2 + h_{2,3}u_3/h_2$$

$$\varepsilon_{4_L} = u_{2,3} - h_{2,3}u_2/h_2 + u_{3,2}/h_2$$

$$\varepsilon_{5_L} = u_{1,3} - h_{1,3}u_1/h_1 + u_{3,1}/h_1$$

$$\varepsilon_{6_L} = u_{1,2}/h_2 - h_{1,2}u_1/(h_1h_2) + u_{2,1}/h_1 - h_{2,1}u_2/(h_1h_2)$$

$$\varepsilon_{1_{NL}} = h_3u_{1,1}^2/(2h_1^2) + h_{1,3}^2h_3u_1^2/(2h_1^2) + h_{1,2}^2h_3u_1^2/(2h_1^2h_2^2) - h_{1,2}u_1u_{2,1}/(h_1^2h_2)$$
$$+ h_3u_{2,1}^2/(2h_1^2) + h_{1,2}u_{1,1}u_2/(h_1^2h_2) + h_{1,2}^2h_3u_2^2/(2h_1^2h_2^2) - h_{1,3}u_1u_{3,1}/h_1^2 + h_3u_{3,1}^2/(2h_1^2)$$
$$+ h_{1,3}u_{1,1}u_3/h_1^2 + h_{1,2}h_{1,3}u_2u_3/(h_1^2h_2) + h_{1,3}^2h_3u_3^2/(2h_1^2)$$

$$\varepsilon_{2_{NL}} = h_3 u_{1,2}^2/(2h_2^2) + h_{2,1}^2 h_3 u_1^2/(2h_1^2 h_2^2) + h_{2,1} u_1 u_{2,2}/(h_1 h_2^2) + h_3 u_{2,2}^3/(2h_2^2)$$
$$- h_{2,1} u_{1,2} u_2/(h_1 h_2^2) + h_{2,1}^2 h_3 u_2^2/(2h_1^2 h_2^2) + h_{2,3}^2 h_3 u_2^2/(2h_2^2) - h_{2,3} u_2 u_{3,2}/h_2^2 + h_3 u_{3,2}^2/(2h_2^2)$$
$$+ h_{2,1} h_{2,3} u_1 u_3/(h_1 h_2^2) + h_{2,3} u_{2,2} u_3/h_2^2 + h_{2,3}^2 h_3 u_3^2/(2h_2^2)$$

$$\varepsilon_{4_{NL}} = u_{1,2} u_{1,3}/h_2 + h_{2,1} u_1 u_{2,3}/(h_1 h_2) + u_{2,2} u_{2,3}/h_2 - h_{2,1} u_{1,3} u_2/(h_1 h_2) - h_{2,3} u_2 u_{3,3}/h_2$$
$$+ u_{3,2} u_{3,3}/h_2 + h_{2,3} u_{2,3} u_3/h_2$$

$$\varepsilon_{5_{NL}} = u_{1,1} u_{1,3}/h_1 - h_{1,2} u_1 u_{2,3}/(h_1 h_2) + u_{2,1} u_{2,3}/h_1 + h_{1,2} u_{1,3} u_2/(h_1 h_2) - h_{1,3} u_1 u_{3,3}/h_1$$
$$+ u_{3,1} u_{3,3}/h_1 + h_{1,3} u_{1,3} u_3/h_1$$

$$\varepsilon_{6_{NL}} = u_{1,1} u_{1,2}/(h_1 h_2) - h_{1,2} h_{2,1} u_1^2/(h_1^2 h_2^2) + h_{2,1} u_1 u_{2,1}/(h_1^2 h_2) - h_{1,2} u_1 u_{2,2}/(h_1 h_2^2)$$
$$+ u_{2,1} u_{2,2}/(h_1 h_2) - h_{2,1} u_{1,1} u_2/(h_1^2 h_2) + h_{1,2} u_{1,2} u_2/(h_1 h_2^2) + h_{1,3} h_{2,3} u_1 u_2/(h_1 h_2)$$
$$- h_{1,2} h_{2,1} u_2^2/(h_1^2 h_2^2) - h_{2,3} u_2 u_{3,1}/(h_1 h_2) - h_{1,3} u_1 u_{3,2}/(h_1 h_2) + u_{3,1} u_{3,2}/(h_1 h_2)$$
$$+ h_{1,3} u_{1,2} u_3/(h_1 h_2) - h_{1,2} h_{2,3} u_1 u_3/(h_1 h_2^2) + h_{2,3} u_{2,1} u_3/(h_1 h_2) - h_{1,3} h_{2,1} u_2 u_3/(h_1^2 h_2)$$

A.2 Midsurface Strain Components for the Arbitrary Shell with a General Quartic Displacement Field Assumption

The expressions listed in the previous section represent strain components for an arbitrary shell where displacement components are unspecified functions of the coordinates (y_1, y_2, y_3). For a shear deformation theory, the displacements are assumed to be functions of the thickness coordinate. Specifically, for a shell with radius R_1 in the y_1-direction and radius R_2 in the y_2-direction, we shall assume a quartic series expansion for u_1 and u_2 as shown below; the u_3 component is assumed to be constant through the thickness of the shell.

$$\begin{aligned} u_1 &= u(1 - y_3/R_1) + \psi_1 y_3 + \phi_1 y_3^2 + \gamma_1 y_3^3 + \theta_1 y_3^4 \\ u_2 &= u(1 - y_3/R_2) + \psi_2 y_3 + \phi_2 y_3^2 + \gamma_2 y_3^3 + \theta_2 y_3^4 \\ u_3 &= w(y_1, y_2) \end{aligned} \tag{A.2}$$

If one substitutes these expressions for the displacements into the previously derived expressions for strain components, the following expressions are obtained for the strain components χ_i^p, where:

$$\varepsilon_{i_L} = \chi_{i_L}^0 + \sum_{p=1}^{n} \chi_{i_L}^p y_3^p \tag{A.3}$$

and

$$\varepsilon_{i_{NL}} = \chi^0_{i_{NL}} + \sum_{p=1}^{n} \chi^p_{i_{NL}} y_3^p \qquad \text{(A.4)}$$

$$\chi^0_{1_L} = u_{,1}/h_1 + h_{1,2}v/(h_1h_2)$$

$$\chi^1_{1_L} = \psi_{1,1}/h_1 + h_{1,2}\psi_2/(h_1h_2) - u_{,1}/(R_1h_1) - h_{1,2}v/(R_2h_1h_2)$$

$$\chi^2_{1_L} = \phi_{1,1}/h_1 + h_{1,2}\phi_2/(h_1h_2)$$

$$\chi^3_{1_L} = \gamma_{1,1}/h_1 + \gamma_2 h_{1,2}/(h_1h_2)$$

$$\chi^4_{1_L} = \theta_{1,1}/h_1 + h_{1,2}\theta_2/(h_1h_2)$$

$$\chi^0_{2_L} = h_{2,1}u/(h_1h_2) + v_{,2}/h_2$$

$$\chi^1_{2_L} = h_{2,1}\psi_1/(h_1h_2) + \psi_{2,2}/h_2 - h_{2,1}u/(R_1h_1h_2) - v_{,2}/(R_2h_2)$$

$$\chi^2_{2_L} = h_{2,1}\phi_1/(h_1h_2) + \phi_{2,2}/h_2$$

$$\chi^3_{2_L} = \gamma_{2,2}/h_2 + \gamma_1 h_{2,1}/(h_1h_2)$$

$$\chi^4_{2_L} = h_{2,1}\theta_1/(h_1h_2) + \theta_{2,2}/h_2$$

$$\chi^0_{4_L} = u_{3,2}/h_2 + \psi_2 - v/R_2$$

$$\chi^1_{4_L} = 2\phi_2 - h_{2,3}\psi_2/h_2 + h_{2,3}v/(R_2h_2)$$

$$\chi^2_{4_L} = 3\gamma_2 - h_{2,3}\phi_2/h_2$$

$$\chi^3_{4_L} = -\gamma_2 h_{2,3}/h_2 + 4\theta_2$$

$$\chi^4_{4_L} = -h_{2,3}\theta_2/h_2$$

$$\chi^0_{5_L} = u_{3,1}/h_1 + \psi_1 - u/R_1$$

$$\chi^1_{5_L} = 2\phi_1 - h_{1,3}\psi_1/h_1 + h_{1,3}u/(R_1h_1)$$

$$\chi^2_{5_L} = 3\gamma_1 - h_{1,3}\phi_1/h_1$$

$$\chi^3_{5_L} = -\gamma_1 h_{1,3}/h_1 + 4\theta_1$$

$$\chi^4_{5_L} = -h_{1,3}\theta_1/h_1$$

$$\chi^0_{6_L} = -h_{1,2}u/(h_1h_2) + u_{,2}/h_2 - h_{2,1}v/(h_1h_2) + v_{,1}/h_1$$

$$\chi^1_{6_L} = \psi_{1,2}/h_2 - h_{1,2}\psi_1/(h_1h_2) + \psi_{2,1}/h_1 - h_{2,1}\psi_2/(h_1h_2) + h_{1,2}u/(R_1h_1h_2) - u_{,2}/(R_1h_2)$$
$$+h_{2,1}v/(R_2h_1h_2) - v_{,1}/(R_2h_1)$$

$$\chi^2_{6_L} = \phi_{1,2}/h_2 - h_{1,2}\phi_1/(h_1h_2) + \phi_{2,1}/h_1 - h_{2,1}\phi_2/(h_1h_2)$$

$$\chi^3_{6_L} = \gamma_{2,1}/h_1 + \gamma_{1,2}/h_2 - \gamma_1 h_{1,2}/(h_1h_2) - \gamma_2 h_{2,1}/(h_1h_2)$$

$$\chi^4_{6_L} = \theta_{1,2}/h_2 - h_{1,2}\theta_1/(h_1h_2) + \theta_{2,1}/h_1 - h_{2,1}\theta_2/(h_1h_2)$$

$$\chi^0_{1_{NL}} = (u_{3,1})^2 h_3/(2h_1^2) + h_{1,2}^2 h_3 u^2/(2h_1^2h_2^2) + h_3 u_{,1}^2/(2h_1^2) + h_{1,2}u_{,1}v/(h_1^2h_2)$$
$$+h_{1,2}^2 h_3 v^2/(2h_1^2h_2^2) - h_{1,2}uv_{,1}/(h_1^2h_2) + h_3 v_{,1}^2/(2h_1^2)$$

$$\chi^1_{1_{NL}} = u_3h_{1,3}\psi_{1,1}/h_1^2 - u_{3,1}h_{1,3}\psi_1/h_1^2 + u_3h_{1,2}h_{1,3}\psi_2/(h_1^2h_2) + u_{3,1}h_{1,3}u/(R_1h_1^2)$$
$$+h_{1,3}^2\psi_1 u/h_1^2 + h_{1,2}^2\psi_1 u/(h_1^2h_2^2) - h_{1,2}\psi_{2,1}u/(h_1^2h_2) - h_{1,3}^2u^2/(R_1h_1^2) - h_{1,2}^2u^2/(R_1h_1^2h_2^2)$$
$$-u_3h_{1,3}u_{,1}/(R_1h_1^2) + \psi_{1,1}u_{,1}/h_1^2 + h_{1,2}\psi_2 u_{,1}/(h_1^2h_2) - u_{,1}^2/(R_1h_1^2) - u_3h_{1,2}h_{1,3}v/(R_2h_1^2h_2)$$
$$+h_{1,2}\psi_{1,1}v/(h_1^2h_2) + h_{1,2}^2\psi_2 v/(h_1^2h_2^2) - h_{1,2}u_{,1}v/(R_1h_1^2h_2) - h_{1,2}u_{,1}v/(R_2h_1^2h_2)$$
$$-h_{1,2}^2v^2/(R_2h_1^2h_2^2) - h_{1,2}\psi_1 v_{,1}/(h_1^2h_2) + \psi_{2,1}v_{,1}/h_1^2 + h_{1,2}uv_{,1}/(R_1h_1^2h_2)$$
$$+h_{1,2}uv_{,1}/(R_2h_1^2h_2) - v_{,1}^2/(R_2h_1^2)$$

$$\chi^2_{1_{NL}} = u_3h_{1,3}\phi_{1,1}/h_1^2 - u_{3,1}h_{1,3}\phi_1/h_1^2 + u_3h_{1,2}h_{1,3}\phi_2/(h_1^2h_2) + h_3\psi_{1,1}^2/(2h_1^2)$$
$$+h_{1,3}^2h_3\psi_1^2/(2h_1^2) + h_{1,2}^2h_3\psi_1^2/(2h_1^2h_2^2) - h_{1,2}\psi_1\psi_{2,1}/(h_1^2h_2) + h_3\psi_{2,1}^2/(2h_1^2)$$
$$+h_{1,2}\psi_{1,1}\psi_2/(h_1^2h_2) + h_{1,2}^2h_3\psi_2^2/(2h_1^2h_2^2) + h_{1,3}^2\phi_1 u/h_1^2 + h_{1,2}^2\phi_1 u/(h_1^2h_2^2) - h_{1,2}\phi_{2,1}u/(h_1^2h_2)$$
$$-h_{1,3}^2\psi_1 u/(R_1h_1^2) - h_{1,2}^2\psi_1 u/(R_1h_1^2h_2^2) + h_{1,2}\psi_{2,1}u/(R_1h_1^2h_2) + h_{1,3}^2h_3u^2/(2R_1^2h_1^2)$$

$$+h_{1,2}^2 h_3 u^2/(2R_1^2 h_1^2 h_2^2) + \phi_{1,1} u_{,1}/h_1^2 + h_{1,2}\phi_2 u_{,1}/(h_1^2 h_2) - \psi_{1,1} u_{,1}/(R_1 h_1^2)$$
$$-h_{1,2}\psi_2 u_{,1}/(R_1 h_1^2 h_2) + h_3 u_{,1}^2/(2R_1^2 h_1^2) + h_{1,2}\phi_{1,1} v/(h_1^2 h_2) + h_{1,2}^2 \phi_2 v/(h_1^2 h_2^2)$$
$$-h_{1,2}\psi_{1,1} v/(R_2 h_1^2 h_2) - h_{1,2}^2 \psi_2 v/(R_2 h_1^2 h_2^2) + h_{1,2} u_{,1} v/(R_1 R_2 h_1^2 h_2) + h_{1,2}^2 h_3 v^2/(2R_2^2 h_1^2 h_2^2)$$
$$-h_{1,2}\phi_1 v_{,1}/(h_1^2 h_2) + \phi_{2,1} v_{,1}/h_1^2 + h_{1,2}\psi_1 v_{,1}/(R_2 h_1^2 h_2) - \psi_{2,1} v_{,1}/(R_2 h_1^2)$$
$$-h_{1,2} u v_{,1}/(R_1 R_2 h_1^2 h_2) + h_3 v_{,1}^2/(2R_2^2 h_1^2)$$

$$\chi_{1_{NL}}^3 = u_3\gamma_{1,1}h_{1,3}/h_1^2 - u_{3,1}\gamma_1 h_{1,3}/h_1^2 + u_3\gamma_2 h_{1,2}h_{1,3}/(h_1^2 h_2) + \phi_{1,1}\psi_{1,1}/h_1^2$$
$$+h_{1,2}\phi_2\psi_{1,1}/(h_1^2 h_2) + h_{1,3}^2\phi_1\psi_1/h_1^2 + h_{1,2}^2\phi_1\psi_1/(h_1^2 h_2^2) - h_{1,2}\phi_{2,1}\psi_1/(h_1^2 h_2)$$
$$-h_{1,2}\phi_1\psi_{2,1}/(h_1^2 h_2) + \phi_{2,1}\psi_{2,1}/h_1^2 + h_{1,2}\phi_{1,1}\psi_2/(h_1^2 h_2) + h_{1,2}^2\phi_2\psi_2/(h_1^2 h_2^2) + \gamma_1 h_{1,3}^2 u/h_1^2$$
$$+\gamma_1 h_{1,2}^2 u/(h_1^2 h_2^2) - \gamma_{2,1}h_{1,2}u/(h_1^2 h_2) - h_{1,3}^2\phi_1 u/(R_1 h_1^2) - h_{1,2}^2\phi_1 u/(R_1 h_1^2 h_2^2)$$
$$+h_{1,2}\phi_{2,1}u/(R_1 h_1^2 h_2) + \gamma_{1,1}u_{,1}/h_1^2 + \gamma_2 h_{1,2}u_{,1}/(h_1^2 h_2) - \phi_{1,1}u_{,1}/(R_1 h_1^2)$$
$$-h_{1,2}\phi_2 u_{,1}/(R_1 h_1^2 h_2) + \gamma_2 h_{1,2}^2 v/(h_1^2 h_2^2) + \gamma_{1,1}h_{1,2}v/(h_1^2 h_2) - h_{1,2}\phi_{1,1}v/(R_2 h_1^2 h_2)$$
$$-h_{1,2}^2\phi_2 v/(R_2 h_1^2 h_2^2) + \gamma_{2,1}v_{,1}/h_1^2 - \gamma_1 h_{1,2}v_{,1}/(h_1^2 h_2) + h_{1,2}\phi_1 v_{,1}/(R_2 h_1^2 h_2) - \phi_{2,1}v_{,1}/(R_2 h_1^2)$$

$$\chi_{1_{NL}}^4 = h_3\phi_{1,1}^2/(2h_1^2) + h_{1,3}^2 h_3\phi_1^2/(2h_1^2) + h_{1,2}^2 h_3\phi_1^2/(2h_1^2 h_2^2) - h_{1,2}\phi_1\phi_{2,1}/(h_1^2 h_2)$$
$$+h_3\phi_{2,1}^2/(2h_1^2) + h_{1,2}\phi_{1,1}\phi_2/(h_1^2 h_2) + h_{1,2}^2 h_3\phi_2^2/(2h_1^2 h_2^2) + \gamma_{1,1}\psi_{1,1}/h_1^2 + \gamma_2 h_{1,2}\psi_{1,1}/(h_1^2 h_2)$$
$$+\gamma_1 h_{1,3}^2\psi_1/h_1^2 + \gamma_1 h_{1,2}^2\psi_1/(h_1^2 h_2^2) - \gamma_{2,1}h_{1,2}\psi_1/(h_1^2 h_2) + \gamma_{2,1}\psi_{2,1}/h_1^2 - \gamma_1 h_{1,2}\psi_{2,1}/(h_1^2 h_2)$$
$$+\gamma_2 h_{1,2}^2\psi_2/(h_1^2 h_2^2) + \gamma_{1,1}h_{1,2}\psi_2/(h_1^2 h_2) + u_3 h_{1,3}\theta_{1,1}/h_1^2 - u_{3,1}h_{1,3}\theta_1/h_1^2$$
$$+u_3 h_{1,2}h_{1,3}\theta_2/(h_1^2 h_2) - \gamma_1 h_{1,3}^2 u/(R_1 h_1^2) - \gamma_1 h_{1,2}^2 u/(R_1 h_1^2 h_2^2) + \gamma_{2,1}h_{1,2}u/(R_1 h_1^2 h_2)$$
$$+h_{1,3}^2\theta_1 u/h_1^2 + h_{1,2}^2\theta_1 u/(h_1^2 h_2^2) - h_{1,2}\theta_{2,1}u/(h_1^2 h_2) - \gamma_{1,1}u_{,1}/(R_1 h_1^2) - \gamma_2 h_{1,2}u_{,1}/(R_1 h_1^2 h_2)$$
$$+\theta_{1,1}u_{,1}/h_1^2 + h_{1,2}\theta_2 u_{,1}/(h_1^2 h_2) - \gamma_2 h_{1,2}^2 v/(R_2 h_1^2 h_2^2) - \gamma_{1,1}h_{1,2}v/(R_2 h_1^2 h_2) + h_{1,2}\theta_{1,1}v/(h_1^2 h_2)$$
$$+h_{1,2}^2\theta_2 v/(h_1^2 h_2^2) - \gamma_{2,1}v_{,1}/(R_2 h_1^2) + \gamma_1 h_{1,2}v_{,1}/(R_2 h_1^2 h_2) - h_{1,2}\theta_1 v_{,1}/(h_1^2 h_2) + \theta_{2,1}v_{,1}/h_1^2$$

$$\chi_{1_{NL}}^5 = \gamma_{1,1}\phi_{1,1}/h_1^2 + \gamma_2 h_{1,2}\phi_{1,1}/(h_1^2 h_2) + \gamma_1 h_{1,3}^2\phi_1/h_1^2 + \gamma_1 h_{1,2}^2\phi_1/(h_1^2 h_2^2)$$
$$-\gamma_{2,1}h_{1,2}\phi_1/(h_1^2 h_2) + \gamma_{2,1}\phi_{2,1}/h_1^2 - \gamma_1 h_{1,2}\phi_{2,1}/(h_1^2 h_2) + \gamma_2 h_{1,2}^2\phi_2/(h_1^2 h_2^2) + \gamma_{1,1}h_{1,2}\phi_2/(h_1^2 h_2)$$
$$+\psi_{1,1}\theta_{1,1}/h_1^2 + h_{1,2}\psi_2\theta_{1,1}/(h_1^2 h_2) + h_{1,3}^2\psi_1\theta_1/h_1^2 + h_{1,2}^2\psi_1\theta_1/(h_1^2 h_2^2) - h_{1,2}\psi_{2,1}\theta_1/(h_1^2 h_2)$$
$$-h_{1,2}\psi_1\theta_{2,1}/(h_1^2 h_2) + \psi_{2,1}\theta_{2,1}/h_1^2 + h_{1,2}\psi_{1,1}\theta_2/(h_1^2 h_2) + h_{1,2}^2\psi_2\theta_2/(h_1^2 h_2^2) - h_{1,3}^2\theta_1 u/(R_1 h_1^2)$$
$$-h_{1,2}^2\theta_1 u/(R_1 h_1^2 h_2^2) + h_{1,2}\theta_{2,1}u/(R_1 h_1^2 h_2) - \theta_{1,1}u_{,1}/(R_1 h_1^2) - h_{1,2}\theta_2 u_{,1}/(R_1 h_1^2 h_2)$$
$$-h_{1,2}\theta_{1,1}v/(R_2 h_1^2 h_2) - h_{1,2}^2\theta_2 v/(R_2 h_1^2 h_2^2) + h_{1,2}\theta_1 v_{,1}/(R_2 h_1^2 h_2) - \theta_{2,1}v_{,1}/(R_2 h_1^2)$$

$$\chi_{1_{NL}}^6 = -\gamma_1\gamma_{2,1}h_{1,2}/(h_1^2 h_2) + \gamma_{1,1}\gamma_2 h_{1,2}/(h_1^2 h_2) + \gamma_{1,1}^2 h_3/(2h_1^2) + \gamma_{2,1}^2 h_3/(2h_1^2)$$
$$+\gamma_1^2 h_{1,3}^2 h_3/(2h_1^2) + \gamma_1^2 h_{1,2}^2 h_3/(2h_1^2 h_2^2) + \gamma_2^2 h_{1,2}^2 h_3/(2h_1^2 h_2^2) + \phi_{1,1}\theta_{1,1}/h_1^2 + h_{1,2}\phi_2\theta_{1,1}/(h_1^2 h_2)$$

$$+h_{1,3}^2\phi_1\theta_1/h_1^2 +h_{1,2}^2\phi_1\theta_1/(h_1^2h_2^2) -h_{1,2}\phi_{2,1}\theta_1/(h_1^2h_2) -h_{1,2}\phi_1\theta_{2,1}/(h_1^2h_2) +\phi_{2,1}\theta_{2,1}/h_1^2$$
$$+h_{1,2}\phi_{1,1}\theta_2/(h_1^2h_2) +h_{1,2}^2\phi_2\theta_2/(h_1^2h_2^2)$$

$$\chi_{1_{NL}}^7 = \gamma_{1,1}\theta_{1,1}/h_1^2 +\gamma_2h_{1,2}\theta_{1,1}/(h_1^2h_2) +\gamma_1h_{1,3}^2\theta_1/h_1^2 +\gamma_1h_{1,2}^2\theta_1/(h_1^2h_2^2) -\gamma_{2,1}h_{1,2}\theta_1/(h_1^2h_2)$$
$$+\gamma_{2,1}\theta_{2,1}/h_1^2 -\gamma_1h_{1,2}\theta_{2,1}/(h_1^2h_2) +\gamma_2h_{1,2}^2\theta_2/(h_1^2h_2^2) +\gamma_{1,1}h_{1,2}\theta_2/(h_1^2h_2)$$

$$\chi_{1_{NL}}^8 = h_3\theta_{1,1}^2/(2h_1^2) +h_{1,3}^2h_3\theta_1^2/(2h_1^2) +h_{1,2}^2h_3\theta_1^2/(2h_1^2h_2^2) -h_{1,2}\theta_1\theta_{2,1}/(h_1^2h_2)$$
$$+h_3\theta_{2,1}^2/(2h_1^2) +h_{1,2}\theta_{1,1}\theta_2/(h_1^2h_2) +h_{1,2}^2h_3\theta_2^2/(2h_1^2h_2^2)$$

$$\chi_{2_{NL}}^0 = (u_{3,2})^2h_3/(2h_2^2) +h_{2,1}^2h_3u^2/(2h_1^2h_2^2) +h_3u_{,2}^2/(2h_2^2) -h_{2,1}u_{,2}v/(h_1h_2^2)$$
$$+h_{2,1}^2h_3v^2/(2h_1^2h_2^2) +h_{2,1}uv_{,2}/(h_1h_2^2) +h_3v_{,2}^3/(2h_2^2)$$

$$\chi_{2_{NL}}^1 = u_3h_{2,1}h_{2,3}\psi_1/(h_1h_2^2) +u_3h_{2,3}\psi_{2,2}/h_2^2 -u_{3,2}h_{2,3}\psi_2/h_2^2 -u_3h_{2,1}h_{2,3}u/(R_1h_1h_2^2)$$
$$+h_{2,1}^2\psi_1u/(h_1^2h_2^2) +h_{2,1}\psi_{2,2}u/(h_1h_2^2) -h_{2,1}^2u^2/(R_1h_1^2h_2^2) +\psi_{1,2}u_{,2}/h_2^2 -h_{2,1}\psi_2u_{,2}/(h_1h_2^2)$$
$$-u_{,2}^2/(R_1h_2^2) +u_{3,2}h_{2,3}v/(R_2h_2^2) -h_{2,1}\psi_{1,2}v/(h_1h_2^2) +h_{2,1}^2\psi_2v/(h_1^2h_2^2) +h_{2,3}^2\psi_2v/h_2^2$$
$$+h_{2,1}u_{,2}v/(R_1h_1h_2^2) +h_{2,1}u_{,2}v/(R_2h_1h_2^2) -h_{2,1}^2v^2/(R_2h_1^2h_2^2) -h_{2,3}^2v^2/(R_2h_2^2)$$
$$-u_3h_{2,3}v_{,2}/(R_2h_2^2) +h_{2,1}\psi_1v_{,2}/(h_1h_2^2) +\psi_{2,2}v_{,2}/h_2^2 -h_{2,1}uv_{,2}/(R_1h_1h_2^2)$$
$$-h_{2,1}uv_{,2}/(R_2h_1h_2^2) -v_{,2}^3/(R_2h_2^2)$$

$$\chi_{2_{NL}}^2 = u_3h_{2,1}h_{2,3}\phi_1/(h_1h_2^2) +u_3h_{2,3}\phi_{2,2}/h_2^2 -u_{3,2}h_{2,3}\phi_2/h_2^2 +h_3\psi_{1,2}^2/(2h_2^2)$$
$$+h_{2,1}^2h_3\psi_1^2/(2h_1^2h_2^2) +h_{2,1}\psi_1\psi_{2,2}/(h_1h_2^2) +h_3\psi_{2,2}^3/(2h_2^2) -h_{2,1}\psi_{1,2}\psi_2/(h_1h_2^2)$$
$$+h_{2,1}^2h_3\psi_2^2/(2h_1^2h_2^2) +h_{2,3}^2h_3\psi_2^2/(2h_2^2) +h_{2,1}^2\phi_1u/(h_1^2h_2^2) +h_{2,1}\phi_{2,2}u/(h_1h_2^2)$$
$$-h_{2,1}^2\psi_1u/(R_1h_1^2h_2^2) -h_{2,1}\psi_{2,2}u/(R_1h_1h_2^2) +h_{2,1}^2h_3u^2/(2R_1^2h_1^2h_2^2) +\phi_{1,2}u_{,2}/h_2^2$$
$$-h_{2,1}\phi_2u_{,2}/(h_1h_2^2) -\psi_{1,2}u_{,2}/(R_1h_2^2) +h_{2,1}\psi_2u_{,2}/(R_1h_1h_2^2) +h_3u_{,2}^2/(2R_1^2h_2^2)$$
$$-h_{2,1}\phi_{1,2}v/(h_1h_2^2) +h_{2,1}^2\phi_2v/(h_1^2h_2^2) +h_{2,3}^2\phi_2v/h_2^2 +h_{2,1}\psi_{1,2}v/(R_2h_1h_2^2)$$
$$-h_{2,1}^2\psi_2v/(R_2h_1^2h_2^2) -h_{2,3}^2\psi_2v/(R_2h_2^2) -h_{2,1}u_{,2}v/(R_1R_2h_1h_2^2) +h_{2,1}^2h_3v^2/(2R_2^2h_1^2h_2^2)$$
$$+h_{2,3}^2h_3v^2/(2R_2^2h_2^2) +h_{2,1}\phi_1v_{,2}/(h_1h_2^2) +\phi_{2,2}v_{,2}/h_2^2 -h_{2,1}\psi_1v_{,2}/(R_2h_1h_2^2) -\psi_{2,2}v_{,2}/(R_2h_2^2)$$
$$+h_{2,1}uv_{,2}/(R_1R_2h_1h_2^2) +h_3v_{,2}^3/(2R_2^2h_2^2)$$

$$\chi_{2_{NL}}^3 = u_3\gamma_{2,2}h_{2,3}/h_2^2 -v_{3,2}\gamma_2h_{2,3}/h_2^2 +u_3\gamma_1h_{2,1}h_{2,3}/(h_1h_2^2) +\phi_{1,2}\psi_{1,2}/h_2^2$$
$$-h_{2,1}\phi_2\psi_{1,2}/(h_1h_2^2) +h_{2,1}^2\phi_1\psi_1/(h_1^2h_2^2) +h_{2,1}\phi_{2,2}\psi_1/(h_1h_2^2) +h_{2,1}\phi_1\psi_{2,2}/(h_1h_2^2)$$
$$+\phi_{2,2}\psi_{2,2}/h_2^2 -h_{2,1}\phi_{1,2}\psi_2/(h_1h_2^2) +h_{2,1}^2\phi_2\psi_2/(h_1^2h_2^2) +h_{2,3}^2\phi_2\psi_2/h_2^2 +\gamma_{2,2}h_{2,1}u/(h_1h_2^2)$$

$$+\gamma_1 h_{2,1}^2 u/(h_1^2 h_2^2) - h_{2,1}^2 \phi_1 u/(R_1 h_1^2 h_2^2) - h_{2,1}\phi_{2,2} u/(R_1 h_1 h_2^2) + \gamma_{1,2} u_{,2}/h_2^2 - \gamma_2 h_{2,1} u_{,2}/(h_1 h_2^2)$$
$$-\phi_{1,2} u_{,2}/(R_1 h_2^2) + h_{2,1}\phi_2 u_{,2}/(R_1 h_1 h_2^2) - \gamma_{1,2} h_{2,1} v/(h_1 h_2^2) + \gamma_2 h_{2,1}^2 v/(h_1^2 h_2^2) + \gamma_2 h_{2,3}^2 v/h_2^2$$
$$+h_{2,1}\phi_{1,2} v/(R_2 h_1 h_2^2) - h_{2,1}^2 \phi_2 v/(R_2 h_1^2 h_2^2) - h_{2,3}^2 \phi_2 v/(R_2 h_2^2) + \gamma_{2,2} v_{,2}/h_2^2 + \gamma_1 h_{2,1} v_{,2}/(h_1 h_2^2)$$
$$-h_{2,1}\phi_1 v_{,2}/(R_2 h_1 h_2^2) - \phi_{2,2} v_{,2}/(R_2 h_2^2)$$

$$\chi_{2_{NL}}^4 = h_3 \phi_{1,2}^2/(2h_2^2) + h_{2,1}^2 h_3 \phi_1^2/(2h_1^2 h_2^2) + h_{2,1}\phi_1\phi_{2,2}/(h_1 h_2^2) + h_3\phi_{2,2}^3/(2h_2^2)$$
$$-h_{2,1}\phi_{1,2}\phi_2/(h_1 h_2^2) + h_{2,1}^2 h_3 \phi_2^2/(2h_1^2 h_2^2) + h_{2,3}^2 h_3 \phi_2^2/(2h_2^2) + \gamma_{1,2}\psi_{1,2}/h_2^2 - \gamma_2 h_{2,1}\psi_{1,2}/(h_1 h_2^2)$$
$$+\gamma_{2,2} h_{2,1}\psi_1/(h_1 h_2^2) + \gamma_1 h_{2,1}^2 \psi_1/(h_1^2 h_2^2) + \gamma_{2,2}\psi_{2,2}/h_2^2 + \gamma_1 h_{2,1}\psi_{2,2}/(h_1 h_2^2)$$
$$-\gamma_{1,2} h_{2,1}\psi_2/(h_1 h_2^2) + \gamma_2 h_{2,1}^2 \psi_2/(h_1^2 h_2^2) + \gamma_2 h_{2,3}^2 \psi_2/h_2^2 + u_3 h_{2,1} h_{2,3}\theta_1/(h_1 h_2^2) + u_3 h_{2,3}\theta_{2,2}/h_2^2$$
$$-u_{3,2} h_{2,3}\theta_2/h_2^2 - \gamma_{2,2} h_{2,1} u/(R_1 h_1 h_2^2) - \gamma_1 h_{2,1}^2 u/(R_1 h_1^2 h_2^2) + h_{2,1}^2 \theta_1 u/(h_1^2 h_2^2)$$
$$+h_{2,1}\theta_{2,2} u/(h_1 h_2^2) - \gamma_{1,2} u_{,2}/(R_1 h_2^2) + \gamma_2 h_{2,1} u_{,2}/(R_1 h_1 h_2^2) + \theta_{1,2} u_{,2}/h_2^2 - h_{2,1}\theta_2 u_{,2}/(h_1 h_2^2)$$
$$+\gamma_{1,2} h_{2,1} v/(R_2 h_1 h_2^2) - \gamma_2 h_{2,1}^2 v/(R_2 h_1^2 h_2^2) - \gamma_2 h_{2,3}^2 v/(R_2 h_2^2) - h_{2,1}\theta_{1,2} v/(h_1 h_2^2)$$
$$+h_{2,1}^2 \theta_2 v/(h_1^2 h_2^2) + h_{2,3}^2 \theta_2 v/h_2^2 - \gamma_{2,2} v_{,2}/(R_2 h_2^2) - \gamma_1 h_{2,1} v_{,2}/(R_2 h_1 h_2^2) + h_{2,1}\theta_1 v_{,2}/(h_1 h_2^2)$$
$$+\theta_{2,2} v_{,2}/h_2^2$$

$$\chi_{2_{NL}}^5 = \gamma_{1,2}\phi_{1,2}/h_2^2 - \gamma_2 h_{2,1}\phi_{1,2}/(h_1 h_2^2) + \gamma_{2,2} h_{2,1}\phi_1/(h_1 h_2^2) + \gamma_1 h_{2,1}^2 \phi_1/(h_1^2 h_2^2) + \gamma_{2,2}\phi_{2,2}/h_2^2$$
$$+\gamma_1 h_{2,1}\phi_{2,2}/(h_1 h_2^2) - \gamma_{1,2} h_{2,1}\phi_2/(h_1 h_2^2) + \gamma_2 h_{2,1}^2 \phi_2/(h_1^2 h_2^2) + \gamma_2 h_{2,3}^2 \phi_2/h_2^2 + \psi_{1,2}\theta_{1,2}/h_2^2$$
$$-h_{2,1}\psi_1\theta_{1,2}/(h_1 h_2^2) + h_{2,1}^2 \psi_1\theta_1/(h_1^2 h_2^2) + h_{2,1}\psi_{2,2}\theta_1/(h_1 h_2^2) + h_{2,1}\psi_1\theta_{2,2}/(h_1 h_2^2)$$
$$+\psi_{2,2}\theta_{2,2}/h_2^2 - h_{2,1}\psi_{1,2}\theta_2/(h_1 h_2^2) + h_{2,1}^2 \psi_2\theta_2/(h_1^2 h_2^2) + h_{2,3}^2 \psi_2\theta_2/h_2^2 - h_{2,1}^2 \theta_1 u/(R_1 h_1^2 h_2^2)$$
$$-h_{2,1}\theta_{2,2} u/(R_1 h_1 h_2^2) - \theta_{1,2} u_{,2}/(R_1 h_2^2) + h_{2,1}\theta_2 u_{,2}/(R_1 h_1 h_2^2) + h_{2,1}\theta_{1,2} v/(R_2 h_1 h_2^2)$$
$$-h_{2,1}^2 \theta_2 v/(R_2 h_1^2 h_2^2) - h_{2,3}^2 \theta_2 v/(R_2 h_2^2) - h_{2,1}\theta_1 v_{,2}/(R_2 h_1 h_2^2) - \theta_{2,2} v_{,2}/(R_2 h_2^2)$$

$$\chi_{2_{NL}}^6 = \gamma_1\gamma_{2,2} h_{2,1}/(h_1 h_2^2) - \gamma_{1,2}\gamma_2 h_{2,1}/(h_1 h_2^2) + \gamma_{1,2}^2 h_3/(2h_2^2) + \gamma_{2,2}^3 h_3/(2h_2^2)$$
$$+\gamma_1^2 h_{2,1}^2 h_3/(2h_1^2 h_2^2) + \gamma_2^2 h_{2,1}^2 h_3/(2h_1^2 h_2^2) + \gamma_2^2 h_{2,3}^2 h_3/(2h_2^2) + \phi_{1,2}\theta_{1,2}/h_2^2 - h_{2,1}\phi_2\theta_{1,2}/(h_1 h_2^2)$$
$$+h_{2,1}^2 \phi_1\theta_1/(h_1^2 h_2^2) + h_{2,1}\phi_{2,2}\theta_1/(h_1 h_2^2) + h_{2,1}\phi_1\theta_{2,2}/(h_1 h_2^2) + \phi_{2,2}\theta_{2,2}/h_2^2 - h_{2,1}\phi_{1,2}\theta_2/(h_1 h_2^2)$$
$$+h_{2,1}^2 \phi_2\theta_2/(h_1^2 h_2^2) + h_{2,3}^2 \phi_2\theta_2/h_2^2$$

$$\chi_{2_{NL}}^7 = \gamma_{1,2}\theta_{1,2}/h_2^2 - \gamma_2 h_{2,1}\theta_{1,2}/(h_1 h_2^2) + \gamma_{2,2} h_{2,1}\theta_1/(h_1 h_2^2) + \gamma_1 h_{2,1}^2 \theta_1/(h_1^2 h_2^2) + \gamma_{2,2}\theta_{2,2}/h_2^2$$
$$+\gamma_1 h_{2,1}\theta_{2,2}/(h_1 h_2^2) - \gamma_{1,2} h_{2,1}\theta_2/(h_1 h_2^2) + \gamma_2 h_{2,1}^2 \theta_2/(h_1^2 h_2^2) + \gamma_2 h_{2,3}^2 \theta_2/h_2^2$$

$$\chi_{2_{NL}}^8 = h_3\theta_{1,2}^2/(2h_2^2) + h_{2,1}^2 h_3\theta_1^2/(2h_1^2 h_2^2) + h_{2,1}\theta_1\theta_{2,2}/(h_1 h_2^2) + h_3\theta_{2,2}^3/(2h_2^2)$$
$$-h_{2,1}\theta_{1,2}\theta_2/(h_1 h_2^2) + h_{2,1}^2 h_3\theta_2^2/(2h_1^2 h_2^2) + h_{2,3}^2 h_3\theta_2^2/(2h_2^2)$$

$$\chi^0_{4NL} = h_{2,1}\psi_2 u/(h_1 h_2) + \psi_1 u_{,2}/h_2 - u u_{,2}/(R_1 h_2) - h_{2,1}\psi_1 v/(h_1 h_2) + h_{2,1} uv/(R_1 h_1 h_2)$$
$$- h_{2,1} uv/(R_2 h_1 h_2) + \psi_2 v_{,2}/h_2 - v v_{,2}/(R_2 h_2)$$

$$\chi^1_{4NL} = 2u_3 h_{2,3}\phi_2/h_2 + \psi_{1,2}\psi_1/h_2 - u_{3,3} h_{2,3}\psi_2/h_2 + \psi_{2,2}\psi_2/h_2 + 2h_{2,1}\phi_2 u/(h_1 h_2)$$
$$- \psi_{1,2} u/(R_1 h_2) + 2\phi_1 u_{,2}/h_2 - \psi_1 u_{,2}/(R_1 h_2) + u u_{,2}/(R_1^2 h_2) + u_{3,3} h_{2,3} v/(R_2 h_2)$$
$$- 2h_{2,1}\phi_1 v/(h_1 h_2) - \psi_{2,2} v/(R_2 h_2) + 2\phi_2 v_{,2}/h_2 - \psi_2 v_{,2}/(R_2 h_2) + v v_{,2}/(R_2^2 h_2)$$

$$\chi^2_{4NL} = 3u_3\gamma_2 h_{2,3}/h_2 - u_{3,3} h_{2,3}\phi_2/h_2 + 2\phi_1\psi_{1,2}/h_2 + \phi_{1,2}\psi_1/h_2 + h_{2,1}\phi_2\psi_1/(h_1 h_2)$$
$$+ 2\phi_2\psi_{2,2}/h_2 - h_{2,1}\phi_1\psi_2/(h_1 h_2) + \phi_{2,2}\psi_2/h_2 + 3\gamma_2 h_{2,1} u/(h_1 h_2) - \phi_{1,2} u/(R_1 h_2)$$
$$- h_{2,1}\phi_2 u/(R_1 h_1 h_2) + 3\gamma_1 u_{,2}/h_2 - 2\phi_1 u_{,2}/(R_1 h_2) - 3\gamma_1 h_{2,1} v/(h_1 h_2) + h_{2,1}\phi_1 v/(R_2 h_1 h_2)$$
$$- \phi_{2,2} v/(R_2 h_2) + 3\gamma_2 v_{,2}/h_2 - 2\phi_2 v_{,2}/(R_2 h_2)$$

$$\chi^3_{4NL} = -u_{3,3}\gamma_2 h_{2,3}/h_2 + 2\phi_{1,2}\phi_1/h_2 + 2\phi_{2,2}\phi_2/h_2 + 3\gamma_1\psi_{1,2}/h_2 + \gamma_{1,2}\psi_1/h_2$$
$$+ 2\gamma_2 h_{2,1}\psi_1/(h_1 h_2) + 3\gamma_2\psi_{2,2}/h_2 + \gamma_{2,2}\psi_2/h_2 - 2\gamma_1 h_{2,1}\psi_2/(h_1 h_2) + u_3 4h_{2,3}\theta_2/h_2$$
$$- \gamma_{1,2} u/(R_1 h_2) - 2\gamma_2 h_{2,1} u/(R_1 h_1 h_2) + 4h_{2,1}\theta_2 u/(h_1 h_2) - 3\gamma_1 u_{,2}/(R_1 h_2) + 4\theta_1 u_{,2}/h_2$$
$$- \gamma_{2,2} v/(R_2 h_2) + 2\gamma_1 h_{2,1} v/(R_2 h_1 h_2) - 4h_{2,1}\theta_1 v/(h_1 h_2) - 3\gamma_2 v_{,2}/(R_2 h_2) + 4\theta_2 v_{,2}/h_2$$

$$\chi^4_{4NL} = 3\gamma_1\phi_{1,2}/h_2 + 2\gamma_{1,2}\phi_1/h_2 + \gamma_2 h_{2,1}\phi_1/(h_1 h_2) + 3\gamma_2\phi_{2,2}/h_2 + 2\gamma_{2,2}\phi_2/h_2$$
$$- \gamma_1 h_{2,1}\phi_2/(h_1 h_2) + \psi_1\theta_{1,2}/h_2 + 4\psi_{1,2}\theta_1/h_2 - 3h_{2,1}\psi_2\theta_1/(h_1 h_2) + \psi_2\theta_{2,2}/h_2 - u_{3,3} h_{2,3}\theta_2/h_2$$
$$+ 3h_{2,1}\psi_1\theta_2/(h_1 h_2) + 4\psi_{2,2}\theta_2/h_2 - \theta_{1,2} u/(R_1 h_2) - 3h_{2,1}\theta_2 u/(R_1 h_1 h_2) - 4\theta_1 u_{,2}/(R_1 h_2)$$
$$+ 3h_{2,1}\theta_1 v/(R_2 h_1 h_2) - \theta_{2,2} v/(R_2 h_2) - 4\theta_2 v_{,2}/(R_2 h_2)$$

$$\chi^5_{4NL} = 3\gamma_{1,2}\gamma_1/h_2 + 3\gamma_{2,2}\gamma_2/h_2 + 2\phi_1\theta_{1,2}/h_2 + 4\phi_{1,2}\theta_1/h_2 - 2h_{2,1}\phi_2\theta_1/(h_1 h_2) + 2\phi_2\theta_{2,2}/h_2$$
$$+ 2h_{2,1}\phi_1\theta_2/(h_1 h_2) + 4\phi_{2,2}\theta_2/h_2$$

$$\chi^6_{4NL} = 3\gamma_1\theta_{1,2}/h_2 + 4\gamma_{1,2}\theta_1/h_2 - \gamma_2 h_{2,1}\theta_1/(h_1 h_2) + 3\gamma_2\theta_{2,2}/h_2 + 4\gamma_{2,2}\theta_2/h_2$$
$$+ \gamma_1 h_{2,1}\theta_2/(h_1 h_2)$$

$$\chi^7_{4NL} = 4\theta_{1,2}\theta_1/h_2 + 4\theta_{2,2}\theta_2/h_2$$

$$\chi^0_{5NL} = -h_{1,2}\psi_2 u/(h_1 h_2) + \psi_1 u_{,1}/h_1 - u u_{,1}/(R_1 h_1) + h_{1,2}\psi_1 v/(h_1 h_2) - h_{1,2} uv/(R_1 h_1 h_2)$$
$$+ h_{1,2} uv/(R_2 h_1 h_2) + \psi_2 v_{,1}/h_1 - v v_{,1}/(R_2 h_1)$$

$$\chi^1_{5_{NL}} = 2u_3h_{1,3}\phi_1/h_1 - u_{3,3}h_{1,3}\psi_1/h_1 + \psi_{1,1}\psi_1/h_1 + \psi_{2,1}\psi_2/h_1 + u_{3,3}h_{1,3}u/(R_1h_1)$$
$$-2h_{1,2}\phi_2u/(h_1h_2) - \psi_{1,1}u/(R_1h_1) + 2\phi_1u_{,1}/h_1 - \psi_1u_{,1}/(R_1h_1) + uu_{,1}/(R_1^2h_1)$$
$$+2h_{1,2}\phi_1v/(h_1h_2) - \psi_{2,1}v/(R_2h_1) + 2\phi_2v_{,1}/h_1 - \psi_2v_{,1}/(R_2h_1) + vv_{,1}/(R_2^2h_1)$$

$$\chi^2_{5_{NL}} = 3u_3\gamma_1h_{1,3}/h_1 - u_{3,3}h_{1,3}\phi_1/h_1 + 2\phi_1\psi_{1,1}/h_1 + \phi_{1,1}\psi_1/h_1 - h_{1,2}\phi_2\psi_1/(h_1h_2)$$
$$+2\phi_2\psi_{2,1}/h_1 + h_{1,2}\phi_1\psi_2/(h_1h_2) + \phi_{2,1}\psi_2/h_1 - 3\gamma_2h_{1,2}u/(h_1h_2) - \phi_{1,1}u/(R_1h_1)$$
$$+h_{1,2}\phi_2u/(R_1h_1h_2) + 3\gamma_1u_{,1}/h_1 - 2\phi_1u_{,1}/(R_1h_1) + 3\gamma_1h_{1,2}v/(h_1h_2) - h_{1,2}\phi_1v/(R_2h_1h_2)$$
$$-\phi_{2,1}v/(R_2h_1) + 3\gamma_2v_{,1}/h_1 - 2\phi_2v_{,1}/(R_2h_1)$$

$$\chi^3_{5_{NL}} = -u_{3,3}\gamma_1h_{1,3}/h_1 + 2\phi_{1,1}\gamma_1/h_1 + 2\phi_{2,1}\phi_2/h_1 + 3\gamma_1\psi_{1,1}/h_1 + \gamma_{1,1}\psi_1/h_1$$
$$-2\gamma_2h_{1,2}\psi_1/(h_1h_2) + 3\gamma_2\psi_{2,1}/h_1 + \gamma_{2,1}\psi_2/h_1 + 2\gamma_1h_{1,2}\psi_2/(h_1h_2) + u_34h_{1,3}\theta_1/h_1$$
$$-\gamma_{1,1}u/(R_1h_1) + 2\gamma_2h_{1,2}u/(R_1h_1h_2) - 4h_{1,2}\theta_2u/(h_1h_2) - 3\gamma_1u_{,1}/(R_1h_1) + 4\theta_1u_{,1}/h_1$$
$$-\gamma_{2,1}v/(R_2h_1) - 2\gamma_1h_{1,2}v/(R_2h_1h_2) + 4h_{1,2}\theta_1v/(h_1h_2) - 3\gamma_2v_{,1}/(R_2h_1) + 4\theta_2v_{,1}/h_1$$

$$\chi^4_{5_{NL}} = 3\gamma_1\phi_{1,1}/h_1 + 2\gamma_{1,1}\phi_1/h_1 - \gamma_2h_{1,2}\phi_1/(h_1h_2) + 3\gamma_2\phi_{2,1}/h_1 + 2\gamma_{2,1}\phi_2/h_1$$
$$+\gamma_1h_{1,2}\phi_2/(h_1h_2) + \psi_1\theta_{1,1}/h_1 - u_{3,3}h_{1,3}\theta_1/h_1 + 4\psi_{1,1}\theta_1/h_1 + 3h_{1,2}\psi_2\theta_1/(h_1h_2) + \psi_2\theta_{2,1}/h_1$$
$$-3h_{1,2}\psi_1\theta_2/(h_1h_2) + 4\psi_{2,1}\theta_2/h_1 - \theta_{1,1}u/(R_1h_1) + 3h_{1,2}\theta_2u/(R_1h_1h_2) - 4\theta_1u_{,1}/(R_1h_1)$$
$$-3h_{1,2}\theta_1v/(R_2h_1h_2) - \theta_{2,1}v/(R_2h_1) - 4\theta_2v_{,1}/(R_2h_1)$$

$$\chi^5_{5_{NL}} = 3\gamma_{1,1}\gamma_1/h_1 + 3\gamma_{2,1}\gamma_2/h_1 + 2\phi_1\theta_{1,1}/h_1 + 4\phi_{1,1}\theta_1/h_1 + 2h_{1,2}\phi_2\theta_1/(h_1h_2) + 2\phi_2\theta_{2,1}/h_1$$
$$-2h_{1,2}\phi_1\theta_2/(h_1h_2) + 4\phi_{2,1}\theta_2/h_1$$

$$\chi^6_{5_{NL}} = 3\gamma_1\theta_{1,1}/h_1 + 4\gamma_{1,1}\theta_1/h_1 + \gamma_2h_{1,2}\theta_1/(h_1h_2) + 3\gamma_2\theta_{2,1}/h_1 + 4\gamma_{2,1}\theta_2/h_1$$
$$-\gamma_1h_{1,2}\theta_2/(h_1h_2)$$

$$\chi^7_{5_{NL}} = 4\theta_{1,1}\theta_1/h_1 + 4\theta_{2,1}\theta_2/h_1$$

$$\chi^0_{6_{NL}} = u_{3,1}u_{3,2}/(h_1h_2) - h_{1,2}h_{2,1}u^2/(h_1^2h_2^2) + u_{,1}u_{,2}/(h_1h_2) - h_{2,1}u_{,1}v/(h_1^2h_2)$$
$$+h_{1,2}u_{,2}v/(h_1h_2^2) - h_{1,2}h_{2,1}v^2/(h_1^2h_2^2) + h_{2,1}uv_{,1}/(h_1^2h_2) - h_{1,2}uv_{,2}/(h_1h_2^2) + v_{,1}v_{,2}/(h_1h_2)$$

$$\chi^1_{6_{NL}} = u_3h_{1,3}\psi_{1,2}/(h_1h_2) - u_3h_{1,2}h_{2,3}\psi_1/(h_1h_2^2) - u_{3,2}h_{1,3}\psi_1/(h_1h_2) + u_3h_{2,3}\psi_{2,1}/(h_1h_2)$$
$$-u_3h_{1,3}h_{2,1}\psi_2/(h_1^2h_2) - u_{3,1}h_{2,3}\psi_2/(h_1h_2) + u_3h_{1,2}h_{2,3}u/(R_1h_1h_2^2) + u_{3,2}h_{1,3}u/(R_1h_1h_2)$$

$$-2h_{1,2}h_{2,1}\psi_1 u/(h_1^2h_2^2) +h_{2,1}\psi_{2,1}u/(h_1^2h_2) -h_{1,2}\psi_{2,2}u/(h_1h_2^2) +h_{1,3}h_{2,3}\psi_2 u/(h_1h_2)$$
$$+2h_{1,2}h_{2,1}u^2/(R_1h_1^2h_2^2) +\psi_{1,2}u_{,1}/(h_1h_2) -h_{2,1}\psi_2 u_{,1}/(h_1^2h_2) -u_3h_{1,3}u_{,2}/(R_1h_1h_2)$$
$$+\psi_{1,1}u_{,2}/(h_1h_2) +h_{1,2}\psi_2 u_{,2}/(h_1h_2^2) -2u_{,1}u_{,2}/(R_1h_1h_2) +u_3h_{1,3}h_{2,1}v/(R_2h_1^2h_2)$$
$$+u_{3,1}h_{2,3}v/(R_2h_1h_2) -h_{2,1}\psi_{1,1}v/(h_1^2h_2) +h_{1,2}\psi_{1,2}v/(h_1h_2^2) +h_{1,3}h_{2,3}\psi_1 v/(h_1h_2)$$
$$-2h_{1,2}h_{2,1}\psi_2 v/(h_1^2h_2^2) -h_{1,3}h_{2,3}uv/(R_1h_1h_2) -h_{1,3}h_{2,3}uv/(R_2h_1h_2) +h_{2,1}u_{,1}v/(R_1h_1^2h_2)$$
$$+h_{2,1}u_{,1}v/(R_2h_1^2h_2) -h_{1,2}u_{,2}v/(R_1h_1h_2^2) -h_{1,2}u_{,2}v/(R_2h_1h_2^2) +2h_{1,2}h_{2,1}v^2/(R_2h_1^2h_2^2)$$
$$-u_3h_{2,3}v_{,1}/(R_2h_1h_2) +h_{2,1}\psi_1 v_{,1}/(h_1^2h_2) +\psi_{2,2}v_{,1}/(h_1h_2) -h_{2,1}uv_{,1}/(R_1h_1^2h_2)$$
$$-h_{2,1}uv_{,1}/(R_2h_1^2h_2) -h_{1,2}\psi_1 v_{,2}/(h_1h_2^2) +\psi_{2,1}v_{,2}/(h_1h_2) +h_{1,2}uv_{,2}/(R_1h_1h_2^2)$$
$$+h_{1,2}uv_{,2}/(R_2h_1h_2^2) -2v_{,1}v_{,2}/(R_2h_1h_2)$$

$$\chi^2_{6_{NL}} = u_3h_{1,3}\phi_{1,2}/(h_1h_2) -u_3h_{1,2}h_{2,3}\phi_1/(h_1h_2^2) -u_{3,2}h_{1,3}\phi_1/(h_1h_2) +u_3h_{2,3}\phi_{2,1}/(h_1h_2)$$
$$-u_3h_{1,3}h_{2,1}\phi_2/(h_1^2h_2) -u_{3,1}h_{2,3}\phi_2/(h_1h_2) +\psi_{1,1}\psi_{1,2}/(h_1h_2) -h_{1,2}h_{2,1}\psi_1^2/(h_1^2h_2^2)$$
$$+h_{2,1}\psi_1\psi_{2,1}/(h_1^2h_2) -h_{1,2}\psi_1\psi_{2,2}/(h_1h_2^2) +\psi_{2,1}\psi_{2,2}/(h_1h_2) -h_{2,1}\psi_{1,1}\psi_2/(h_1^2h_2)$$
$$+h_{1,2}\psi_{1,2}\psi_2/(h_1h_2^2) +h_{1,3}h_{2,3}\psi_1\psi_2/(h_1h_2) -h_{1,2}h_{2,1}\psi_2^2/(h_1^2h_2^2) -2h_{1,2}h_{2,1}\phi_1 u/(h_1^2h_2^2)$$
$$+h_{2,1}\phi_{2,1}u/(h_1^2h_2) -h_{1,2}\phi_{2,2}u/(h_1h_2^2) +h_{1,3}h_{2,3}\phi_2 u/(h_1h_2) +2h_{1,2}h_{2,1}\psi_1 u/(R_1h_1^2h_2^2)$$
$$-h_{2,1}\psi_{2,1}u/(R_1h_1^2h_2) +h_{1,2}\psi_{2,2}u/(R_1h_1h_2^2) -h_{1,3}h_{2,3}\psi_2 u/(R_1h_1h_2) -h_{1,2}h_{2,1}u^2/(R_1^2h_1^2h_2^2)$$
$$+\phi_{1,2}u_{,1}/(h_1h_2) -h_{2,1}\phi_2 u_{,1}/(h_1^2h_2) -\psi_{1,2}u_{,1}/(R_1h_1h_2) +h_{2,1}\psi_2 u_{,1}/(R_1h_1^2h_2)$$
$$+\phi_{1,1}u_{,2}/(h_1h_2) +h_{1,2}\phi_2 u_{,2}/(h_1h_2^2) -\psi_{1,1}u_{,2}/(R_1h_1h_2) -h_{1,2}\psi_2 u_{,2}/(R_1h_1h_2^2)$$
$$+u_{,1}u_{,2}/(R_1^2h_1h_2) -h_{2,1}\phi_{1,1}v/(h_1^2h_2) +h_{1,2}\phi_{1,2}v/(h_1h_2^2) +h_{1,3}h_{2,3}\phi_1 v/(h_1h_2)$$
$$-2h_{1,2}h_{2,1}\phi_2 v/(h_1^2h_2^2) +h_{2,1}\psi_{1,1}v/(R_2h_1^2h_2) -h_{1,2}\psi_{1,2}v/(R_2h_1h_2^2) -h_{1,3}h_{2,3}\psi_1 v/(R_2h_1h_2)$$
$$+2h_{1,2}h_{2,1}\psi_2 v/(R_2h_1^2h_2^2) +h_{1,3}h_{2,3}uv/(R_1R_2h_1h_2) -h_{2,1}u_{,1}v/(R_1R_2h_1^2h_2)$$
$$+h_{1,2}u_{,2}v/(R_1R_2h_1h_2^2) -h_{1,2}h_{2,1}v^2/(R_2^2h_1^2h_2^2) +h_{2,1}\phi_1 v_{,1}/(h_1^2h_2) +\phi_{2,2}v_{,1}/(h_1h_2)$$
$$-h_{2,1}\psi_1 v_{,1}/(R_2h_1^2h_2) -\psi_{2,2}v_{,1}/(R_2h_1h_2) +h_{2,1}uv_{,1}/(R_1R_2h_1^2h_2) -h_{1,2}\phi_1 v_{,2}/(h_1h_2^2)$$
$$+\phi_{2,1}v_{,2}/(h_1h_2) +h_{1,2}\psi_1 v_{,2}/(R_2h_1h_2^2) -\psi_{2,1}v_{,2}/(R_2h_1h_2) -h_{1,2}uv_{,2}/(R_1R_2h_1h_2^2)$$
$$+v_{,1}v_{,2}/(R_2^2h_1h_2)$$

$$\chi^3_{6_{NL}} = -u_3\gamma_1h_{1,2}h_{2,3}/(h_1h_2^2) +u_3\gamma_{1,2}h_{1,3}/(h_1h_2) -u_{3,2}\gamma_1h_{1,3}/(h_1h_2)$$
$$-u_3\gamma_2h_{1,3}h_{2,1}/(h_1^2h_2) +u_3\gamma_{2,1}h_{2,3}/(h_1h_2) -u_{3,1}\gamma_2h_{2,3}/(h_1h_2) +\phi_{1,2}\psi_{1,1}/(h_1h_2)$$
$$-h_{2,1}\phi_2\psi_{1,1}/(h_1^2h_2) +\phi_{1,1}\psi_{1,2}/(h_1h_2) +h_{1,2}\phi_2\psi_{1,2}/(h_1h_2^2) -2h_{1,2}h_{2,1}\phi_1\psi_1/(h_1^2h_2^2)$$
$$+h_{2,1}\phi_{2,1}\psi_1/(h_1^2h_2) -h_{1,2}\phi_{2,2}\psi_1/(h_1h_2^2) +h_{1,3}h_{2,3}\phi_2\psi_1/(h_1h_2) +h_{2,1}\phi_1\psi_{2,1}/(h_1^2h_2)$$
$$+\phi_{2,2}\psi_{2,1}/(h_1h_2) -h_{1,2}\phi_1\psi_{2,2}/(h_1h_2^2) +\phi_{2,1}\psi_{2,2}/(h_1h_2) -h_{2,1}\phi_{1,1}\psi_2/(h_1^2h_2)$$

$$+h_{1,2}\phi_{1,2}\psi_2/(h_1h_2^2)+h_{1,3}h_{2,3}\phi_1\psi_2/(h_1h_2)-2h_{1,2}h_{2,1}\phi_2\psi_2/(h_1^2h_2^2)-\gamma_{2,2}h_{1,2}u/(h_1h_2^2)$$
$$-2\gamma_1h_{1,2}h_{2,1}u/(h_1^2h_2^2)+\gamma_{2,1}h_{2,1}u/(h_1^2h_2)+\gamma_2h_{1,3}h_{2,3}u/(h_1h_2)+2h_{1,2}h_{2,1}\phi_1u/(R_1h_1^2h_2^2)$$
$$-h_{2,1}\phi_{2,1}u/(R_1h_1^2h_2)+h_{1,2}\phi_{2,2}u/(R_1h_1h_2^2)-h_{1,3}h_{2,3}\phi_2u/(R_1h_1h_2)+\gamma_{1,2}u_{,1}/(h_1h_2)$$
$$-\gamma_2h_{2,1}u_{,1}/(h_1^2h_2)-\phi_{1,2}u_{,1}/(R_1h_1h_2)+h_{2,1}\phi_2u_{,1}/(R_1h_1^2h_2)+\gamma_2h_{1,2}u_{,2}/(h_1h_2^2)$$
$$+\gamma_{1,1}u_{,2}/(h_1h_2)-\phi_{1,1}u_{,2}/(R_1h_1h_2)-h_{1,2}\phi_2u_{,2}/(R_1h_1h_2^2)+\gamma_{1,2}h_{1,2}v/(h_1h_2^2)$$
$$-2\gamma_2h_{1,2}h_{2,1}v/(h_1^2h_2^2)-\gamma_{1,1}h_{2,1}v/(h_1^2h_2)+\gamma_1h_{1,3}h_{2,3}v/(h_1h_2)+h_{2,1}\phi_{1,1}v/(R_2h_1^2h_2)$$
$$-h_{1,2}\phi_{1,2}v/(R_2h_1h_2^2)-h_{1,3}h_{2,3}\phi_1v/(R_2h_1h_2)+2h_{1,2}h_{2,1}\phi_2v/(R_2h_1^2h_2^2)+\gamma_{2,2}v_{,1}/(h_1h_2)$$
$$+\gamma_1h_{2,1}v_{,1}/(h_1^2h_2)-h_{2,1}\phi_1v_{,1}/(R_2h_1^2h_2)-\phi_{2,2}v_{,1}/(R_2h_1h_2)-\gamma_1h_{1,2}v_{,2}/(h_1h_2^2)$$
$$+\gamma_{2,1}v_{,2}/(h_1h_2)+h_{1,2}\phi_1v_{,2}/(R_2h_1h_2^2)-\phi_{2,1}v_{,2}/(R_2h_1h_2)$$

$$\chi^4_{6_{NL}}=\phi_{1,1}\phi_{1,2}/(h_1h_2)-h_{1,2}h_{2,1}\phi_1^2/(h_1^2h_2^2)+h_{2,1}\phi_1\phi_{2,1}/(h_1^2h_2)-h_{1,2}\phi_1\phi_{2,2}/(h_1h_2^2)$$
$$+\phi_{2,1}\phi_{2,2}/(h_1h_2)-h_{2,1}\phi_{1,1}\phi_2/(h_1^2h_2)+h_{1,2}\phi_{1,2}\phi_2/(h_1h_2^2)+h_{1,3}h_{2,3}\phi_1\phi_2/(h_1h_2)$$
$$-h_{1,2}h_{2,1}\phi_2^2/(h_1^2h_2^2)+\gamma_{1,2}\psi_{1,1}/(h_1h_2)-\gamma_2h_{2,1}\psi_{1,1}/(h_1^2h_2)+\gamma_2h_{1,2}\psi_{1,2}/(h_1h_2^2)$$
$$+\gamma_{1,1}\psi_{1,2}/(h_1h_2)-\gamma_{2,2}h_{1,2}\psi_1/(h_1h_2^2)-2\gamma_1h_{1,2}h_{2,1}\psi_1/(h_1^2h_2^2)+\gamma_{2,1}h_{2,1}\psi_1/(h_1^2h_2)$$
$$+\gamma_2h_{1,3}h_{2,3}\psi_1/(h_1h_2)+\gamma_{2,2}\psi_{2,1}/(h_1h_2)+\gamma_1h_{2,1}\psi_{2,1}/(h_1^2h_2)-\gamma_1h_{1,2}\psi_{2,2}/(h_1h_2^2)$$
$$+\gamma_{2,1}\psi_{2,2}/(h_1h_2)+\gamma_{1,2}h_{1,2}\psi_2/(h_1h_2^2)-2\gamma_2h_{1,2}h_{2,1}\psi_2/(h_1^2h_2^2)-\gamma_{1,1}h_{2,1}\psi_2/(h_1^2h_2)$$
$$+\gamma_1h_{1,3}h_{2,3}\psi_2/(h_1h_2)+u_3h_{1,3}\theta_{1,2}/(h_1h_2)-u_3h_{1,2}h_{2,3}\theta_1/(h_1h_2^2)-u_{3,2}h_{1,3}\theta_1/(h_1h_2)$$
$$+u_3h_{2,3}\theta_{2,1}/(h_1h_2)-u_3h_{1,3}h_{2,1}\theta_2/(h_1^2h_2)-u_{3,1}h_{2,3}\theta_2/(h_1h_2)+\gamma_{2,2}h_{1,2}u/(R_1h_1h_2^2)$$
$$+2\gamma_1h_{1,2}h_{2,1}u/(R_1h_1^2h_2^2)-\gamma_{2,1}h_{2,1}u/(R_1h_1^2h_2)-\gamma_2h_{1,3}h_{2,3}u/(R_1h_1h_2)$$
$$-2h_{1,2}h_{2,1}\theta_1u/(h_1^2h_2^2)+h_{2,1}\theta_{2,1}u/(h_1^2h_2)-h_{1,2}\theta_{2,2}u/(h_1h_2^2)+h_{1,3}h_{2,3}\theta_2u/(h_1h_2)$$
$$-\gamma_{1,2}u_{,1}/(R_1h_1h_2)+\gamma_2h_{2,1}u_{,1}/(R_1h_1^2h_2)+\theta_{1,2}u_{,1}/(h_1h_2)-h_{2,1}\theta_2u_{,1}/(h_1^2h_2)$$
$$-\gamma_2h_{1,2}u_{,2}/(R_1h_1h_2^2)-\gamma_{1,1}u_{,2}/(R_1h_1h_2)+\theta_{1,1}u_{,2}/(h_1h_2)+h_{1,2}\theta_2u_{,2}/(h_1h_2^2)$$
$$-\gamma_{1,2}h_{1,2}v/(R_2h_1h_2^2)+2\gamma_2h_{1,2}h_{2,1}v/(R_2h_1^2h_2^2)+\gamma_{1,1}h_{2,1}v/(R_2h_1^2h_2)$$
$$-\gamma_1h_{1,3}h_{2,3}v/(R_2h_1h_2)-h_{2,1}\theta_{1,1}v/(h_1^2h_2)+h_{1,2}\theta_{1,2}v/(h_1h_2^2)+h_{1,3}h_{2,3}\theta_1v/(h_1h_2)$$
$$-2h_{1,2}h_{2,1}\theta_2v/(h_1^2h_2^2)-\gamma_{2,2}v_{,1}/(R_2h_1h_2)-\gamma_1h_{2,1}v_{,1}/(R_2h_1^2h_2)+h_{2,1}\theta_1v_{,1}/(h_1^2h_2)$$
$$+\theta_{2,2}v_{,1}/(h_1h_2)+\gamma_1h_{1,2}v_{,2}/(R_2h_1h_2^2)-\gamma_{2,1}v_{,2}/(R_2h_1h_2)-h_{1,2}\theta_1v_{,2}/(h_1h_2^2)$$
$$+\theta_{2,1}v_{,2}/(h_1h_2)$$

$$\chi^5_{6_{NL}}=\gamma_{1,2}\phi_{1,1}/(h_1h_2)-\gamma_2h_{2,1}\phi_{1,1}/(h_1^2h_2)+\gamma_2h_{1,2}\phi_{1,2}/(h_1h_2^2)+\gamma_{1,1}\phi_{1,2}/(h_1h_2)$$
$$-\gamma_{2,2}h_{1,2}\phi_1/(h_1h_2^2)-2\gamma_1h_{1,2}h_{2,1}\phi_1/(h_1^2h_2^2)+\gamma_{2,1}h_{2,1}\phi_1/(h_1^2h_2)+\gamma_2h_{1,3}h_{2,3}\phi_1/(h_1h_2)$$
$$+\gamma_{2,2}\phi_{2,1}/(h_1h_2)+\gamma_1h_{2,1}\phi_{2,1}/(h_1^2h_2)-\gamma_1h_{1,2}\phi_{2,2}/(h_1h_2^2)+\gamma_{2,1}\phi_{2,2}/(h_1h_2)$$

$$+\gamma_{1,2}h_{1,2}\phi_2/(h_1h_2^2) -2\gamma_2h_{1,2}h_{2,1}\phi_2/(h_1^2h_2^2) -\gamma_{1,1}h_{2,1}\phi_2/(h_1^2h_2) +\gamma_1h_{1,3}h_{2,3}\phi_2/(h_1h_2)$$
$$+\psi_{1,2}\theta_{1,1}/(h_1h_2) -h_{2,1}\psi_2\theta_{1,1}/(h_1^2h_2) +\psi_{1,1}\theta_{1,2}/(h_1h_2) +h_{1,2}\psi_2\theta_{1,2}/(h_1h_2^2)$$
$$-2h_{1,2}h_{2,1}\psi_1\theta_1/(h_1^2h_2^2) +h_{2,1}\psi_{2,1}\theta_1/(h_1^2h_2) -h_{1,2}\psi_{2,2}\theta_1/(h_1h_2^2) +h_{1,3}h_{2,3}\psi_2\theta_1/(h_1h_2)$$
$$+h_{2,1}\psi_1\theta_{2,1}/(h_1^2h_2) +\psi_{2,2}\theta_{2,1}/(h_1h_2) -h_{1,2}\psi_1\theta_{2,2}/(h_1h_2^2) +\psi_{2,1}\theta_{2,2}/(h_1h_2)$$
$$-h_{2,1}\psi_{1,1}\theta_2/(h_1^2h_2) +h_{1,2}\psi_{1,2}\theta_2/(h_1h_2^2) +h_{1,3}h_{2,3}\psi_1\theta_2/(h_1h_2) -2h_{1,2}h_{2,1}\psi_2\theta_2/(h_1^2h_2^2)$$
$$+2h_{1,2}h_{2,1}\theta_1u/(R_1h_1^2h_2^2) -h_{2,1}\theta_{2,1}u/(R_1h_1^2h_2) +h_{1,2}\theta_{2,2}u/(R_1h_1h_2^2)$$
$$-h_{1,3}h_{2,3}\theta_2u/(R_1h_1h_2) -\theta_{1,2}u_{,1}/(R_1h_1h_2) +h_{2,1}\theta_2u_{,1}/(R_1h_1^2h_2) -\theta_{1,1}u_{,2}/(R_1h_1h_2)$$
$$-h_{1,2}\theta_2u_{,2}/(R_1h_1h_2^2) +h_{2,1}\theta_{1,1}v/(R_2h_1^2h_2) -h_{1,2}\theta_{1,2}v/(R_2h_1h_2^2) -h_{1,3}h_{2,3}\theta_1v/(R_2h_1h_2)$$
$$+2h_{1,2}h_{2,1}\theta_2v/(R_2h_1^2h_2^2) -h_{2,1}\theta_1v_{,1}/(R_2h_1^2h_2) -\theta_{2,2}v_{,1}/(R_2h_1h_2) +h_{1,2}\theta_1v_{,2}/(R_2h_1h_2^2)$$
$$-\theta_{2,1}v_{,2}/(R_2h_1h_2)$$

$$\chi^6_{6_{NL}} = -\gamma_1\gamma_{2,2}h_{1,2}/(h_1h_2^2) +\gamma_{1,2}\gamma_2h_{1,2}/(h_1h_2^2) -\gamma_1^2h_{1,2}h_{2,1}/(h_1^2h_2^2) -\gamma_2^2h_{1,2}h_{2,1}/(h_1^2h_2^2)$$
$$+\gamma_{1,1}\gamma_{1,2}/(h_1h_2) +\gamma_{2,1}\gamma_{2,2}/(h_1h_2) +\gamma_1\gamma_{2,1}h_{2,1}/(h_1^2h_2) -\gamma_{1,1}\gamma_2h_{2,1}/(h_1^2h_2)$$
$$+\gamma_1\gamma_2h_{1,3}h_{2,3}/(h_1h_2) +\phi_{1,2}\theta_{1,1}/(h_1h_2) -h_{2,1}\phi_2\theta_{1,1}/(h_1^2h_2) +\phi_{1,1}\theta_{1,2}/(h_1h_2)$$
$$+h_{1,2}\phi_2\theta_{1,2}/(h_1h_2^2) -2h_{1,2}h_{2,1}\phi_1\theta_1/(h_1^2h_2^2) +h_{2,1}\phi_{2,1}\theta_1/(h_1^2h_2) -h_{1,2}\phi_{2,2}\theta_1/(h_1h_2^2)$$
$$+h_{1,3}h_{2,3}\phi_2\theta_1/(h_1h_2) +h_{2,1}\phi_1\theta_{2,1}/(h_1^2h_2) +\phi_{2,2}\theta_{2,1}/(h_1h_2) -h_{1,2}\phi_1\theta_{2,2}/(h_1h_2^2)$$
$$+\phi_{2,1}\theta_{2,2}/(h_1h_2) -h_{2,1}\phi_{1,1}\theta_2/(h_1^2h_2) +h_{1,2}\phi_{1,2}\theta_2/(h_1h_2^2) +h_{1,3}h_{2,3}\phi_1\theta_2/(h_1h_2)$$
$$-2h_{1,2}h_{2,1}\phi_2\theta_2/(h_1^2h_2^2)$$

$$\chi^7_{6_{NL}} = \gamma_{1,2}\theta_{1,1}/(h_1h_2) -\gamma_2h_{2,1}\theta_{1,1}/(h_1^2h_2) +\gamma_2h_{1,2}\theta_{1,2}/(h_1h_2^2) +\gamma_{1,1}\theta_{1,2}/(h_1h_2)$$
$$-\gamma_{2,2}h_{1,2}\theta_1/(h_1h_2^2) -2\gamma_1h_{1,2}h_{2,1}\theta_1/(h_1^2h_2^2) +\gamma_{2,1}h_{2,1}\theta_1/(h_1^2h_2) +\gamma_2h_{1,3}h_{2,3}\theta_1/(h_1h_2)$$
$$+\gamma_{2,2}\theta_{2,1}/(h_1h_2) +\gamma_1h_{2,1}\theta_{2,1}/(h_1^2h_2) -\gamma_1h_{1,2}\theta_{2,2}/(h_1h_2^2) +\gamma_{2,1}\theta_{2,2}/(h_1h_2)$$
$$+\gamma_{1,2}h_{1,2}\theta_2/(h_1h_2^2) -2\gamma_2h_{1,2}h_{2,1}\theta_2/(h_1^2h_2^2) -\gamma_{1,1}h_{2,1}\theta_2/(h_1^2h_2) +\gamma_1h_{1,3}h_{2,3}\theta_2/(h_1h_2)$$

$$\chi^8_{6_{NL}} = \theta_{1,1}\theta_{1,2}/(h_1h_2) -h_{1,2}h_{2,1}\theta_1^2/(h_1^2h_2^2) +h_{2,1}\theta_1\theta_{2,1}/(h_1^2h_2) -h_{1,2}\theta_1\theta_{2,2}/(h_1h_2^2)$$
$$+\theta_{2,1}\theta_{2,2}/(h_1h_2) -h_{2,1}\theta_{1,1}\theta_2/(h_1^2h_2) +h_{1,2}\theta_{1,2}\theta_2/(h_1h_2^2) +h_{1,3}h_{2,3}\theta_1\theta_2/(h_1h_2)$$
$$-h_{1,2}h_{2,1}\theta_2^2/(h_1^2h_2^2)$$

A.3 Approximation of 60 Shell Shape Factor Functions with Second Order Taylor's Series Expansions

Most of the expressions listed in the previous section contain the shape functions h_1 and h_2 or their derivatives. If one factors out all of these functions, there are 60 different

combinations possible. For a shell with radius R_1 in the y_1 direction and radius R_2 in the y_2 direction, the shape factors h_1 and h_2 are as shown below:

$$h_1 = A_1\,(1 - y_3/R_1) \qquad h_2 = A_2\,(1 - y_3/R_2) \tag{A.5}$$

where $A_1 = \sqrt{a_{11}}$ and $A_2 = \sqrt{a_{22}}$ are the Lamé parameters of the surface. The 60 possible combinations of the functions are listed below along with their quadratic Taylor's series approximation.

$$\hat{H}_1 = h_{1,2}/h_1 \cong [\,A_{1,2}/A_1\,] + [\,R_{1,2}/R_1^2\,]\,y_3 + [\,R_{1,2}/R_1^3\,]\,y_3^2$$

$$\hat{H}_2 = h_{1,3}/h_1 \cong [\,A_{1,3}/A_1 - 1/R_1\,] + [\,-1/R_1^2 + R_{1,3}/R_1^2\,]\,y_3 + [\,-1/R_1^3 + R_{1,3}/R_1^3\,]\,y_3^2$$

$$\hat{H}_3 = 1/h_1^2 \cong [\,1/A_1^2\,] + [\,2/(A_1^2 R_1)\,]\,y_3 + [\,3/(A_1^2 R_1^2)\,]\,y_3^2$$

$$\hat{H}_4 = h_{1,2}^2/h_1^2 \cong [\,A_{1,2}^2/A_1^2\,] + [\,2A_{1,2}R_{1,2}/(A_1 R_1^2)\,]\,y_3 + [\,2A_{1,2}R_{1,2}/(A_1 R_1^3) + R_{1,2}^2/R_1^4\,]\,y_3^2$$

$$\begin{aligned}\hat{H}_5 = h_{1,2}^2/h_2^2 \cong\ & [\,A_{1,2}^2/A_2^2\,] + [\,-2A_{1,2}^2/(A_2^2 R_1) + 2A_{1,2}A_1 R_{1,2}/(A_2^2 R_1^2) + 2A_{1,2}^2/(A_2^2 R_2)\,]\,y_3 \\ & + [\,A_{1,2}^2/(A_2^2 R_1^2) - 2A_{1,2}A_1 R_{1,2}/(A_2^2 R_1^3) + A_1^2 R_{1,2}^2/(A_2^2 R_1^4) - 4A_{1,2}^2/(A_2^2 R_1 R_2) \\ & + 4A_{1,2}A_1 R_{1,2}/(A_2^2 R_1^2 R_2) + 3A_{1,2}^2/(A_2^2 R_2^2)\,]\,y_3^2\end{aligned}$$

$$\begin{aligned}\hat{H}_6 = h_{1,3}^2/h_1^2 \cong\ & [\,A_{1,3}^2/A_1^2 - 2A_{1,3}/(A_1 R_1) + 1/R_1^2\,] + [\,-2A_{1,3}/(A_1 R_1^2) \\ & + 2A_{1,3}R_{1,3}/(A_1 R_1^2) + 2/R_1^3 - 2R_{1,3}/R_1^3\,]\,y_3 + [\,-2A_{1,3}/(A_1 R_1^3) + 2A_{1,3}R_{1,3}/(A_1 R_1^3) \\ & + 3/R_1^4 - 4R_{1,3}/R_1^4 + R_{1,3}^2/R_1^4\,]\,y_3^2\end{aligned}$$

$$\begin{aligned}\hat{H}_7 = h_{1,3}^2 \cong\ & [\,A_{1,3}^2 - 2A_{1,3}A_1/R_1 + A_1^2/R_1^2\,] + [\,-2A_{1,3}^2/R_1 + 2A_{1,3}A_1/R_1^2 \\ & + 2A_{1,3}A_1 R_{1,3}/R_1^2 - 2A_1^2 R_{1,3}/R_1^3\,]\,y_3 + [\,A_{1,3}^2/R_1^2 - 2A_{1,3}A_1 R_{1,3}/R_1^3 + A_1^2 R_{1,3}^2/R_1^4\,]\,y_3^2\end{aligned}$$

$$\begin{aligned}\hat{H}_8 = h_{1,2}h_{1,3}/h_1^2 \cong\ & [\,A_{1,2}A_{1,3}/A_1^2 - A_{1,2}/(A_1 R_1)\,] + [\,-A_{1,2}/(A_1 R_1^2) + A_{1,3}R_{1,2}/(A_1 R_1^2) \\ & + A_{1,2}R_{1,3}/(A_1 R_1^2) - R_{1,2}/R_1^3\,]\,y_3 + [\,-A_{1,2}/(A_1 R_1^3) + A_{1,3}R_{1,2}/(A_1 R_1^3) + A_{1,2}R_{1,3}/(A_1 R_1^3) \\ & - 2R_{1,2}/R_1^4 + R_{1,2}R_{1,3}/R_1^4\,]\,y_3^2\end{aligned}$$

$$\hat{H}_9 = h_{2,3}/h_2 \cong [\,A_{2,3}/A_2 - 1/R_2\,] + [\,-1/R_2^2 + R_{2,3}/R_2^2\,]\,y_3 + [\,-1/R_2^3 + R_{2,3}/R_2^3\,]\,y_3^2$$

$$\hat{H}_{10} = h_{2,1}/h_2 \cong [\, A_{2,1}/A_2 \,] + [\, R_{2,1}/R_2^2 \,] y_3 + [\, R_{2,1}/R_2^3 \,] y_3^2$$

$$\hat{H}_{11} = 1/h_2^2 \cong [\, 1/A_2^2 \,] + [\, 2/(A_2^2 R_2) \,] y_3 + [\, 3/(A_2^2 R_2^2) \,] y_3^2$$

$$\hat{H}_{12} = h_{2,1}^2/h_2^2 \cong [\, A_{2,1}^2/A_2^2 \,] + [\, 2A_{2,1}R_{2,1}/(A_2 R_2^2) \,] y_3 + [\, 2A_{2,1}R_{2,1}/(A_2 R_2^3) + R_{2,1}^2/R_2^4 \,] y_3^2$$

$$\hat{H}_{13} = h_{2,1}^2/h_1^2 \cong [\, A_{2,1}^2/A_1^2 \,] + [\, 2A_{2,1}^2/(A_1^2 R_1) - 2A_{2,1}^2/(A_1^2 R_2) + 2A_{2,1}A_2 R_{2,1}/(A_1^2 R_2^2) \,] y_3$$
$$+ [\, 3A_{2,1}^2/(A_1^2 R_1^2) - 4A_{2,1}^2/(A_1^2 R_1 R_2) + A_{2,1}^2/(A_1^2 R_2^2) + 4A_{2,1}A_2 R_{2,1}/(A_1^2 R_1 R_2^2)$$
$$- 2A_{2,1}A_2 R_{2,1}/(A_1^2 R_2^3) + A_2^2 R_{2,1}^2/(A_1^2 R_2^4) \,] y_3^2$$

$$\hat{H}_{14} = h_{2,3}^2/h_2^2 \cong [\, A_{2,3}^2/A_2^2 - 2A_{2,3}/(A_2 R_2) + 1/R_2^2 \,] + [\, -2A_{2,3}/(A_2 R_2^2)$$
$$+ 2A_{2,3}R_{2,3}/(A_2 R_2^2) + 2/R_2^3 - 2R_{2,3}/R_2^3 \,] y_3 + [\, -2A_{2,3}/(A_2 R_2^3) + 2A_{2,3}R_{2,3}/(A_2 R_2^3)$$
$$+ 3/R_2^4 - 4R_{2,3}/R_2^4 + R_{2,3}^2/R_2^4 \,] y_3^2$$

$$\hat{H}_{15} = h_{2,3}^2 \cong [\, A_{2,3}^2 - 2A_{2,3}A_2/R_2 + A_2^2/R_2^2 \,] + [\, -2A_{2,3}^2/R_2 + 2A_{2,3}A_2/R_2^2$$
$$+ 2A_{2,3}A_2 R_{2,3}/R_2^2 - 2A_2^2 R_{2,3}/R_2^3 \,] y_3 + [\, A_{2,3}^2/R_2^2 - 2A_{2,3}A_2 R_{2,3}/R_2^3 + A_2^2 R_{2,3}^2/R_2^4 \,] y_3^2$$

$$\hat{H}_{16} = h_{2,1}h_{2,3}/h_2^2 \cong [\, A_{2,1}A_{2,3}/A_2^2 - A_{2,1}/(A_2 R_2) \,] + [\, -A_{2,1}/(A_2 R_2^2) + A_{2,3}R_{2,1}/(A_2 R_2^2)$$
$$+ A_{2,1}R_{2,3}/(A_2 R_2^2) - R_{2,1}/R_2^3 \,] y_3 + [\, -A_{2,1}/(A_2 R_2^3) + A_{2,3}R_{2,1}/(A_2 R_2^3) + A_{2,1}R_{2,3}/(A_2 R_2^3)$$
$$- 2R_{2,1}/R_2^4 + R_{2,1}R_{2,3}/R_2^4 \,] y_3^2$$

$$\hat{H}_{17} = 1/h_2 \cong [\, 1/A_2 \,] + [\, 1/(A_2 R_2) \,] y_3 + [\, 1/(A_2 R_2^2) \,] y_3^2$$

$$\hat{H}_{18} = 1/h_1 \cong [\, 1/A_1 \,] + [\, 1/(A_1 R_1) \,] y_3 + [\, 1/(A_1 R_1^2) \,] y_3^2$$

$$\hat{H}_{19} = h_{2,1}/h_1 \cong [\, A_{2,1}/A_1 \,] + [\, A_{2,1}/(A_1 R_1) - A_{2,1}/(A_1 R_2) + A_2 R_{2,1}/(A_1 R_2^2) \,] y_3$$
$$+ [\, A_{2,1}/(A_1 R_1^2) - A_{2,1}/(A_1 R_1 R_2) + A_2 R_{2,1}/(A_1 R_1 R_2^2) \,] y_3^2$$

$$\hat{H}_{20} = h_{1,2}/h_2 \cong [\, A_{1,2}/A_2 \,] + [\, -A_{1,2}/(A_2 R_1) + A_1 R_{1,2}/(A_2 R_1^2) + A_{1,2}/(A_2 R_2) \,] y_3$$
$$+ [\, -A_{1,2}/(A_2 R_1 R_2) + A_1 R_{1,2}/(A_2 R_1^2 R_2) + A_{1,2}/(A_2 R_2^2) \,] y_3^2$$

$$\hat{H}_{21} = 1/(h_1 h_2) \cong [\, 1/(A_1 A_2) \,] + [\, 1/(A_1 A_2 R_1) + 1/(A_1 A_2 R_2) \,] y_3 + [\, 1/(A_1 A_2 R_1^2)$$
$$+ 1/(A_1 A_2 R_1 R_2) + 1/(A_1 A_2 R_2^2) \,] y_3^2$$

$$\hat{H}_{22} = h_{1,3}/h_2 \cong [\, A_{1,3}/A_2 - A_1/(A_2R_1)\,] + [\, -A_{1,3}/(A_2R_1) + A_1R_{1,3}/(A_2R_1^2)$$
$$+A_{1,3}/(A_2R_2) - A_1/(A_2R_1R_2)\,]\,y_3 + [\, -A_{1,3}/(A_2R_1R_2) + A_1R_{1,3}/(A_2R_1^2R_2)$$
$$+A_{1,3}/(A_2R_2^2) - A_1/(A_2R_1R_2^2)\,]\,y_3^2$$

$$\hat{H}_{23} = h_{2,3}/h_1 \cong [\, A_{2,3}/A_1 - A_2/(A_1R_2)\,] + [\, A_{2,3}/(A_1R_1) - A_{2,3}/(A_1R_2) - A_2/(A_1R_1R_2)$$
$$+A_2R_{2,3}/(A_1R_2^2)\,]\,y_3 + [\, A_{2,3}/(A_1R_1^2) - A_{2,3}/(A_1R_1R_2) - A_2/(A_1R_1^2R_2)$$
$$+A_2R_{2,3}/(A_1R_1R_2^2)\,]\,y_3^2$$

$$\hat{H}_{24} = h_{1,2}h_{2,1}/h_1^2 \cong [\, A_{1,2}A_{2,1}/A_1^2\,] + [\, A_{1,2}A_{2,1}/(A_1^2R_1) + A_{2,1}R_{1,2}/(A_1R_1^2)$$
$$-A_{1,2}A_{2,1}/(A_1^2R_2) + A_{1,2}A_2R_{2,1}/(A_1^2R_2^2)\,]\,y_3 + [\, A_{1,2}A_{2,1}/(A_1^2R_1^2) + 2A_{2,1}R_{1,2}/(A_1R_1^3)$$
$$-A_{1,2}A_{2,1}/(A_1^2R_1R_2) - A_{2,1}R_{1,2}/(A_1R_1^2R_2) + A_{1,2}A_2R_{2,1}/(A_1^2R_1R_2^2)$$
$$+A_2R_{1,2}R_{2,1}/(A_1R_1^2R_2^2)\,]\,y_3^2$$

$$\hat{H}_{25} = h_{1,2}h_{2,1}/h_2^2 \cong [\, A_{1,2}A_{2,1}/A_2^2\,] + [\, -A_{1,2}A_{2,1}/(A_2^2R_1) + A_1A_{2,1}R_{1,2}/(A_2^2R_1^2)$$
$$+A_{1,2}A_{2,1}/(A_2^2R_2) + A_{1,2}R_{2,1}/(A_2R_2^2)\,]\,y_3 + [\, -A_{1,2}A_{2,1}/(A_2^2R_1R_2)$$
$$+A_1A_{2,1}R_{1,2}/(A_2^2R_1^2R_2) + A_{1,2}A_{2,1}/(A_2^2R_2^2) - A_{1,2}R_{2,1}/(A_2R_1R_2^2) + A_1R_{1,2}R_{2,1}/(A_2R_1^2R_2^2)$$
$$+2A_{1,2}R_{2,1}/(A_2R_2^3)\,]\,y_3^2$$

$$\hat{H}_{26} = h_{1,3}h_{2,3} \cong [\, A_{1,3}A_{2,3} - A_1A_{2,3}/R_1 - A_{1,3}A_2/R_2 + A_1A_2/(R_1R_2)\,] + [\, -A_{1,3}A_{2,3}/R_1$$
$$+A_1A_{2,3}R_{1,3}/R_1^2 - A_{1,3}A_{2,3}/R_2 + A_1A_{2,3}/(R_1R_2) + A_{1,3}A_2/(R_1R_2) - A_1A_2R_{1,3}/(R_1^2R_2)$$
$$+A_{1,3}A_2R_{2,3}/R_2^2 - A_1A_2R_{2,3}/(R_1R_2^2)\,]\,y_3 + [\, A_{1,3}A_{2,3}/(R_1R_2) - A_1A_{2,3}R_{1,3}/(R_1^2R_2)$$
$$-A_{1,3}A_2R_{2,3}/(R_1R_2^2) + A_1A_2R_{1,3}R_{2,3}/(R_1^2R_2^2)\,]\,y_3^2$$

$$\hat{H}_{27} = h_{1,3}h_{2,1}/h_1^2 \cong [\, A_{1,3}A_{2,1}/A_1^2 - A_{2,1}/(A_1R_1)\,] + [\, A_{1,3}A_{2,1}/(A_1^2R_1) - 2A_{2,1}/(A_1R_1^2)$$
$$+A_{2,1}R_{1,3}/(A_1R_1^2) - A_{1,3}A_{2,1}/(A_1^2R_2) + A_{2,1}/(A_1R_1R_2) + A_{1,3}A_2R_{2,1}/(A_1^2R_2^2)$$
$$-A_2R_{2,1}/(A_1R_1R_2^2)\,]\,y_3 + [\, A_{1,3}A_{2,1}/(A_1^2R_1^2) - 3A_{2,1}/(A_1R_1^3) + 2A_{2,1}R_{1,3}/(A_1R_1^3)$$
$$-A_{1,3}A_{2,1}/(A_1^2R_1R_2) + 2A_{2,1}/(A_1R_1^2R_2) - A_{2,1}R_{1,3}/(A_1R_1^2R_2) + A_{1,3}A_2R_{2,1}/(A_1^2R_1R_2^2)$$
$$-2A_2R_{2,1}/(A_1R_1^2R_2^2) + A_2R_{1,3}R_{2,1}/(A_1R_1^2R_2^2)\,]\,y_3^2$$

$$\hat{H}_{28} = h_{1,2}h_{2,3}/h_2^2 \cong [\, A_{1,2}A_{2,3}/A_2^2 - A_{1,2}/(A_2R_2)\,] + [\, -A_{1,2}A_{2,3}/(A_2^2R_1)$$
$$+A_1A_{2,3}R_{1,2}/(A_2^2R_1^2) + A_{1,2}A_{2,3}/(A_2^2R_2) + A_{1,2}/(A_2R_1R_2) - A_1R_{1,2}/(A_2R_1^2R_2)$$
$$-2A_{1,2}/(A_2R_2^2) + A_{1,2}R_{2,3}/(A_2R_2^2)\,]\,y_3 + [\, -A_{1,2}A_{2,3}/(A_2^2R_1R_2) + A_1A_{2,3}R_{1,2}/(A_2^2R_1^2R_2)$$

$$+A_{1,2}A_{2,3}/(A_2^2R_2^2) +2A_{1,2}/(A_2R_1R_2^2) -2A_1R_{1,2}/(A_2R_1^2R_2^2) -A_{1,2}R_{2,3}/(A_2R_1R_2^2)$$
$$+A_1R_{1,2}R_{2,3}/(A_2R_1^2R_2^2) -3A_{1,2}/(A_2R_2^3) +2A_{1,2}R_{2,3}/(A_2R_2^3)]\, y_3^2.$$

$$\hat{H}_{29} = h_{1,2}/(h_1h_2) \cong [\, A_{1,2}/(A_1A_2) \,] + [\, R_{1,2}/(A_2R_1^2) +A_{1,2}/(A_1A_2R_2) \,]\, y_3$$
$$+ [\, R_{1,2}/(A_2R_1^3) +R_{1,2}/(A_2R_1^2R_2) +A_{1,2}/(A_1A_2R_2^2) \,]\, y_3^2$$

$$\hat{H}_{30} = h_{1,2}^2/(h_1^2h_2) \cong [\, A_{1,2}^2/(A_1^2A_2) \,] + [\, 2A_{1,2}R_{1,2}/(A_1A_2R_1^2) +A_{1,2}^2/(A_1^2A_2R_2) \,]\, y_3$$
$$+ [\, 2A_{1,2}R_{1,2}/(A_1A_2R_1^3) +R_{1,2}^2/(A_2R_1^4) +2A_{1,2}R_{1,2}/(A_1A_2R_1^2R_2) +A_{1,2}^2/(A_1^2A_2R_2^2) \,]\, y_3^2$$

$$\hat{H}_{31} = h_{1,2}^2/(h_1h_2^2) \cong [\, A_{1,2}^2/(A_1A_2^2) \,] + [\, -A_{1,2}^2/(A_1A_2^2R_1) +2A_{1,2}R_{1,2}/(A_2^2R_1^2)$$
$$+2A_{1,2}^2/(A_1A_2^2R_2) \,]\, y_3 + [\, A_1R_{1,2}^2/(A_2^2R_1^4) -2A_{1,2}^2/(A_1A_2^2R_1R_2) +4A_{1,2}R_{1,2}/(A_2^2R_1^2R_2)$$
$$+3A_{1,2}^2/(A_1A_2^2R_2^2) \,]\, y_3^2$$

$$\hat{H}_{32} = h_{1,3}^2/h_1 \cong [\, A_{1,3}^2/A_1 -2A_{1,3}/R_1 +A_1/R_1^2 \,] + [\, -A_{1,3}^2/(A_1R_1) +2A_{1,3}R_{1,3}/R_1^2$$
$$+A_1/R_1^3 -2A_1R_{1,3}/R_1^3 \,]\, y_3 + [\, A_1/R_1^4 -2A_1R_{1,3}/R_1^4 +A_1R_{1,3}^2/R_1^4 \,]\, y_3^2$$

$$\hat{H}_{33} = h_{1,2}/h_1^2 \cong [\, A_{1,2}/A_1^2 \,] + [\, A_{1,2}/(A_1^2R_1) +R_{1,2}/(A_1R_1^2) \,]\, y_3 + [\, A_{1,2}/(A_1^2R_1^2)$$
$$+2R_{1,2}/(A_1R_1^3) \,]\, y_3^2$$

$$\hat{H}_{34} = h_{1,3}/h_1^2 \cong [\, A_{1,3}/A_1^2 -1/(A_1R_1) \,] + [\, A_{1,3}/(A_1^2R_1) -2/(A_1R_1^2) +R_{1,3}/(A_1R_1^2) \,]\, y_3$$
$$+ [\, A_{1,3}/(A_1^2R_1^2) -3/(A_1R_1^3) +2R_{1,3}/(A_1R_1^3) \,]\, y_3^2$$

$$\hat{H}_{35} = h_{1,2}h_{1,3}/(h_1^2h_2) \cong [\, A_{1,2}A_{1,3}/(A_1^2A_2) -A_{1,2}/(A_1A_2R_1) \,] + [\, -A_{1,2}/(A_1A_2R_1^2)$$
$$+A_{1,3}R_{1,2}/(A_1A_2R_1^2) +A_{1,2}R_{1,3}/(A_1A_2R_1^2) -R_{1,2}/(A_2R_1^3) +A_{1,2}A_{1,3}/(A_1^2A_2R_2)$$
$$-A_{1,2}/(A_1A_2R_1R_2) \,]\, y_3 + [\, -A_{1,2}/(A_1A_2R_1^3) +A_{1,3}R_{1,2}/(A_1A_2R_1^3) +A_{1,2}R_{1,3}/(A_1A_2R_1^3)$$
$$-2R_{1,2}/(A_2R_1^4) +R_{1,2}R_{1,3}/(A_2R_1^4) -A_{1,2}/(A_1A_2R_1^2R_2) +A_{1,3}R_{1,2}/(A_1A_2R_1^2R_2)$$
$$+A_{1,2}R_{1,3}/(A_1A_2R_1^2R_2) -R_{1,2}/(A_2R_1^3R_2) +A_{1,2}A_{1,3}/(A_1^2A_2R_2^2) -A_{1,2}/(A_1A_2R_1R_2^2) \,]\, y_3^2$$

$$\hat{H}_{36} = h_{2,1}/(h_1h_2) \cong [\, A_{2,1}/(A_1A_2) \,] + [\, A_{2,1}/(A_1A_2R_1) +R_{2,1}/(A_1R_2^2) \,]\, y_3$$
$$+ [\, A_{2,1}/(A_1A_2R_1^2) +R_{2,1}/(A_1R_1R_2^2) +R_{2,1}/(A_1R_2^3) \,]\, y_3^2$$

$$\hat{H}_{37} = h_{2,1}^2/(h_1h_2^2) \cong [\, A_{2,1}^2/(A_1A_2^2) \,] + [\, A_{2,1}^2/(A_1A_2^2R_1) +2A_{2,1}R_{2,1}/(A_1A_2R_2^2) \,]\, y_3$$
$$+ [\, A_{2,1}^2/(A_1A_2^2R_1^2) +2A_{2,1}R_{2,1}/(A_1A_2R_1R_2^2) +2A_{2,1}R_{2,1}/(A_1A_2R_2^3) +R_{2,1}^2/(A_1R_2^4) \,]\, y_3^2$$

$$\hat{H}_{38} = h_{2,1}^2/(h_1^2 h_2) \cong [\, A_{2,1}^2/(A_1^2 A_2)\,] + [\, 2A_{2,1}^2/(A_1^2 A_2 R_1) - A_{2,1}^2/(A_1^2 A_2 R_2)$$
$$+2A_{2,1}R_{2,1}/(A_1^2 R_2^2)\,]\, y_3 + [\, 3A_{2,1}^2/(A_1^2 A_2 R_1^2) - 2A_{2,1}^2/(A_1^2 A_2 R_1 R_2) + 4A_{2,1}R_{2,1}/(A_1^2 R_1 R_2^2)$$
$$+A_2 R_{2,1}^2/(A_1^2 R_2^4)\,]\, y_3^2$$

$$\hat{H}_{39} = h_{2,3}^2/h_2 \cong [\, A_{2,3}^2/A_2 - 2A_{2,3}/R_2 + A_2/R_2^2\,] + [\, -A_{2,3}^2/(A_2 R_2) + 2A_{2,3}R_{2,3}/R_2^2$$
$$+A_2/R_2^3 - 2A_2 R_{2,3}/R_2^3\,]\, y_3 + [\, A_2/R_2^4 - 2A_2 R_{2,3}/R_2^4 + A_2 R_{2,3}^2/R_2^4\,]\, y_3^2$$

$$\hat{H}_{40} = h_{2,1}/h_2^2 \cong [\, A_{2,1}/A_2^2\,] + [\, A_{2,1}/(A_2^2 R_2) + R_{2,1}/(A_2 R_2^2)\,]\, y_3 + [\, A_{2,1}/(A_2^2 R_2^2)$$
$$+2R_{2,1}/(A_2 R_2^3)\,]\, y_3^2$$

$$\hat{H}_{41} = h_{2,1}h_{2,3}/(h_1 h_2^2) \cong [\, A_{2,1}A_{2,3}/(A_1 A_2^2) - A_{2,1}/(A_1 A_2 R_2)\,] + [\, A_{2,1}A_{2,3}/(A_1 A_2^2 R_1)$$
$$-A_{2,1}/(A_1 A_2 R_1 R_2) - A_{2,1}/(A_1 A_2 R_2^2) + A_{2,3}R_{2,1}/(A_1 A_2 R_2^2) + A_{2,1}R_{2,3}/(A_1 A_2 R_2^2)$$
$$-R_{2,1}/(A_1 R_2^3)\,]\, y_3 + [\, A_{2,1}A_{2,3}/(A_1 A_2^2 R_1^2) - A_{2,1}/(A_1 A_2 R_1^2 R_2) - A_{2,1}/(A_1 A_2 R_1 R_2^2)$$
$$+A_{2,3}R_{2,1}/(A_1 A_2 R_1 R_2^2) + A_{2,1}R_{2,3}/(A_1 A_2 R_1 R_2^2) - A_{2,1}/(A_1 A_2 R_2^3) + A_{2,3}R_{2,1}/(A_1 A_2 R_2^3)$$
$$-R_{2,1}/(A_1 R_1 R_2^3) + A_{2,1}R_{2,3}/(A_1 A_2 R_2^3) - 2R_{2,1}/(A_1 R_2^4) + R_{2,1}R_{2,3}/(A_1 R_2^4)\,]\, y_3^2$$

$$\hat{H}_{42} = h_{2,3}/h_2^2 \cong [\, A_{2,3}/A_2^2 - 1/(A_2 R_2)\,] + [\, A_{2,3}/(A_2^2 R_2) - 2/(A_2 R_2^2) + R_{2,3}/(A_2 R_2^2)\,]\, y_3$$
$$+[\, A_{2,3}/(A_2^2 R_2^2) - 3/(A_2 R_2^3) + 2R_{2,3}/(A_2 R_2^3)\,]\, y_3^2$$

$$\hat{H}_{43} = h_{1,2}/h_2^2 \cong [\, A_{1,2}/A_2^2\,] + [\, -A_{1,2}/(A_2^2 R_1) + A_1 R_{1,2}/(A_2^2 R_1^2) + 2A_{1,2}/(A_2^2 R_2)\,]\, y_3$$
$$+[\, -2A_{1,2}/(A_2^2 R_1 R_2) + 2A_1 R_{1,2}/(A_2^2 R_1^2 R_2) + 3A_{1,2}/(A_2^2 R_2^2)\,]\, y_3^2$$

$$\hat{H}_{44} = h_{2,1}/h_1^2 \cong [\, A_{2,1}/A_1^2\,] + [\, 2A_{2,1}/(A_1^2 R_1) - A_{2,1}/(A_1^2 R_2) + A_2 R_{2,1}/(A_1^2 R_2^2)\,]\, y_3$$
$$+[\, 3A_{2,1}/(A_1^2 R_1^2) - 2A_{2,1}/(A_1^2 R_1 R_2) + 2A_2 R_{2,1}/(A_1^2 R_1 R_2^2)\,]\, y_3^2$$

$$\hat{H}_{45} = h_{1,3}/(h_1 h_2) \cong [\, A_{1,3}/(A_1 A_2) - 1/(A_2 R_1)\,] + [\, -1/(A_2 R_1^2) + R_{1,3}/(A_2 R_1^2)$$
$$+A_{1,3}/(A_1 A_2 R_2) - 1/(A_2 R_1 R_2)\,]\, y_3 + [\, -1/(A_2 R_1^3) + R_{1,3}/(A_2 R_1^3) - 1/(A_2 R_1^2 R_2)$$
$$+R_{1,3}/(A_2 R_1^2 R_2) + A_{1,3}/(A_1 A_2 R_2^2) - 1/(A_2 R_1 R_2^2)\,]\, y_3^2$$

$$\hat{H}_{46} = h_{2,3}/(h_1 h_2) \cong [\, A_{2,3}/(A_1 A_2) - 1/(A_1 R_2)\,] + [\, A_{2,3}/(A_1 A_2 R_1) - 1/(A_1 R_1 R_2)$$
$$-1/(A_1 R_2^2) + R_{2,3}/(A_1 R_2^2)\,]\, y_3 + [\, A_{2,3}/(A_1 A_2 R_1^2) - 1/(A_1 R_1^2 R_2) - 1/(A_1 R_1 R_2^2)$$
$$+R_{2,3}/(A_1 R_1 R_2^2) - 1/(A_1 R_2^3) + R_{2,3}/(A_1 R_2^3)\,]\, y_3^2$$

$$\hat{H}_{47} = h_{1,2}h_{2,1}/(h_1^2h_2) \cong [\, A_{1,2}A_{2,1}/(A_1^2A_2)\,] + [\, A_{1,2}A_{2,1}/(A_1^2A_2R_1) + A_{2,1}R_{1,2}/(A_1A_2R_1^2) + A_{1,2}R_{2,1}/(A_1^2R_2^2)\,]\, y_3 + [\, A_{1,2}A_{2,1}/(A_1^2A_2R_1^2) + 2A_{2,1}R_{1,2}/(A_1A_2R_1^3) + A_{1,2}R_{2,1}/(A_1^2R_1R_2^2) + R_{1,2}R_{2,1}/(A_1R_1^2R_2^2) + A_{1,2}R_{2,1}/(A_1^2R_2^3)\,]\, y_3^2$$

$$\hat{H}_{48} = h_{1,2}h_{2,1}/(h_1h_2^2) \cong [\, A_{1,2}A_{2,1}/(A_1A_2^2)\,] + [\, A_{2,1}R_{1,2}/(A_2^2R_1^2) + A_{1,2}A_{2,1}/(A_1A_2^2R_2) + A_{1,2}R_{2,1}/(A_1A_2R_2^2)\,]\, y_3 + [\, A_{2,1}R_{1,2}/(A_2^2R_1^3) + A_{2,1}R_{1,2}/(A_2^2R_1^2R_2) + A_{1,2}A_{2,1}/(A_1A_2^2R_2^2) + R_{1,2}R_{2,1}/(A_2R_1^2R_2^2) + 2A_{1,2}R_{2,1}/(A_1A_2R_2^3)\,]\, y_3^2$$

$$\hat{H}_{49} = h_{1,3}h_{2,1}/(h_1^2h_2) \cong [\, A_{1,3}A_{2,1}/(A_1^2A_2) - A_{2,1}/(A_1A_2R_1)\,] + [\, A_{1,3}A_{2,1}/(A_1^2A_2R_1) - 2A_{2,1}/(A_1A_2R_1^2) + A_{2,1}R_{1,3}/(A_1A_2R_1^2) + A_{1,3}R_{2,1}/(A_1^2R_2^2) - R_{2,1}/(A_1R_1R_2^2)\,]\, y_3 + [\, A_{1,3}A_{2,1}/(A_1^2A_2R_1^2) - 3A_{2,1}/(A_1A_2R_1^3) + 2A_{2,1}R_{1,3}/(A_1A_2R_1^3) + A_{1,3}R_{2,1}/(A_1^2R_1R_2^2) - 2R_{2,1}/(A_1R_1^2R_2^2) + R_{1,3}R_{2,1}/(A_1R_1^2R_2^2) + A_{1,3}R_{2,1}/(A_1^2R_2^3) - R_{2,1}/(A_1R_1R_2^3)\,]\, y_3^2$$

$$\hat{H}_{50} = h_{1,2}h_{2,3}/(h_1h_2^2) \cong [\, A_{1,2}A_{2,3}/(A_1A_2^2) - A_{1,2}/(A_1A_2R_2)\,] + [\, A_{2,3}R_{1,2}/(A_2^2R_1^2) + A_{1,2}A_{2,3}/(A_1A_2^2R_2) - R_{1,2}/(A_2R_1^2R_2) - 2A_{1,2}/(A_1A_2R_2^2) + A_{1,2}R_{2,3}/(A_1A_2R_2^2)\,]\, y_3 + [\, A_{2,3}R_{1,2}/(A_2^2R_1^3) + A_{2,3}R_{1,2}/(A_2^2R_1^2R_2) - R_{1,2}/(A_2R_1^3R_2) + A_{1,2}A_{2,3}/(A_1A_2^2R_2^2) - 2R_{1,2}/(A_2R_1^2R_2^2) + R_{1,2}R_{2,3}/(A_2R_1^2R_2^2) - 3A_{1,2}/(A_1A_2R_2^3) + 2A_{1,2}R_{2,3}/(A_1A_2R_2^3)\,]\, y_3^2$$

$$\hat{H}_{51} = h_{1,3}h_{2,3}/h_2 \cong [\, A_{1,3}A_{2,3}/A_2 - A_1A_{2,3}/(A_2R_1) - A_{1,3}/R_2 + A_1/(R_1R_2)\,] + [\, - A_{1,3}A_{2,3}/(A_2R_1) + A_1A_{2,3}R_{1,3}/(A_2R_1^2) + A_{1,3}/(R_1R_2) - A_1R_{1,3}/(R_1^2R_2) - A_{1,3}/R_2^2 + A_1/(R_1R_2^2) + A_{1,3}R_{2,3}/R_2^2 - A_1R_{2,3}/(R_1R_2^2)\,]\, y_3 + [\, A_{1,3}/(R_1R_2^2) - A_1R_{1,3}/(R_1^2R_2^2) - A_{1,3}R_{2,3}/(R_1R_2^2) + A_1R_{1,3}R_{2,3}/(R_1^2R_2^2) - A_{1,3}/R_2^3 + A_1/(R_1R_2^3) + A_{1,3}R_{2,3}/R_2^3 - A_1R_{2,3}/(R_1R_2^3)\,]\, y_3^2$$

$$\hat{H}_{52} = h_{1,3}h_{2,3}/h_1 \cong [\, A_{1,3}A_{2,3}/A_1 - A_{2,3}/R_1 - A_{1,3}A_2/(A_1R_2) + A_2/(R_1R_2)\,] + [\, - A_{2,3}/R_1^2 + A_{2,3}R_{1,3}/R_1^2 - A_{1,3}A_{2,3}/(A_1R_2) + A_{2,3}/(R_1R_2) + A_2/(R_1^2R_2) - A_2R_{1,3}/(R_1^2R_2) + A_{1,3}A_2R_{2,3}/(A_1R_2^2) - A_2R_{2,3}/(R_1R_2^2)\,]\, y_3 + [\, - A_{2,3}/R_1^3 + A_{2,3}R_{1,3}/R_1^3 + A_{2,3}/(R_1^2R_2) - A_{2,3}R_{1,3}/(R_1^2R_2) + A_2/(R_1^3R_2) - A_2R_{1,3}/(R_1^3R_2) - A_2R_{2,3}/(R_1^2R_2^2) + A_2R_{1,3}R_{2,3}/(R_1^2R_2^2)\,]\, y_3^2$$

$$\hat{H}_{53} = h_{1,2}^2/(h_1^2h_2^2) \cong [\, A_{1,2}^2/(A_1^2A_2^2)\,] + [\, 2A_{1,2}R_{1,2}/(A_1A_2^2R_1^2) + 2A_{1,2}^2/(A_1^2A_2^2R_2)\,]\, y_3 + [\, 2A_{1,2}R_{1,2}/(A_1A_2^2R_1^3) + R_{1,2}^2/(A_2^2R_1^4) + 4A_{1,2}R_{1,2}/(A_1A_2^2R_1^2R_2) + 3A_{1,2}^2/(A_1^2A_2^2R_2^2)\,]\, y_3^2$$

$$\hat{H}_{54} = h_{1,2}/(h_1^2 h_2) \cong [\, A_{1,2}/(A_1^2 A_2) \,] + [\, A_{1,2}/(A_1^2 A_2 R_1) + R_{1,2}/(A_1 A_2 R_1^2) + A_{1,2}/(A_1^2 A_2 R_2) \,] y_3 + [\, A_{1,2}/(A_1^2 A_2 R_1^2) + 2R_{1,2}/(A_1 A_2 R_1^3) + A_{1,2}/(A_1^2 A_2 R_1 R_2) + R_{1,2}/(A_1 A_2 R_1^2 R_2) + A_{1,2}/(A_1^2 A_2 R_2^2) \,] y_3^2$$

$$\hat{H}_{55} = h_{2,1}^2/(h_1^2 h_2^2) \cong [\, A_{2,1}^2/(A_1^2 A_2^2) \,] + [\, 2A_{2,1}^2/(A_1^2 A_2^2 R_1) + 2A_{2,1} R_{2,1}/(A_1^2 A_2 R_2^2) \,] y_3 + [\, 3A_{2,1}^2/(A_1^2 A_2^2 R_1^2) + 4A_{2,1} R_{2,1}/(A_1^2 A_2 R_1 R_2^2) + 2A_{2,1} R_{2,1}/(A_1^2 A_2 R_2^3) + R_{2,1}^2/(A_1^2 R_2^4) \,] y_3^2$$

$$\hat{H}_{56} = h_{2,1}/(h_1 h_2^2) \cong [\, A_{2,1}/(A_1 A_2^2) \,] + [\, A_{2,1}/(A_1 A_2^2 R_1) + A_{2,1}/(A_1 A_2^2 R_2) + R_{2,1}/(A_1 A_2 R_2^2) \,] y_3 + [\, A_{2,1}/(A_1 A_2^2 R_1^2) + A_{2,1}/(A_1 A_2^2 R_1 R_2) + A_{2,1}/(A_1 A_2^2 R_2^2) + R_{2,1}/(A_1 A_2 R_1 R_2^2) + 2R_{2,1}/(A_1 A_2 R_2^3) \,] y_3^2$$

$$\hat{H}_{57} = h_{1,2}/(h_1 h_2^2) \cong [\, A_{1,2}/(A_1 A_2^2) \,] + [\, R_{1,2}/(A_2^2 R_1^2) + 2A_{1,2}/(A_1 A_2^2 R_2) \,] y_3 + [\, R_{1,2}/(A_2^2 R_1^3) + 2R_{1,2}/(A_2^2 R_1^2 R_2) + 3A_{1,2}/(A_1 A_2^2 R_2^2) \,] y_3^2$$

$$\hat{H}_{58} = h_{2,1}/(h_1^2 h_2) \cong [\, A_{2,1}/(A_1^2 A_2) \,] + [\, 2A_{2,1}/(A_1^2 A_2 R_1) + R_{2,1}/(A_1^2 R_2^2) \,] y_3 + [\, 3A_{2,1}/(A_1^2 A_2 R_1^2) + 2R_{2,1}/(A_1^2 R_1 R_2^2) + R_{2,1}/(A_1^2 R_2^3) \,] y_3^2$$

$$\hat{H}_{59} = h_{1,2} h_{2,1}/(h_1^2 h_2^2) \cong [\, A_{1,2} A_{2,1}/(A_1^2 A_2^2) \,] + [\, A_{1,2} A_{2,1}/(A_1^2 A_2^2 R_1) + A_{2,1} R_{1,2}/(A_1 A_2^2 R_1^2) + A_{1,2} A_{2,1}/(A_1^2 A_2^2 R_2) + A_{1,2} R_{2,1}/(A_1^2 A_2 R_2^2) \,] y_3 + [\, A_{1,2} A_{2,1}/(A_1^2 A_2^2 R_1^2) + 2A_{2,1} R_{1,2}/(A_1 A_2^2 R_1^3) + A_{1,2} A_{2,1}/(A_1^2 A_2^2 R_1 R_2) + A_{2,1} R_{1,2}/(A_1 A_2^2 R_1^2 R_2) + A_{1,2} A_{2,1}/(A_1^2 A_2^2 R_2^2) + A_{1,2} R_{2,1}/(A_1^2 A_2 R_1 R_2^2) + R_{1,2} R_{2,1}/(A_1 A_2 R_1^2 R_2^2) + 2A_{1,2} R_{2,1}/(A_1^2 A_2 R_2^3) \,] y_3^2$$

$$\hat{H}_{60} = h_{1,3} h_{2,3}/(h_1 h_2) \cong [\, A_{1,3} A_{2,3}/(A_1 A_2) - A_{2,3}/(A_2 R_1) - A_{1,3}/(A_1 R_2) + 1/(R_1 R_2) \,] + [\, -A_{2,3}/(A_2 R_1^2) + A_{2,3} R_{1,3}/(A_2 R_1^2) + 1/(R_1^2 R_2) - R_{1,3}/(R_1^2 R_2) - A_{1,3}/(A_1 R_2^2) + 1/(R_1 R_2^2) + A_{1,3} R_{2,3}/(A_1 R_2^2) - R_{2,3}/(R_1 R_2^2) \,] y_3 + [\, -A_{2,3}/(A_2 R_1^3) + A_{2,3} R_{1,3}/(A_2 R_1^3) + 1/(R_1^3 R_2) - R_{1,3}/(R_1^3 R_2) + 1/(R_1^2 R_2^2) - R_{1,3}/(R_1^2 R_2^2) - R_{2,3}/(R_1^2 R_2^2) + R_{1,3} R_{2,3}/(R_1^2 R_2^2) - A_{1,3}/(A_1 R_2^3) + 1/(R_1 R_2^3) + A_{1,3} R_{2,3}/(A_1 R_2^3) - R_{2,3}/(R_1 R_2^3) \,] y_3^2$$

Appendix B. *Strain Displacement Relations for C000/C003 Elemental Codes*

The strain displacement relations of this appendix are for the case of a circular cylindrical shell with its longitudinal axis in the y_1 direction and a radius of R_2. The y_2 coordinate is the circumferential distance $dy_2 = R_2 d\theta$. The kinematic displacement within the shell is assumed to be of the form:

$$\vec{U} = u_1\vec{e}_1 + u_2\vec{e}_2 + u_3\vec{e}_3 \tag{B.1}$$

where

$$\begin{aligned} u_1(y_1, y_2, y_3) &= u + y_3\psi_1 + k(\psi_1 + w_{,1})y_3^3 \\ u_2(y_1, y_2, y_3) &= v(1 - cy_3) + \psi_2 y_3 + k(\psi_2 + w_{,2})y_3^3 \\ u_3(y_1, y_2, y_3) &= w \end{aligned} \tag{B.2}$$

The seven degrees of freedom, $u, v, w, w_{,1}, w_{,2}, \psi_1$ and ψ_2, are functions of midsurface coordinates (y_1, y_2) only. The ψ_i are rotations of the normals and $c = 1/R_2$ and $k = -4/(3h^2)$. For this case, the 60 shell geometric functions $\hat{H}_i$ are simplified, because $h_1 = h_3 = 1$ and the quadratic terms of the expansions are neglected. The simplified nonzero functions of Appendix A are listed in Eq (B.3)

$$\begin{aligned} \hat{H}_3 &= 1 & \hat{H}_9 &= -c - c^2 y_3 \\ \hat{H}_{11} &= 1 + 2cy_3 & \hat{H}_{14} &= c^2 + 2c^3 y_3 \\ \hat{H}_{15} &= c^2 & \hat{H}_{17} &= 1 + cy_3 \\ \hat{H}_{21} &= 1 + cy_3 & \hat{H}_{18} &= 1 \\ \hat{H}_{21} &= 1 + cy_3 & \hat{H}_{23} &= -c \\ \hat{H}_{39} &= c^2 + c^3 y_3 & \hat{H}_{42} &= -c - 2c^2 y_3 \\ \hat{H}_{46} &= -c - c^2 y_3 \end{aligned} \tag{B.3}$$

The strain equations listed below are the parts of the linear and nonlinear strain components for the C000 and C003 elemental codes. Contracted notation is used, where $\varepsilon_1 = \varepsilon_{11}$, $\varepsilon_2 = \varepsilon_{22}$, $\varepsilon_3 = \varepsilon_{33}$, $\varepsilon_4 = \varepsilon_{23}$, $\varepsilon_5 = \varepsilon_{13}$, and $\varepsilon_6 = \varepsilon_{12}$. The strain components ε_i are given by

the series expansion shown in Eq (B.4).

$$\varepsilon_i = \sum_{p=0}^{n} \chi_i^p y_3^p \tag{B.4}$$

The nonzero χ_i^p are listed below for each component of the C003 nonlinear HTSD theory code. The C000 quasi-nonlinear HTSD theory is given by neglecting the nonlinear terms of χ_4^p and χ_5^p.

$$\chi_1^0 = u_{,1} + u_{,1}^2/2 + v_{,1}^2/2 + w_{,1}^2/2$$

$$\chi_1^1 = -cv_{,1}^2 + \psi_{1,1} + u_{,1}\psi_{1,1} + v_{,1}\psi_{2,1}$$

$$\chi_1^2 = c^2 v_{,1}^2/2 + \psi_{1,1}^2/2 - cv_{,1}\psi_{2,1} + \psi_{2,1}^2/2$$

$$\chi_1^3 = kw_{,11} + ku_{,1}w_{,11} + kv_{,1}w_{,12} + k\psi_{1,1} + ku_{,1}\psi_{1,1} + kv_{,1}\psi_{2,1}$$

$$\chi_1^4 = -ckv_{,1}w_{,12} + kw_{,11}\psi_{1,1} + k\psi_{1,1}^2 - ckv_{,1}\psi_{2,1} + kw_{,12}\psi_{2,1} + k\psi_{2,1}^2$$

$$\chi_1^6 = k^2 w_{,11}^2/2 + k^2 w_{,12}^2/2 + k^2 w_{,11}\psi_{1,1} + k^2\psi_{1,1}^2/2 + k^2 w_{,12}\psi_{2,1} + k^2\psi_{2,1}^2/2$$

$$\chi_2^0 = u_{,2}^2/2 + c^2 v^2/2 + v_{,2} + v_{,2}^2/2 - cw - cv_{,2}w + c^2 w^2/2 + cvw_{,2} + w_{,2}^2/2$$

$$\chi_2^1 = cu_{,2}^2 - c^2 w - c^2 v_{,2}w + c^3 w^2 + c^2 vw_{,2} + cw_{,2}^2 + u_{,2}\psi_{1.2} + \psi_{2,2} + v_{,2}\psi_{2,2} - cw\psi_{2,2} + c^2 v\psi_2 + cw_{,2}\psi_2$$

$$\chi_2^2 = -3c^4 v^2/2 - c^2 v_{,2} - 3c^2 v_{,2}^2/2 + 2c^3 v_{,2}w - 2c^3 vw_{,2} + 2cu_{,2}\psi_{1,2} + \psi_{1,2}^2/2 + c\psi_{2,2} + cv_{,2}\psi_{2,2} - 2c^2 w\psi_{2,2} + \psi_{2,2}^2/2 + c^3 v\psi_2 + 2c^2 w_{,2}\psi_2 + c^2\psi_2^2/2$$

$$\chi_2^3 = c^5 v^2 + c^3 v_{,2}^2 + ku_{,2}w_{,12} + kw_{,22} + kv_{,2}w_{,22} - ckww_{,22} + c^2 kvw_{,2} + ckw_{,2}^2 + ku_{,2}\psi_{1,2} + c\psi_{1,2}^2 + k\psi_{2,2} - 2c^2 v_{,2}\psi_{2,2} + kv_{,2}\psi_{2,2} - ckw\psi_{2,2} + c\psi_{2,2}^2 - 2c^4 v\psi_2 + c^2 kv\psi_2 + ckw_{,2}\psi_2 + c^3\psi_2^2$$

$$\chi_2^4 = 2cku_{,2}w_{,12} + ckw_{,22} + ckv_{,2}w_{,22} - 2c^2 kww_{,22} + c^3 kvw_{,2} + 2c^2 kw_{,2}^2 + 2cku_{,2}\psi_{1,2} + kw_{,12}\psi_{1,2} + k\psi_{1,2}^2 + ck\psi_{2,2} + ckv_{,2}\psi_{2,2} - 2c^2 kw\psi_{2,2} + kw_{,22}\psi_{2,2} + k\psi_{2,2}^2 + c^3 kv\psi_2 + 3c^2 kw_{,2}\psi_2 + c^2 k\psi_2^2$$

$$\chi_2^5 = -2c^2kv_{,2}w_{,22} -2c^4kvw_{,2} +2ckw_{,12}\psi_{1,2} +2ck\psi_{1,2}^2 -2c^2kv_{,2}\psi_{2,2} +2ckw_{,22}\psi_{2,2} +2ck\psi_{2,2}^2 -2c^4kv\psi_2 +2c^3kw_{,2}\psi_2 +2c^3k\psi_2^2$$

$$\chi_2^6 = k^2w_{,12}^2/2 +k^2w_{,22}^2/2 +c^2k^2w_{,2}^2/2 +k^2w_{,12}\psi_{1,2} +k^2\psi_{1,2}^2/2 +k^2w_{,22}\psi_{2,2} +k^2\psi_{2,2}^2/2 +c^2k^2w_{,2}\psi_2 +c^2k^2\psi_2^2/2$$

$$\chi_2^7 = ck^2w_{,12}^2 +ck^2w_{,22}^2 +c^3k^2w_{,2}^2 +2ck^2w_{,12}\psi_{1,2} +ck^2\psi_{1,2}^2 +2ck^2w_{,22}\psi_{2,2} +ck^2\psi_{2,2}^2 +2c^3k^2w_{,2}\psi_2 +c^3k^2\psi_2^2$$

$$\chi_4^0 = -cvv_{,2} +c^2vw +w_{,2} +u_{,2}\psi_1 +\psi_2 +v_{,2}\psi_2 -cw\psi_2$$

$$\chi_4^1 = c^3vw +cw_{,2} +cu_{,2}\psi_1 +\psi_{1,2}\psi_1 -cv\psi_{2,2} +c\psi_2 -c^2w\psi_2 +\psi_{2,2}\psi_2$$

$$\chi_4^2 = c^3vv_{,2} -3ckvv_{,2} +3c^2kvw +3ku_{,2}w_{,1} +3kw_{,2} +3kv_{,2}w_{,2} -3ckww_{,2} +6ku_{,2}\psi_1 +c\psi_{1,2}\psi_1 -c^2v\psi_{2,2} +3k\psi_2 -c^2v_{,2}\psi_2 +6kv_{,2}\psi_2 -6ckw\psi_2 +c\psi_{2,2}\psi_2$$

$$\chi_4^3 = 3c^3kvw +3cku_{,2}w_{,1} -ckvw_{,22} +ckw_{,2} -3c^2kww_{,2} +3kw_{,1}\psi_{1,2} +6cku_{,2}\psi_1 +kw_{,12}\psi_1 +7k\psi_{1,2}\psi_1 -4ckv\psi_{2,2} +3kw_{,2}\psi_{2,2} +ck\psi_2 -6c^2kw\psi_2 +kw_{,22}\psi_2 +7k\psi_{2,2}\psi_2$$

$$\chi_4^4 = 3c^3kvv_{,2} +9k^2u_{,2}w_{,1} -c^2kvw_{,22} -2c^2kw_{,2} -3c^2kv_{,2}w_{,2} +9k^2v_{,2}w_{,2} -9ck^2ww_{,2} +3ckw_{,1}\psi_{1,2} +9k^2u_{,2}\psi_1 +ckw_{,12}\psi_1 +7ck\psi_{1,2}\psi_1 -4c^2kv\psi_{2,2} +3ckw_{,2}\psi_{2,2} -2c^2k\psi_2 -6c^2kv_{,2}\psi_2 +9k^2v_{,2}\psi_2 -9ck^2w\psi_2 +ckw_{,22}\psi_2 +7ck\psi_{2,2}\psi_2$$

$$\chi_4^5 = 9ck^2u_{,2}w_{,1} +3k^2w_{,12}w_{,1} -3ck^2vw_{,22} -9c^2k^2ww_{,2} +3k^2w_{,22}w_{,2} +12k^2w_{,1}\psi_{1,2} +9ck^2u_{,2}\psi_1 +6k^2w_{,12}\psi_1 +15k^2\psi_{1,2}\psi_1 -3ck^2v\psi_{2,2} +12k^2w_{,2}\psi_{2,2} -9c^2k^2w\psi_2 +6k^2w_{,22}\psi_2 +15k^2\psi_{2,2}\psi_2$$

$$\chi_4^6 = 3ck^2w_{,12}w_{,1} -3c^2k^2vw_{,22} -9c^2k^2v_{,2}w_{,2} +3ck^2w_{,22}w_{,2} +12ck^2w_{,1}\psi_{1,2} +6ck^2w_{,12}\psi_1 +15ck^2\psi_{1,2}\psi_1 -3c^2k^2v\psi_{2,2} +12ck^2w_{,2}\psi_{2,2} -9c^2k^2v_{,2}\psi_2 +6ck^2w_{,22}\psi_2 +15ck^2\psi_{2,2}\psi_2$$

$$\chi_4^7 = 9k^3w_{,12}w_{,1} +9k^3w_{,22}w_{,2} +9k^3w_{,1}\psi_{1,2} +9k^3w_{,12}\psi_1 +9k^3\psi_{1,2}\psi_1 +9k^3w_{,2}\psi_{2,2} +9k^3w_{,22}\psi_2 +9k^3\psi_{2,2}\psi_2$$

$$\chi_4^8 = 9ck^3w_{,12}w_{,1} +9ck^3w_{,22}w_{,2} +9ck^3w_{,1}\psi_{1,2} +9ck^3w_{,12}\psi_1 +9ck^3\psi_{1,2}\psi_1 +9ck^3w_{,2}\psi_{2,2} +9ck^3w_{,22}\psi_2 +9ck^3\psi_{2,2}\psi_2$$

$$\chi_5^0 = -cvv_{,1} +w_{,1} +\psi_1 +u_{,1}\psi_1 +v_{,1}\psi_2$$

$$\chi_5^1 = c^2vv_{,1} +\psi_{1,1}\psi_1 -cv\psi_{2,1} -cv_{,1}\psi_2 +\psi_{2,1}\psi_2$$

$$\chi_5^2 = -3ckvv_{,1} +3kw_{,1} +3ku_{,1}w_{,1} +3kv_{,1}w_{,2} +3k\psi_1 +6ku_{,1}\psi_1 +6kv_{,1}\psi_2$$

$$\chi_5^3 = 3c^2kvv_{,1} -ckvw_{,12} -3ckv_{,1}w_{,2} +3kw_{,1}\psi_{1,1} +kw_{,11}\psi_1 +7k\psi_{1,1}\psi_1 -4ckv\psi_{2,1} +3kw_{,2}\psi_{2,1} -6ckv_{,1}\psi_2 +kw_{,12}\psi_2 +7k\psi_{2,1}\psi_2$$

$$\chi_5^4 = 9k^2u_{,1}w_{,1} +9k^2v_{,1}w_{,2} +9k^2u_{,1}\psi_1 +9k^2v_{,1}\psi_2$$

$$\chi_5^5 = -3ck^2vw_{,12} +3k^2w_{,11}w_{,1} -9ck^2v_{,1}w_{,2} +3k^2w_{,12}w_{,2} +12k^2w_{,1}\psi_{1,1} +6k^2w_{,11}\psi_1 +15k^2\psi_{1,1}\psi_1 -3ck^2v\psi_{2,1} +12k^2w_{,2}\psi_{2,1} -9ck^2v_{,1}\psi_2 +6k^2w_{,12}\psi_2 +15k^2\psi_{2,1}\psi_2$$

$$\chi_5^7 = 9k^3w_{,11}w_{,1} +9k^3w_{,12}w_{,2} +9k^3w_{,1}\psi_{1,1} +9k^3w_{,11}\psi_1 +9k^3\psi_{1,1}\psi_1 +9k^3w_{,2}\psi_{2,1} +9k^3w_{,12}\psi_2 +9k^3\psi_{2,1}\psi_2$$

$$\chi_6^0 = u_{,2} +u_{,1}u_{,2} +v_{,1} +v_{,1}v_{,2} -cv_{,1}w +cvw_{,1} +w_{,1}w_{,2}$$

$$\chi_6^1 = cu_{,2} +cu_{,1}u_{,2} -cv_{,1} -cv_{,1}v_{,2} +cw_{,1}w_{,2} +u_{,2}\psi_{1,1} +\psi_{1,2} +u_{,1}\psi_{1,2} +\psi_{2,1} +v_{,2}\psi_{2,1} -cw\psi_{2,1} +v_{,1}\psi_{2,2} +cw_{,1}\psi_2$$

$$\chi_6^2 = -c^2v_{,1}v_{,2} +c^3v_{,1}w -c^3vw_{,1} +cu_{,2}\psi_{1,1} +c\psi_{1,2} +cu_{,1}\psi_{1,2} +\psi_{1,1}\psi_{1,2} -c^2w\psi_{2,1} +\psi_{2,1}\psi_{2,2} +c^2w_{,1}\psi_2$$

$$\chi_6^3 = c^3v_{,1}v_{,2} +ku_{,2}w_{,11} +2kw_{,12} +ku_{,1}w_{,12} +kv_{,2}w_{,12} -ckww_{,12} +kv_{,1}w_{,22} +ckw_{,1}w_{,2} +ku_{,2}\psi_{1,1} +k\psi_{1,2} +ku_{,1}\psi_{1,2} +c\psi_{1,1}\psi_{1,2} +k\psi_{2,1} -c^2v_{,2}\psi_{2,1} +kv_{,2}\psi_{2,1} -ckw\psi_{2,1} -c^2v_{,1}\psi_{2,2} +kv_{,1}\psi_{2,2} +c\psi_{2,1}\psi_{2,2} +ckw_{,1}\psi_2$$

$$\chi_6^4 = cku_{,2}w_{,11} + ckw_{,12} + cku_{,1}w_{,12} - c^2kww_{,12} + c^2kw_{,1}w_{,2} + cku_{,2}\psi_{1,1} + kw_{,12}\psi_{1,1} + ck\psi_{1,2} + cku_{,1}\psi_{1,2} + kw_{,11}\psi_{1,2} + 2k\psi_{1,1}\psi_{1,2} - c^2kw\psi_{2,1} + kw_{,22}\psi_{2,1} + kw_{,12}\psi_{2,2} + 2k\psi_{2,1}\psi_{2,2} + c^2kw_{,1}\psi_2$$

$$\chi_6^5 = -c^2kv_{,2}w_{,12} - c^2kv_{,1}w_{,22} + ckw_{,12}\psi_{1,1} + ckw_{,11}\psi_{1,2} + 2ck\psi_{1,1}\psi_{1,2} - c^2kv_{,2}\psi_{2,1} + ckw_{,22}\psi_{2,1} - c^2kv_{,1}\psi_{2,2} + ckw_{,12}\psi_{2,2} + 2ck\psi_{2,1}\psi_{2,2}$$

$$\chi_6^6 = k^2w_{,11}w_{,12} + k^2w_{,12}w_{,22} + k^2w_{,12}\psi_{1,1} + k^2w_{,11}\psi_{1,2} + k^2\psi_{1,1}\psi_{1,2} + k^2w_{,22}\psi_{2,1} + k^2w_{,12}\psi_{2,2} + k^2\psi_{2,1}\psi_{2,2}$$

$$\chi_6^7 = ck^2w_{,11}w_{,12} + ck^2w_{,12}w_{,22} + ck^2w_{,12}\psi_{1,1} + ck^2w_{,11}\psi_{1,2} + ck^2\psi_{1,1}\psi_{1,2} + ck^2w_{,22}\psi_{2,1} + ck^2w_{,12}\psi_{2,2} + ck^2\psi_{2,1}\psi_{2,2}$$

Appendix C. *Strain Displacement Relations for C020/C023 Elemental Codes*

The strain displacement relations of this appendix are for the case of a circular cylindrical shell with its longitudinal axis in the y_1 direction and a radius of R_2 . The y_2 coordinate is the circumferential distance $dy_2 = R_2 d\theta$. The kinematic displacement within the shell is assumed to be of the form:

$$\vec{U} = u_1\vec{e}_1 + u_2\vec{e}_2 + u_3\vec{e}_3 \tag{C.1}$$

where

$$\begin{aligned} u_1(y_1, y_2, y_3) &= u + y_3\psi_1 + k(\psi_1 + w_{,1})y_3^3 \\ u_2(y_1, y_2, y_3) &= v(1 - cy_3) + \psi_2 y_3 + k(\psi_2 + w_{,2})y_3^3 \\ u_3(y_1, y_2, y_3) &= w \end{aligned} \tag{C.2}$$

The seven degrees of freedom $u, v, w, w_{,1}, w_{,2}, \psi_1$ and ψ_2, are functions of midsurface coordinates (y_1, y_2) only. The ψ_i are rotations of the normals and $c = 1/R_2$ and $k = -4/(3h^2)$. For this case, the 60 shell geometric functions $\hat{H}_i$ are quadratic in order and are simplified because $h_1 = h_3 = 1$. The simplified nonzero functions of Appendix A are listed in Eq (C.3)

$$\begin{aligned} \hat{H}_3 &= 1 & \hat{H}_9 &= -c - c^2y_3 - c^3y_3^2 \\ \hat{H}_{11} &= 1 + 2cy_3 + 3c^2y_3^2 & \hat{H}_{14} &= c^2 + 2c^3y_3 + 3c^4y_3^2 \\ \hat{H}_{15} &= c^2 & \hat{H}_{17} &= 1 + cy_3 + c^2y_3^2 \\ \hat{H}_{21} &= 1 + cy_3 + c^2y_3^2 & \hat{H}_{18} &= 1 \\ \hat{H}_{21} &= 1 + cy_3 + c^2y_3^2 & \hat{H}_{23} &= -c \\ \hat{H}_{39} &= c^2 + c^3y_3 + c^4y_3^2 & \hat{H}_{42} &= -c - 2c^2y_3 - 3c^3y_3^2 \\ \hat{H}_{46} &= -c - c^2y_3 - c^3y_3^2 \end{aligned} \tag{C.3}$$

The strain equations listed below are the parts of the linear and nonlinear strain components for the C020 and C023 elemental codes. Contracted notation is used, where $\varepsilon_1 = \varepsilon_{11}$, $\varepsilon_2 = \varepsilon_{22}$, $\varepsilon_3 = \varepsilon_{33}$, $\varepsilon_4 = \varepsilon_{23}$, $\varepsilon_5 = \varepsilon_{13}$, and $\varepsilon_6 = \varepsilon_{12}$. The strain components ε_i are given by the series expansion shown in Eq (C.4).

$$\varepsilon_i = \sum_{p=0}^{n} \chi_i^p y_3^p \tag{C.4}$$

The nonzero χ_i^p are listed below for each component of the nonlinear C023 elemental code. The C020 quasi-nonlinear HTSD theory is given by neglecting the nonlinear terms of χ_4^p and χ_5^p.

$$\chi_1^0 = u_{,1} + u_{,1}^2/2 + v_{,1}^2/2 + w_{,1}^2/2$$

$$\chi_1^1 = -cv_{,1}^2 + \psi_{1,1} + u_{,1}\psi_{1,1} + v_{,1}\psi_{2,1}$$

$$\chi_1^2 = c^2v_{,1}^2/2 + \psi_{1,1}^2/2 - cv_{,1}\psi_{2,1} + \psi_{2,1}^2/2$$

$$\chi_1^3 = kw_{,11} + ku_{,1}w_{,11} + kv_{,1}w_{,12} + k\psi_{1,1} + ku_{,1}\psi_{1,1} + kv_{,1}\psi_{2,1}$$

$$\chi_1^4 = -ckv_{,1}w_{,12} + kw_{,11}\psi_{1,1} + k\psi_{1,1}^2 - ckv_{,1}\psi_{2,1} + kw_{,12}\psi_{2,1} + k\psi_{2,1}^2$$

$$\chi_1^6 = k^2w_{,11}^2/2 + k^2w_{,12}^2/2 + k^2w_{,11}\psi_{1,1} + k^2\psi_{1,1}^2/2 + k^2w_{,12}\psi_{2,1} + k^2\psi_{2,1}^2/2$$

$$\chi_2^0 = u_{,2}^2/2 + c^2v^2/2 + v_{,2} + v_{,2}^2/2 - cw - cv_{,2}w + c^2w^2/2 + cvw_{,2} + w_{,2}^2/2$$

$$\chi_2^1 = cu_{,2}^2 - c^2w - c^2v_{,2}w + c^3w^2 + c^2vw_{,2} + cw_{,2}^2 + u_{,2}\psi_{1,2} + \psi_{2,2} + v_{,2}\psi_{2,2} - cw\psi_{2,2} + c^2v\psi_2 + cw_{,2}\psi_2$$

$$\chi_2^2 = 3c^2u_{,2}^2/2 - c^3w - c^3v_{,2}w + 3c^4w^2/2 + c^3vw_{,2} + 3c^2w_{,2}^2/2 + 2cu_{,2}\psi_{1,2} + \psi_{1,2}^2/2 + c\psi_{2,2} + cv_{,2}\psi_{2,2} - 2c^2w\psi_{2,2} + \psi_{2,2}^2/2 + c^3v\psi_2 + 2c^2w_{,2}\psi_2 + c^2\psi_2^2/2$$

$$\chi_2^3 = -2c^5v^2 - c^3v_{,2} - 2c^3v_{,2}^2 + 3c^4v_{,2}w + ku_{,2}w_{,12} + kw_{,22} + kv_{,2}w_{,22} - ckww_{,22} - 3c^4vw_{,2} + c^2kvw_{,2} + ckw_{,2}^2 + 3c^2u_{,2}\psi_{1,2} + ku_{,2}\psi_{1,2} + c\psi_{1,2}^2 + c^2\psi_{2,2} + k\psi_{2,2} + c^2v_{,2}\psi_{2,2} + kv_{,2}\psi_{2,2} - 3c^3w\psi_{2,2} - ckw\psi_{2,2} + c\psi_{2,2}^2 + c^4v\psi_2 + c^2kv\psi_2 + 3c^3w_{,2}\psi_2 + ckw_{,2}\psi_2 + c^3\psi_2^2$$

$$\chi_2^4 = 3c^6v^2/2 + 3c^4v_{,2}^2/2 + 2cku_{,2}w_{,12} + ckw_{,22} + ckv_{,2}w_{,22} - 2c^2kww_{,22} + c^3kvw_{,2} + 2c^2kw_{,2}^2 + 2cku_{,2}\psi_{1,2} + kw_{,12}\psi_{1,2} + 3c^2\psi_{1,2}^2/2 + k\psi_{1,2}^2 + ck\psi_{2,2} - 3c^3v_{,2}\psi_{2,2} + ckv_{,2}\psi_{2,2} - 2c^2kw\psi_{2,2} + kw_{,22}\psi_{2,2} + 3c^2\psi_{2,2}^2/2 + k\psi_{2,2}^2 - 3c^5v\psi_2 + c^3kv\psi_2 + 3c^2kw_{,2}\psi_2 + 3c^4\psi_2^2/2 + c^2k\psi_2^2$$

$$\chi_2^5 = 3c^2ku_{,2}w_{,12} + c^2kw_{,22} + c^2kv_{,2}w_{,22} - 3c^3kww_{,22} + c^4kvw_{,2} + 3c^3kw_{,2}^2 + 3c^2ku_{,2}\psi_{1,2}$$
$$+ 2ckw_{,12}\psi_{1,2} + 2ck\psi_{1,2}^2 + c^2k\psi_{2,2} + c^2kv_{,2}\psi_{2,2} - 3c^3kw\psi_{2,2} + 2ckw_{,22}\psi_{2,2} + 2ck\psi_{2,2}^2$$
$$+ c^4kv\psi_2 + 5c^3kw_{,2}\psi_2 + 2c^3k\psi_2^2$$

$$\chi_2^6 = k^2w_{,12}^2/2 - 3c^3kv_{,2}w_{,22} + k^2w_{,22}^2/2 - 3c^5kvw_{,2} + c^2k^2w_{,2}^2/2 + 3c^2kw_{,12}\psi_{1,2}$$
$$+ k^2w_{,12}\psi_{1,2} + 3c^2k\psi_{1,2}^2 + k^2\psi_{1,2}^2/2 - 3c^3kv_{,2}\psi_{2,2} + 3c^2kw_{,22}\psi_{2,2} + k^2w_{,22}\psi_{2,2} + 3c^2k\psi_{2,2}^2$$
$$+ k^2\psi_{2,2}^2/2 - 3c^5kv\psi_2 + 3c^4kw_{,2}\psi_2 + c^2k^2w_{,2}\psi_2 + 3c^4k\psi_2^2 + c^2k^2\psi_2^2/2$$

$$\chi_2^7 = ck^2w_{,12}^2 + ck^2w_{,22}^2 + c^3k^2w_{,2}^2 + 2ck^2w_{,12}\psi_{1,2} + ck^2\psi_{1,2}^2 + 2ck^2w_{,22}\psi_{2,2} + ck^2\psi_{2,2}^2$$
$$+ 2c^3k^2w_{,2}\psi_2 + c^3k^2\psi_2^2$$

$$\chi_2^8 = 3c^2k^2w_{,12}^2/2 + 3c^2k^2w_{,22}^2/2 + 3c^4k^2w_{,2}^2/2 + 3c^2k^2w_{,12}\psi_{1,2} + 3c^2k^2\psi_{1,2}^2/2$$
$$+ 3c^2k^2w_{,22}\psi_{2,2} + 3c^2k^2\psi_{2,2}^2/2 + 3c^4k^2w_{,2}\psi_2 + 3c^4k^2\psi_2^2/2$$

$$\chi_4^0 = -cvv_{,2} + c^2vw + w_{,2} + u_{,2}\psi_1 + \psi_2 + v_{,2}\psi_2 - cw\psi_2$$

$$\chi_4^1 = c^3vw + cw_{,2} + cu_{,2}\psi_1 + \psi_{1,2}\psi_1 - cv\psi_{2,2} + c\psi_2 - c^2w\psi_2 + \psi_{2,2}\psi_2$$

$$\chi_4^2 = -3ckvv_{,2} + c^4vw + 3c^2kvw + 3ku_{,2}w_{,1} + c^2w_{,2} + 3kw_{,2} + 3kv_{,2}w_{,2} - 3ckww_{,2} + c^2u_{,2}\psi_1$$
$$+ 6ku_{,2}\psi_1 + c\psi_{1,2}\psi_1 - c^2v\psi_{2,2} + c^2\psi_2 + 3k\psi_2 + 6kv_{,2}\psi_2 - c^3w\psi_2 - 6ckw\psi_2 + c\psi_{2,2}\psi_2$$

$$\chi_4^3 = c^4vv_{,2} + 3c^3kvw + 3cku_{,2}w_{,1} - ckvw_{,22} + ckw_{,2} - 3c^2kww_{,2} + 3kw_{,1}\psi_{1,2} + 6cku_{,2}\psi_1$$
$$+ kw_{,12}\psi_1 + c^2\psi_{1,2}\psi_1 + 7k\psi_{1,2}\psi_1 - c^3v\psi_{2,2} - 4ckv\psi_{2,2} + 3kw_{,2}\psi_{2,2} + ck\psi_2 - c^3v_{,2}\psi_2$$
$$- 6c^2kw\psi_2 + kw_{,22}\psi_2 + c^2\psi_{2,2}\psi_2 + 7k\psi_{2,2}\psi_2$$

$$\chi_4^4 = 3c^4kvw + 3c^2ku_{,2}w_{,1} + 9k^2u_{,2}w_{,1} - c^2kvw_{,22} + c^2kw_{,2} + 9k^2v_{,2}w_{,2} - 3c^3kww_{,2}$$
$$- 9ck^2ww_{,2} + 3ckw_{,1}\psi_{1,2} + 6c^2ku_{,2}\psi_1 + 9k^2u_{,2}\psi_1 + ckw_{,12}\psi_1 + 7ck\psi_{1,2}\psi_1 - 4c^2kv\psi_{2,2}$$
$$+ 3ckw_{,2}\psi_{2,2} + c^2k\psi_2 + 9k^2v_{,2}\psi_2 - 6c^3kw\psi_2 - 9ck^2w\psi_2 + ckw_{,22}\psi_2 + 7ck\psi_{2,2}\psi_2$$

$$\chi_4^5 = 3c^4kvv_{,2} + 9ck^2u_{,2}w_{,1} + 3k^2w_{,12}w_{,1} - c^3kvw_{,22} - 3ck^2vw_{,22} - 2c^3kw_{,2} - 3c^3kv_{,2}w_{,2}$$
$$- 9c^2k^2ww_{,2} + 3k^2w_{,22}w_{,2} + 3c^2kw_{,1}\psi_{1,2} + 12k^2w_{,1}\psi_{1,2} + 9ck^2u_{,2}\psi_1 + c^2kw_{,12}\psi_1 + 6k^2w_{,12}\psi_1$$
$$+ 7c^2k\psi_{1,2}\psi_1 + 15k^2\psi_{1,2}\psi_1 - 4c^3kv\psi_{2,2} - 3ck^2v\psi_{2,2} + 3c^2kw_{,2}\psi_{2,2} + 12k^2w_{,2}\psi_{2,2} - 2c^3k\psi_2$$
$$- 6c^3kv_{,2}\psi_2 - 9c^2k^2w\psi_2 + c^2kw_{,22}\psi_2 + 6k^2w_{,22}\psi_2 + 7c^2k\psi_{2,2}\psi_2 + 15k^2\psi_{2,2}\psi_2$$

$$\chi_4^6 = 9c^2k^2u_{,2}w_{,1} +3ck^2w_{,12}w_{,1} -3c^2k^2vw_{,22} -9c^3k^2ww_{,2} +3ck^2w_{,22}w_{,2} +12ck^2w_{,1}\psi_{1,2} +9c^2k^2u_{,2}\psi_1 +6ck^2w_{,12}\psi_1 +15ck^2\psi_{1,2}\psi_1 -3c^2k^2v\psi_{2,2} +12ck^2w_{,2}\psi_{2,2} -9c^3k^2w\psi_2 +6ck^2w_{,22}\psi_2 +15ck^2\psi_{2,2}\psi_2$$

$$\chi_4^7 = 3c^2k^2w_{,12}w_{,1} +9k^3w_{,12}w_{,1} -3c^3k^2vw_{,22} -9c^3k^2v_{,2}w_{,2} +3c^2k^2w_{,22}w_{,2} +9k^3w_{,22}w_{,2} +12c^2k^2w_{,1}\psi_{1,2} +9k^3w_{,1}\psi_{1,2} +6c^2k^2w_{,12}\psi_1 +9k^3w_{,12}\psi_1 +15c^2k^2\psi_{1,2}\psi_1 +9k^3\psi_{1,2}\psi_1 -3c^3k^2v\psi_{2,2} +12c^2k^2w_{,2}\psi_{2,2} +9k^3w_{,2}\psi_{2,2} -9c^3k^2v_{,2}\psi_2 +6c^2k^2w_{,22}\psi_2 +9k^3w_{,22}\psi_2 +15c^2k^2\psi_{2,2}\psi_2 +9k^3\psi_{2,2}\psi_2$$

$$\chi_4^8 = 9ck^3w_{,12}w_{,1} +9ck^3w_{,22}w_{,2} +9ck^3w_{,1}\psi_{1,2} +9ck^3w_{,12}\psi_1 +9ck^3\psi_{1,2}\psi_1 +9ck^3w_{,2}\psi_{2,2} +9ck^3w_{,22}\psi_2 +9ck^3\psi_{2,2}\psi_2$$

$$\chi_4^9 = 9c^2k^3w_{,12}w_{,1} +9c^2k^3w_{,22}w_{,2} +9c^2k^3w_{,1}\psi_{1,2} +9c^2k^3w_{,12}\psi_1 +9c^2k^3\psi_{1,2}\psi_1 +9c^2k^3w_{,2}\psi_{2,2} +9c^2k^3w_{,22}\psi_2 +9c^2k^3\psi_{2,2}\psi_2$$

$$\chi_5^0 = -cvv_{,1} +w_{,1} +\psi_1 +u_{,1}\psi_1 +v_{,1}\psi_2$$

$$\chi_5^1 = c^2vv_{,1} +\psi_{1,1}\psi_1 -cv\psi_{2,1} -cv_{,1}\psi_2 +\psi_{2,1}\psi_2$$

$$\chi_5^2 = -3ckvv_{,1} +3kw_{,1} +3ku_{,1}w_{,1} +3kv_{,1}w_{,2} +3k\psi_1 +6ku_{,1}\psi_1 +6kv_{,1}\psi_2$$

$$\chi_5^3 = 3c^2kvv_{,1} -ckvw_{,12} -3ckv_{,1}w_{,2} +3kw_{,1}\psi_{1,1} +kw_{,11}\psi_1 +7k\psi_{1,1}\psi_1 -4ckv\psi_{2,1} +3kw_{,2}\psi_{2,1} -6ckv_{,1}\psi_2 +kw_{,12}\psi_2 +7k\psi_{2,1}\psi_2$$

$$\chi_5^4 = 9k^2u_{,1}w_{,1} +9k^2v_{,1}w_{,2} +9k^2u_{,1}\psi_1 +9k^2v_{,1}\psi_2$$

$$\chi_5^5 = -3ck^2vw_{,12} +3k^2w_{,11}w_{,1} -9ck^2v_{,1}w_{,2} +3k^2w_{,12}w_{,2} +12k^2w_{,1}\psi_{1,1} +6k^2w_{,11}\psi_1 +15k^2\psi_{1,1}\psi_1 -3ck^2v\psi_{2,1} +12k^2w_{,2}\psi_{2,1} -9ck^2v_{,1}\psi_2 +6k^2w_{,12}\psi_2 +15k^2\psi_{2,1}\psi_2$$

$$\chi_5^7 = 9k^3w_{,11}w_{,1} +9k^3w_{,12}w_{,2} +9k^3w_{,1}\psi_{1,1} +9k^3w_{,11}\psi_1 +9k^3\psi_{1,1}\psi_1 +9k^3w_{,2}\psi_{2,1} +9k^3w_{,12}\psi_2 +9k^3\psi_{2,1}\psi_2$$

$$\chi_6^0 = u_{,2} +u_{,1}u_{,2} +v_{,1} +v_{,1}v_{,2} -cv_{,1}w +cvw_{,1} +w_{,1}w_{,2}$$

$$\chi_6^1 = cu_{,2} + cu_{,1}u_{,2} - cv_{,1} - cv_{,1}v_{,2} + cw_{,1}w_{,2} + u_{,2}\psi_{1,1} + \psi_{1,2} + u_{,1}\psi_{1,2} + \psi_{2,1} + v_{,2}\psi_{2,1} - cw\psi_{2,1} + v_{,1}\psi_{2,2} + cw_{,1}\psi_2$$

$$\chi_6^2 = c^2u_{,2} + c^2u_{,1}u_{,2} + c^2w_{,1}w_{,2} + cu_{,2}\psi_{1,1} + c\psi_{1,2} + cu_{,1}\psi_{1,2} + \psi_{1,1}\psi_{1,2} - c^2w\psi_{2,1} + \psi_{2,1}\psi_{2,2} + c^2w_{,1}\psi_2$$

$$\chi_6^3 = -c^3v_{,1}v_{,2} + c^4v_{,1}w + ku_{,2}w_{,11} + 2kw_{,12} + ku_{,1}w_{,12} + kv_{,2}w_{,12} - ckww_{,12} - c^4vw_{,1} + kv_{,1}w_{,22} + ckw_{,1}w_{,2} + c^2u_{,2}\psi_{1,1} + ku_{,2}\psi_{1,1} + c^2\psi_{1,2} + k\psi_{1,2} + c^2u_{,1}\psi_{1,2} + ku_{,1}\psi_{1,2} + c\psi_{1,1}\psi_{1,2} + k\psi_{2,1} + kv_{,2}\psi_{2,1} - c^3w\psi_{2,1} - ckw\psi_{2,1} + kv_{,1}\psi_{2,2} + c\psi_{2,1}\psi_{2,2} + c^3w_{,1}\psi_2 + ckw_{,1}\psi_2$$

$$\chi_6^4 = c^4v_{,1}v_{,2} + cku_{,2}w_{,11} + ckw_{,12} + cku_{,1}w_{,12} - c^2kww_{,12} + c^2kw_{,1}w_{,2} + cku_{,2}\psi_{1,1} + kw_{,12}\psi_{1,1} + ck\psi_{1,2} + cku_{,1}\psi_{1,2} + kw_{,11}\psi_{1,2} + c^2\psi_{1,1}\psi_{1,2} + 2k\psi_{1,1}\psi_{1,2} - c^3v_{,2}\psi_{2,1} - c^2kw\psi_{2,1} + kw_{,22}\psi_{2,1} - c^3v_{,1}\psi_{2,2} + kw_{,12}\psi_{2,2} + c^2\psi_{2,1}\psi_{2,2} + 2k\psi_{2,1}\psi_{2,2} + c^2kw_{,1}\psi_2$$

$$\chi_6^5 = c^2ku_{,2}w_{,11} + c^2kw_{,12} + c^2ku_{,1}w_{,12} - c^3kww_{,12} + c^3kw_{,1}w_{,2} + c^2ku_{,2}\psi_{1,1} + ckw_{,12}\psi_{1,1} + c^2k\psi_{1,2} + c^2ku_{,1}\psi_{1,2} + ckw_{,11}\psi_{1,2} + 2ck\psi_{1,1}\psi_{1,2} - c^3kw\psi_{2,1} + ckw_{,22}\psi_{2,1} + ckw_{,12}\psi_{2,2} + 2ck\psi_{2,1}\psi_{2,2} + c^3kw_{,1}\psi_2$$

$$\chi_6^6 = -c^3kv_{,2}w_{,12} + k^2w_{,11}w_{,12} - c^3kv_{,1}w_{,22} + k^2w_{,12}w_{,22} + c^2kw_{,12}\psi_{1,1} + k^2w_{,12}\psi_{1,1} + c^2kw_{,11}\psi_{1,2} + k^2w_{,11}\psi_{1,2} + 2c^2k\psi_{1,1}\psi_{1,2} + k^2\psi_{1,1}\psi_{1,2} - c^3kv_{,2}\psi_{2,1} + c^2kw_{,22}\psi_{2,1} + k^2w_{,22}\psi_{2,1} - c^3kv_{,1}\psi_{2,2} + c^2kw_{,12}\psi_{2,2} + k^2w_{,12}\psi_{2,2} + 2c^2k\psi_{2,1}\psi_{2,2} + k^2\psi_{2,1}\psi_{2,2}$$

$$\chi_6^7 = ck^2w_{,11}w_{,12} + ck^2w_{,12}w_{,22} + ck^2w_{,12}\psi_{1,1} + ck^2w_{,11}\psi_{1,2} + ck^2\psi_{1,1}\psi_{1,2} + ck^2w_{,22}\psi_{2,1} + ck^2w_{,12}\psi_{2,2} + ck^2\psi_{2,1}\psi_{2,2}$$

$$\chi_6^8 = c^2k^2w_{,11}w_{,12} + c^2k^2w_{,12}w_{,22} + c^2k^2w_{,12}\psi_{1,1} + c^2k^2w_{,11}\psi_{1,2} + c^2k^2\psi_{1,1}\psi_{1,2} + c^2k^2w_{,22}\psi_{2,1} + c^2k^2w_{,12}\psi_{2,2} + c^2k^2\psi_{2,1}\psi_{2,2}$$

Appendix D. *Strain Displacement Relations for C100/C103 Elemental Codes*

The strain displacement relations of this appendix are for the case of a circular cylindrical shell with its longitudinal axis in the y_1 direction and a radius of R_2 . The y_2 coordinate is the circumferential distance $dy_2 = R_2 d\theta$. The kinematic displacement within the shell is assumed to be of the form:

$$\vec{U} = u_1\vec{e}_1 + u_2\vec{e}_2 + u_3\vec{e}_3 \tag{D.1}$$

where

$$\begin{aligned} u_1(y_1, y_2, y_3) &= u + y_3\psi_1 + k(\psi_1 + w_{,1})y_3^3 \\ u_2(y_1, y_2, y_3) &= v(1 - cy_3) + \psi_2 y_3(\psi_2 + w_{,2})\left[-c + ky_3 - cky_3^2\right] y_3^2 \\ u_3(y_1, y_2, y_3) &= w \end{aligned} \tag{D.2}$$

The seven degrees of freedom $u, v, w, w_{,1}, w_{,2}, \psi_1$ and ψ_2, are functions of midsurface coordinates (y_1, y_2) only. The ψ_i are rotations of the normals and $c = 1/R_2$ and $k = -4/(3h^2)$. For this case, the 60 shell geometric functions $\hat{H}_i$ are simplified because $h_1 = h_3 = 1$ and the quadratic terms of the expansions are neglected. The simplified nonzero functions of Appendix A are listed in Eq (D.3)

$$\begin{aligned} \hat{H}_3 &= 1 & \hat{H}_9 &= -c - c^2 y_3 \\ \hat{H}_{11} &= 1 + 2cy_3 & \hat{H}_{14} &= c^2 + 2c^3 y_3 \\ \hat{H}_{15} &= c^2 & \hat{H}_{17} &= 1 + cy_3 \\ \hat{H}_{21} &= 1 + cy_3 & \hat{H}_{18} &= 1 \\ \hat{H}_{21} &= 1 + cy_3 & \hat{H}_{23} &= -c \\ \hat{H}_{39} &= c^2 + c^3 y_3 & \hat{H}_{42} &= -c - 2c^2 y_3 \\ \hat{H}_{46} &= -c - c^2 y_3 \end{aligned} \tag{D.3}$$

The strain equations listed below are the parts of the linear and nonlinear strain components for the C100 and C103 elemental codes. Contracted notation is used, where $\varepsilon_1 = \varepsilon_{11}$, $\varepsilon_2 = \varepsilon_{22}, \varepsilon_3 = \varepsilon_{33}, \varepsilon_4 = \varepsilon_{23}, \varepsilon_5 = \varepsilon_{13}$, and $\varepsilon_6 = \varepsilon_{12}$. The strain components ε_i are given by

the series expansion shown in Eq (D.4).

$$\varepsilon_i = \sum_{p=0}^{n} \chi_i^p y_3^p \tag{D.4}$$

The nonzero χ_i^p are listed below for each component of the nonlinear C103 code. The C100 quasi-nonlinear theory components are the same except for neglect of all nonlinear terms of the χ_4^p and χ_5^p strain components.

$$\chi_1^0 = u_{,1} + u_{,1}^2/2 + v_{,1}^2/2 + w_{,1}^2/2$$

$$\chi_1^1 = -cv_{,1}^2 + \psi_{1,1} + u_{,1}\psi_{1,1} + v_{,1}\psi_{2,1}$$

$$\chi_1^2 = c^2 v_{,1}^2/2 - cv_{,1}w_{,12} + \psi_{1,1}^2/2 - 2cv_{,1}\psi_{2,1} + \psi_{2,1}^2/2$$

$$\chi_1^3 = kw_{,11} + ku_{,1}w_{,11} + c^2 v_{,1}w_{,12} + kv_{,1}w_{,12} + k\psi_{1,1} + ku_{,1}\psi_{1,1} + c^2 v_{,1}\psi_{2,1} + kv_{,1}\psi_{2,1} - cw_{,12}\psi_{2,1} - c\psi_{2,1}^2$$

$$\chi_1^4 = -2ckv_{,1}w_{,12} + c^2 w_{,12}^2/2 + kw_{,11}\psi_{1,1} + k\psi_{1,1}^2 - 2ckv_{,1}\psi_{2,1} + c^2 w_{,12}\psi_{2,1} + kw_{,12}\psi_{2,1} + c^2\psi_{2,1}^2/2 + k\psi_{2,1}^2$$

$$\chi_1^5 = c^2 kv_{,1}w_{,12} - ckw_{,12}^2 + c^2 kv_{,1}\psi_{2,1} - 3ckw_{,12}\psi_{2,1} - 2ck\psi_{2,1}^2$$

$$\chi_1^6 = k^2 w_{,11}^2/2 + c^2 kw_{,12}^2 + k^2 w_{,12}^2/2 + k^2 w_{,11}\psi_{1,1} + k^2\psi_{1,1}^2/2 + 2c^2 kw_{,12}\psi_{2,1} + k^2 w_{,12}\psi_{2,1} + c^2 k\psi_{2,1}^2 + k^2\psi_{2,1}^2/2$$

$$\chi_1^7 = -ck^2 w_{,12}^2 - 2ck^2 w_{,12}\psi_{2,1} - ck^2\psi_{2,1}^2$$

$$\chi_1^8 = c^2 k^2 w_{,12}^2/2 + c^2 k^2 w_{,12}\psi_{2,1} + c^2 k^2\psi_{2,1}^2/2$$

$$\chi_2^0 = u_{,2}^2/2 + c^2 v^2/2 + v_{,2} + v_{,2}^2/2 - cw - cv_{,2}w + c^2 w^2/2 + cvw_{,2} + w_{,2}^2/2$$

$$\chi_2^1 = cu_{,2}^2 - c^2 w - c^2 v_{,2}w + c^3 w^2 + c^2 vw_{,2} + cw_{,2}^2 + u_{,2}\psi_{1,2} + \psi_{2,2} + v_{,2}\psi_{2,2} - cw\psi_{2,2} + c^2 v\psi_2 + cw_{,2}\psi_2$$

$$\chi_2^2 = -3c^4v^2/2 - c^2v_{,2} - 3c^2v_{,2}^2/2 + 2c^3v_{,2}w - cw_{,22} - cv_{,2}w_{,22} + c^2ww_{,22} - 3c^3vw_{,2} - c^2w_{,2}^2 + 2cu_{,2}\psi_{1,2} + \psi_{1,2}^2/2 - c^2w\psi_{2,2} + \psi_{2,2}^2/2 + c^2w_{,2}\psi_2 + c^2\psi_2^2/2$$

$$\chi_2^3 = c^5v^2 + c^3v_{,2}^2 + ku_{,2}w_{,12} - c^2w_{,22} + kw_{,22} - c^2v_{,2}w_{,22} + kv_{,2}w_{,22} + 2c^3ww_{,22} - ckww_{,22} - c^4vw_{,2} + c^2kvw_{,2} - 2c^3w_{,2}^2 + ckw_{,2}^2 + ku_{,2}\psi_{1,2} + c\psi_{1,2}^2 - c^2\psi_{2,2} + k\psi_{2,2} - 3c^2v_{,2}\psi_{2,2} + kv_{,2}\psi_{2,2} + 2c^3w\psi_{2,2} - ckw\psi_{2,2} - cw_{,22}\psi_{2,2} - 3c^4v\psi_2 + c^2kv\psi_2 - 3c^3w_{,2}\psi_2 + ckw_{,2}\psi_2$$

$$\chi_2^4 = 2cku_{,2}w_{,12} + 2c^3v_{,2}w_{,22} - c^2kww_{,22} + c^2w_{,22}^2/2 + 2c^5vw_{,2} + c^4w_{,2}^2/2 + c^2kw_{,2}^2 + 2cku_{,2}\psi_{1,2} + kw_{,12}\psi_{1,2} + k\psi_{1,2}^2 + 2c^3v_{,2}\psi_{2,2} - c^2kw\psi_{2,2} - c^2w_{,22}\psi_{2,2} + kw_{,22}\psi_{2,2} - 3c^2\psi_{2,2}^2/2 + k\psi_{2,2}^2 + 2c^5v\psi_2 - c^4w_{,2}\psi_2 + 2c^2kw_{,2}\psi_2 - 3c^4\psi_2^2/2 + c^2k\psi_2^2$$

$$\chi_2^5 = -c^2kw_{,22} - 3c^2kv_{,2}w_{,22} + 2c^3kww_{,22} + c^3w_{,22}^2 - ckw_{,22}^2 - 3c^4kvw_{,2} + c^5w_{,2}^2 - 3c^3kw_{,2}^2 + 2ckw_{,12}\psi_{1,2} + 2ck\psi_{1,2}^2 - c^2k\psi_{2,2} - 3c^2kv_{,2}\psi_{2,2} + 2c^3kw\psi_{2,2} + 2c^3w_{,22}\psi_{2,2} - ckw_{,22}\psi_{2,2} + c^3\psi_{2,2}^2 - 3c^4kv\psi_2 + 2c^5w_{,2}\psi_2 - 3c^3kw_{,2}\psi_2 + c^5\psi_2^2$$

$$\chi_2^6 = k^2w_{,12}^2/2 + 2c^3kv_{,2}w_{,22} - c^2kw_{,22}^2 + k^2w_{,22}^2/2 + 2c^5kw_{,2} - c^4kw_{,2}^2 + c^2k^2w_{,2}^2/2 + k^2w_{,12}\psi_{1,2} + k^2\psi_{1,2}^2/2 + 2c^3kv_{,2}\psi_{2,2} - 4c^2kw_{,22}\psi_{2,2} + k^2w_{,22}\psi_{2,2} - 3c^2k\psi_{2,2}^2 + k^2\psi_{2,2}^2/2 + 2c^5kv\psi_2 - 4c^4kw_{,2}\psi_2 + c^2k^2w_{,2}\psi_2 - 3c^4k\psi_2^2 + c^2k^2\psi_2^2/2$$

$$\chi_2^7 = ck^2w_{,12}^2 + 2c^3kw_{,22}^2 + 2c^5kw_{,2}^2 + 2ck^2w_{,12}\psi_{1,2} + ck^2\psi_{1,2}^2 + 4c^3kw_{,22}\psi_{2,2} + 2c^3k\psi_{2,2}^2 + 4c^5kw_{,2}\psi_2 + 2c^5k\psi_2^2$$

$$\chi_2^8 = -3c^2k^2w_{,22}^2/2 - 3c^4k^2w_{,2}^2/2 - 3c^2k^2w_{,22}\psi_{2,2} - 3c^2k^2\psi_{2,2}^2/2 - 3c^4k^2w_{,2}\psi_2 - 3c^4k^2\psi_2^2/2$$

$$\chi_2^9 = c^3k^2w_{,22}^2 + c^5k^2w_{,2}^2 + 2c^3k^2w_{,22}\psi_{2,2} + c^3k^2\psi_{2,2}^2 + 2c^5k^2w_{,2}\psi_2 + c^5k^2\psi_2^2$$

$$\chi_4^0 = -cvv_{,2} + c^2vw + w_{,2} + u_{,2}\psi_1 + \psi_2 + v_{,2}\psi_2 - cw\psi_2$$

$$\chi_4^1 = c^3vw - cw_{,2} - 2cv_{,2}w_{,2} + 2c^2ww_{,2} + cu_{,2}\psi_1 + \psi_{1,2}\psi_1 - cv\psi_{2,2} - c\psi_2 - 2cv_{,2}\psi_2 + c^2w\psi_2 + \psi_{2,2}\psi_2$$

$$\chi_4^2 = c^3vv_{,2} - 3ckvv_{,2} + 3c^2kvw + 3ku_{,2}u_{,1} + c^2vw_{,22} - c^2w_{,2} + 3kw_{,2} + 3kv_{,2}w_{,2} + 2c^3ww_{,2} - 3ckww_{,2} + 6ku_{,2}\psi_1 + c\psi_{1,2}\psi_1 - 2cw_{,2}\psi_{2,2} - c^2\psi_2 + 3k\psi_2 - c^2v_{,2}\psi_2 + 6kv_{,2}\psi_2 + 2c^3w\psi_2 - 6ckw\psi_2 - cw_{,22}\psi_2 - 2c\psi_{2,2}\psi_2$$

$$\chi_4^3 = 3c^3kvw +3cku_{,2}w_{,1} +c^3vw_{,22} -ckvw_{,22} +c^3w_{,2} -3ckw_{,2} +2c^3v_{,2}w_{,2} -10ckv_{,2}w_{,2}$$
$$+7c^2kww_{,2} +2c^2w_{,22}w_{,2} +3kw_{,1}\psi_{1,2} +6cku_{,2}\psi_1 +kw_{,12}\psi_1 +7k\psi_{1,2}\psi_1 +c^3v\psi_{2,2} -4ckv\psi_{2,2}$$
$$+3kw_{,2}\psi_{2,2} +c^3\psi_2 -3ck\psi_2 +2c^3v_{,2}\psi_2 -10ckv_{,2}\psi_2 +7c^2kw\psi_2 +c^2w_{,22}\psi_2 +kw_{,22}\psi_2$$
$$-c^2\psi_{2,2}\psi_2 +7k\psi_{2,2}\psi_2$$

$$\chi_4^4 = 3c^3kvv_{,2} +9k^2u_{,2}w_{,1} +3c^2kvw_{,22} -3c^2kw_{,2} -3c^3v_{,2}w_{,2} +9k^2v_{,2}w_{,2} +10c^3kww_{,2}$$
$$-9ck^2ww_{,2} +2c^3w_{,22}w_{,2} -5ckw_{,22}w_{,2} +3ckw_{,1}\psi_{1,2} +9k^2u_{,2}\psi_1 +ckw_{,12}\psi_1 +7ck\psi_{1,2}\psi_1$$
$$+2c^3w_{,2}\psi_{2,2} -12ckw_{,2}\psi_{2,2} -3c^2k\psi_2 -6c^2kv_{,2}\psi_2 +9k^2v_{,2}\psi_2 +10c^3kw\psi_2 -9ck^2w\psi_2$$
$$+2c^3w_{,22}\psi_2 -8ckw_{,22}\psi_2 +2c^3\psi_{2,2}\psi_2 -12ck\psi_{2,2}\psi_2$$

$$\chi_4^5 = 9ck^2u_{,2}w_{,1} +3k^2w_{,12}w_{,1} +4c^3kvw_{,22} -3ck^2vw_{,22} +3c^3kw_{,2} +10c^3kv_{,2}w_{,2}$$
$$-12ck^2v_{,2}w_{,2} +3c^2k^2ww_{,2} +7c^2kw_{,22}w_{,2} +3k^2w_{,22}w_{,2} +12k^2w_{,1}\psi_{1,2} +9ck^2u_{,2}\psi_1$$
$$+6k^2w_{,12}\psi_1 +15k^2\psi_{1,2}\psi_1 +4c^3kv\psi_{2,2} -3ck^2v\psi_{2,2} -3c^2kw_{,2}\psi_{2,2} +12k^2w_{,2}\psi_{2,2} +3c^3k\psi_2$$
$$+10c^3kv_{,2}\psi_2 -12ck^2v_{,2}\psi_2 +3c^2k^2w\psi_2 +3c^2kw_{,22}\psi_2 +6k^2w_{,22}\psi_2 -7c^2k\psi_{2,2}\psi_2$$
$$+15k^2\psi_{2,2}\psi_2$$

$$\chi_4^6 = 3ck^2w_{,12}w_{,1} -9c^2k^2v_{,2}w_{,2} +12c^3k^2ww_{,2} +12c^3kw_{,22}w_{,2} -19ck^2w_{,22}w_{,2}$$
$$+12ck^2w_{,1}\psi_{1,2} +6ck^2w_{,12}\psi_1 +15ck^2w_{,2}\psi_1 +12c^3kw_{,2}\psi_{2,2} -22ck^2w_{,2}\psi_{2,2} -9c^2k^2v_{,2}\psi_2$$
$$+12c^3k^2w\psi_2 +12c^3kw_{,22}\psi_2 -19ck^2w_{,22}\psi_2 +12c^3k\psi_{2,2}\psi_2 -22ck^2\psi_{2,2}\psi_2$$

$$\chi_4^7 = 9k^3w_{,12}w_{,1} +3c^3k^2vw_{,22} +12c^3k^2v_{,2}w_{,2} +9k^3w_{,22}w_{,2} +9k^3w_{,1}\psi_{1,2} +9k^3w_{,12}\psi_1$$
$$+9k^3\psi_{1,2}\psi_1 +3c^3k^2v\psi_{2,2} -12c^2k^2w_{,2}\psi_{2,2} +9k^3w_{,2}\psi_{2,2} +12c^3k^2v_{,2}\psi_2 -3c^2k^2w_{,22}\psi_2$$
$$+9k^3w_{,22}\psi_2 -15c^2k^2\psi_{2,2}\psi_2 +9k^3\psi_{2,2}\psi_2$$

$$\chi_4^8 = 9ck^3w_{,12}w_{,1} +22c^3k^2w_{,22}w_{,2} -12ck^3w_{,22}w_{,2} +9ck^3w_{,1}\psi_{1,2} +9ck^3w_{,12}\psi_1 +9ck^3\psi_{1,2}\psi_1$$
$$+22c^3k^2w_{,2}\psi_{2,2} -12ck^3w_{,2}\psi_{2,2} +22c^3k^2w_{,22}\psi_2 -12ck^3w_{,22}\psi_2 +22c^3k^2\psi_{2,2}\psi_2$$
$$-12ck^3\psi_{2,2}\psi_2$$

$$\chi_4^9 = -9c^2k^3w_{,22}w_{,2} -9c^2k^3w_{,2}\psi_{2,2} -9c^2k^3w_{,22}\psi_2 -9c^2k^3\psi_{2,2}\psi_2$$

$$\chi_4^{10} = 12c^3k^3w_{,22}w_{,2} +12c^3k^3w_{,2}\psi_{2,2} +12c^3k^3w_{,22}\psi_2 +12c^3k^3\psi_{2,2}\psi_2$$

$$\chi_5^0 = -cvv_{,1} +w_{,1} +\psi_1 +u_{,1}\psi_1 +v_{,1}\psi_2$$

$$\chi_5^1 = c^2 v v_{,1} - 2c v_{,1} w_{,2} + \psi_{1,1}\psi_1 - c v \psi_{2,1} - 3c v_{,1}\psi_2 + \psi_{2,1}\psi_2$$

$$\chi_5^2 = -3ckvv_{,1} + c^2 v w_{,1} + 3kw_{,1} + 3ku_{,1}w_{,1} + 2c^2 v_{,1}w_{,2} + 3kv_{,1}w_{,2} + 3k\psi_1 + 6ku_{,1}\psi_1$$
$$+ c^2 v\psi_{2,1} - 2cw_{,2}\psi_{2,1} + 2c^2 v_{,1}\psi_2 + 6kv_{,1}\psi_2 - cw_{,12}\psi_2 - 3c\psi_{2,1}\psi_2$$

$$\chi_5^3 = 3c^2 k v v_{,1} - ckvw_{,12} - 13ckv_{,1}w_{,2} + 2c^2 w_{,12}w_{,2} + 3kw_{,1}\psi_{1,1} + kw_{,11}\psi_1 + 7k\psi_{1,1}\psi_1$$
$$- 4ckv\psi_{2,1} + 2c^2 w_{,2}\psi_{2,1} + 3kw_{,2}\psi_{2,1} - 2^4 ckv_{,1}\psi_2 + 2c^2 w_{,12}\psi_2 + kw_{,12}\psi_2 + 2c^2\psi_{2,1}\psi_2$$
$$+ 7k\psi_{2,1}\psi_2$$

$$\chi_5^4 = 4c^2 kvw_{,12} + 9k^2 u_{,1}w_{,1} + 10c^2 kv_{,1}w_{,2} + 9k^2 v_{,1}w_{,2} - 5ckw_{,12}w_{,2} + 9k^2 u_{,1}\psi_1 + 4c^2 kv\psi_{2,1}$$
$$- 15ckw_{,2}\psi_{2,1} + 10c^2 kv_{,1}\psi_2 + 9k^2 v_{,1}\psi_2 - 9ckw_{,12}\psi_2 - 19ck\psi_{2,1}\psi_2$$

$$\chi_5^5 = -3ck^2 vw_{,12} + 3k^2 w_{,11}w_{,1} - 21ck^2 v_{,1}w_{,2} + 12c^2 kw_{,12}w_{,2} + 3k^2 w_{,12}w_{,2} + 12k^2 w_{,1}\psi_{1,1}$$
$$+ 6k^2 w_{,11}\psi_1 + 15k^2\psi_{1,1}\psi_1 - 3ck^2 v\psi_{2,1} + 12c^2 kw_{,2}\psi_{2,1} + 12k^2 w_{,2}\psi_{2,1} - 21ck^2 v_{,1}\psi_2$$
$$+ 12c^2 kw_{,12}\psi_2 + 6k^2 w_{,12}\psi_2 + 12c^2 k\psi_{2,1}\psi_2 + 15k^2\psi_{2,1}\psi_2$$

$$\chi_5^6 = 3c^2 k^2 vw_{,12} + 12c^2 k^2 v_{,1}w_{,2} - 22ck^2 w_{,12}w_{,2} + 3c^2 k^2 v\psi_{2,1} - 34ck^2 w_{,2}\psi_{2,1} + 12c^2 k^2 v_{,1}\psi_2$$
$$- 25ck^2 w_{,12}\psi_2 - 37ck^2\psi_{2,1}\psi_2$$

$$\chi_5^7 = 9k^3 w_{,11}w_{,1} + 22c^2 k^2 w_{,12}w_{,2} + 9k^3 w_{,12}w_{,2} + 9k^3 w_{,1}\psi_{1,1} + 9k^3 w_{,11}\psi_1 + 9k^3\psi_{1,1}\psi_1$$
$$+ 22c^2 k^2 w_{,2}\psi_{2,1} + 9k^3 w_{,2}\psi_{2,1} + 22c^2 k^2 w_{,12}\psi_2 + 9k^3 w_{,12}\psi_2 + 22c^2 k^2\psi_{2,1}\psi_2 + 9k^3\psi_{2,1}\psi_2$$

$$\chi_5^8 = -21ck^3 w_{,12}w_{,2} - 21ck^3 w_{,2}\psi_{2,1} - 21ck^3 w_{,12}\psi_2 - 21ck^3\psi_{2,1}\psi_2$$

$$\chi_5^9 = 12c^2 k^3 w_{,12}w_{,2} + 12c^2 k^3 w_{,2}\psi_{2,1} + 12c^2 k^3 w_{,12}\psi_2 + 12c^2 k^3\psi_{2,1}\psi_2$$

$$\chi_6^0 = u_{,2} + u_{,1}u_{,2} + v_{,1} + v_{,1}v_{,2} - cv_{,1}w + cvw_{,1} + w_{,1}w_{,2}$$

$$\chi_6^1 = cu_{,2} + cu_{,1}u_{,2} - cv_{,1} - cv_{,1}v_{,2} + cw_{,1}w_{,2} + u_{,2}\psi_{1,1} + \psi_{1,2} + u_{,1}\psi_{1,2} + \psi_{2,1} + v_{,2}\psi_{2,1}$$
$$- cw\psi_{2,1} + v_{,1}\psi_{2,2} + cw_{,1}\psi_2$$

$$\chi_6^2 = -c^2 v_{,1}v_{,2} + c^3 v_{,1}w - cw_{,12} - cv_{,2}w_{,12} + c^2 ww_{,12} - c^3 vw_{,1} - cv_{,1}w_{,22} - c^2 w_{,1}w_{,2}$$
$$+ cu_{,2}\psi_{1,1} + c\psi_{1,2} + cu_{,1}\psi_{1,2} + \psi_{1,1}\psi_{1,2} - c\psi_{2,1} - cv_{,2}\psi_{2,1} - cv_{,1}\psi_{2,2} + \psi_{2,1}\psi_{2,2}$$

$$\chi_6^3 = c^3 v_{,1} v_{,2} + k u_{,2} w_{,11} + 2k w_{,12} + k u_{,1} w_{,12} + k v_{,2} w_{,12} + c^3 w w_{,12} - ckw w_{,12} + k v_{,1} w_{,22}$$
$$- c^3 w_{,1} w_{,2} + ckw_{,1} w_{,2} + k u_{,2} \psi_{1,1} + k \psi_{1,2} + k u_{,1} \psi_{1,2} + c \psi_{1,1} \psi_{1,2} + k \psi_{2,1} - c^2 v_{,2} \psi_{2,1} + k v_{,2} \psi_{2,1}$$
$$+ c^3 w \psi_{2,1} - ckw \psi_{2,1} - c w_{,22} \psi_{2,1} - c^2 v_{,1} \psi_{2,2} + k v_{,1} \psi_{2,2} - c w_{,12} \psi_{2,2} - c \psi_{2,1} \psi_{2,2} - c^3 w_{,1} \psi_2$$
$$+ ckw_{,1} \psi_2$$

$$\chi_6^4 = cku_{,2} w_{,11} + cku_{,1} w_{,12} + c^3 v_{,2} w_{,12} - ckv_{,2} w_{,12} + c^3 v_{,1} w_{,22} - ckv_{,1} w_{,22} + c^2 w_{,12} w_{,22}$$
$$+ cku_{,2} \psi_{1,1} + kw_{,12} \psi_{1,1} + ck \psi_{1,2} + cku_{,1} \psi_{1,2} + kw_{,11} \psi_{1,2} + 2k \psi_{1,1} \psi_{1,2} - ck \psi_{2,1} + c^3 v_{,2} \psi_{2,1}$$
$$- ckv_{,2} \psi_{2,1} + kw_{,22} \psi_{2,1} + c^3 v_{,1} \psi_{2,2} - ckv_{,1} \psi_{2,2} + kw_{,12} \psi_{2,2} - c^2 \psi_{2,1} \psi_{2,2} + 2k \psi_{2,1} \psi_{2,2}$$

$$\chi_6^5 = -c^2 k v_{,2} w_{,12} + c^3 k w w_{,12} - c^2 k v_{,1} w_{,22} + c^3 w_{,12} w_{,22} - 2ckw_{,12} w_{,22} - c^3 k w_{,1} w_{,2}$$
$$+ ckw_{,12} \psi_{1,1} + ckw_{,11} \psi_{1,2} + 2ck \psi_{1,1} \psi_{1,2} - c^2 k v_{,2} \psi_{2,1} + c^3 k w \psi_{2,1} + c^3 w_{,22} \psi_{2,1} - 2ckw_{,22} \psi_{2,1}$$
$$- c^2 k v_{,1} \psi_{2,2} + c^3 w_{,12} \psi_{2,2} - 2ckw_{,12} \psi_{2,2} + c^3 \psi_{2,1} \psi_{2,2} - 2ck \psi_{2,1} \psi_{2,2} - c^3 k w_{,1} \psi_2$$

$$\chi_6^6 = c^3 k v_{,2} w_{,12} + k^2 w_{,11} w_{,12} + c^3 k v_{,1} w_{,22} + k^2 w_{,12} w_{,22} + k^2 w_{,12} \psi_{1,1} + k^2 w_{,11} \psi_{1,2}$$
$$+ k^2 \psi_{1,1} \psi_{1,2} + c^3 k v_{,2} \psi_{2,1} - c^2 k w_{,22} \psi_{2,1} + k^2 w_{,22} \psi_{2,1} + c^3 k v_{,1} \psi_{2,2} - c^2 k w_{,12} \psi_{2,2} + k^2 w_{,12} \psi_{2,2}$$
$$- 2c^2 k \psi_{2,1} \psi_{2,2} + k^2 \psi_{2,1} \psi_{2,2}$$

$$\chi_6^7 = -ck^2 w_{,11} w_{,12} + 2c^3 k w_{,12} w_{,22} - ck^2 w_{,12} w_{,22} + ck^2 w_{,12} \psi_{1,1} + ck^2 w_{,11} \psi_{1,2} + ck^2 \psi_{1,1} \psi_{1,2}$$
$$+ 2c^3 k w_{,22} \psi_{2,1} - ck^2 w_{,22} \psi_{2,1} + 2c^3 k w_{,12} \psi_{2,2} - ck^2 w_{,12} \psi_{2,2} + 2c^3 k \psi_{2,1} \psi_{2,2} - ck^2 \psi_{2,1} \psi_{2,2}$$

$$\chi_6^8 = -c^2 k^2 w_{,12} w_{,22} - c^2 k^2 w_{,22} \psi_{2,1} - c^2 k^2 w_{,12} \psi_{2,2} - c^2 k^2 \psi_{2,1} \psi_{2,2}$$

$$\chi_6^9 = c^3 k^2 w_{,12} w_{,22} + c^3 k^2 w_{,22} \psi_{2,1} + c^3 k^2 w_{,12} \psi_{2,2} + c^3 k^2 \psi_{2,1} \psi_{2,2}$$

Appendix E. *Strain Displacement Relations for C120/C123 Elemental Codes*

The strain displacement relations of this appendix are for the case of a circular cylindrical shell with its longitudinal axis in the y_1 direction and a radius of R_2 . The y_2 coordinate is the circumferential distance $dy_2 = R_2 d\theta$. The kinematic displacement within the shell is assumed to be of the form:

$$\vec{U} = u_1\vec{e}_1 + u_2\vec{e}_2 + u_3\vec{e}_3 \tag{E.1}$$

where

$$\begin{aligned} u_1(y_1, y_2, y_3) &= u + y_3\psi_1 + k(\psi_1 + w_{,1})y_3^3 \\ u_2(y_1, y_2, y_3) &= v(1 - cy_3) + \psi_2 y_3(\psi_2 + w_{,2})\left[-c + ky_3 - cky_3^2\right] y_3^2 \\ u_3(y_1, y_2, y_3) &= w \end{aligned} \tag{E.2}$$

The seven degrees of freedom $u, v, w, w_{,1}, w_{,2}, \psi_1$ and ψ_2, are functions of midsurface coordinates (y_1, y_2) only. The ψ_i are rotations of the normals and $c = 1/R_2$ and $k = -4/(3h^2)$. For this case, the 60 shell geometric functions $\hat{H}_i$ are only simplified because $h_1 = h_3 = 1$. The quadratic terms of the expansions are retained. The simplified nonzero functions of Appendix A are listed in Eq (E.3)

$$\begin{aligned} \hat{H}_3 &= 1 & \hat{H}_9 &= -c - c^2y_3 - c^3y_3^2 \\ \hat{H}_{11} &= 1 + 2cy_3 + 3c^2y_3^2 & \hat{H}_{14} &= c^2 + 2c^3y_3 + 3c^4y_3^2 \\ \hat{H}_{15} &= c^2 & \hat{H}_{17} &= 1 + cy_3 + c^2y_3^2 \\ \hat{H}_{21} &= 1 + cy_3 + c^2y_3^2 & \hat{H}_{18} &= 1 \\ \hat{H}_{21} &= 1 + cy_3 + c^2y_3^2 & \hat{H}_{23} &= -c \\ \hat{H}_{39} &= c^2 + c^3y_3 + c^4y_3^2 & \hat{H}_{42} &= -c - 2c^2y_3 - 3c^3y_3^2 \\ \hat{H}_{46} &= -c - c^2y_3 - c^3y_3^2 \end{aligned} \tag{E.3}$$

The strain equations listed below are the parts of the linear and nonlinear strain compo nents for the C120 and C123 elemental codes. Contracted notation is used, where $\varepsilon_1 = \varepsilon_{11}$, $\varepsilon_2 = \varepsilon_{22}, \varepsilon_3 = \varepsilon_{33}, \varepsilon_4 = \varepsilon_{23}, \varepsilon_5 = \varepsilon_{13}$, and $\varepsilon_6 = \varepsilon_{12}$. The strain components ε_i are given by

the series expansion shown in Eq (E.4).

$$\varepsilon_i = \sum_{p=0}^{n} \chi_i^p y_3^p \tag{E.4}$$

The nonzero χ_i^p, are listed below for each component of the C123 elemental code. The C120 quasi-nonlinear HTSD theory is given by neglecting the nonlinear terms of χ_4^p and χ_5^p.

$$\chi_1^0 = u_{,1} + u_{,1}^2/2 + v_{,1}^2/2 + w_{,1}^2/2$$

$$\chi_1^1 = -cv_{,1}^2 + \psi_{1,1} + u_{,1}\psi_{1,1} + v_{,1}\psi_{2,1}$$

$$\chi_1^2 = c^2 v_{,1}^2/2 - cv_{,1}w_{,12} + \psi_{1,1}^2/2 - 2cv_{,1}\psi_{2,1} + \psi_{2,1}^2/2$$

$$\chi_1^3 = kw_{,11} + ku_{,1}w_{,11} + c^2 v_{,1}w_{,12} + kv_{,1}w_{,12} + k\psi_{1,1} + ku_{,1}\psi_{1,1} + c^2 v_{,1}\psi_{2,1} + kv_{,1}\psi_{2,1} - cw_{,12}\psi_{2,1} - c\psi_{2,1}^2$$

$$\chi_1^4 = -2ckv_{,1}w_{,12} + c^2 w_{,12}^2/2 + kw_{,11}\psi_{1,1} + k\psi_{1,1}^2 - 2ckv_{,1}\psi_{2,1} + c^2 w_{,12}\psi_{2,1} + kw_{,12}\psi_{2,1} + c^2\psi_{2,1}^2/2 + k\psi_{2,1}^2$$

$$\chi_1^5 = c^2 kv_{,1}w_{,12} - ckw_{,12}^2 + c^2 kv_{,1}\psi_{2,1} - 3ckw_{,12}\psi_{2,1} - 2ck\psi_{2,1}^2$$

$$\chi_1^6 = k^2 w_{,11}^2/2 + c^2 kw_{,12}^2 + k^2 w_{,12}^2/2 + k^2 w_{,11}\psi_{1,1} + k^2\psi_{1,1}^2/2 + 2c^2 kw_{,12}\psi_{2,1} + k^2 w_{,12}\psi_{2,1} + c^2 k\psi_{2,1}^2 + k^2\psi_{2,1}^2/2$$

$$\chi_1^7 = -ck^2 w_{,12}^2 - 2ck^2 w_{,12}\psi_{2,1} - ck^2\psi_{2,1}^2$$

$$\chi_1^8 = c^2 k^2 w_{,12}^2/2 + c^2 k^2 w_{,12}\psi_{2,1} + c^2 k^2\psi_{2,1}^2/2$$

$$\chi_2^0 = u_{,2}^2/2 + c^2 v^2/2 + v_{,2} + v_{,2}^2/2 - cw - cv_{,2}w + c^2 w^2/2 + cvw_{,2} + w_{,2}^2/2$$

$$\chi_2^1 = cu_{,2}^2 - c^2 w - c^2 v_{,2}w + c^3 w^2 + c^2 vw_{,2} + cw_{,2}^2 + u_{,2}\psi_{1,2} + \psi_{2,2} + v_{,2}\psi_{2,2} - cw\psi_{2,2} + c^2 v\psi_2 + cw_{,2}\psi_2$$

$$\chi_2^2 = 3c^2u_{,2}^2/2 - c^3w - c^3v_{,2}w + 3c^4w^2/2 - cw_{,22} - cv_{,2}w_{,22} + c^2ww_{,22} + c^2w_{,2}^2/2 + 2cu_{,2}\psi_{1,2} + \psi_{1,2}^2/2 - c^2w\psi_{2,2} + \psi_{2,2}^2/2 + c^2w_{,2}\psi_2 + c^2\psi_2^2/2$$

$$\chi_2^3 = -2c^5v^2 - c^3v_{,2} - 2c^3v_{,2}^2 + 3c^4v_{,2}w + ku_{,2}w_{,12} - c^2w_{,22} + kw_{,22} - c^2v_{,2}w_{,22} + kv_{,2}w_{,22} + 2c^3ww_{,22} - ckww_{,22} - 4c^4vw_{,2} + c^2kvw_{,2} - 2c^3w_{,2}^2 + ckw_{,2}^2 + 3c^2u_{,2}\psi_{1,2} + ku_{,2}\psi_{1,2} + c\psi_{1,2}^2 + k\psi_{2,2} + kv_{,2}\psi_{2,2} - c^3w\psi_{2,2} - ckw\psi_{2,2} - cw_{,22}\psi_{2,2} + c^2kv\psi_2 + ckw_{,2}\psi_2$$

$$\chi_2^4 = 3c^6v^2/2 + 3c^4v_{,2}^2/2 + 2cku_{,2}w_{,12} - c^3w_{,22} - c^3v_{,2}w_{,22} + 3c^4ww_{,22} - c^2kww_{,22} + c^2w_{,22}^2/2 - c^5vw_{,2} - 5c^4w_{,2}^2/2 + c^2kw_{,2}^2 + 2cku_{,2}\psi_{1,2} + kw_{,12}\psi_{1,2} + 3c^2\psi_{1,2}^2/2 + k\psi_{1,2}^2 - c^3\psi_{2,2} - 4c^3v_{,2}\psi_{2,2} + 3c^4w\psi_{2,2} - c^2kw\psi_{2,2} - c^2w_{,22}\psi_{2,2} + kw_{,22}\psi_{2,2} + k\psi_{2,2}^2 - 4c^5v\psi_2 - 4c^4w_{,2}\psi_2 + 2c^2kw_{,2}\psi_2 + c^2k\psi_2^2$$

$$\chi_2^5 = 3c^2ku_{,2}w_{,12} + 3c^4v_{,2}w_{,22} - c^3kww_{,22} + c^3w_{,22}^2 - ckw_{,22}^2 + 3c^6vw_{,2} + c^5w_{,2}^2 + 3c^2ku_{,2}\psi_{1,2} + 2ckw_{,12}\psi_{1,2} + 2ck\psi_{1,2}^2 + 3c^4v_{,2}\psi_{2,2} - c^3kw\psi_{2,2} - c^3w_{,22}\psi_{2,2} - ckw_{,22}\psi_{2,2} - 2c^3\psi_{2,2}^2 + 3c^6v\psi_2 - c^5w_{,2}\psi_2 - 2c^5\psi_2^2$$

$$\chi_2^6 = k^2w_{,12}^2/2 - c^3kw_{,22} - 4c^3kv_{,2}w_{,22} + 3c^4kww_{,22} + 3c^4w_{,22}^2/2 - c^2kw_{,22}^2 + k^2w_{,22}^2/2 - 4c^5kvw_{,2} + 3c^6w_{,2}^2/2 - 4c^4kw_{,2}^2 + c^2k^2w_{,2}^2/2 + 3c^2kw_{,12}\psi_{1,2} + k^2w_{,12}\psi_{1,2} + 3c^2k\psi_{1,2}^2 + k^2\psi_{1,2}^2/2 - c^3k\psi_{2,2} - 4c^3kv_{,2}\psi_{2,2} + 3c^4kw\psi_{2,2} + 3c^4w_{,22}\psi_{2,2} - c^2kw_{,22}\psi_{2,2} + k^2w_{,22}\psi_{2,2} + 3c^4\psi_{2,2}^2/2 + k^2\psi_{2,2}^2/2 - 4c^5kv\psi_2 + 3c^6w_{,2}\psi_2 - 4c^4kw_{,2}\psi_2 + c^2k^2w_{,2}\psi_2 + 3c^6\psi_2^2/2 + c^2k^2\psi_2^2/2$$

$$\chi_2^7 = ck^2w_{,12}^2 + 3c^4kv_{,2}w_{,22} - c^3kw_{,22}^2 + 3c^6kvw_{,2} - c^5kw_{,2}^2 + 2ck^2w_{,12}\psi_{1,2} + ck^2\psi_{1,2}^2 + 3c^4kv_{,2}\psi_{2,2} - 5c^3kw_{,22}\psi_{2,2} - 4c^3k\psi_{2,2}^2 + 3c^6kv\psi_2 - 5c^5kw_{,2}\psi_2 - 4c^5k\psi_2^2$$

$$\chi_2^8 = 3c^2k^2w_{,12}^2/2 + 3c^4kw_{,22}^2 + 3c^6kw_{,2}^2 + 3c^2k^2w_{,12}\psi_{1,2} + 3c^2k^2\psi_{1,2}^2/2 + 6c^4kw_{,22}\psi_{2,2} + 3c^4k\psi_{2,2}^2 + 6c^6kw_{,2}\psi_2 + 3c^6k\psi_2^2$$

$$\chi_2^9 = -2c^3k^2w_{,22}^2 - 2c^5k^2w_{,2}^2 - 4c^3k^2w_{,22}\psi_{2,2} - 2c^3k^2\psi_{2,2}^2 - 4c^5k^2w_{,2}\psi_2 - 2c^5k^2\psi_2^2$$

$$\chi_2^{10} = 3c^4k^2w_{,22}^2/2 + 3c^6k^2w_{,2}^2/2 + 3c^4k^2w_{,22}\psi_{2,2} + 3c^4k^2\psi_{2,2}^2/2 + 3c^6k^2w_{,2}\psi_2 + 3c^6k^2\psi_2^2/2$$

$$\chi_4^0 = -cvv_{,2} + c^2vw + w_{,2} + u_{,2}\psi_1 + \psi_2 + v_{,2}\psi_2 - cw\psi_2$$

$$\chi_4^1 = c^3vw - cw_{,2} - 2cv_{,2}w_{,2} + 2c^2ww_{,2} + cu_{,2}\psi_1 + \psi_{1,2}\psi_1 - cv\psi_{2,2} - c\psi_2 - 2cv_{,2}\psi_2 + c^2w\psi_2 + \psi_{2,2}\psi_2$$

$$\chi_4^2 = -3ckvv_{,2} + c^4vw + 3c^2kvw + 3ku_{,2}w_{,1} + c^2vw_{,22} + 3kw_{,2} + 3kv_{,2}w_{,2} + 2c^3ww_{,2} - 3ckww_{,2} + c^2u_{,2}\psi_1 + 6ku_{,2}\psi_1 + c\psi_{1,2}\psi_1 - 2cw_{,2}\psi_{2,2} + 3k\psi_2 + 6kv_{,2}\psi_2 + c^3w\psi_2 - 6ckw\psi_2 - cw_{,22}\psi_2 - 2c\psi_{2,2}\psi_2$$

$$\chi_4^3 = c^4vv_{,2} + 3c^3kvw + 3cku_{,2}w_{,1} + c^3vw_{,22} - ckvw_{,22} - c^3w_{,2} - 3ckw_{,2} - 10ckv_{,2}w_{,2} + 2c^4ww_{,2} + 7c^2kww_{,2} + 2c^2w_{,22}w_{,2} + 3kw_{,1}\psi_{1,2} + 6cku_{,2}\psi_1 + kw_{,12}\psi_1 + c^2\psi_{1,2}\psi_1 + 7k\psi_{1,2}\psi_1 - 4ckv\psi_{2,2} + 3kw_{,2}\psi_{2,2} - c^3\psi_2 - 3ck\psi_2 - c^3v_{,2}\psi_2 - 10ckv_{,2}\psi_2 + 2c^4w\psi_2 + 4c^2kw\psi_2 + c^2w_{,22}\psi_2 + kw_{,22}\psi_2 + 7k\psi_{2,2}\psi_2$$

$$\chi_4^4 = 3c^4kvw + 3c^2ku_{,2}w_{,1} + 9k^2u_{,2}w_{,1} + c^4vw_{,22} + 3c^2kvw_{,22} + c^4w_{,2} + 2c^4v_{,2}w_{,2} + 9k^2v_{,2}w_{,2} + 7c^3kww_{,2} - 9ck^2ww_{,2} + 2c^3w_{,22}w_{,2} - 5ckw_{,22}w_{,2} + 3ckw_{,1}\psi_{1,2} + 6c^2ku_{,2}\psi_1 + 9k^2u_{,2}\psi_1 + ckw_{,12}\psi_1 + 7ck\psi_{1,2}\psi_1 + c^4v\psi_{2,2} - 12ckw_{,2}\psi_{2,2} + c^4\psi_2 + 2c^4v_{,2}\psi_2 + 9k^2v_{,2}\psi_2 + 4c^3kw\psi_2 - 9ck^2w\psi_2 + c^3w_{,22}\psi_2 - 8ckw_{,22}\psi_2 - c^3\psi_{2,2}\psi_2 - 12ck\psi_{2,2}\psi_2$$

$$\chi_4^5 = 3c^4kvv_{,2} + 9ck^2u_{,2}w_{,1} + 3k^2w_{,12}w_{,1} + 3c^3kvw_{,22} - 3ck^2vw_{,22} - 3c^3kw_{,2} - 3c^3kv_{,2}w_{,2} - 12ck^2v_{,2}w_{,2} + 10c^4kww_{,2} + 3c^2k^2ww_{,2} + 2c^4w_{,22}w_{,2} + 7c^2kw_{,22}w_{,2} + 3k^2w_{,22}w_{,2} + 3c^2kw_{,1}\psi_{1,2} + 12k^2w_{,1}\psi_{1,2} + 9ck^2u_{,2}\psi_1 + c^2kw_{,12}\psi_1 + 6k^2w_{,12}\psi_1 + 7c^2k\psi_{1,2}\psi_1 + 15k^2\psi_{1,2}\psi_1 - 3ck^2v\psi_{2,2} + 2c^4w_{,2}\psi_{2,2} + 12k^2w_{,2}\psi_{2,2} - 3c^3k\psi_2 - 6c^3kv_{,2}\psi_2 - 12ck^2v_{,2}\psi_2 + 10c^4kw\psi_2 + 3c^2k^2w\psi_2 + 2c^4w_{,22}\psi_2 + 4c^2kw_{,22}\psi_2 + 6k^2w_{,22}\psi_2 + 2c^4\psi_{2,2}\psi_2 + 15k^2\psi_{2,2}\psi_2$$

$$\chi_4^6 = 9c^2k^2u_{,2}w_{,1} + 3ck^2w_{,12}w_{,1} + 4c^4kvw_{,22} + 3c^4kw_{,2} + 10c^4kv_{,2}w_{,2} + 3c^3k^2ww_{,2} + 7c^3kw_{,22}w_{,2} - 19ck^2w_{,22}w_{,2} + 12ck^2w_{,1}\psi_{1,2} + 9c^2k^2u_{,2}\psi_1 + 6ck^2w_{,12}\psi_1 + 15ck^2\psi_{1,2}\psi_1 + 4c^4kv\psi_{2,2} - 3c^3kw_{,2}\psi_{2,2} - 22ck^2w_{,2}\psi_{2,2} + 3c^4k\psi_2 + 10c^4kv_{,2}\psi_2 + 3c^3k^2w\psi_2 + 3c^3kw_{,22}\psi_2 - 19ck^2w_{,22}\psi_2 - 7c^3k\psi_{2,2}\psi_2 - 22ck^2\psi_{2,2}\psi_2$$

$$\chi_4^7 = 3c^2k^2w_{,12}w_{,1} + 9k^3w_{,12}w_{,1} - 9c^3k^2v_{,2}w_{,2} + 12c^4k^2ww_{,2} + 12c^4kw_{,22}w_{,2} + 3c^2k^2w_{,22}w_{,2} + 9k^3w_{,22}w_{,2} + 12c^2k^2w_{,1}\psi_{1,2} + 9k^3w_{,1}\psi_{1,2} + 6c^2k^2w_{,12}\psi_1 + 9k^3w_{,12}\psi_1 + 15c^2k^2\psi_{1,2}\psi_1 + 9k^3\psi_{1,2}\psi_1 + 12c^4kw_{,2}\psi_{2,2} + 9k^3w_{,2}\psi_{2,2} - 9c^3k^2v_{,2}\psi_2 + 12c^4k^2w\psi_2 + 12c^4kw_{,22}\psi_2 + 3c^2k^2w_{,22}\psi_2 + 9k^3w_{,22}\psi_2 + 12c^4k\psi_{2,2}\psi_2 + 9k^3\psi_{2,2}\psi_2$$

$$\chi_4^8 = 9ck^3w_{,12}w_{,1} +3c^4k^2vw_{,22} +12c^4k^2v_{,2}w_{,2} -12ck^3w_{,22}w_{,2} +9ck^3w_{,1}\psi_{1,2} +9ck^3w_{,12}\psi_1 +9ck^3\psi_{1,2}\psi_1 +3c^4k^2v\psi_{2,2} -12c^3k^2w_{,2}\psi_{2,2} -12ck^3w_{,2}\psi_{2,2} +12c^4k^2v_{,2}\psi_2 -3c^3k^2w_{,22}\psi_2 -12ck^3w_{,22}\psi_2 -15c^3k^2\psi_{2,2}\psi_2 -12ck^3\psi_{2,2}\psi_2$$

$$\chi_4^9 = 9c^2k^3w_{,12}w_{,1} +22c^4k^2w_{,22}w_{,2} +9c^2k^3w_{,1}\psi_{1,2} +9c^2k^3w_{,12}\psi_1 +9c^2k^3\psi_{1,2}\psi_1 +22c^4k^2w_{,2}\psi_{2,2} +22c^4k^2w_{,22}\psi_2 +22c^4k^2\psi_{2,2}\psi_2$$

$$\chi_4^{10} = -9c^3k^3w_{,22}w_{,2} -9c^3k^3w_{,2}\psi_{2,2} -9c^3k^3w_{,22}\psi_2 -9c^3k^3\psi_{2,2}\psi_2$$

$$\chi_4^{11} = 12c^4k^3w_{,22}w_{,2} +12c^4k^3w_{,2}\psi_{2,2} +12c^4k^3w_{,22}\psi_2 +12c^4k^3\psi_{2,2}\psi_2$$

$$\chi_5^0 = -cvv_{,1} +w_{,1} +\psi_1 +u_{,1}\psi_1 +v_{,1}\psi_2$$

$$\chi_5^1 = c^2vv_{,1} -2cv_{,1}w_{,2} +\psi_{1,1}\psi_1 -cv\psi_{2,1} -3cv_{,1}\psi_2 +\psi_{2,1}\psi_2$$

$$\chi_5^2 = -3ckvv_{,1} +c^2vw_{,12} +3kw_{,1} +3ku_{,1}w_{,1} +2c^2v_{,1}w_{,2} +3kv_{,1}w_{,2} +3k\psi_1 +6ku_{,1}\psi_1 +c^2v\psi_{2,1} -2cw_{,2}\psi_{2,1} +2c^2v_{,1}\psi_2 +6kv_{,1}\psi_2 -cw_{,12}\psi_2 -3c\psi_{2,1}\psi_2$$

$$\chi_5^3 = 3c^2kvv_{,1} -ckvw_{,12} -13ckv_{,1}w_{,2} +2c^2w_{,12}w_{,2} +3kw_{,1}\psi_{1,1} +kw_{,11}\psi_1 +7k\psi_{1,1}\psi_1 -4ckv\psi_{2,1} +2c^2w_{,2}\psi_{2,1} +3kw_{,2}\psi_{2,1} -2^4ckv_{,1}\psi_2 +2c^2w_{,12}\psi_2 +kw_{,12}\psi_2 +2c^2\psi_{2,1}\psi_2 +7k\psi_{2,1}\psi_2$$

$$\chi_5^4 = 4c^2kvw_{,12} +9k^2u_{,1}w_{,1} +10c^2kv_{,1}w_{,2} +9k^2v_{,1}w_{,2} -5ckw_{,12}w_{,2} +9k^2u_{,1}\psi_1 +4c^2kv\psi_{2,1} -15ckw_{,2}\psi_{2,1} +10c^2kv_{,1}\psi_2 +9k^2v_{,1}\psi_2 -9ckw_{,12}\psi_2 -19ck\psi_{2,1}\psi_2$$

$$\chi_5^5 = -3ck^2vw_{,12} +3k^2w_{,11}w_{,1} -21ck^2v_{,1}w_{,2} +12c^2kw_{,12}w_{,2} +3k^2w_{,12}w_{,2} +12k^2w_{,1}\psi_{1,1} +6k^2w_{,11}\psi_1 +15k^2\psi_{1,1}\psi_1 -3ck^2v\psi_{2,1} +12c^2kw_{,2}\psi_{2,1} +12k^2w_{,2}\psi_{2,1} -21ck^2v_{,1}\psi_2 +12c^2kw_{,12}\psi_2 +6k^2w_{,12}\psi_2 +12c^2k\psi_{2,1}\psi_2 +15k^2\psi_{2,1}\psi_2$$

$$\chi_5^6 = 3c^2k^2vw_{,12} +12c^2k^2v_{,1}w_{,2} -22ck^2w_{,12}w_{,2} +3c^2k^2v\psi_{2,1} -34ck^2w_{,2}\psi_{2,1} +12c^2k^2v_{,1}\psi_2 -25ck^2w_{,12}\psi_2 -37ck^2\psi_{2,1}\psi_2$$

$$\chi_5^7 = 9k^3w_{,11}w_{,1} +22c^2k^2w_{,12}w_{,2} +9k^3w_{,12}w_{,2} +9k^3w_{,1}\psi_{1,1} +9k^3w_{,11}\psi_1 +9k^3\psi_{1,1}\psi_1 +22c^2k^2w_{,2}\psi_{2,1} +9k^3w_{,2}\psi_{2,1} +22c^2k^2w_{,12}\psi_2 +9k^3w_{,12}\psi_2 +22c^2k^2\psi_{2,1}\psi_2 +9k^3\psi_{2,1}\psi_2$$

$$\chi_5^8 = -21ck^3w_{,12}w_{,2} -21ck^3w_{,2}\psi_{2,1} -21ck^3w_{,12}\psi_2 -21ck^3\psi_{2,1}\psi_2$$

$$\chi_5^9 = 12c^2k^3w_{,12}w_{,2} +12c^2k^3w_{,2}\psi_{2,1} +12c^2k^3w_{,12}\psi_2 +12c^2k^3\psi_{2,1}\psi_2$$

$$\chi_6^0 = u_{,2} +u_{,1}u_{,2} +v_{,1} +v_{,1}v_{,2} -cv_{,1}w +cvw_{,1} +w_{,1}w_{,2}$$

$$\chi_6^1 = cu_{,2} +cu_{,1}u_{,2} -cv_{,1} -cv_{,1}v_{,2} +cw_{,1}w_{,2} +u_{,2}\psi_{1,1} +\psi_{1,2} +u_{,1}\psi_{1,2} +\psi_{2,1} +v_{,2}\psi_{2,1} -cw\psi_{2,1} +v_{,1}\psi_{2,2} +cw_{,1}\psi_2$$

$$\chi_6^2 = c^2u_{,2} +c^2u_{,1}u_{,2} -cw_{,12} -cv_{,2}w_{,12} +c^2ww_{,12} -cv_{,1}w_{,22} +cu_{,2}\psi_{1,1} +c\psi_{1,2} +cu_{,1}\psi_{1,2} +\psi_{1,1}\psi_{1,2} -c\psi_{2,1} -cv_{,2}\psi_{2,1} -cv_{,1}\psi_{2,2} +\psi_{2,1}\psi_{2,2}$$

$$\chi_6^3 = -c^3v_{,1}v_{,2} +c^4v_{,1}w +ku_{,2}w_{,11} +2kw_{,12} +ku_{,1}w_{,12} +kv_{,2}w_{,12} +c^3ww_{,12} -ckww_{,12} -c^4vw_{,1} +kv_{,1}w_{,22} -c^3w_{,1}w_{,2} +ckw_{,1}w_{,2} +c^2u_{,2}\psi_{1,1} +ku_{,2}\psi_{1,1} +c^2\psi_{1,2} +k\psi_{1,2} +c^2u_{,1}\psi_{1,2} +ku_{,1}\psi_{1,2} +c\psi_{1,1}\psi_{1,2} +k\psi_{2,1} +kv_{,2}\psi_{2,1} -ckw\psi_{2,1} -cw_{,22}\psi_{2,1} +kv_{,1}\psi_{2,2} -cw_{,12}\psi_{2,2} -c\psi_{2,1}\psi_{2,2} +ckw_{,1}\psi_2$$

$$\chi_6^4 = c^4v_{,1}v_{,2} +cku_{,2}w_{,11} +cku_{,1}w_{,12} -ckv_{,2}w_{,12} +c^4ww_{,12} -ckv_{,1}w_{,22} +c^2w_{,12}w_{,22} -c^4w_{,1}w_{,2} +cku_{,2}\psi_{1,1} +kw_{,12}\psi_{1,1} +ck\psi_{1,2} +cku_{,1}\psi_{1,2} +kw_{,11}\psi_{1,2} +c^2\psi_{1,1}\psi_{1,2} +2k\psi_{1,1}\psi_{1,2} -ck\psi_{2,1} -c^3v_{,2}\psi_{2,1} -ckv_{,2}\psi_{2,1} +c^4w\psi_{2,1} +kw_{,22}\psi_{2,1} -c^3v_{,1}\psi_{2,2} -ckv_{,1}\psi_{2,2} +kw_{,12}\psi_{2,2} +2k\psi_{2,1}\psi_{2,2} -c^4w_{,1}\psi_2$$

$$\chi_6^5 = c^2ku_{,2}w_{,11} +c^2kw_{,12} +c^2ku_{,1}w_{,12} +c^4v_{,2}w_{,12} +c^4v_{,1}w_{,22} +c^3w_{,12}w_{,22} -2ckw_{,12}w_{,22} +c^2ku_{,2}\psi_{1,1} +ckw_{,12}\psi_{1,1} +c^2k\psi_{1,2} +c^2ku_{,1}\psi_{1,2} +ckw_{,11}\psi_{1,2} +2ck\psi_{1,1}\psi_{1,2} +c^4v_{,2}\psi_{2,1} -2ckw_{,22}\psi_{2,1} +c^4v_{,1}\psi_{2,2} -2ckw_{,12}\psi_{2,2} -c^3\psi_{2,1}\psi_{2,2} -2ck\psi_{2,1}\psi_{2,2}$$

$$\chi_6^6 = -c^3kv_{,2}w_{,12} +c^4kww_{,12} +k^2w_{,11}w_{,12} -c^3kv_{,1}w_{,22} +c^4w_{,12}w_{,22} +k^2w_{,12}w_{,22} -c^4kw_{,1}w_{,2} +c^2kw_{,12}\psi_{1,1} +k^2w_{,12}\psi_{1,1} +c^2kw_{,11}\psi_{1,2} +k^2w_{,11}\psi_{1,2} +2c^2k\psi_{1,1}\psi_{1,2} +k^2\psi_{1,1}\psi_{1,2} -c^3kv_{,2}\psi_{2,1} +c^4kw\psi_{2,1} +c^4w_{,22}\psi_{2,1} +k^2w_{,22}\psi_{2,1} -c^3kv_{,1}\psi_{2,2} +c^4w_{,12}\psi_{2,2} +k^2w_{,12}\psi_{2,2} +c^4\psi_{2,1}\psi_{2,2} +k^2\psi_{2,1}\psi_{2,2} -c^4kw_{,1}\psi_2$$

$$\chi_6^7 = c^4kv_{,2}w_{,12} +ck^2w_{,11}w_{,12} +c^4kv_{,1}w_{,22} -ck^2w_{,12}w_{,22} +ck^2w_{,12}\psi_{1,1} +ck^2w_{,11}\psi_{1,2} +ck^2\psi_{1,1}\psi_{1,2} +c^4kv_{,2}\psi_{2,1} -c^3kw_{,22}\psi_{2,1} -ck^2w_{,22}\psi_{2,1} +c^4kv_{,1}\psi_{2,2} -c^3kw_{,12}\psi_{2,2} -ck^2w_{,12}\psi_{2,2} -2c^3k\psi_{2,1}\psi_{2,2} -ck^2\psi_{2,1}\psi_{2,2}$$

$$\chi_6^8 = c^2k^2w_{,11}w_{,12} + 2c^4kw_{,12}w_{,22} + c^2k^2w_{,12}\psi_{1,1} + c^2k^2w_{,11}\psi_{1,2} + c^2k^2\psi_{1,1}\psi_{1,2}$$
$$+ 2c^4kw_{,22}\psi_{2,1} + 2c^4kw_{,12}\psi_{2,2} + 2c^4k\psi_{2,1}\psi_{2,2}$$

$$\chi_6^9 = -c^3k^2w_{,12}w_{,22} - c^3k^2w_{,22}\psi_{2,1} - c^3k^2w_{,12}\psi_{2,2} - c^3k^2\psi_{2,1}\psi_{2,2}$$

$$\chi_6^{10} = c^4k^2w_{,12}w_{,22} + c^4k^2w_{,22}\psi_{2,1} + c^4k^2w_{,12}\psi_{2,2} + c^4k^2\psi_{2,1}\psi_{2,2}$$

Appendix F. *Strain Displacement Relations for the Modified Donnell Theory with Higher-Order Transverse Shear Deformation (CDON)*

The strain displacement relations of this appendix are for the case of a circular cylindrical shell with its longitudinal axis in the y_1 direction and a radius of R_2 . The y_2 coordinate is the circumferential distance $dy_2 = R_2 d\theta$. The kinematic displacement within the shell is assumed to be of the form:

$$\vec{U} = u_1\vec{e}_1 + u_2\vec{e}_2 + u_3\vec{e}_3 \tag{F.1}$$

where

$$\begin{aligned} u_1(y_1, y_2, y_3) &= u + y_3\psi_1 + k(\psi_1 + w_{,1})y_3^3 \\ u_2(y_1, y_2, y_3) &= v(1 - cy_3) + \psi_2 y_3 + k(\psi_2 + w_{,2})y_3^3 \\ u_3(y_1, y_2, y_3) &= w \end{aligned} \tag{F.2}$$

The seven degrees of freedom $u, v, w, w_{,1}, w_{,2}, \psi_1$ and ψ_2, are functions of midsurface coordinates (y_1, y_2) only. The ψ_i are rotations of the normals and $c = 1/R_2$ and $k = -4/(3h^2)$. For this case, the 60 shell geometric functions $\hat{H}_i$ are simplified because $h_1 = h_2 = h_3 = 1$. The simplified nonzero functions of Appendix A are listed in Eq (F.3)

$$\begin{aligned} \hat{H}_3 &= 1 \qquad \hat{H}_{11} = 1 \\ \hat{H}_{17} &= 1 \qquad \hat{H}_{21} = 1 \\ \hat{H}_{18} &= 1 \qquad \hat{H}_{21} = 1 \end{aligned} \tag{F.3}$$

The strain equations listed below are the parts of the linear strain components for the modified Donnell theory. Contracted notation is used, where $\varepsilon_1 = \varepsilon_{11}$, $\varepsilon_2 = \varepsilon_{22}$, $\varepsilon_3 = \varepsilon_{33}$, $\varepsilon_4 = \varepsilon_{23}, \varepsilon_5 = \varepsilon_{13}$, and $\varepsilon_6 = \varepsilon_{12}$. The strain components ε_i are given by the series expansion shown in Eq (F.4).

$$\varepsilon_i = \sum_{p=0}^{n} \chi_i^p y_3^p \tag{F.4}$$

The nonzero χ_i^p are listed below for each component of the CDON code.

$$\chi_1^0 = u_{,1} + w_{,1}^2/2 \qquad \chi_1^1 = \psi_{1,1} \qquad \chi_1^3 = kw_{,11} + k\psi_{1,1}$$

$$\chi_2^0 = v_{,2} - cw + w_{,2}^2/2 \qquad \chi_2^1 = -cv_{,2} + \psi_{2,2} \qquad \chi_2^3 = kw_{,22} + k\psi_{2,2}$$

$$\chi_4^0 = \psi_2 + w_{,2} \qquad \chi_4^2 = k\psi_2 + w_{,2}$$

$$\chi_5^0 = \psi_1 + w_{,1} \qquad \chi_5^2 = k\psi_1 + w_{,1}$$

$$\chi_6^0 = u_{,2} + v_{,1} + w_{,1}w_{,2} \qquad \chi_6^1 = -cv_{,1} + \psi_{1,2} + \psi_{2,1} \qquad \chi_6^3 = 2kw_{,12} + k\psi_{1,2} + k\psi_{2,1}$$

Appendix G. *MACSYMA Routine for Elemental Codes Generation*

```
/*********************************************************************/
/*   MACSYMA ROUTINE FOR ELEMENTAL CODES GENERATION BY R. A. SMITH   */
/*   CREATED AS PART OF AIR FORCE INSTITUTE OF TECHNOLOGY (AFIT)     */
/*   PHD PROGRAM IN AERONAUTICAL ENGINEERING  ---  JULY 1991         */
/*              MACSYMA IS A REGISTERED TRADEMARK OF                 */
/*          THE MASSACHUSETTS INSTITUTE OF TECHNOLOGY.               */
/*********************************************************************/

/*   INITIALIZE MACSYMA PARAMETERS AND DECLARE VARIABLE PROPERTIES   */
[DYNAMALLOC:TRUE,DISKGC:TRUE,DERIVABBREV:TRUE,POWERDISP:TRUE]$
DEPENDS([U1D,U1R,U2D,U2R,U3,P1,P2,H1,H2],[Y1,Y2,Y3])$
DEPENDS([R1,R2,M1,M2,PSI1,PSI2,PHI1,PHI2],[Y1,Y2,Y3])$
DEPENDS([GAMMA1,GAMMA2,THETA1,THETA2,U,V,W],[Y1,Y2])$
DECLARE([R,C,AR1,AR2,AR3,AR4,H3],CONSTANT)$

/*   SET THEORETICAL ATTRIBUTES FOR SPECIFIC ELEMENTAL CODE          */
H3:1$                 /*  H3=1 FOR A SHELL                          */
AR1:1$                /*  AR1=0 FOR INCOMPLETE CUBIC KINEMATICS     */
                      /*  AR1=1 FOR COMPLETE QUARTIC KINEMATICS     */
AR2:1$                /*  AR2=0 FOR LINEAR H1/H2 APPROXIMATIONS     */
                      /*  AR2=1 FOR QUADRATIC    APPROXIMATIONS     */
AR3:1$                /*  AR3=0 FOR LINEAR TRANSVERSE STRAIN        */
                      /*  AR3=1 FOR NONLINEAR TRANSVERSE STRAIN     */

/*********************************************************************/
/*  SUBLIST IS A VARIABLE CONTAINING THE DEFINITIONS OF DISPLACEMENT */
/*  PARAMETERS Q(1) THROUGH Q(18).  ALL SYMBOLIC MANIPULATION OF     */
/*  STRAIN COMPONENTS IS DONE WITH THE NAMES TO THE LEFT OF THE EQUAL*/
/*  SIGNS IN SUBLIST.  THE Q(XX) DEFINITIONS ARE REQUIRED ONLY FOR   */
/*  GENERATION OF ELEMENT INDEPENDENT STRAIN DEFINITION ARRAYS LO    */
/*  THROUGH SS12, ETC.                                               */
/*********************************************************************/
SUBLIST:[ DIFF(U,Y1)=Q(2), DIFF(U,Y2)=Q(3), U=Q(1), DIFF(V,Y1)=Q(5),
DIFF(V,Y2)=Q(6), V=Q(4), DIFF(W,Y1,2)=Q(10), DIFF(W,Y2,2)=Q(11),
DIFF(W,Y1,1,Y2,1)=Q(12), DIFF(W,Y1)=Q(8), DIFF(W,Y2)=Q(9), W=Q(7),
DIFF(PSI1,Y1)=Q(14), DIFF(PSI1,Y2)=Q(15), PSI1=Q(13),
DIFF(PSI2,Y1)=Q(17), DIFF(PSI2,Y2)=Q(18), PSI2=Q(16)]$

/*********************************************************************/
/*  BEGIN GENERATING THE DISPLACEMENT FIELD COMPONENTS U1, U2, U3    */
/*  THESE NEXT STEPS HAVE BEEN SPECIALIZED FOR A CYLINDRICAL SHELL   */
/*  R2=1/C, R1=INFINITY, K=-4/(3*H^2).  THE VALUES OF C AND K WILL BE */
/*  INPUT AS PART OF THE FORTRAN PROGRAM.  THEY ARE UNSPECIFIED      */
/*  CONSTANTS AS FAR AS MACSYMA IS CONCERNED .                       */
/*********************************************************************/
P1:U$ P2:V*(1-Y3*C)$ P11:DIFF(U,Y1)$ P12:DIFF(U,Y2)$
P21:DIFF(V,Y1)*(1-Y3*C)$ P22:DIFF(V,Y2)*(1-Y3*C)$
```

```
L11:DIFF(PSI1,Y1)$ L22:DIFF(PSI2,Y2)$ L12:DIFF(PSI1,Y2)$
L21:DIFF(PSI2,Y1)$ M1:K*(DIFF(W,Y1)+PSI1)$ M2:K*(DIFF(W,Y2)+PSI2)$

U1D:P1+Y3*PSI1+Y3**3*M1; /* INCOMPLETE CUBIC U1 DISPLACEMENT OF DENNIS */
U2D:P2+Y3*PSI2+Y3**3*M2; /* INCOMPLETE CUBIC U2 DISPLACEMENT OF DENNIS */

/*************************************************************************/
/* COMPLETE QUARTIC U2 OF SMITH = U2D+U2R WHERE U2R ARE THE CURVATURE  */
/* CORRECTION TERMS.  NOTE: U1R=0, SINCE R1=INFINITY.                  */
/*************************************************************************/
U2R:(-M2*(1+K*Y3**2)*Y3**2/(K/C)); U2:U2D+U2R*AR1;
U1:U1D; U3:W$

/* SYMBOLICALLY COMPUTE THE DERIVATIVES OF U1 AND U2                   */
DU11:P11+L11*Y3+DIFF(M1,Y1)*Y3**3+DIFF(U1R,Y1);
DU21:P21+L21*Y3+DIFF(M2,Y1)*Y3**3+DIFF(U2R,Y1);
DU12:P12+L12*Y3+DIFF(M1,Y2)*Y3**3+DIFF(U1R,Y2);
DU22:P22+L22*Y3+DIFF(M2,Y2)*Y3**3+DIFF(U2R,Y2);

/*************************************************************************/
/* SYMBOLICALLY GENERATE THE GREEN-LAGARANGE STRAIN COMPONENTS DIVIDED  */
/* BY THE APPROPRIATE SHELL LAME PARAMETERS H1, H2, TO GIVE THE PHYSICAL*/
/* STRAINS EPSILON11,EPSILON22,EPSILON12,EPSILON23,EPSILON13,EPSILON33  */
/*************************************************************************/

/* EPSILON11 COMPONENT OF STRAIN. LINE 1 IS LINEAR TERMS. LINES 2-4 N.L. */
ER[1]:(H1*DU11+H1*U2/H2*DIFF(H1,Y2)+H1*U3/H3*DIFF(H1,Y3)+
1/2*(DU11+U2/H2*DIFF(H1,Y2)+U3/H3*DIFF(H1,Y3))^2+
1/2*(DU21-U1/H2*DIFF(H1,Y2))^2+
1/2*(DIFF(U3,Y1)-U1/H3*DIFF(H1,Y3))^2)/H1^2;

/* EPSILON22 COMPONENT OF STRAIN. LINE 1 IS LINEAR TERMS. LINES 2-4 N.L. */
ER[2]:(H2*DU22+H2*U3/H3*DIFF(H2,Y3)+H2*U1/H1*DIFF(H2,Y1)+
1/2*(DU22+U3/H3*DIFF(H2,Y3)+U1/H1*DIFF(H2,Y1))^2+
1/2*(DIFF(U3,Y2)-U2/H3*DIFF(H2,Y3))^2+
1/2*(DU12-U2/H1*DIFF(H2,Y1))^2)/H2^2;

/* EPSILON12 COMPONENT OF STRAIN. LINE 1 IS LINEAR TERMS. LINES 2-4 N.L. */
ER[6]:((H1*DU12+H2*DU21-U2*DIFF(H2,Y1)-U1*DIFF(H1,Y2))+
(DU12-U2/H1*DIFF(H2,Y1))*(DU11+U2/H2*DIFF(H1,Y2)+U3/H3*DIFF(H1,Y3))+
(DU21-U1/H2*DIFF(H1,Y2))*(DU22+U1/H1*DIFF(H2,Y1)+U3/H3*DIFF(H2,Y3))+
(DIFF(U3,Y1)-U1/H3*DIFF(H1,Y3))*(DIFF(U3,Y2)-U2/H3*DIFF(H2,Y3)))/(H1*H2);

/* EPSILON23 COMPONENT OF STRAIN. LINE 1 IS LINEAR TERMS. LINE 2-8 N.L.  */
/* F(Z)=1+3*K*Y3^2 PARABOLIC FORCING FUNCTION APPLIED ONLY TO N.L. TERMS */
ER[4]:(DIFF(U3,Y2)+(1-C*Y3)*DIFF(U2,Y3)-U2*(-C))/(H2*H3);
ERNL[4]:(1+3*K*Y3^2)*(
(DIFF(U2,Y3)-U3/H2*DIFF(H3,Y2))*
          (DIFF(U2,Y2)+U3/H3*DIFF(H2,Y3)+U1/H1*DIFF(H2,Y1))+
(DIFF(U3,Y2)-U2/H3*DIFF(H2,Y3))*
          (DIFF(U3,Y3)+U2/H2*DIFF(H3,Y2)+U1/H1*DIFF(H3,Y1))+
```

```
(DIFF(U1,Y2)-U2/H1*DIFF(H2,Y1))*
          (DIFF(U1,Y3)-U3/H1*DIFF(H3,Y1)))/(H2*H3);
ER[4]:ER[4]+ERNL[4]*AR3;

/* EPSILON13 COMPONENT OF STRAIN. LINE 1 IS LINEAR TERMS. LINE 2-8 N.L.  */
/* F(Z)=1+3*K*Y3^2 PARABOLIC FORCING FUNCTION APPLIED ONLY TO N.L. TERMS */
ER[5]:(H3*DIFF(U3,Y1)+H1*DIFF(U1,Y3)-U1*(0))/(H1*H3);
ERNL[5]:(1+3*K*Y3^2)*(
(DIFF(U1,Y3)-U3/H1*DIFF(H3,Y1))*
          (DIFF(U1,Y1)+U3/H3*DIFF(H1,Y3)+U2/H2*DIFF(H1,Y2))+
(DIFF(U3,Y1)-U1/H3*DIFF(H1,Y3))*
          (DIFF(U3,Y3)+U1/H1*DIFF(H3,Y1)+U2/H2*DIFF(H3,Y2))+
(DIFF(U2,Y1)-U1/H2*DIFF(H1,Y2))*
          (DIFF(U2,Y3)-U3/H2*DIFF(H3,Y2)))/(H1*H3);
ER[5]:ER[5]+ERNL[5]*AR3;

/* EPSILON33 COMPONENT OF STRAIN IS ZERO.  IT IS HOWEVER INCLUDED IN THE
*  CONSTITUTIVE RELATIONS THROUGH THE ELASTICITY SUBROUTINE OF THE CODE
*  WRITTEN BY DENNIS.                                                    */
ER[3]:0;

/* SUBSTITUTE THE Q(1) THROUGH Q(18) DEFINITIONS OF SUBLIST AND DISPLAY
*  STRAIN COMPONENTS INDIVIDUALLY                                        */
FOR I THRU 6 DO (ER[I]:EXPAND(ER[I]),
ER[I]:EXPAND(SUBST(SUBLIST,ER[I])),DISPLAY(ER[I])     )$

/*************************************************************************/
/*   THE NEXT 60 EXPRESSIONS ARE THE POSSIBLE COMBINATIONS OF LAME       */
/*   PARAMETERS APPEARING IN THE STRAIN EXPRESSIONS FOR A ANY SHELL,     */
/*   WHERE, H3=1 AND H1,H2 DEPEND UPON Y1,Y2, AND Y3.                    */
/*************************************************************************/
HREXP[1]:(DIFF(H1,Y2)/H1)$
HREXP[2]:(DIFF(H1,Y3)/H1)$
HREXP[3]:(1/(H1**2))$
HREXP[4]:(DIFF(H1,Y2)**2/(H1**2))$
HREXP[5]:(DIFF(H1,Y2)**2/(H2**2))$
HREXP[6]:(DIFF(H1,Y3)**2/(H1**2))$
HREXP[7]:(DIFF(H1,Y3)**2)$
HREXP[8]:(DIFF(H1,Y2)*DIFF(H1,Y3)/(H1**2))$
HREXP[9]:(DIFF(H2,Y3)/H2)$
HREXP[10]:(DIFF(H2,Y1)/H2)$
HREXP[11]:(1/(H2**2))$
HREXP[12]:(DIFF(H2,Y1)**2/(H2**2))$
HREXP[13]:(DIFF(H2,Y1)**2/(H1**2))$
HREXP[14]:(DIFF(H2,Y3)**2/(H2**2))$
HREXP[15]:DIFF(H2,Y3)**2$
HREXP[16]:(DIFF(H2,Y3)*DIFF(H2,Y1)/(H2**2))$
HREXP[17]:(1/H2)$
HREXP[18]:(1/H1)$
HREXP[19]:(DIFF(H2,Y1)/H1)$
HREXP[20]:(DIFF(H1,Y2)/H2)$
```

```
HREXP[21]:(1/(H1*H2))$
HREXP[22]:(DIFF(H1,Y3)/H2)$
HREXP[23]:(DIFF(H2,Y3)/H1)$
HREXP[24]:(DIFF(H2,Y1)*DIFF(H1,Y2)/(H1**2))$
HREXP[25]:(DIFF(H2,Y1)*DIFF(H1,Y2)/(H2**2))$
HREXP[26]:(DIFF(H1,Y3)*DIFF(H2,Y3))$
HREXP[27]:(DIFF(H1,Y3)*DIFF(H2,Y1)/(H1**2))$
HREXP[28]:(DIFF(H2,Y3)*DIFF(H1,Y2)/(H2**2))$
HREXP[29]:(DIFF(H1,Y2)/(H1*H2))$
HREXP[30]:(DIFF(H1,Y2)**2/(H1**2*H2))$
HREXP[31]:(DIFF(H1,Y2)**2/(H2**2*H1))$
HREXP[32]:(DIFF(H1,Y3)**2/H1)$
HREXP[33]:(DIFF(H1,Y2)/(H1**2))$
HREXP[34]:(DIFF(H1,Y3)/(H1**2))$
HREXP[35]:(DIFF(H1,Y2)*DIFF(H1,Y3)/(H1**2*H2))$
HREXP[36]:(DIFF(H2,Y1)/(H1*H2))$
HREXP[37]:(DIFF(H2,Y1)**2/(H1*H2**2))$
HREXP[38]:(DIFF(H2,Y1)**2/(H2*H1**2))$
HREXP[39]:(DIFF(H2,Y3)**2/H2)$
HREXP[40]:(DIFF(H2,Y1)/(H2**2))$
HREXP[41]:(DIFF(H2,Y3)*DIFF(H2,Y1)/(H1*H2**2))$
HREXP[42]:(DIFF(H2,Y3)/(H2**2))$
HREXP[43]:(DIFF(H1,Y2)/(H2**2))$
HREXP[44]:(DIFF(H2,Y1)/(H1**2))$
HREXP[45]:(DIFF(H1,Y3)/(H1*H2))$
HREXP[46]:(DIFF(H2,Y3)/(H1*H2))$
HREXP[47]:(DIFF(H2,Y1)*DIFF(H1,Y2)/(H1**2*H2))$
HREXP[48]:(DIFF(H1,Y2)*DIFF(H2,Y1)/(H2**2*H1))$
HREXP[49]:(DIFF(H1,Y3)*DIFF(H2,Y1)/(H1**2*H2))$
HREXP[50]:(DIFF(H2,Y3)*DIFF(H1,Y2)/(H2**2*H1))$
HREXP[51]:(DIFF(H1,Y3)*DIFF(H2,Y3)/H2)$
HREXP[52]:(DIFF(H1,Y3)*DIFF(H2,Y3)/H1)$
HREXP[53]:(DIFF(H1,Y2)**2/(H1**2*H2**2))$
HREXP[54]:(DIFF(H1,Y2)/(H1**2*H2))$
HREXP[55]:(DIFF(H2,Y1)**2/(H1**2*H2**2))$
HREXP[56]:(DIFF(H2,Y1)/(H2**2*H1))$
HREXP[57]:(DIFF(H1,Y2)/(H1*H2**2))$
HREXP[58]:(DIFF(H2,Y1)/(H2*H1**2))$
HREXP[59]:(DIFF(H2,Y1)*DIFF(H1,Y2)/(H1**2*H2**2))$
HREXP[60]:(DIFF(H1,Y3)*DIFF(H2,Y3)/(H1*H2))$

/*************************************************************************/
/*   THIS MACRO HRTAY(X,I)::= GENERATES THE COEFFICIENTS F, G, AND H OF */
/*   THE TAYLOR'S SERIES EXPANSION OF THE EXPRESSION X ABOUT THE POINT  */
/*   Y3=0 FOR A CYLINDRICAL SHELL WITH H1=1 AND H2=1-Y3/R2              */
/*************************************************************************/
HRTAY(X,I)::= BUILDQ([X,I],(
PRINT("  THE TAYLOR SERIES SCALE FACTOR EXPANSION OF
"),DISPLAY(X),
PRINT("  IS EQUAL TO F + G*Y3 + H*Y3**2 + H.O.T., WHERE "),
(X:TAYLOR(FACTOROUT(EXPAND(RAT(EV(X,H1=1,H2=(1-Y3*C),DIFF))),C),Y3,0,3)),
```

```
 F[I]:EXPAND(COEFF(X,Y3,0)),DISPLAY(F[I]),
 G[I]:EXPAND(COEFF(X,Y3,1)),DISPLAY(G[I]),
 H[I]:EXPAND(COEFF(X,Y3,2)),DISPLAY(H[I]))$

/*   COMPUTE THE COEFFICIENTS F, G, H, FOR ALL 60 HREXP EXPRESSIONS     */
FOR I THRU 60 DO HRTAY(HREXP[I],I)$

/*********************************************************************/
/*   MACRO HRSUB(X) TAKES ANY ONE-TERM EXPRESSION X, (PRODUCTS ARE OK,  */
/*   BUT [+-] OPERATORS ARE NOT) AND SUBSTITUTES THE APPROXIMATE SERIES */
/*   EXPANSION F+G*Y3+AR2*H*Y3^2  FOR THE FUNCTION OF LAME PARAMETERS   */
/*********************************************************************/
HRSUB(X)::=BUILDQ([X],(
XO:X,
X:NUM(X)/SUBST(D[1],H1,DENOM(X)),
X:NUM(X)/SUBST(D[2],H2,DENOM(X)),
X:NUM(X)/RATSUBST(D[3],D[1]*D[1],DENOM(X)),
X:NUM(X)/RATSUBST(D[4],D[2]*D[2],DENOM(X)),
X:NUM(X)/RATSUBST(D[5],D[1]*D[2],DENOM(X)),
X:NUM(X)/RATSUBST(D[6],D[1]*D[4],DENOM(X)),
X:NUM(X)/RATSUBST(D[7],D[2]*D[3],DENOM(X)),
X:NUM(X)/RATSUBST(D[8],D[3]*D[4],DENOM(X)),
XD:X,
X:NUM(X)/RATSUBST(1/D[1],D[1],DENOM(X)),
X:NUM(X)/RATSUBST(1/D[2],D[2],DENOM(X)),
X:NUM(X)/RATSUBST(1/D[3],D[3],DENOM(X)),
X:NUM(X)/RATSUBST(1/D[4],D[4],DENOM(X)),
X:NUM(X)/RATSUBST(1/D[5],D[5],DENOM(X)),
X:NUM(X)/RATSUBST(1/D[6],D[6],DENOM(X)),
X:NUM(X)/RATSUBST(1/D[7],D[7],DENOM(X)),
X:NUM(X)/RATSUBST(1/D[8],D[8],DENOM(X)),
XN:X,
X:RATSUBST(F[59]+Y3*G[59]+Y3**2*AR2*H[59],'DIFF(H2,Y1)*'DIFF(H1,Y2)*D[8],X),
X:RATSUBST(F[55]+Y3*G[55]+Y3**2*AR2*H[55],'DIFF(H2,Y1)**2*D[8],X),
X:RATSUBST(F[53]+Y3*G[53]+Y3**2*AR2*H[53],'DIFF(H1,Y2)**2*D[8],X),
X:RATSUBST(F[50]+Y3*G[50]+Y3**2*AR2*H[50],'DIFF(H2,Y3)*'DIFF(H1,Y2)*D[6],X),
X:RATSUBST(F[49]+Y3*G[49]+Y3**2*AR2*H[49],'DIFF(H1,Y3)*'DIFF(H2,Y1)*D[7],X),
X:RATSUBST(F[48]+Y3*G[48]+Y3**2*AR2*H[48],'DIFF(H1,Y2)*'DIFF(H2,Y1)*D[6],X),
X:RATSUBST(F[47]+Y3*G[47]+Y3**2*AR2*H[47],'DIFF(H2,Y1)*'DIFF(H1,Y2)*D[7],X),
X:RATSUBST(F[41]+Y3*G[41]+Y3**2*AR2*H[41],'DIFF(H2,Y3)*'DIFF(H2,Y1)*D[6],X),
X:RATSUBST(F[38]+Y3*G[38]+Y3**2*AR2*H[38],'DIFF(H2,Y1)**2*D[7],X),
X:RATSUBST(F[37]+Y3*G[37]+Y3**2*AR2*H[37],'DIFF(H2,Y1)**2*D[6],X),
X:RATSUBST(F[35]+Y3*G[35]+Y3**2*AR2*H[35],'DIFF(H1,Y2)*'DIFF(H1,Y3)*D[7],X),
X:RATSUBST(F[31]+Y3*G[31]+Y3**2*AR2*H[31],'DIFF(H1,Y2)**2*D[6],X),
X:RATSUBST(F[30]+Y3*G[30]+Y3**2*AR2*H[30],'DIFF(H1,Y2)**2*D[7],X),
X:RATSUBST(F[58]+Y3*G[58]+Y3**2*AR2*H[58],'DIFF(H2,Y1)*D[7],X),
X:RATSUBST(F[57]+Y3*G[57]+Y3**2*AR2*H[57],'DIFF(H1,Y2)*D[6],X),
X:RATSUBST(F[56]+Y3*G[56]+Y3**2*AR2*H[56],'DIFF(H2,Y1)*D[6],X),
X:RATSUBST(F[54]+Y3*G[54]+Y3**2*AR2*H[54],'DIFF(H1,Y2)*D[7],X),
X:RATSUBST(F[60]+Y3*G[60]+Y3**2*AR2*H[60],'DIFF(H1,Y3)*'DIFF(H2,Y3)*D[5],X),
X:RATSUBST(F[28]+Y3*G[28]+Y3**2*AR2*H[28],'DIFF(H2,Y3)*'DIFF(H1,Y2)*D[4],X),
```

```
X:RATSUBST(F[27]+Y3*G[27]+Y3**2*AR2*H[27],'DIFF(H1,Y3)*'DIFF(H2,Y1)*D[3],X),
X:RATSUBST(F[25]+Y3*G[25]+Y3**2*AR2*H[25],'DIFF(H2,Y1)*'DIFF(H1,Y2)*D[4],X),
X:RATSUBST(F[24]+Y3*G[24]+Y3**2*AR2*H[24],'DIFF(H2,Y1)*'DIFF(H1,Y2)*D[3],X),
X:RATSUBST(F[16]+Y3*G[16]+Y3**2*AR2*H[16],'DIFF(H2,Y3)*'DIFF(H2,Y1)*D[4],X),
X:RATSUBST(F[8]+Y3*G[8]+Y3**2*AR2*H[8],'DIFF(H1,Y2)*'DIFF(H1,Y3)*D[3],X),
X:RATSUBST(F[14]+Y3*G[14]+Y3**2*AR2*H[14],'DIFF(H2,Y3)**2*D[4],X),
X:RATSUBST(F[13]+Y3*G[13]+Y3**2*AR2*H[13],'DIFF(H2,Y1)**2*D[3],X),
X:RATSUBST(F[12]+Y3*G[12]+Y3**2*AR2*H[12],'DIFF(H2,Y1)**2*D[4],X),
X:RATSUBST(F[6]+Y3*G[6]+Y3**2*AR2*H[6],'DIFF(H1,Y3)**2*D[3],X),
X:RATSUBST(F[5]+Y3*G[5]+Y3**2*AR2*H[5],'DIFF(H1,Y2)**2*D[4],X),
X:RATSUBST(F[4]+Y3*G[4]+Y3**2*AR2*H[4],'DIFF(H1,Y2)**2*D[3],X),
X:RATSUBST(F[46]+Y3*G[46]+Y3**2*AR2*H[46],'DIFF(H2,Y3)*D[5],X),
X:RATSUBST(F[45]+Y3*G[45]+Y3**2*AR2*H[45],'DIFF(H1,Y3)*D[5],X),
X:RATSUBST(F[44]+Y3*G[44]+Y3**2*AR2*H[44],'DIFF(H2,Y1)*D[3],X),
X:RATSUBST(F[43]+Y3*G[43]+Y3**2*AR2*H[43],'DIFF(H1,Y2)*D[4],X),
X:RATSUBST(F[42]+Y3*G[42]+Y3**2*AR2*H[42],'DIFF(H2,Y3)*D[4],X),
X:RATSUBST(F[40]+Y3*G[40]+Y3**2*AR2*H[40],'DIFF(H2,Y1)*D[4],X),
X:RATSUBST(F[36]+Y3*G[36]+Y3**2*AR2*H[36],'DIFF(H2,Y1)*D[5],X),
X:RATSUBST(F[34]+Y3*G[34]+Y3**2*AR2*H[34],'DIFF(H1,Y3)*D[3],X),
X:RATSUBST(F[33]+Y3*G[33]+Y3**2*AR2*H[33],'DIFF(H1,Y2)*D[3],X),
X:RATSUBST(F[29]+Y3*G[29]+Y3**2*AR2*H[29],'DIFF(H1,Y2)*D[5],X),
X:RATSUBST(F[3]+Y3*G[3]+Y3**2*AR2*H[3],1*D[3],X),
X:RATSUBST(F[21]+Y3*G[21]+Y3**2*AR2*H[21],1*D[5],X),
X:RATSUBST(F[11]+Y3*G[11]+Y3**2*AR2*H[11],1*D[4],X),
X:RATSUBST(F[52]+Y3*G[52]+Y3**2*AR2*H[52],'DIFF(H1,Y3)*'DIFF(H2,Y3)*D[1],X),
X:RATSUBST(F[51]+Y3*G[51]+Y3**2*AR2*H[51],'DIFF(H1,Y3)*'DIFF(H2,Y3)*D[2],X),
X:RATSUBST(F[39]+Y3*G[39]+Y3**2*AR2*H[39],'DIFF(H2,Y3)**2*D[2],X),
X:RATSUBST(F[32]+Y3*G[32]+Y3**2*AR2*H[32],'DIFF(H1,Y3)**2*D[1],X),
X:RATSUBST(F[23]+Y3*G[23]+Y3**2*AR2*H[23],'DIFF(H2,Y3)*D[1],X),
X:RATSUBST(F[22]+Y3*G[22]+Y3**2*AR2*H[22],'DIFF(H1,Y3)*D[2],X),
X:RATSUBST(F[20]+Y3*G[20]+Y3**2*AR2*H[20],'DIFF(H1,Y2)*D[2],X),
X:RATSUBST(F[19]+Y3*G[19]+Y3**2*AR2*H[19],'DIFF(H2,Y1)*D[1],X),
X:RATSUBST(F[10]+Y3*G[10]+Y3**2*AR2*H[10],'DIFF(H2,Y1)*D[2],X),
X:RATSUBST(F[9]+Y3*G[9]+Y3**2*AR2*H[9],'DIFF(H2,Y3)*D[2],X),
X:RATSUBST(F[1]+Y3*G[1]+Y3**2*AR2*H[1],'DIFF(H1,Y2)*D[1],X),
X:RATSUBST(F[2]+Y3*G[2]+Y3**2*AR2*H[2],'DIFF(H1,Y3)*D[1],X),
X:RATSUBST(F[17]+Y3*G[17]+Y3**2*AR2*H[17],1*D[2],X),
X:RATSUBST(F[18]+Y3*G[18]+Y3**2*AR2*H[18],1*D[1],X),
X:RATSUBST(F[15]+Y3*G[15]+Y3**2*AR2*H[15],'DIFF(H2,Y3)**2,X),
X:RATSUBST(F[7]+Y3*G[7]+Y3**2*AR2*H[7],'DIFF(H1,Y3)**2,X),
X:RATSUBST(F[26]+Y3*G[26]+Y3**2*AR2*H[26],'DIFF(H1,Y3)*'DIFF(H2,Y3),X)))$

/*********************************************************************/
/*   MACRO PICK(XXX) TAKES ANY EXPRESSION XXX (PREVIOUSLY EXPANDED)  */
/*   AND SEPARATES IT INTO SINGLE EXPRESSIONS LABELED E(I).  IT THEN */
/*   CALLS MACRO HRSUB(X) TO FIND THE APPROPRIATE LAME PARAMETER     */
/*   APPROXIMATION FOR EACH EXPRESSION AND THEN SUMS ALL THE EXPRES- */
/*   SIONS TO YIELD THE EXPRESSION XXX WITH ALL TERMS FULLY APPROXIMATED*/
/*********************************************************************/
E(I):=CONCAT(E,I)$
PICK(XXX)::=BUILDQ([XXX],(
```

```
I1:LINENUM,
NT:NTERMS(XXX),
I2:I1+NT-1,
PRINT(" THIS EXPRESSION HAS",NT,"TERMS TO BE RESOLVED"),
PICKAPART(XXX,1),
FOR K:I1 THRU I2 DO EXH[K]:EV(E(K),EVAL),
FOR K:I1 THRU I2 DO HRSUB(EXH[K]),
XXX:SUM(EXH[K],K,I1,I2),
DISPLAY(XXX)                ))$

/*************************************************************************/
/*    USE MACRO PICK(XXX) TO APPROXIMATE LAME PARAMETER FUNCTIONS OF     */
/*    THE STRAIN COMPONENTS                                              */
/*************************************************************************/
ERR4:ER[4]$ ERR5:ER[5]$
PICK(ERR4); PICK(ERR5);
ER[4]:ERR4$ ER[5]:ERR5$
ERR1:ER[1]$ ERR2:ER[2]$ ERR6:ER[6]$
PICK(ERR1); PICK(ERR2); PICK(ERR6);
ER[1]:ERR1$ ER[2]:ERR2$ ER[6]:ERR6$
SAVE("ER123.SV",ER);

/*************************************************************************/
/*    THIS MACRO, CHIFORM(XX,YY,K)::= EXPANDS A 6X1 VECTOR CALLED XX,    */
/*    THEN DETERMINES AND DISPLAYS THE COEFFICIENTS OF Y3 UPTO THE       */
/*    KTH POWER.   THESE ARE CALLED YY[I,K].                             */
/*************************************************************************/
CHIFORM(XX,YY,K)::=BUILDQ([XX,YY,K],
(FOR I THRU 6 DO FOR JJ THRU K+1 DO
(XY[I]:FACTOROUT(EXPAND(RAT(XX[I])),[H1,H2]),
YY[I,JJ-1]:COEFF(XY[I],Y3,JJ-1),
DISPLAY(YY[I,JJ-1]))))$

POWERDISP:TRUE$ CHIFORM(ER,XR,12); KILL(ER); SAVE("XR123.SV",XR);

/*************************************************************************/
/*    THIS MACRO, DECOMPOSE(XR)::= DETERMINES AND DISPLAYS THE COEFFIC-  */
/*    IENTS OF DISPLACEMENT VARIABLES Q(1) THROUGH Q(18) AND CREATES A   */
/*    6X13X18 ARRAY CALLED LMAT OF THE CONSTANT COEFFICIENTS OF LINEAR   */
/*    DISPLACEMENT TERMS, AND A 6X13X18X18 ARRAY CALLED HMAT OF THE      */
/*    CONSTANT COEFFICIENTS OF THE QUADRATIC DISPLACEMENT TERMS.         */
/*************************************************************************/
DECOMPOSE(XR)::=BUILDQ([XR],
(FOR I THRU 6 DO (PRINT("DECOMPOSING STRAIN COMPONENT",I),
(FOR J:0 THRU 12 DO
(FOR K THRU 18 DO
(IF HIPOW(XR[I,J],Q(K))=2 THEN
XQUAD[I,J,K].RATCOEFF(XR[I,J],Q(K),2)*Q(K)*2+RATCOEFF(XR[I,J],Q(K),1) ELSE
XQUAD[I,J,K]:RATCOEFF(XR[I,J],Q(K),1),
FOR L THRU 18 DO HMAT[I,J,K,L]:RATCOEFF(XQUAD[I,J,K],Q(L),1),
LMAT[I,J,K]:EXPAND(XQUAD[I,J,K]-SUM(HMAT[I,J,K,L]*Q(L),L,1,18)))))))$
```

```
DECOMPOSE(XR);
KILL(XR);
SAVE("LHMAT.SV-123",LMAT,HMAT);

/*************************************************************************/
/*   GENERATE ELEMENT-INDEPENDENT STRAIN DEFINITION ARRAYS LX AND HXX    */
/*   FOR INPLANE STRAINS AND SX AND SSXX FOR TRANSVERSE SHEAR STRAINS.   */
/*   X AND XX REPRESENT THE POWER OF Y3 FOR WHICH THE COEFFICIENTS       */
/*   APPLY.  NOTE LX HAS 3 COLUMNS.  COLUMN 1 CONTAINS COEFFICIENTS OF   */
/*   THE EPSILON11 TERMS WHICH ARE LINEAR IN DISPLACEMENTS Q(1)-Q(18).   */
/*   COLUMN 2 CONTAINS EPSILON22 TERMS AND COLUMN 3 CONTAINS EPSILON12   */
/*   TERMS.  LIKEWISE HXX HAS 3 PARTITIONS.  COLUMNS 1-18 CONTAINS       */
/*   COEFFICIENTS OF EPSILON11 TERMS WHICH ARE QUADRATIC IN DISPLACE-    */
/*   MENT.  COLUMNS 19-36 CONTAIN THE EPSILON22 TERMS AND COLUMNS 37-54  */
/*   CONTAIN THE EPSILON12 TERMS.  SIMILARLY, SX CONTAINS 2 COLUMNS      */
/*   PERTAINING TO THE COEFFICIENTS OF LINEAR TERMS OF EPSILON23 AND     */
/*   EPSILON13, RESPECTIVELY.  SSXX HAS 2 PARTITIONS.  COLUMNS 1-18      */
/*   PERTAIN TO THE COEFFICIENTS OF THE QUADRATIC TERMS OF EPSILON23     */
/*   AND EPSILON13, RESPECTIVELY.                                        */
/*************************************************************************/
FOR NN THRU 18 DO  (
L0[NN,1]:LMAT[1,0,NN],L0[NN,2]:LMAT[2,0,NN],L0[NN,3]:LMAT[6,0,NN],
L1[NN,1]:LMAT[1,1,NN],L1[NN,2]:LMAT[2,1,NN],L1[NN,3]:LMAT[6,1,NN],
L2[NN,1]:LMAT[1,2,NN],L2[NN,2]:LMAT[2,2,NN],L2[NN,3]:LMAT[6,2,NN],
L3[NN,1]:LMAT[1,3,NN],L3[NN,2]:LMAT[2,3,NN],L3[NN,3]:LMAT[6,3,NN],
L4[NN,1]:LMAT[1,4,NN],L4[NN,2]:LMAT[2,4,NN],L4[NN,3]:LMAT[6,4,NN],
L5[NN,1]:LMAT[1,5,NN],L5[NN,2]:LMAT[2,5,NN],L5[NN,3]:LMAT[6,5,NN],
L6[NN,1]:LMAT[1,6,NN],L6[NN,2]:LMAT[2,6,NN],L6[NN,3]:LMAT[6,6,NN],
L7[NN,1]:LMAT[1,7,NN],L7[NN,2]:LMAT[2,7,NN],L7[NN,3]:LMAT[6,7,NN],
S0[NN,1]:LMAT[4,0,NN],S0[NN,2]:LMAT[5,0,NN],
S1[NN,1]:LMAT[4,1,NN],S1[NN,2]:LMAT[5,1,NN],
S2[NN,1]:LMAT[4,2,NN],S2[NN,2]:LMAT[5,2,NN],
S3[NN,1]:LMAT[4,3,NN],S3[NN,2]:LMAT[5,3,NN],
S4[NN,1]:LMAT[4,4,NN],S4[NN,2]:LMAT[5,4,NN],
S5[NN,1]:LMAT[4,5,NN],S5[NN,2]:LMAT[5,5,NN],
S6[NN,1]:LMAT[4,6,NN],S6[NN,2]:LMAT[5,6,NN],
S7[NN,1]:LMAT[4,7,NN],S7[NN,2]:LMAT[5,7,NN],
FOR MM THRU 18 DO (
H0[NN,MM]:HMAT[1,0,NN,MM],H0[NN,MM+18]:HMAT[2,0,NN,MM],
H0[NN,MM+36]:HMAT[6,0,NN,MM],
H1[NN,MM]:HMAT[1,1,NN,HM],H1[NN,MM+18]:HMAT[2,1,NN,MM],
H1[NN,MM+36]:HMAT[6,1,NN,MM],
H2[NN,MM]:HMAT[1,2,NN,MM],H2[NN,MM+18]:HMAT[2,2,NN,MM],
H2[NN,MM+36]:HMAT[6,2,NN,MM],
H3[NN,MM]:HMAT[1,3,NN,MM],H3[NN,MM+18]:HMAT[2,3,NN,MM],
H3[NN,MM+36]:HMAT[6,3,NN,MM],
H4[NN,MM]:HMAT[1,4,NN,MM],H4[NN,MM+18]:HMAT[2,4,NN,MM],
H4[NN,MM+36]:HMAT[6,4,NN,MM],
H5[NN,MM]:HMAT[1,5,NN,MM],H5[NN,MM+18]:HMAT[2,5,NN,MM],
H5[NN,MM+36]:HMAT[6,5,NN,MM],
```

```
H6[NN,MM]:HMAT[1,6,NN,MM],H6[NN,MM+18]:HMAT[2,6,NN,MM],
H6[NN,MM+36]:HMAT[6,6,NN,MM],
H7[NN,MM]:HMAT[1,7,NN,MM],H7[NN,MM+18]:HMAT[2,7,NN,MM],
H7[NN,MM+36]:HMAT[6,7,NN,MM],
H8[NN,MM]:HMAT[1,8,NN,MM],H8[NN,MM+18]:HMAT[2,8,NN,MM],
H8[NN,MM+36]:HMAT[6,8,NN,MM],
H9[NN,MM]:HMAT[1,9,NN,MM],H9[NN,MM+18]:HMAT[2,9,NN,MM],
H9[NN,MM+36]:HMAT[6,9,NN,MM],
H10[NN,MM]:HMAT[1,10,NN,MM],H10[NN,MM+18]:HMAT[2,10,NN,MM],
H10[NN,MM+36]:HMAT[6,10,NN,MM],
H11[NN,MM]:HMAT[1,11,NN,MM],H11[NN,MM+18]:HMAT[2,11,NN,MM],
H11[NN,MM+36]:HMAT[6,11,NN,MM],
H12[NN,MM]:HMAT[1,12,NN,MM],H12[NN,MM+18]:HMAT[2,12,NN,MM],
H12[NN,MM+36]:HMAT[6,12,NN,MM],
SS0[NN,MM]:HMAT[4,0,NN,MM],SS0[NN,MM+18]:HMAT[5,0,NN,MM],
SS1[NN,MM]:HMAT[4,1,NN,MM],SS1[NN,MM+18]:HMAT[5,1,NN,MM],
SS2[NN,MM]:HMAT[4,2,NN,MM],SS2[NN,MM+18]:HMAT[5,2,NN,MM],
SS3[NN,MM]:HMAT[4,3,NN,MM],SS3[NN,MM+18]:HMAT[5,3,NN,MM],
SS4[NN,MM]:HMAT[4,4,NN,MM],SS4[NN,MM+18]:HMAT[5,4,NN,MM],
SS5[NN,MM]:HMAT[4,5,NN,MM],SS5[NN,MM+18]:HMAT[5,5,NN,MM],
SS6[NN,MM]:HMAT[4,6,NN,MM],SS6[NN,MM+18]:HMAT[5,6,NN,MM],
SS7[NN,MM]:HMAT[4,7,NN,MM],SS7[NN,MM+18]:HMAT[5,7,NN,MM],
SS8[NN,MM]:HMAT[4,8,NN,MM],SS8[NN,MM+18]:HMAT[5,8,NN,MM],
SS9[NN,MM]:HMAT[4,9,NN,MM],SS9[NN,MM+18]:HMAT[5,9,NN,MM],
SS11[NN,MM]:HMAT[4,11,NN,MM],SS11[NN,MM+18]:HMAT[5,11,NN,MM],
SS12[NN,MM]:HMAT[4,12,NN,MM],SS12[NN,MM+18]:HMAT[5,12,NN,MM],
SS10[NN,MM]:HMAT[4,10,NN,MM],SS10[NN,MM+18]:HMAT[5,10,NN,MM]))$

/*   FORM MACSYMA MATRICES FROM THE ABOVE DEFINED ARRAYS.                */
L0:GENMATRIX(L0,18,3)$ L1:GENMATRIX(L1,18,3)$ L2:GENMATRIX(L2,18,3)$
L3:GENMATRIX(L3,18,3)$ L4:GENMATRIX(L4,18,3)$ L5:GENMATRIX(L5,18,3)$
L6:GENMATRIX(L6,18,3)$ L7:GENMATRIX(L7,18,3)$
S0:GENMATRIX(S0,18,2)$ S1:GENMATRIX(S1,18,2)$ S2:GENMATRIX(S2,18,2)$
S3:GENMATRIX(S3,18,2)$ S4:GENMATRIX(S4,18,2)$ S5:GENMATRIX(S5,18,2)$
S6:GENMATRIX(S6,18,2)$ S7:GENMATRIX(S7,18,2)$
H0:GENMATRIX(H0,18,54)$ H1:GENMATRIX(H1,18,54)$ H2:GENMATRIX(H2,18,54)$
H3:GENMATRIX(H3,18,54)$ H4:GENMATRIX(H4,18,54)$ H5:GENMATRIX(H5,18,54)$
H6:GENMATRIX(H6,18,54)$ H7:GENMATRIX(H7,18,54)$ H8:GENMATRIX(H8,18,54)$
H9:GENMATRIX(H9,18,54)$ H10:GENMATRIX(H10,18,54)$
H11:GENMATRIX(H11,18,54)$ H12:GENMATRIX(H12,18,54)$
SS0:GENMATRIX(SS0,18,36)$ SS1:GENMATRIX(SS1,18,36)$
SS2:GENMATRIX(SS2,18,36)$ SS3:GENMATRIX(SS3,18,36)$
SS4:GENMATRIX(SS4,18,36)$ SS5:GENMATRIX(SS5,18,36)$
SS6:GENMATRIX(SS6,18,36)$ SS7:GENMATRIX(SS7,18,36)$
SS8:GENMATRIX(SS8,18,36)$ SS9:GENMATRIX(SS9,18,36)$
SS10:GENMATRIX(SS10,18,36)$ SS11:GENMATRIX(SS11,18,36)$
SS12:GENMATRIX(SS12,18,36)$
SAVE("LSMAT123.SV",L0,L1,L2,L3,L4,L5,L6,L7,S0,S1,S2,S3,S4,S5,S6,S7);
SAVE("HMAT123.SV",H0,H1,H2,H3,H4,H5,H6,H7,H8,H9,H10,H11,H12);
SAVE("SSMAT123.SV",SS0,SS1,SS2,SS3,SS4,SS5,SS6,SS7,SS8,SS9,SS10,SS11,SS12);
KILL(ALL)$
```

```
/*************************************************************************/
/*   GENERATE THE LINEAR ELEMENT-INDEPENDENT STIFFNESS ARRAY K.          */
/*************************************************************************/

/* ASSEMBLE MATRIX KO */
LOADFILE("LSMAT123.SV")$
LO:SUBST([K=K1,C=P1],LO)$ L1:SUBST([K=K1,C=P1],L1)$
L2:SUBST([K=K1,C=P1],L2)$ L3:SUBST([K=K1,C=P1],L3)$
L4:SUBST([K=K1,C=P1],L4)$ L5:SUBST([K=K1,C=P1],L5)$
L6:SUBST([K=K1,C=P1],L6)$ L7:SUBST([K=K1,C=P1],L7)$
LOT:TRANSPOSE(LO); L1T:TRANSPOSE(L1); L2T:TRANSPOSE(L2);
L3T:TRANSPOSE(L3); L4T:TRANSPOSE(L4); L5T:TRANSPOSE(L5);
L6T:TRANSPOSE(L6); L7T:TRANSPOSE(L7); KM:ZEROMATRIX(18,18)$

FOR II THRU 3 DO FOR JJ THRU 3 DO (PRINT(II,JJ),
KM:KM+A[II,JJ]*(COL(LO,II).ROW(LOT,JJ))+
    DD[II,JJ]*(COL(L1,II).ROW(L1T,JJ)+
               COL(LO,II).ROW(L2T,JJ)+
               COL(L2,II).ROW(LOT,JJ))+
    F[II,JJ]*(COL(L2,II).ROW(L2T,JJ)+
              COL(L1,II).ROW(L3T,JJ)+ COL(L3,II).ROW(L1T,JJ)+
              COL(LO,II).ROW(L4T,JJ)+ COL(L4,II).ROW(LOT,JJ))+
    H[II,JJ]*(COL(L3,II).ROW(L3T,JJ)+
              COL(L2,II).ROW(L4T,JJ)+COL(L4,II).ROW(L2T,JJ)+
              COL(L1,II).ROW(L5T,JJ)+COL(L5,II).ROW(L1T,JJ)+
              COL(LO,II).ROW(L6T,JJ)+COL(L6,II).ROW(LOT,JJ))+
    J[II,JJ]*(COL(L4,II).ROW(L4T,JJ)+
              COL(L3,II).ROW(L5T,JJ)+COL(L5,II).ROW(L3T,JJ)+
              COL(L2,II).ROW(L6T,JJ)+COL(L6,II).ROW(L2T,JJ)+
              COL(L1,II).ROW(L7T,JJ)+COL(L7,II).ROW(L1T,JJ))+
    L[II,JJ]*(COL(L5,II).ROW(L5T,JJ)+
              COL(L4,II).ROW(L6T,JJ)+COL(L6,II).ROW(L4T,JJ)+
              COL(L3,II).ROW(L7T,JJ)+COL(L7,II).ROW(L3T,JJ) )+
    R[II,JJ]*(COL(L6,II).ROW(L6T,JJ)+
              COL(L5,II).ROW(L7T,JJ)+COL(L7,II).ROW(L5T,JJ)));

/*************************************************************************/
/*   THE FOLLOWING STATEMENTS GENERATE A FORTRAN STATEMENT FOR EACH      */
/*   NONZERO ELEMENT OF STK(I,J).  THESE STATEMENTS ARE OF THE FORM      */
/*         STK(2,2)=A(1,1)                                               */
/*   EACH STATEMENT IS WRITTEN TO A SEPARATE FILE CALLED TT2XXX,         */
/*   WHERE XXX STARTS AT 001 FOR THE FIRST NONZERO ENTRY AND CON-        */
/*   TINUES SEQUENTIALLY UNTIL ALL NONZERO ENTRIES THROUGH STK(18,18)    */
/*   ARE GENERATED.  THE MACSYMA FUNCTION GENTRAN WILL ALSO BREAK        */
/*   STATEMENTS EXCEEDING 800 CHARACTERS INTO SHORTER EXPRESSIONS TO     */
/*   AVOID TOO MANY CONTINUATION LINES.  MACSYMA AUTOMATICALLY MAKES     */
/*   CONTINUATION LINES COMPLETE WITH A LEGAL CHARACTER IN COLUMN 6.     */
/*************************************************************************/

KO:ZEROMATRIX(18,18)$
```

```
FOR III THRU 18 DO FOR JJJ:III THRU 18 DO
KO[III,JJJ]:KM[III,JJJ]$
FRAME(I,J):=CONCAT(TT,EV(18*(I-1)+J+1000))$
FOR I THRU 18 DO FOR J:I THRU 18 DO
(IF KO[I,J]#0 THEN (PT:1,GENTRAN(STK[EVAL(I),EVAL(J)]:EVAL(KO[I,J]),
[EVAL(FRAME(I,J))])))$
IF PT#1 THEN GENTRAN(PT:EVAL(PT),[TT2000])$


/*********************************************************************/
/*   GENERATE THE LINEAR ELEMENT-INDEPENDENT STIFFNESS ARRAY KS.     */
/*********************************************************************/

/* ASSEMBLE MATRIX KS */
LOADFILE("LSMAT123.SV")$
SO:SUBST([K=K1,C=P1],SO)$ S1:SUBST([K=K1,C=P1],S1)$ S2:SUBST([K=K1,C=P1],S2)$
S3:SUBST([K=K1,C=P1],S3)$ S4:SUBST([K=K1,C=P1],S4)$ S5:SUBST([K=K1,C=P1],S5)$
S6:SUBST([K=K1,C=P1],S6)$ S7:SUBST([K=K1,C=P1],S7)$
SOT:TRANSPOSE(SO); S1T:TRANSPOSE(S1); S2T:TRANSPOSE(S2);
S3T:TRANSPOSE(S3); S4T:TRANSPOSE(S4); S5T:TRANSPOSE(S5);
S6T:TRANSPOSE(S6); S7T:TRANSPOSE(S7); KS:ZEROMATRIX(18,18)$

FOR II THRU 2 DO FOR JJ THRU 2 DO (PRINT(II,JJ),
KS:KS+AS[II,JJ]*(COL(SO,II).ROW(SOT,JJ))+
    DS[II,JJ]*(COL(S1,II).ROW(S1T,JJ)+
               COL(SO,II).ROW(S2T,JJ)+COL(S2,II).ROW(SOT,JJ))+
    FS[II,JJ]*(COL(S2,II).ROW(S2T,JJ)+
              COL(S1,II).ROW(S3T,JJ)+COL(S3,II).ROW(S1T,JJ)+
              COL(SO,II).ROW(S4T,JJ)+COL(S4,II).ROW(SOT,JJ))+
    HS[II,JJ]*(COL(S3,II).ROW(S3T,JJ)+
              COL(S2,II).ROW(S4T,JJ)+COL(S4,II).ROW(S2T,JJ)+
              COL(S1,II).ROW(S5T,JJ)+COL(S5,II).ROW(S1T,JJ)+
              COL(SO,II).ROW(S6T,JJ)+COL(S6,II).ROW(SOT,JJ))+
    JS[II,JJ]*(COL(S4,II).ROW(S4T,JJ)+
              COL(S3,II).ROW(S5T,JJ)+COL(S5,II).ROW(S3T,JJ)+
              COL(S2,II).ROW(S6T,JJ)+COL(S6,II).ROW(S2T,JJ)+
              COL(S1,II).ROW(S7T,JJ)+COL(S7,II).ROW(S1T,JJ))+
    LS[II,JJ]*(COL(S5,II).ROW(S5T,JJ)+
              COL(S4,II).ROW(S6T,JJ)+COL(S6,II).ROW(S4T,JJ)+
              COL(S3,II).ROW(S7T,JJ)+COL(S7,II).ROW(S3T,JJ))+
    RS[II,JJ]*(COL(S6,II).ROW(S6T,JJ)+
              COL(S5,II).ROW(S7T,JJ)+COL(S7,II).ROW(S5T,JJ)));

KO:ZEROMATRIX(18,18)$
FOR III THRU 18 DO FOR JJJ:III THRU 18 DO
KO[III,JJJ]:KS[III,JJJ]$
FRAME(I,J):=CONCAT(TT,EV(18*(I-1)+J+1000))$
FOR I THRU 18 DO FOR J:I THRU 18 DO
(IF KO[I,J]#0 THEN (PT:1,GENTRAN(STKS[EVAL(I),EVAL(J)]:EVAL(KO[I,J]),
[EVAL(FRAME(I,J))])))$
IF PT#1 THEN GENTRAN(PT:EVAL(PT),[TT2000])$
```

```
/*************************************************************************/
/*   GENERATE THE NONLINEAR ELEMENT-INDEPENDENT STIFFNESS ARRAY N1.      */
/*************************************************************************/

/* ASSEMBLE MATRIX N1 */
TQ:MATRIX([Q(1),Q(2),Q(3),Q(4),Q(5),Q(6),Q(7),Q(8),Q(9),Q(10),
           Q(11),Q(12),Q(13),Q(14),Q(15),Q(16),Q(17),Q(18)])$
Q:TRANSPOSE(TQ)$
LOADFILE("LSMAT123.SV")$ LOADFILE("HMAT123.SV")$
L0:SUBST([K=K1,C=P1],L0)$ L1:SUBST([K=K1,C=P1],L1)$
L2:SUBST([K=K1,C=P1],L2)$ L3:SUBST([K=K1,C=P1],L3)$
L4:SUBST([K=K1,C=P1],L4)$ L5:SUBST([K=K1,C=P1],L5)$
L6:SUBST([K=K1,C=P1],L6)$ L7:SUBST([K=K1,C=P1],L7)$
L0T:TRANSPOSE(L0)$ L1T:TRANSPOSE(L1)$ L2T:TRANSPOSE(L2)$
L3T:TRANSPOSE(L3)$ L4T:TRANSPOSE(L4)$ L5T:TRANSPOSE(L5)$
L6T:TRANSPOSE(L6)$ L7T:TRANSPOSE(L7)$
H0:SUBST([K=K1,C=P1],H0)$ H1:SUBST([K=K1,C=P1],H1)$
H2:SUBST([K=K1,C=P1],H2)$ H3:SUBST([K=K1,C=P1],H3)$
H4:SUBST([K=K1,C=P1],H4)$ H5:SUBST([K=K1,C=P1],H5)$
H6:SUBST([K=K1,C=P1],H6)$ H7:SUBST([K=K1,C=P1],H7)$
H8:SUBST([K=K1,C=P1],H8)$ H9:SUBST([K=K1,C=P1],H9)$
H10:SUBST([K=K1,C=P1],H10)$ H11:SUBST([K=K1,C=P1],H11)$
H12:SUBST([K=K1,C=P1],H12)$ N1:ZEROMATRIX(18,18)$

FOR II THRU 3 DO FOR JJ THRU 3 DO (PRINT(II,JJ),
(I1:3*(-9*II^2+33*II-12), J2:3*( 9*JJ^2-39*JJ+48),
 J1:3*(-9*JJ^2+33*JJ-12), I2:3*( 9*II^2-39*II+48),
SUBI0:SUBMATRIX(H0,I1,I1-1,I1-2,I1-3,I1-4,I1-5,I1-6,I1-7,I1-8,I1-9,
                I1-10,I1-11,I1-12,I1-13,I1-14,I1-15,I1-16,I1-17,
                I2,I2-1,I2-2,I2-3,I2-4,I2-5,I2-6,I2-7,I2-8,I2-9,
                I2-10,I2-11,I2-12,I2-13,I2-14,I2-15,I2-16,I2-17),
SUBJ0:SUBMATRIX(H0,J1,J1-1,J1-2,J1-3,J1-4,J1-5,J1-6,J1-7,J1-8,J1-9,
                J1-10,J1-11,J1-12,J1-13,J1-14,J1-15,J1-16,J1-17,
                J2,J2-1,J2-2,J2-3,J2-4,J2-5,J2-6,J2-7,J2-8,J2-9,
                J2-10,J2-11,J2-12,J2-13,J2-14,J2-15,J2-16,J2-17),
SUBI1:SUBMATRIX(H1,I1,I1-1,I1-2,I1-3,I1-4,I1-5,I1-6,I1-7,I1-8,I1-9,
                I1-10,I1-11,I1-12,I1-13,I1-14,I1-15,I1-16,I1-17,
                I2,I2-1,I2-2,I2-3,I2-4,I2-5,I2-6,I2-7,I2-8,I2-9,
                I2-10,I2-11,I2-12,I2-13,I2-14,I2-15,I2-16,I2-17),
SUBJ1:SUBMATRIX(H1,J1,J1-1,J1-2,J1-3,J1-4,J1-5,J1-6,J1-7,J1-8,J1-9,
                J1-10,J1-11,J1-12,J1-13,J1-14,J1-15,J1-16,J1-17,
                J2,J2-1,J2-2,J2-3,J2-4,J2-5,J2-6,J2-7,J2-8,J2-9,
                J2-10,J2-11,J2-12,J2-13,J2-14,J2-15,J2-16,J2-17),
SUBI2:SUBMATRIX(H2,I1,I1-1,I1-2,I1-3,I1-4,I1-5,I1-6,I1-7,I1-8,I1-9,
                I1-10,I1-11,I1-12,I1-13,I1-14,I1-15,I1-16,I1-17,
                I2,I2-1,I2-2,I2-3,I2-4,I2-5,I2-6,I2-7,I2-8,I2-9,
                I2-10,I2-11,I2-12,I2-13,I2-14,I2-15,I2-16,I2-17),
SUBJ2:SUBMATRIX(H2,J1,J1-1,J1-2,J1-3,J1-4,J1-5,J1-6,J1-7,J1-8,J1-9,
                J1-10,J1-11,J1-12,J1-13,J1-14,J1-15,J1-16,J1-17,
                J2,J2-1,J2-2,J2-3,J2-4,J2-5,J2-6,J2-7,J2-8,J2-9,
```

```
                    J2-10,J2-11,J2-12,J2-13,J2-14,J2-15,J2-16,J2-17),
SUBI3:SUBMATRIX(H3,I1,I1-1,I1-2,I1-3,I1-4,I1-5,I1-6,I1-7,I1-8,I1-9,
                    I1-10,I1-11,I1-12,I1-13,I1-14,I1-15,I1-16,I1-17,
                    I2,I2-1,I2-2,I2-3,I2-4,I2-5,I2-6,I2-7,I2-8,I2-9,
                    I2-10,I2-11,I2-12,I2-13,I2-14,I2-15,I2-16,I2-17),
SUBJ3:SUBMATRIX(H3,J1,J1-1,J1-2,J1-3,J1-4,J1-5,J1-6,J1-7,J1-8,J1-9,
                    J1-10,J1-11,J1-12,J1-13,J1-14,J1-15,J1-16,J1-17,
                    J2,J2-1,J2-2,J2-3,J2-4,J2-5,J2-6,J2-7,J2-8,J2-9,
                    J2-10,J2-11,J2-12,J2-13,J2-14,J2-15,J2-16,J2-17),
SUBI4:SUBMATRIX(H4,I1,I1-1,I1-2,I1-3,I1-4,I1-5,I1-6,I1-7,I1-8,I1-9,
                    I1-10,I1-11,I1-12,I1-13,I1-14,I1-15,I1-16,I1-17,
                    I2,I2-1,I2-2,I2-3,I2-4,I2-5,I2-6,I2-7,I2-8,I2-9,
                    I2-10,I2-11,I2-12,I2-13,I2-14,I2-15,I2-16,I2-17),
SUBJ4:SUBMATRIX(H4,J1,J1-1,J1-2,J1-3,J1-4,J1-5,J1-6,J1-7,J1-8,J1-9,
                    J1-10,J1-11,J1-12,J1-13,J1-14,J1-15,J1-16,J1-17,
                    J2,J2-1,J2-2,J2-3,J2-4,J2-5,J2-6,J2-7,J2-8,J2-9,
                    J2-10,J2-11,J2-12,J2-13,J2-14,J2-15,J2-16,J2-17),
SUBI5:SUBMATRIX(H5,I1,I1-1,I1-2,I1-3,I1-4,I1-5,I1-6,I1-7,I1-8,I1-9,
                    I1-10,I1-11,I1-12,I1-13,I1-14,I1-15,I1-16,I1-17,
                    I2,I2-1,I2-2,I2-3,I2-4,I2-5,I2-6,I2-7,I2-8,I2-9,
                    I2-10,I2-11,I2-12,I2-13,I2-14,I2-15,I2-16,I2-17),
SUBJ5:SUBMATRIX(H5,J1,J1-1,J1-2,J1-3,J1-4,J1-5,J1-6,J1-7,J1-8,J1-9,
                    J1-10,J1-11,J1-12,J1-13,J1-14,J1-15,J1-16,J1-17,
                    J2,J2-1,J2-2,J2-3,J2-4,J2-5,J2-6,J2-7,J2-8,J2-9,
                    J2-10,J2-11,J2-12,J2-13,J2-14,J2-15,J2-16,J2-17),
SUBI6:SUBMATRIX(H6,I1,I1-1,I1-2,I1-3,I1-4,I1-5,I1-6,I1-7,I1-8,I1-9,
                    I1-10,I1-11,I1-12,I1-13,I1-14,I1-15,I1-16,I1-17,
                    I2,I2-1,I2-2,I2-3,I2-4,I2-5,I2-6,I2-7,I2-8,I2-9,
                    I2-10,I2-11,I2-12,I2-13,I2-14,I2-15,I2-16,I2-17),
SUBJ6:SUBMATRIX(H6,J1,J1-1,J1-2,J1-3,J1-4,J1-5,J1-6,J1-7,J1-8,J1-9,
                    J1-10,J1-11,J1-12,J1-13,J1-14,J1-15,J1-16,J1-17,
                    J2,J2-1,J2-2,J2-3,J2-4,J2-5,J2-6,J2-7,J2-8,J2-9,
                    J2-10,J2-11,J2-12,J2-13,J2-14,J2-15,J2-16,J2-17),
SUBI7:SUBMATRIX(H7,I1,I1-1,I1-2,I1-3,I1-4,I1-5,I1-6,I1-7,I1-8,I1-9,
                    I1-10,I1-11,I1-12,I1-13,I1-14,I1-15,I1-16,I1-17,
                    I2,I2-1,I2-2,I2-3,I2-4,I2-5,I2-6,I2-7,I2-8,I2-9,
                    I2-10,I2-11,I2-12,I2-13,I2-14,I2-15,I2-16,I2-17),
SUBJ7:SUBMATRIX(H7,J1,J1-1,J1-2,J1-3,J1-4,J1-5,J1-6,J1-7,J1-8,J1-9,
                    J1-10,J1-11,J1-12,J1-13,J1-14,J1-15,J1-16,J1-17,
                    J2,J2-1,J2-2,J2-3,J2-4,J2-5,J2-6,J2-7,J2-8,J2-9,
                    J2-10,J2-11,J2-12,J2-13,J2-14,J2-15,J2-16,J2-17),
SUBI8:SUBMATRIX(H8,I1,I1-1,I1-2,I1-3,I1-4,I1-5,I1-6,I1-7,I1-8,I1-9,
                    I1-10,I1-11,I1-12,I1-13,I1-14,I1-15,I1-16,I1-17,
                    I2,I2-1,I2-2,I2-3,I2-4,I2-5,I2-6,I2-7,I2-8,I2-9,
                    I2-10,I2-11,I2-12,I2-13,I2-14,I2-15,I2-16,I2-17),
SUBJ8:SUBMATRIX(H8,J1,J1-1,J1-2,J1-3,J1-4,J1-5,J1-6,J1-7,J1-8,J1-9,
                    J1-10,J1-11,J1-12,J1-13,J1-14,J1-15,J1-16,J1-17,
                    J2,J2-1,J2-2,J2-3,J2-4,J2-5,J2-6,J2-7,J2-8,J2-9,
                    J2-10,J2-11,J2-12,J2-13,J2-14,J2-15,J2-16,J2-17),
SUBI9:SUBMATRIX(H9,I1,I1-1,I1-2,I1-3,I1-4,I1-5,I1-6,I1-7,I1-8,I1-9,
                    I1-10,I1-11,I1-12,I1-13,I1-14,I1-15,I1-16,I1-17,
```

```
                    I2,I2-1,I2-2,I2-3,I2-4,I2-5,I2-6,I2-7,I2-8,I2-9,
                    I2-10,I2-11,I2-12,I2-13,I2-14,I2-15,I2-16,I2-17),
SUBJ9:SUBMATRIX(H9,J1,J1-1,J1-2,J1-3,J1-4,J1-5,J1-6,J1-7,J1-8,J1-9,
                    J1-10,J1-11,J1-12,J1-13,J1-14,J1-15,J1-16,J1-17,
                    J2,J2-1,J2-2,J2-3,J2-4,J2-5,J2-6,J2-7,J2-8,J2-9,
                    J2-10,J2-11,J2-12,J2-13,J2-14,J2-15,J2-16,J2-17),
SUBI10:SUBMATRIX(H10,I1,I1-1,I1-2,I1-3,I1-4,I1-5,I1-6,I1-7,I1-8,I1-9,
                    I1-10,I1-11,I1-12,I1-13,I1-14,I1-15,I1-16,I1-17,
                    I2,I2-1,I2-2,I2-3,I2-4,I2-5,I2-6,I2-7,I2-8,I2-9,
                    I2-10,I2-11,I2-12,I2-13,I2-14,I2-15,I2-16,I2-17),
SUBJ10:SUBMATRIX(H10,J1,J1-1,J1-2,J1-3,J1-4,J1-5,J1-6,J1-7,J1-8,J1-9,
                    J1-10,J1-11,J1-12,J1-13,J1-14,J1-15,J1-16,J1-17,
                    J2,J2-1,J2-2,J2-3,J2-4,J2-5,J2-6,J2-7,J2-8,J2-9,
                    J2-10,J2-11,J2-12,J2-13,J2-14,J2-15,J2-16,J2-17),
SUBI11:SUBMATRIX(H11,I1,I1-1,I1-2,I1-3,I1-4,I1-5,I1-6,I1-7,I1-8,I1-9,
                    I1-10,I1-11,I1-12,I1-13,I1-14,I1-15,I1-16,I1-17,
                    I2,I2-1,I2-2,I2-3,I2-4,I2-5,I2-6,I2-7,I2-8,I2-9,
                    I2-10,I2-11,I2-12,I2-13,I2-14,I2-15,I2-16,I2-17),
SUBJ11:SUBMATRIX(H11,J1,J1-1,J1-2,J1-3,J1-4,J1-5,J1-6,J1-7,J1-8,J1-9,
                    J1-10,J1-11,J1-12,J1-13,J1-14,J1-15,J1-16,J1-17,
                    J2,J2-1,J2-2,J2-3,J2-4,J2-5,J2-6,J2-7,J2-8,J2-9,
                    J2-10,J2-11,J2-12,J2-13,J2-14,J2-15,J2-16,J2-17),
SUBI12:SUBMATRIX(H12,I1,I1-1,I1-2,I1-3,I1-4,I1-5,I1-6,I1-7,I1-8,I1-9,
                    I1-10,I1-11,I1-12,I1-13,I1-14,I1-15,I1-16,I1-17,
                    I2,I2-1,I2-2,I2-3,I2-4,I2-5,I2-6,I2-7,I2-8,I2-9,
                    I2-10,I2-11,I2-12,I2-13,I2-14,I2-15,I2-16,I2-17),
SUBJ12:SUBMATRIX(H12,J1,J1-1,J1-2,J1-3,J1-4,J1-5,J1-6,J1-7,J1-8,J1-9,
                    J1-10,J1-11,J1-12,J1-13,J1-14,J1-15,J1-16,J1-17,
                    J2,J2-1,J2-2,J2-3,J2-4,J2-5,J2-6,J2-7,J2-8,J2-9,
                    J2-10,J2-11,J2-12,J2-13,J2-14,J2-15,J2-16,J2-17),

N1:N1+A[II,JJ]*(
COL(L0,II).TQ.SUBJ0+(TQ.COL(L0,II))*SUBJ0+SUBI0.Q.ROW(L0T,JJ)),
N1:N1+DD[II,JJ]*(
COL(L0,II).TQ.SUBJ2+(TQ.COL(L0,II))*SUBJ2+SUBI2.Q.ROW(L0T,JJ)+
COL(L2,II).TQ.SUBJ0+(TQ.COL(L2,II))*SUBJ0+SUBI0.Q.ROW(L2T,JJ)+
COL(L1,II).TQ.SUBJ1+(TQ.COL(L1,II))*SUBJ1+SUBI1.Q.ROW(L1T,JJ)),
N1:N1+ F[II,JJ]*(
COL(L0,II).TQ.SUBJ4+(TQ.COL(L0,II))*SUBJ4+SUBI4.Q.ROW(L0T,JJ)+
COL(L1,II).TQ.SUBJ3+(TQ.COL(L1,II))*SUBJ3+SUBI3.Q.ROW(L1T,JJ)+
COL(L2,II).TQ.SUBJ2+(TQ.COL(L2,II))*SUBJ2+SUBI2.Q.ROW(L2T,JJ)+
COL(L3,II).TQ.SUBJ1+(TQ.COL(L3,II))*SUBJ1+SUBI1.Q.ROW(L3T,JJ)+
COL(L4,II).TQ.SUBJ0+(TQ.COL(L4,II))*SUBJ0+SUBI0.Q.ROW(L4T,JJ)),
N1:N1+ H[II,JJ]*(
COL(L0,II).TQ.SUBJ6+(TQ.COL(L0,II))*SUBJ6+SUBI6.Q.ROW(L0T,JJ)+
COL(L1,II).TQ.SUBJ5+(TQ.COL(L1,II))*SUBJ5+SUBI5.Q.ROW(L1T,JJ)+
COL(L2,II).TQ.SUBJ4+(TQ.COL(L2,II))*SUBJ4+SUBI4.Q.ROW(L2T,JJ)+
COL(L3,II).TQ.SUBJ3+(TQ.COL(L3,II))*SUBJ3+SUBI3.Q.ROW(L3T,JJ)+
COL(L4,II).TQ.SUBJ2+(TQ.COL(L4,II))*SUBJ2+SUBI2.Q.ROW(L4T,JJ)+
COL(L5,II).TQ.SUBJ1+(TQ.COL(L5,II))*SUBJ1+SUBI1.Q.ROW(L5T,JJ)+
COL(L6,II).TQ.SUBJ0+(TQ.COL(L6,II))*SUBJ0+SUBI0.Q.ROW(L6T,JJ)),
```

```
N1:N1+ J[II,JJ]*(
COL(L0,II).TQ.SUBJ8+(TQ.COL(L0,II))*SUBJ8+SUBI8.Q.ROW(L0T,JJ)+
COL(L1,II).TQ.SUBJ7+(TQ.COL(L1,II))*SUBJ7+SUBI7.Q.ROW(L1T,JJ)+
COL(L2,II).TQ.SUBJ6+(TQ.COL(L2,II))*SUBJ6+SUBI6.Q.ROW(L2T,JJ)+
COL(L3,II).TQ.SUBJ5+(TQ.COL(L3,II))*SUBJ5+SUBI5.Q.ROW(L3T,JJ)+
COL(L4,II).TQ.SUBJ4+(TQ.COL(L4,II))*SUBJ4+SUBI4.Q.ROW(L4T,JJ)+
COL(L5,II).TQ.SUBJ3+(TQ.COL(L5,II))*SUBJ3+SUBI3.Q.ROW(L5T,JJ)+
COL(L6,II).TQ.SUBJ2+(TQ.COL(L6,II))*SUBJ2+SUBI2.Q.ROW(L6T,JJ)+
COL(L7,II).TQ.SUBJ1+(TQ.COL(L7,II))*SUBJ1+SUBI1.Q.ROW(L7T,JJ)),
N1:N1+ L[II,JJ]*(
COL(L0,II).TQ.SUBJ10+(TQ.COL(L0,II))*SUBJ10+SUBI10.Q.ROW(L0T,JJ)+
COL(L1,II).TQ.SUBJ9+(TQ.COL(L1,II))*SUBJ9+SUBI9.Q.ROW(L1T,JJ)+
COL(L2,II).TQ.SUBJ8+(TQ.COL(L2,II))*SUBJ8+SUBI8.Q.ROW(L2T,JJ)+
COL(L3,II).TQ.SUBJ7+(TQ.COL(L3,II))*SUBJ7+SUBI7.Q.ROW(L3T,JJ)+
COL(L4,II).TQ.SUBJ6+(TQ.COL(L4,II))*SUBJ6+SUBI6.Q.ROW(L4T,JJ)+
COL(L5,II).TQ.SUBJ5+(TQ.COL(L5,II))*SUBJ5+SUBI5.Q.ROW(L5T,JJ)+
COL(L6,II).TQ.SUBJ4+(TQ.COL(L6,II))*SUBJ4+SUBI4.Q.ROW(L6T,JJ)+
COL(L7,II).TQ.SUBJ3+(TQ.COL(L7,II))*SUBJ3+SUBI3.Q.ROW(L7T,JJ)),
N1:N1+ R[II,JJ]*(
COL(L0,II).TQ.SUBJ12+(TQ.COL(L0,II))*SUBJ12+SUBI12.Q.ROW(L0T,JJ)+
COL(L1,II).TQ.SUBJ11+(TQ.COL(L1,II))*SUBJ11+SUBI11.Q.ROW(L1T,JJ)+
COL(L2,II).TQ.SUBJ10+(TQ.COL(L2,II))*SUBJ10+SUBI10.Q.ROW(L2T,JJ)+
COL(L3,II).TQ.SUBJ9+(TQ.COL(L3,II))*SUBJ9+SUBI9.Q.ROW(L3T,JJ)+
COL(L4,II).TQ.SUBJ8+(TQ.COL(L4,II))*SUBJ8+SUBI8.Q.ROW(L4T,JJ)+
COL(L5,II).TQ.SUBJ7+(TQ.COL(L5,II))*SUBJ7+SUBI7.Q.ROW(L5T,JJ)+
COL(L6,II).TQ.SUBJ6+(TQ.COL(L6,II))*SUBJ6+SUBI6.Q.ROW(L6T,JJ)+
COL(L7,II).TQ.SUBJ5+(TQ.COL(L7,II))*SUBJ5+SUBI5.Q.ROW(L7T,JJ)),
N1:N1+ T[II,JJ]*(
COL(L2,II).TQ.SUBJ12+(TQ.COL(L2,II))*SUBJ12+SUBI12.Q.ROW(L2T,JJ)+
COL(L3,II).TQ.SUBJ11+(TQ.COL(L3,II))*SUBJ11+SUBI11.Q.ROW(L3T,JJ)+
COL(L4,II).TQ.SUBJ10+(TQ.COL(L4,II))*SUBJ10+SUBI10.Q.ROW(L4T,JJ)+
COL(L5,II).TQ.SUBJ9+(TQ.COL(L5,II))*SUBJ9+SUBI9.Q.ROW(L5T,JJ)+
COL(L6,II).TQ.SUBJ8+(TQ.COL(L6,II))*SUBJ8+SUBI8.Q.ROW(L6T,JJ)+
COL(L7,II).TQ.SUBJ7+(TQ.COL(L7,II))*SUBJ7+SUBI7.Q.ROW(L7T,JJ)),
N1:N1+XH[II,JJ]*(
COL(L4,II).TQ.SUBJ12+(TQ.COL(L4,II))*SUBJ12+SUBI12.Q.ROW(L4T,JJ)+
COL(L5,II).TQ.SUBJ11+(TQ.COL(L5,II))*SUBJ11+SUBI11.Q.ROW(L5T,JJ)+
COL(L6,II).TQ.SUBJ10+(TQ.COL(L6,II))*SUBJ10+SUBI10.Q.ROW(L6T,JJ)+
COL(L7,II).TQ.SUBJ9+(TQ.COL(L7,II))*SUBJ9+SUBI9.Q.ROW(L7T,JJ)),
N1:N1+XJ[II,JJ]*(
COL(L6,II).TQ.SUBJ12+(TQ.COL(L6,II))*SUBJ12+SUBI12.Q.ROW(L6T,JJ)+
COL(L7,II).TQ.SUBJ11+(TQ.COL(L7,II))*SUBJ11+SUBI11.Q.ROW(L7T,JJ)),

KILL(SUBJ12,SUBI12,SUBJ11,SUBI11),
KILL(SUBJ0,SUBJ1,SUBJ2,SUBJ3,SUBJ4,SUBJ5,SUBJ6,SUBJ7,SUBJ8,SUBJ9,SUBJ10),
KILL(SUBI0,SUBI1,SUBI2,SUBI3,SUBI4,SUBI5,SUBI6,SUBI7,SUBI8,SUBI9,SUBI10)))$

KILL(L0,L1,L2,L3,L4,L5,L6,L7,L0T,L1T,L2T,L3T,L4T,L5T,L6T,L7T)$
KILL(H0,H1,H2,H3,H4,H5,H6,H7,H8,H9,H10,H11,H12)$
N1SYM:ZEROMATRIX(18,18)$
FOR II THRU 18 DO FOR JJ:II THRU 18 DO N1SYM[II,JJ]:N1[II,JJ]$
```

```
PRINT("SYMMETRIC N1 FORMED")$
KILL(N1)$
N1:ZEROMATRIX(18,18)$
KILL(Q,TQ)$
FOR II THRU 18 DO FOR JJ:II THRU 18 DO
N1[II,JJ]:FACTOROUT(N1SYM[II,JJ],Q(1),Q(2),Q(3),Q(4),Q(5),Q(6),
Q(7),Q(8),Q(9),Q(10),Q(11),Q(12),Q(13),Q(14),Q(15),Q(16),Q(17),Q(18))$
FRAME(I,J):=CONCAT(TT,EV(18*(I-1)+J+1000))$
FOR I THRU 18 DO FOR J:I THRU 18 DO
(IF N1[I,J]#0 THEN (PT:1,GENTRAN(SN1[EVAL(I),EVAL(J)]:EVAL(N1[I,J]),
[EVAL(FRAME(I,J))])))$
IF PT#1 THEN GENTRAN(PT:EVAL(PT),[TT2000])$

/*************************************************************************/
/*   GENERATE THE NONLINEAR ELEMENT-INDEPENDENT STIFFNESS ARRAY N1S.     */
/*************************************************************************/

/* ASSEMBLE MATRIX N1AS */
TQ:MATRIX([Q(1),Q(2),Q(3),Q(4),Q(5),Q(6),Q(7),Q(8),Q(9),Q(10),
           Q(11),Q(12),Q(13),Q(14),Q(15),Q(16),Q(17),Q(18)])$
Q:TRANSPOSE(TQ)$ LOADFILE("LSMAT123.SV")$
S0:SUBST([K=K1,C=P1],S0)$ S1:SUBST([K=K1,C=P1],S1)$
S2:SUBST([K=K1,C=P1],S2)$ S3:SUBST([K=K1,C=P1],S3)$
S4:SUBST([K=K1,C=P1],S4)$ S5:SUBST([K=K1,C=P1],S5)$
S6:SUBST([K=K1,C=P1],S6)$ S7:SUBST([K=K1,C=P1],S7)$
S0T:TRANSPOSE(S0)$ S1T:TRANSPOSE(S1)$ S2T:TRANSPOSE(S2)$
S3T:TRANSPOSE(S3)$ S4T:TRANSPOSE(S4)$ S5T:TRANSPOSE(S5)$
S6T:TRANSPOSE(S6)$ S7T:TRANSPOSE(S7)$
LOADFILE("SSMAT123.SV")$
SS0:SUBST([K=K1,C=P1],SS0)$ SS1:SUBST([K=K1,C=P1],SS1)$
SS2:SUBST([K=K1,C=P1],SS2)$ SS3:SUBST([K=K1,C=P1],SS3)$
SS4:SUBST([K=K1,C=P1],SS4)$ SS5:SUBST([K=K1,C=P1],SS5)$
SS6:SUBST([K=K1,C=P1],SS6)$ SS7:SUBST([K=K1,C=P1],SS7)$
SS8:SUBST([K=K1,C=P1],SS8)$ SS9:SUBST([K=K1,C=P1],SS9)$
SS10:SUBST([K=K1,C=P1],SS10)$ SS11:SUBST([K=K1,C=P1],SS11)$
SS12:SUBST([K=K1,C=P1],SS12)$ N1S:ZEROMATRIX(18,18)$

FOR II THRU 2 DO FOR JJ THRU 2 DO (PRINT(II,JJ),
 J2:3*( 9*(JJ+1)^2-39*(JJ+1)+48), I2:3*( 9*(II+1)^2-39*(II+1)+48),
SUBIS0:SUBMATRIX(SS0, I2,I2-1,I2-2,I2-3,I2-4,I2-5,I2-6,I2-7,I2-8,I2-9,
                 I2-10,I2-11,I2-12,I2-13,I2-14,I2-15,I2-16,I2-17),
SUBJS0:SUBMATRIX(SS0, J2,J2-1,J2-2,J2-3,J2-4,J2-5,J2-6,J2-7,J2-8,J2-9,
                 J2-10,J2-11,J2-12,J2-13,J2-14,J2-15,J2-16,J2-17),
SUBIS1:SUBMATRIX(SS1, I2,I2-1,I2-2,I2-3,I2-4,I2-5,I2-6,I2-7,I2-8,I2-9,
                 I2-10,I2-11,I2-12,I2-13,I2-14,I2-15,I2-16,I2-17),
SUBJS1:SUBMATRIX(SS1, J2,J2-1,J2-2,J2-3,J2-4,J2-5,J2-6,J2-7,J2-8,J2-9,
                 J2-10,J2-11,J2-12,J2-13,J2-14,J2-15,J2-16,J2-17),
SUBIS2:SUBMATRIX(SS2, I2,I2-1,I2-2,I2-3,I2-4,I2-5,I2-6,I2-7,I2-8,I2-9,
                 I2-10,I2-11,I2-12,I2-13,I2-14,I2-15,I2-16,I2-17),
SUBJS2:SUBMATRIX(SS2, J2,J2-1,J2-2,J2-3,J2-4,J2-5,J2-6,J2-7,J2-8,J2-9,
                 J2-10,J2-11,J2-12,J2-13,J2-14,J2-15,J2-16,J2-17),
```

```
SUBIS3:SUBMATRIX(SS3, I2,I2-1,I2-2,I2-3,I2-4,I2-5,I2-6,I2-7,I2-8,I2-9,
                 I2-10,I2-11,I2-12,I2-13,I2-14,I2-15,I2-16,I2-17),
SUBJS3:SUBMATRIX(SS3, J2,J2-1,J2-2,J2-3,J2-4,J2-5,J2-6,J2-7,J2-8,J2-9,
                 J2-10,J2-11,J2-12,J2-13,J2-14,J2-15,J2-16,J2-17),
SUBIS4:SUBMATRIX(SS4, I2,I2-1,I2-2,I2-3,I2-4,I2-5,I2-6,I2-7,I2-8,I2-9,
                 I2-10,I2-11,I2-12,I2-13,I2-14,I2-15,I2-16,I2-17),
SUBJS4:SUBMATRIX(SS4, J2,J2-1,J2-2,J2-3,J2-4,J2-5,J2-6,J2-7,J2-8,J2-9,
                 J2-10,J2-11,J2-12,J2-13,J2-14,J2-15,J2-16,J2-17),
SUBIS5:SUBMATRIX(SS5, I2,I2-1,I2-2,I2-3,I2-4,I2-5,I2-6,I2-7,I2-8,I2-9,
                 I2-10,I2-11,I2-12,I2-13,I2-14,I2-15,I2-16,I2-17),
SUBJS5:SUBMATRIX(SS5, J2,J2-1,J2-2,J2-3,J2-4,J2-5,J2-6,J2-7,J2-8,J2-9,
                 J2-10,J2-11,J2-12,J2-13,J2-14,J2-15,J2-16,J2-17),
SUBIS6:SUBMATRIX(SS6, I2,I2-1,I2-2,I2-3,I2-4,I2-5,I2-6,I2-7,I2-8,I2-9,
                 I2-10,I2-11,I2-12,I2-13,I2-14,I2-15,I2-16,I2-17),
SUBJS6:SUBMATRIX(SS6, J2,J2-1,J2-2,J2-3,J2-4,J2-5,J2-6,J2-7,J2-8,J2-9,
                 J2-10,J2-11,J2-12,J2-13,J2-14,J2-15,J2-16,J2-17),
SUBIS7:SUBMATRIX(SS7, I2,I2-1,I2-2,I2-3,I2-4,I2-5,I2-6,I2-7,I2-8,I2-9,
                 I2-10,I2-11,I2-12,I2-13,I2-14,I2-15,I2-16,I2-17),
SUBJS7:SUBMATRIX(SS7, J2,J2-1,J2-2,J2-3,J2-4,J2-5,J2-6,J2-7,J2-8,J2-9,
                 J2-10,J2-11,J2-12,J2-13,J2-14,J2-15,J2-16,J2-17),
SUBIS8:SUBMATRIX(SS8, I2,I2-1,I2-2,I2-3,I2-4,I2-5,I2-6,I2-7,I2-8,I2-9,
                 I2-10,I2-11,I2-12,I2-13,I2-14,I2-15,I2-16,I2-17),
SUBJS8:SUBMATRIX(SS8, J2,J2-1,J2-2,J2-3,J2-4,J2-5,J2-6,J2-7,J2-8,J2-9,
                 J2-10,J2-11,J2-12,J2-13,J2-14,J2-15,J2-16,J2-17),
SUBIS9:SUBMATRIX(SS9, I2,I2-1,I2-2,I2-3,I2-4,I2-5,I2-6,I2-7,I2-8,I2-9,
                 I2-10,I2-11,I2-12,I2-13,I2-14,I2-15,I2-16,I2-17),
SUBJS9:SUBMATRIX(SS9, J2,J2-1,J2-2,J2-3,J2-4,J2-5,J2-6,J2-7,J2-8,J2-9,
                 J2-10,J2-11,J2-12,J2-13,J2-14,J2-15,J2-16,J2-17),
SUBIS10:SUBMATRIX(SS10, I2,I2-1,I2-2,I2-3,I2-4,I2-5,I2-6,I2-7,I2-8,I2-9,
                 I2-10,I2-11,I2-12,I2-13,I2-14,I2-15,I2-16,I2-17),
SUBJS10:SUBMATRIX(SS10, J2,J2-1,J2-2,J2-3,J2-4,J2-5,J2-6,J2-7,J2-8,J2-9,
                 J2-10,J2-11,J2-12,J2-13,J2-14,J2-15,J2-16,J2-17),
SUBIS11:SUBMATRIX(SS11, I2,I2-1,I2-2,I2-3,I2-4,I2-5,I2-6,I2-7,I2-8,I2-9,
                 I2-10,I2-11,I2-12,I2-13,I2-14,I2-15,I2-16,I2-17),
SUBJS11:SUBMATRIX(SS11, J2,J2-1,J2-2,J2-3,J2-4,J2-5,J2-6,J2-7,J2-8,J2-9,
                 J2-10,J2-11,J2-12,J2-13,J2-14,J2-15,J2-16,J2-17),
SUBIS12:SUBMATRIX(SS12, I2,I2-1,I2-2,I2-3,I2-4,I2-5,I2-6,I2-7,I2-8,I2-9,
                 I2-10,I2-11,I2-12,I2-13,I2-14,I2-15,I2-16,I2-17),
SUBJS12:SUBMATRIX(SS12, J2,J2-1,J2-2,J2-3,J2-4,J2-5,J2-6,J2-7,J2-8,J2-9,
                 J2-10,J2-11,J2-12,J2-13,J2-14,J2-15,J2-16,J2-17),
N1S:N1S+AS[II,JJ]*(
 COL(S0,II).TQ.SUBJS0+(TQ.COL(S0,II))*SUBJS0+SUBIS0.Q.ROW(S0T,JJ)),
N1S:N1S+DS[II,JJ]*(
COL(S0,II).TQ.SUBJS2+(TQ.COL(S0,II))*SUBJS2+SUBIS2.Q.ROW(S0T,JJ)+
COL(S2,II).TQ.SUBJS0+(TQ.COL(S2,II))*SUBJS0+SUBIS0.Q.ROW(S2T,JJ)+
COL(S1,II).TQ.SUBJS1+(TQ.COL(S1,II))*SUBJS1+SUBIS1.Q.ROW(S1T,JJ)),
N1S:N1S+FS[II,JJ]*(
COL(S0,II).TQ.SUBJS4+(TQ.COL(S0,II))*SUBJS4+SUBIS4.Q.ROW(S0T,JJ)+
COL(S1,II).TQ.SUBJS3+(TQ.COL(S1,II))*SUBJS3+SUBIS3.Q.ROW(S1T,JJ)+
COL(S2,II).TQ.SUBJS2+(TQ.COL(S2,II))*SUBJS2+SUBIS2.Q.ROW(S2T,JJ)+
COL(S3,II).TQ.SUBJS1+(TQ.COL(S3,II))*SUBJS1+SUBIS1.Q.ROW(S3T,JJ)+
```

```
COL(S4,II).TQ.SUBJS0+(TQ.COL(S4,II))*SUBJS0+SUBIS0.Q.ROW(S4T,JJ)),
N1S:N1S+HS[II,JJ]*(
COL(S0,II).TQ.SUBJS6+(TQ.COL(S0,II))*SUBJS6+SUBIS6.Q.ROW(S0T,JJ)+
COL(S1,II).TQ.SUBJS5+(TQ.COL(S1,II))*SUBJS5+SUBIS5.Q.ROW(S1T,JJ)+
COL(S2,II).TQ.SUBJS4+(TQ.COL(S2,II))*SUBJS4+SUBIS4.Q.ROW(S2T,JJ)+
COL(S3,II).TQ.SUBJS3+(TQ.COL(S3,II))*SUBJS3+SUBIS3.Q.ROW(S3T,JJ)+
COL(S4,II).TQ.SUBJS2+(TQ.COL(S4,II))*SUBJS2+SUBIS2.Q.ROW(S4T,JJ)+
COL(S5,II).TQ.SUBJS1+(TQ.COL(S5,II))*SUBJS1+SUBIS1.Q.ROW(S5T,JJ)+
COL(S6,II).TQ.SUBJS0+(TQ.COL(S6,II))*SUBJS0+SUBIS0.Q.ROW(S6T,JJ)),
N1S:N1S+JS[II,JJ]*(
COL(S0,II).TQ.SUBJS8+(TQ.COL(S0,II))*SUBJS8+SUBIS8.Q.ROW(S0T,JJ)+
COL(S1,II).TQ.SUBJS7+(TQ.COL(S1,II))*SUBJS7+SUBIS7.Q.ROW(S1T,JJ)+
COL(S2,II).TQ.SUBJS6+(TQ.COL(S2,II))*SUBJS6+SUBIS6.Q.ROW(S2T,JJ)+
COL(S3,II).TQ.SUBJS5+(TQ.COL(S3,II))*SUBJS5+SUBIS5.Q.ROW(S3T,JJ)+
COL(S4,II).TQ.SUBJS4+(TQ.COL(S4,II))*SUBJS4+SUBIS4.Q.ROW(S4T,JJ)+
COL(S5,II).TQ.SUBJS3+(TQ.COL(S5,II))*SUBJS3+SUBIS3.Q.ROW(S5T,JJ)+
COL(S6,II).TQ.SUBJS2+(TQ.COL(S6,II))*SUBJS2+SUBIS2.Q.ROW(S6T,JJ)+
COL(S7,II).TQ.SUBJS1+(TQ.COL(S7,II))*SUBJS1+SUBIS1.Q.ROW(S7T,JJ)),
N1S:N1S+LS[II,JJ]*(
COL(S0,II).TQ.SUBJS10+(TQ.COL(S0,II))*SUBJS10+SUBIS10.Q.ROW(S0T,JJ)+
COL(S1,II).TQ.SUBJS9+(TQ.COL(S1,II))*SUBJS9+SUBIS9.Q.ROW(S1T,JJ)+
COL(S2,II).TQ.SUBJS8+(TQ.COL(S2,II))*SUBJS8+SUBIS8.Q.ROW(S2T,JJ)+
COL(S3,II).TQ.SUBJS7+(TQ.COL(S3,II))*SUBJS7+SUBIS7.Q.ROW(S3T,JJ)+
COL(S4,II).TQ.SUBJS6+(TQ.COL(S4,II))*SUBJS6+SUBIS6.Q.ROW(S4T,JJ)+
COL(S5,II).TQ.SUBJS5+(TQ.COL(S5,II))*SUBJS5+SUBIS5.Q.ROW(S5T,JJ)+
COL(S6,II).TQ.SUBJS4+(TQ.COL(S6,II))*SUBJS4+SUBIS4.Q.ROW(S6T,JJ)+
COL(S7,II).TQ.SUBJS3+(TQ.COL(S7,II))*SUBJS3+SUBIS3.Q.ROW(S7T,JJ)),
N1S:N1S+RS[II,JJ]*(
COL(S0,II).TQ.SUBJS12+(TQ.COL(S0,II))*SUBJS12+SUBIS12.Q.ROW(S0T,JJ)+
COL(S1,II).TQ.SUBJS11+(TQ.COL(S1,II))*SUBJS11+SUBIS11.Q.ROW(S1T,JJ)+
COL(S2,II).TQ.SUBJS10+(TQ.COL(S2,II))*SUBJS10+SUBIS10.Q.ROW(S2T,JJ)+
COL(S3,II).TQ.SUBJS9+(TQ.COL(S3,II))*SUBJS9+SUBIS9.Q.ROW(S3T,JJ)+
COL(S4,II).TQ.SUBJS8+(TQ.COL(S4,II))*SUBJS8+SUBIS8.Q.ROW(S4T,JJ)+
COL(S5,II).TQ.SUBJS7+(TQ.COL(S5,II))*SUBJS7+SUBIS7.Q.ROW(S5T,JJ)+
COL(S6,II).TQ.SUBJS6+(TQ.COL(S6,II))*SUBJS6+SUBIS6.Q.ROW(S6T,JJ)+
COL(S7,II).TQ.SUBJS5+(TQ.COL(S7,II))*SUBJS5+SUBIS5.Q.ROW(S7T,JJ)),
N1S:N1S+TS[II,JJ]*(
COL(S2,II).TQ.SUBJS12+(TQ.COL(S2,II))*SUBJS12+SUBIS12.Q.ROW(S2T,JJ)+
COL(S3,II).TQ.SUBJS11+(TQ.COL(S3,II))*SUBJS11+SUBIS11.Q.ROW(S3T,JJ)+
COL(S4,II).TQ.SUBJS10+(TQ.COL(S4,II))*SUBJS10+SUBIS10.Q.ROW(S4T,JJ)+
COL(S5,II).TQ.SUBJS9+(TQ.COL(S5,II))*SUBJS9+SUBIS9.Q.ROW(S5T,JJ)+
COL(S6,II).TQ.SUBJS8+(TQ.COL(S6,II))*SUBJS8+SUBIS8.Q.ROW(S6T,JJ)+
COL(S7,II).TQ.SUBJS7+(TQ.COL(S7,II))*SUBJS7+SUBIS7.Q.ROW(S7T,JJ)),
N1S:N1S+XHS[II,JJ]*(
COL(S4,II).TQ.SUBJS12+(TQ.COL(S4,II))*SUBJS12+SUBIS12.Q.ROW(S4T,JJ)+
COL(S5,II).TQ.SUBJS11+(TQ.COL(S5,II))*SUBJS11+SUBIS11.Q.ROW(S5T,JJ)+
COL(S6,II).TQ.SUBJS10+(TQ.COL(S6,II))*SUBJS10+SUBIS10.Q.ROW(S6T,JJ)+
COL(S7,II).TQ.SUBJS9+(TQ.COL(S7,II))*SUBJS9+SUBIS9.Q.ROW(S7T,JJ)),
N1S:N1S+XJS[II,JJ]*(
COL(S6,II).TQ.SUBJS12+(TQ.COL(S6,II))*SUBJS12+SUBIS12.Q.ROW(S6T,JJ)+
COL(S7,II).TQ.SUBJS11+(TQ.COL(S7,II))*SUBJS11+SUBIS11.Q.ROW(S7T,JJ)),
```

```
KILL(SUBJS0,SUBJS1,SUBJS2,SUBJS3,SUBJS4,SUBJS5,
     SUBJS6,SUBJS7,SUBJS8,SUBJS9,SUBJS10,SUBJS11,SUBJS12),
KILL(SUBIS0,SUBIS1,SUBIS2,SUBIS3,SUBIS4,SUBIS5,
     SUBIS6,SUBIS7,SUBIS8,SUBIS9,SUBIS10,SUBIS11,SUBIS12))$

KILL(SS0,SS1,SS2,SS3,SS4,SS5,SS6,SS7,SS8,SS9,SS10,SS11,SS12)$
KILL(S0,S1,S2,S3,S4,S5,S6,S7,S0T,S1T,S2T,S3T,S4T,S5T,S6T,S7T)$
N1SYM:ZEROMATRIX(18,18)$
FOR II THRU 18 DO FOR JJ:II THRU 18 DO N1SYM[II,JJ]:N1S[II,JJ]$
PRINT("SYMMETRIC N1 FORMED")$
KILL(N1,N1S)$
N1:ZEROMATRIX(18,18)$
KILL(Q,TQ)$
FOR II THRU 18 DO FOR JJ:II THRU 18 DO
N1[II,JJ]:FACTOROUT(N1SYM[II,JJ],Q(1),Q(2),Q(3),Q(4),Q(5),Q(6),
Q(7),Q(8),Q(9),Q(10),Q(11),Q(12),Q(13),Q(14),Q(15),Q(16),Q(17),Q(18))$
FRAME(I,J):=CONCAT(TT,EV(18*(I-1)+J+1000))$
FOR I THRU 18 DO FOR J:I THRU 18 DO
(IF N1[I,J]#0 THEN (PT:1,GENTRAN(SN1S[EVAL(I),EVAL(J)]:EVAL(N1[I,J]),
[EVAL(FRAME(I,J))]))))$
IF PT#1 THEN GENTRAN(PT:EVAL(PT),[TT2000])$

/*************************************************************************/
/*   GENERATE THE NONLINEAR ELEMENT-INDEPENDENT STIFFNESS ARRAY N2.      */
/*************************************************************************/

/* ASSEMBLE MATRIX N2A */
TQ:MATRIX([Q(1),Q(2),Q(3),Q(4),Q(5),Q(6),Q(7),Q(8),Q(9),Q(10),
          Q(11),Q(12),Q(13),Q(14),Q(15),Q(16),Q(17),Q(18)])$
Q:TRANSPOSE(TQ)$ LOADFILE("HMAT123.SV")$
H0:SUBST([K=K1,C=P1],H0)$ H1:SUBST([K=K1,C=P1],H1)$
H2:SUBST([K=K1,C=P1],H2)$ H3:SUBST([K=K1,C=P1],H3)$
H4:SUBST([K=K1,C=P1],H4)$ H5:SUBST([K=K1,C=P1],H5)$
H6:SUBST([K=K1,C=P1],H6)$ H7:SUBST([K=K1,C=P1],H7)$
H8:SUBST([K=K1,C=P1],H8)$ H9:SUBST([K=K1,C=P1],H9)$
H10:SUBST([K=K1,C=P1],H10)$ H11:SUBST([K=K1,C=P1],H11)$
H12:SUBST([K=K1,C=P1],H12)$ N2:ZEROMATRIX(18,18)$

FOR II THRU 3 DO FOR JJ THRU 3 DO (PRINT(II,JJ),
(I1:3*(-9*II^2+33*II-12), J2:3*( 9*JJ^2-39*JJ+48),
 J1:3*(-9*JJ^2+33*JJ-12), I2:3*( 9*II^2-39*II+48),
SUBI0:SUBMATRIX(H0,I1,I1-1,I1-2,I1-3,I1-4,I1-5,I1-6,I1-7,I1-8,I1-9,
                I1-10,I1-11,I1-12,I1-13,I1-14,I1-15,I1-16,I1-17,
                I2,I2-1,I2-2,I2-3,I2-4,I2-5,I2-6,I2-7,I2-8,I2-9,
                I2-10,I2-11,I2-12,I2-13,I2-14,I2-15,I2-16,I2-17),
SUBJ0:SUBMATRIX(H0,J1,J1-1,J1-2,J1-3,J1-4,J1-5,J1-6,J1-7,J1-8,J1-9,
                J1-10,J1-11,J1-12,J1-13,J1-14,J1-15,J1-16,J1-17,
                J2,J2-1,J2-2,J2-3,J2-4,J2-5,J2-6,J2-7,J2-8,J2-9,
                J2-10,J2-11,J2-12,J2-13,J2-14,J2-15,J2-16,J2-17),
SUBI1:SUBMATRIX(H1,I1,I1-1,I1-2,I1-3,I1-4,I1-5,I1-6,I1-7,I1-8,I1-9,
```

```
                    I1-10,I1-11,I1-12,I1-13,I1-14,I1-15,I1-16,I1-17,
                    I2,I2-1,I2-2,I2-3,I2-4,I2-5,I2-6,I2-7,I2-8,I2-9,
                    I2-10,I2-11,I2-12,I2-13,I2-14,I2-15,I2-16,I2-17),
SUBJ1:SUBMATRIX(H1,J1,J1-1,J1-2,J1-3,J1-4,J1-5,J1-6,J1-7,J1-8,J1-9,
                    J1-10,J1-11,J1-12,J1-13,J1-14,J1-15,J1-16,J1-17,
                    J2,J2-1,J2-2,J2-3,J2-4,J2-5,J2-6,J2-7,J2-8,J2-9,
                    J2-10,J2-11,J2-12,J2-13,J2-14,J2-15,J2-16,J2-17),
SUBI2:SUBMATRIX(H2,I1,I1-1,I1-2,I1-3,I1-4,I1-5,I1-6,I1-7,I1-8,I1-9,
                    I1-10,I1-11,I1-12,I1-13,I1-14,I1-15,I1-16,I1-17,
                    I2,I2-1,I2-2,I2-3,I2-4,I2-5,I2-6,I2-7,I2-8,I2-9,
                    I2-10,I2-11,I2-12,I2-13,I2-14,I2-15,I2-16,I2-17),
SUBJ2:SUBMATRIX(H2,J1,J1-1,J1-2,J1-3,J1-4,J1-5,J1-6,J1-7,J1-8,J1-9,
                    J1-10,J1-11,J1-12,J1-13,J1-14,J1-15,J1-16,J1-17,
                    J2,J2-1,J2-2,J2-3,J2-4,J2-5,J2-6,J2-7,J2-8,J2-9,
                    J2-10,J2-11,J2-12,J2-13,J2-14,J2-15,J2-16,J2-17),
SUBI3:SUBMATRIX(H3,I1,I1-1,I1-2,I1-3,I1-4,I1-5,I1-6,I1-7,I1-8,I1-9,
                    I1-10,I1-11,I1-12,I1-13,I1-14,I1-15,I1-16,I1-17,
                    I2,I2-1,I2-2,I2-3,I2-4,I2-5,I2-6,I2-7,I2-8,I2-9,
                    I2-10,I2-11,I2-12,I2-13,I2-14,I2-15,I2-16,I2-17),
SUBJ3:SUBMATRIX(H3,J1,J1-1,J1-2,J1-3,J1-4,J1-5,J1-6,J1-7,J1-8,J1-9,
                    J1-10,J1-11,J1-12,J1-13,J1-14,J1-15,J1-16,J1-17,
                    J2,J2-1,J2-2,J2-3,J2-4,J2-5,J2-6,J2-7,J2-8,J2-9,
                    J2-10,J2-11,J2-12,J2-13,J2-14,J2-15,J2-16,J2-17),
SUBI4:SUBMATRIX(H4,I1,I1-1,I1-2,I1-3,I1-4,I1-5,I1-6,I1-7,I1-8,I1-9,
                    I1-10,I1-11,I1-12,I1-13,I1-14,I1-15,I1-16,I1-17,
                    I2,I2-1,I2-2,I2-3,I2-4,I2-5,I2-6,I2-7,I2-8,I2-9,
                    I2-10,I2-11,I2-12,I2-13,I2-14,I2-15,I2-16,I2-17),
SUBJ4:SUBMATRIX(H4,J1,J1-1,J1-2,J1-3,J1-4,J1-5,J1-6,J1-7,J1-8,J1-9,
                    J1-10,J1-11,J1-12,J1-13,J1-14,J1-15,J1-16,J1-17,
                    J2,J2-1,J2-2,J2-3,J2-4,J2-5,J2-6,J2-7,J2-8,J2-9,
                    J2-10,J2-11,J2-12,J2-13,J2-14,J2-15,J2-16,J2-17),
SUBI5:SUBMATRIX(H5,I1,I1-1,I1-2,I1-3,I1-4,I1-5,I1-6,I1-7,I1-8,I1-9,
                    I1-10,I1-11,I1-12,I1-13,I1-14,I1-15,I1-16,I1-17,
                    I2,I2-1,I2-2,I2-3,I2-4,I2-5,I2-6,I2-7,I2-8,I2-9,
                    I2-10,I2-11,I2-12,I2-13,I2-14,I2-15,I2-16,I2-17),
SUBJ5:SUBMATRIX(H5,J1,J1-1,J1-2,J1-3,J1-4,J1-5,J1-6,J1-7,J1-8,J1-9,
                    J1-10,J1-11,J1-12,J1-13,J1-14,J1-15,J1-16,J1-17,
                    J2,J2-1,J2-2,J2-3,J2-4,J2-5,J2-6,J2-7,J2-8,J2-9,
                    J2-10,J2-11,J2-12,J2-13,J2-14,J2-15,J2-16,J2-17),
SUBI6:SUBMATRIX(H6,I1,I1-1,I1-2,I1-3,I1-4,I1-5,I1-6,I1-7,I1-8,I1-9,
                    I1-10,I1-11,I1-12,I1-13,I1-14,I1-15,I1-16,I1-17,
                    I2,I2-1,I2-2,I2-3,I2-4,I2-5,I2-6,I2-7,I2-8,I2-9,
                    I2-10,I2-11,I2-12,I2-13,I2-14,I2-15,I2-16,I2-17),
SUBJ6:SUBMATRIX(H6,J1,J1-1,J1-2,J1-3,J1-4,J1-5,J1-6,J1-7,J1-8,J1-9,
                    J1-10,J1-11,J1-12,J1-13,J1-14,J1-15,J1-16,J1-17,
                    J2,J2-1,J2-2,J2-3,J2-4,J2-5,J2-6,J2-7,J2-8,J2-9,
                    J2-10,J2-11,J2-12,J2-13,J2-14,J2-15,J2-16,J2-17),
SUBI7:SUBMATRIX(H7,I1,I1-1,I1-2,I1-3,I1-4,I1-5,I1-6,I1-7,I1-8,I1-9,
                    I1-10,I1-11,I1-12,I1-13,I1-14,I1-15,I1-16,I1-17,
                    I2,I2-1,I2-2,I2-3,I2-4,I2-5,I2-6,I2-7,I2-8,I2-9,
                    I2-10,I2-11,I2-12,I2-13,I2-14,I2-15,I2-16,I2-17),
```

```
SUBJ7:SUBMATRIX(H7,J1,J1-1,J1-2,J1-3,J1-4,J1-5,J1-6,J1-7,J1-8,J1-9,
                J1-10,J1-11,J1-12,J1-13,J1-14,J1-15,J1-16,J1-17,
                J2,J2-1,J2-2,J2-3,J2-4,J2-5,J2-6,J2-7,J2-8,J2-9,
                J2-10,J2-11,J2-12,J2-13,J2-14,J2-15,J2-16,J2-17),
SUBI8:SUBMATRIX(H8,I1,I1-1,I1-2,I1-3,I1-4,I1-5,I1-6,I1-7,I1-8,I1-9,
                I1-10,I1-11,I1-12,I1-13,I1-14,I1-15,I1-16,I1-17,
                I2,I2-1,I2-2,I2-3,I2-4,I2-5,I2-6,I2-7,I2-8,I2-9,
                I2-10,I2-11,I2-12,I2-13,I2-14,I2-15,I2-16,I2-17),
SUBJ8:SUBMATRIX(H8,J1,J1-1,J1-2,J1-3,J1-4,J1-5,J1-6,J1-7,J1-8,J1-9,
                J1-10,J1-11,J1-12,J1-13,J1-14,J1-15,J1-16,J1-17,
                J2,J2-1,J2-2,J2-3,J2-4,J2-5,J2-6,J2-7,J2-8,J2-9,
                J2-10,J2-11,J2-12,J2-13,J2-14,J2-15,J2-16,J2-17),
SUBI9:SUBMATRIX(H9,I1,I1-1,I1-2,I1-3,I1-4,I1-5,I1-6,I1-7,I1-8,I1-9,
                I1-10,I1-11,I1-12,I1-13,I1-14,I1-15,I1-16,I1-17,
                I2,I2-1,I2-2,I2-3,I2-4,I2-5,I2-6,I2-7,I2-8,I2-9,
                I2-10,I2-11,I2-12,I2-13,I2-14,I2-15,I2-16,I2-17),
SUBJ9:SUBMATRIX(H9,J1,J1-1,J1-2,J1-3,J1-4,J1-5,J1-6,J1-7,J1-8,J1-9,
                J1-10,J1-11,J1-12,J1-13,J1-14,J1-15,J1-16,J1-17,
                J2,J2-1,J2-2,J2-3,J2-4,J2-5,J2-6,J2-7,J2-8,J2-9,
                J2-10,J2-11,J2-12,J2-13,J2-14,J2-15,J2-16,J2-17),
SUBI10:SUBMATRIX(H10,I1,I1-1,I1-2,I1-3,I1-4,I1-5,I1-6,I1-7,I1-8,I1-9,
                I1-10,I1-11,I1-12,I1-13,I1-14,I1-15,I1-16,I1-17,
                I2,I2-1,I2-2,I2-3,I2-4,I2-5,I2-6,I2-7,I2-8,I2-9,
                I2-10,I2-11,I2-12,I2-13,I2-14,I2-15,I2-16,I2-17),
SUBJ10:SUBMATRIX(H10,J1,J1-1,J1-2,J1-3,J1-4,J1-5,J1-6,J1-7,J1-8,J1-9,
                J1-10,J1-11,J1-12,J1-13,J1-14,J1-15,J1-16,J1-17,
                J2,J2-1,J2-2,J2-3,J2-4,J2-5,J2-6,J2-7,J2-8,J2-9,
                J2-10,J2-11,J2-12,J2-13,J2-14,J2-15,J2-16,J2-17),
SUBI11:SUBMATRIX(H11,I1,I1-1,I1-2,I1-3,I1-4,I1-5,I1-6,I1-7,I1-8,I1-9,
                I1-10,I1-11,I1-12,I1-13,I1-14,I1-15,I1-16,I1-17,
                I2,I2-1,I2-2,I2-3,I2-4,I2-5,I2-6,I2-7,I2-8,I2-9,
                I2-10,I2-11,I2-12,I2-13,I2-14,I2-15,I2-16,I2-17),
SUBJ11:SUBMATRIX(H11,J1,J1-1,J1-2,J1-3,J1-4,J1-5,J1-6,J1-7,J1-8,J1-9,
                J1-10,J1-11,J1-12,J1-13,J1-14,J1-15,J1-16,J1-17,
                J2,J2-1,J2-2,J2-3,J2-4,J2-5,J2-6,J2-7,J2-8,J2-9,
                J2-10,J2-11,J2-12,J2-13,J2-14,J2-15,J2-16,J2-17),
SUBI12:SUBMATRIX(H12,I1,I1-1,I1-2,I1-3,I1-4,I1-5,I1-6,I1-7,I1-8,I1-9,
                I1-10,I1-11,I1-12,I1-13,I1-14,I1-15,I1-16,I1-17,
                I2,I2-1,I2-2,I2-3,I2-4,I2-5,I2-6,I2-7,I2-8,I2-9,
                I2-10,I2-11,I2-12,I2-13,I2-14,I2-15,I2-16,I2-17),
SUBJ12:SUBMATRIX(H12,J1,J1-1,J1-2,J1-3,J1-4,J1-5,J1-6,J1-7,J1-8,J1-9,
                J1-10,J1-11,J1-12,J1-13,J1-14,J1-15,J1-16,J1-17,
                J2,J2-1,J2-2,J2-3,J2-4,J2-5,J2-6,J2-7,J2-8,J2-9,
                J2-10,J2-11,J2-12,J2-13,J2-14,J2-15,J2-16,J2-17),

CA:0.5$ CB:1./3.$ CC:2./3.$

N2:N2+ A[II,JJ]*( SUBI0.Q.TQ.SUBJ0+CA*(TQ.SUBJ0.Q)*SUBI0 ),
N2:N2+DD[II,JJ]*( CB*(SUBI0.Q.TQ.SUBJ2+CA*(TQ.SUBI0.Q)*SUBJ2+
                   SUBI2.Q.TQ.SUBJ0+CA*(TQ.SUBI2.Q)*SUBJ0)+
                     SUBI1.Q.TQ.SUBJ1+CA*(TQ.SUBJ1.Q)*SUBI1 ),
```

```
N2:N2+ F[II,JJ]*( CB*(SUBI0.Q.TQ.SUBJ4+CA*(TQ.SUBI0.Q)*SUBJ4+
                    SUBI4.Q.TQ.SUBJ0+CA*(TQ.SUBI4.Q)*SUBJ0)+
                  CC*(SUBI1.Q.TQ.SUBJ3+CA*(TQ.SUBI1.Q)*SUBJ3+
                    SUBI3.Q.TQ.SUBJ1+CA*(TQ.SUBI3.Q)*SUBJ1)+
                      SUBI2.Q.TQ.SUBJ2+CA*(TQ.SUBJ2.Q)*SUBI2 ),
N2:N2+ H[II,JJ]*( CB*(SUBI0.Q.TQ.SUBJ6+CA*(TQ.SUBI0.Q)*SUBJ6+
                    SUBI6.Q.TQ.SUBJ0+CA*(TQ.SUBI6.Q)*SUBJ0)+
                  CC*(SUBI1.Q.TQ.SUBJ5+CA*(TQ.SUBI1.Q)*SUBJ5+
                    SUBI5.Q.TQ.SUBJ1+CA*(TQ.SUBI5.Q)*SUBJ1)+
                  CC*(SUBI2.Q.TQ.SUBJ4+CA*(TQ.SUBI2.Q)*SUBJ4+
                    SUBI4.Q.TQ.SUBJ2+CA*(TQ.SUBI4.Q)*SUBJ2)+
                      SUBI3.Q.TQ.SUBJ3+CA*(TQ.SUBJ3.Q)*SUBI3 ),
N2:N2+ J[II,JJ]*( CB*(SUBI0.Q.TQ.SUBJ8+CA*(TQ.SUBI0.Q)*SUBJ8+
                    SUBI8.Q.TQ.SUBJ0+CA*(TQ.SUBI8.Q)*SUBJ0)+
                  CC*(SUBI1.Q.TQ.SUBJ7+CA*(TQ.SUBI1.Q)*SUBJ7+
                    SUBI7.Q.TQ.SUBJ1+CA*(TQ.SUBI7.Q)*SUBJ1)+
                  CC*(SUBI2.Q.TQ.SUBJ6+CA*(TQ.SUBI2.Q)*SUBJ6+
                    SUBI6.Q.TQ.SUBJ2+CA*(TQ.SUBI6.Q)*SUBJ2)+
                  CC*(SUBI3.Q.TQ.SUBJ5+CA*(TQ.SUBI3.Q)*SUBJ5+
                    SUBI5.Q.TQ.SUBJ3+CA*(TQ.SUBI5.Q)*SUBJ3)+
                      SUBI4.Q.TQ.SUBJ4+CA*(TQ.SUBJ4.Q)*SUBI4 ),
N2:N2+ L[II,JJ]*( CB*(SUBI0.Q.TQ.SUBJ10+CA*(TQ.SUBI0.Q)*SUBJ10+
                    SUBI10.Q.TQ.SUBJ0+CA*(TQ.SUBI10.Q)*SUBJ0)+
                  CC*(SUBI1.Q.TQ.SUBJ9+CA*(TQ.SUBI1.Q)*SUBJ9+
                    SUBI9.Q.TQ.SUBJ1+CA*(TQ.SUBI9.Q)*SUBJ1)+
                  CC*(SUBI2.Q.TQ.SUBJ8+CA*(TQ.SUBI2.Q)*SUBJ8+
                    SUBI8.Q.TQ.SUBJ2+CA*(TQ.SUBI8.Q)*SUBJ2)+
                  CC*(SUBI3.Q.TQ.SUBJ7+CA*(TQ.SUBI3.Q)*SUBJ7+
                    SUBI7.Q.TQ.SUBJ3+CA*(TQ.SUBI7.Q)*SUBJ3)+
                  CC*(SUBI4.Q.TQ.SUBJ6+CA*(TQ.SUBI4.Q)*SUBJ6+
                    SUBI6.Q.TQ.SUBJ4+CA*(TQ.SUBI6.Q)*SUBJ4)+
                      SUBI5.Q.TQ.SUBJ5+CA*(TQ.SUBJ5.Q)*SUBI5 ),
N2:N2+ R[II,JJ]*( CB*(SUBI0.Q.TQ.SUBJ12+CA*(TQ.SUBI0.Q)*SUBJ12+
                    SUBI12.Q.TQ.SUBJ0+CA*(TQ.SUBI12.Q)*SUBJ0)+
                  CC*(SUBI1.Q.TQ.SUBJ11+CA*(TQ.SUBI1.Q)*SUBJ11+
                    SUBI11.Q.TQ.SUBJ1+CA*(TQ.SUBI11.Q)*SUBJ1)+
                  CC*(SUBI2.Q.TQ.SUBJ10+CA*(TQ.SUBI2.Q)*SUBJ10+
                    SUBI10.Q.TQ.SUBJ2+CA*(TQ.SUBI10.Q)*SUBJ2)+
                  CC*(SUBI3.Q.TQ.SUBJ9+CA*(TQ.SUBI3.Q)*SUBJ9+
                    SUBI9.Q.TQ.SUBJ3+CA*(TQ.SUBI9.Q)*SUBJ3)+
                  CC*(SUBI4.Q.TQ.SUBJ8+CA*(TQ.SUBI4.Q)*SUBJ8+
                    SUBI8.Q.TQ.SUBJ4+CA*(TQ.SUBI8.Q)*SUBJ4)+
                  CC*(SUBI5.Q.TQ.SUBJ7+CA*(TQ.SUBI5.Q)*SUBJ7+
                    SUBI7.Q.TQ.SUBJ5+CA*(TQ.SUBI7.Q)*SUBJ5)+
                      SUBI6.Q.TQ.SUBJ6+CA*(TQ.SUBJ6.Q)*SUBI6 ),
N2:N2+ T[II,JJ]*( CC*(SUBI2.Q.TQ.SUBJ12+CA*(TQ.SUBI2.Q)*SUBJ12+
                    SUBI12.Q.TQ.SUBJ2+CA*(TQ.SUBI12.Q)*SUBJ2)+
                  CC*(SUBI3.Q.TQ.SUBJ11+CA*(TQ.SUBI3.Q)*SUBJ11+
                    SUBI11.Q.TQ.SUBJ3+CA*(TQ.SUBI11.Q)*SUBJ3)+
                  CC*(SUBI4.Q.TQ.SUBJ10+CA*(TQ.SUBI4.Q)*SUBJ10+
                    SUBI10.Q.TQ.SUBJ4+CA*(TQ.SUBI10.Q)*SUBJ4)+
```

```
                    CC*(SUBI5.Q.TQ.SUBJ9+CA*(TQ.SUBI5.Q)*SUBJ9+
                      SUBI9.Q.TQ.SUBJ5+CA*(TQ.SUBI9.Q)*SUBJ5)+
                    CC*(SUBI6.Q.TQ.SUBJ8+CA*(TQ.SUBI6.Q)*SUBJ8+
                      SUBI8.Q.TQ.SUBJ6+CA*(TQ.SUBI8.Q)*SUBJ6)+
                        SUBI7.Q.TQ.SUBJ7+CA*(TQ.SUBJ7.Q)*SUBI7 ),
N2:N2+ XH[II,JJ]*(CC*(SUBI4.Q.TQ.SUBJ12+CA*(TQ.SUBI4.Q)*SUBJ12+
                      SUBI12.Q.TQ.SUBJ4+CA*(TQ.SUBI12.Q)*SUBJ4)+
                    CC*(SUBI5.Q.TQ.SUBJ11+CA*(TQ.SUBI5.Q)*SUBJ11+
                      SUBI11.Q.TQ.SUBJ5+CA*(TQ.SUBI11.Q)*SUBJ5)+
                    CC*(SUBI6.Q.TQ.SUBJ10+CA*(TQ.SUBI6.Q)*SUBJ10+
                      SUBI10.Q.TQ.SUBJ6+CA*(TQ.SUBI10.Q)*SUBJ6)+
                    CC*(SUBI7.Q.TQ.SUBJ9+CA*(TQ.SUBI7.Q)*SUBJ9+
                      SUBI9.Q.TQ.SUBJ7+CA*(TQ.SUBI9.Q)*SUBJ7)+
                        SUBI8.Q.TQ.SUBJ8+CA*(TQ.SUBJ8.Q)*SUBI8 ),
N2:N2+ XJ[II,JJ]*( CC*(SUBI6.Q.TQ.SUBJ12+CA*(TQ.SUBI6.Q)*SUBJ12+
                      SUBI12.Q.TQ.SUBJ6+CA*(TQ.SUBI12.Q)*SUBJ6)+
                    CC*(SUBI7.Q.TQ.SUBJ11+CA*(TQ.SUBI7.Q)*SUBJ11+
                      SUBI11.Q.TQ.SUBJ7+CA*(TQ.SUBI11.Q)*SUBJ7)+
                    CC*(SUBI8.Q.TQ.SUBJ10+CA*(TQ.SUBI8.Q)*SUBJ10+
                      SUBI10.Q.TQ.SUBJ8+CA*(TQ.SUBI10.Q)*SUBJ8)+
                        SUBI9.Q.TQ.SUBJ9+CA*(TQ.SUBJ9.Q)*SUBI9 ),
N2:N2+ XL[II,JJ]*( CC*(SUBI8.Q.TQ.SUBJ12+CA*(TQ.SUBI8.Q)*SUBJ12+
                      SUBI12.Q.TQ.SUBJ8+CA*(TQ.SUBI12.Q)*SUBJ8)+
                    CC*(SUBI9.Q.TQ.SUBJ11+CA*(TQ.SUBI9.Q)*SUBJ11+
                      SUBI11.Q.TQ.SUBJ9+CA*(TQ.SUBI11.Q)*SUBJ9)+
                    SUBI10.Q.TQ.SUBJ10+CA*(TQ.SUBJ10.Q)*SUBI10 ),
N2:N2+ XR[II,JJ]*( CC*(SUBI10.Q.TQ.SUBJ12+CA*(TQ.SUBI10.Q)*SUBJ12+
                      SUBI12.Q.TQ.SUBJ10+CA*(TQ.SUBI12.Q)*SUBJ10)+
                    SUBI11.Q.TQ.SUBJ11+CA*(TQ.SUBJ11.Q)*SUBI11 ),
N2:N2+ XT[II,JJ]*( SUBI12.Q.TQ.SUBJ12+CA*(TQ.SUBJ12.Q)*SUBI12 ),

KILL(SUBJ12,SUBI12,SUBJ11,SUBJ11),
KILL(SUBJ0,SUBJ1,SUBJ2,SUBJ3,SUBJ4,SUBJ5,SUBJ6,SUBJ7,SUBJ8,SUBJ9,SUBJ10),
KILL(SUBI0,SUBI1,SUBI2,SUBI3,SUBI4,SUBI5,SUBI6,SUBI7,SUBI8,SUBI9,SUBI10)))$

KILL(H0,H1,H2,H3,H4,H5,H6,H7,H8,H9,H10,H11,H12)$
N2SYM:ZEROMATRIX(18,18)$
FOR II THRU 18 DO FOR JJ:II THRU 18 DO N2SYM[II,JJ]:N2[II,JJ]$
PRINT("SYMMETRIC N2 FORMED")$
KILL(N2)$
N2:ZEROMATRIX(18,18)$
KILL(Q,TQ)$
FOR II THRU 18 DO FOR JJ:II THRU 18 DO
N2[II,JJ]:FACTOROUT(N2SYM[II,JJ],Q(1),Q(2),Q(3),Q(4),Q(5),Q(6),
Q(7),Q(8),Q(9),Q(10),Q(11),Q(12),Q(13),Q(14),Q(15),Q(16),Q(17),Q(18))$
FRAME(I,J):=CONCAT(TT,EV(18*(I-1)+J+1000))$
FOR I THRU 18 DO FOR J:I THRU 18 DO
(IF N2[I,J]#0 THEN (PT:1,GENTRAN(SN2[EVAL(I),EVAL(J)]:EVAL(N2[I,J]),
[EVAL(FRAME(I,J))])))$
IF PT#1 THEN GENTRAN(PT:EVAL(PT),[TT2000])$
```

```
/*************************************************************************/
/*   GENERATE THE NONLINEAR ELEMENT-INDEPENDENT STIFFNESS ARRAY N2S.     */
/*************************************************************************/

/* ASSEMBLE MATRIX N2AS */
TQ:MATRIX([Q(1),Q(2),Q(3),Q(4),Q(5),Q(6),Q(7),Q(8),Q(9),Q(10),
          Q(11),Q(12),Q(13),Q(14),Q(15),Q(16),Q(17),Q(18)])$
Q:TRANSPOSE(TQ)$ LOADFILE("SSMAT123.SV")$
SS0:SUBST([K=K1,C=P1],SS0)$ SS1:SUBST([K=K1,C=P1],SS1)$
SS2:SUBST([K=K1,C=P1],SS2)$ SS3:SUBST([K=K1,C=P1],SS3)$
SS4:SUBST([K=K1,C=P1],SS4)$ SS5:SUBST([K=K1,C=P1],SS5)$
SS6:SUBST([K=K1,C=P1],SS6)$ SS7:SUBST([K=K1,C=P1],SS7)$
SS8:SUBST([K=K1,C=P1],SS8)$ SS9:SUBST([K=K1,C=P1],SS9)$
SS10:SUBST([K=K1,C=P1],SS10)$ SS11:SUBST([K=K1,C=P1],SS11)$
SS12:SUBST([K=K1,C=P1],SS12)$ N2S:ZEROMATRIX(18,18)$

FOR II THRU 2 DO FOR JJ THRU 2 DO (PRINT(II,JJ),
( J2:3*( 9*(JJ+1)^2-39*(JJ+1)+48), I2:3*( 9*(II+1)^2-39*(II+1)+48),
SUBIS0:SUBMATRIX(SS0, I2,I2-1,I2-2,I2-3,I2-4,I2-5,I2-6,I2-7,I2-8,I2-9,
                 I2-10,I2-11,I2-12,I2-13,I2-14,I2-15,I2-16,I2-17),
SUBJS0:SUBMATRIX(SS0, J2,J2-1,J2-2,J2-3,J2-4,J2-5,J2-6,J2-7,J2-8,J2-9,
                 J2-10,J2-11,J2-12,J2-13,J2-14,J2-15,J2-16,J2-17),
SUBIS1:SUBMATRIX(SS1, I2,I2-1,I2-2,I2-3,I2-4,I2-5,I2-6,I2-7,I2-8,I2-9,
                 I2-10,I2-11,I2-12,I2-13,I2-14,I2-15,I2-16,I2-17),
SUBJS1:SUBMATRIX(SS1, J2,J2-1,J2-2,J2-3,J2-4,J2-5,J2-6,J2-7,J2-8,J2-9,
                 J2-10,J2-11,J2-12,J2-13,J2-14,J2-15,J2-16,J2-17),
SUBIS2:SUBMATRIX(SS2, I2,I2-1,I2-2,I2-3,I2-4,I2-5,I2-6,I2-7,I2-8,I2-9,
                 I2-10,I2-11,I2-12,I2-13,I2-14,I2-15,I2-16,I2-17),
SUBJS2:SUBMATRIX(SS2, J2,J2-1,J2-2,J2-3,J2-4,J2-5,J2-6,J2-7,J2-8,J2-9,
                 J2-10,J2-11,J2-12,J2-13,J2-14,J2-15,J2-16,J2-17),
SUBIS3:SUBMATRIX(SS3, I2,I2-1,I2-2,I2-3,I2-4,I2-5,I2-6,I2-7,I2-8,I2-9,
                 I2-10,I2-11,I2-12,I2-13,I2-14,I2-15,I2-16,I2-17),
SUBJS3:SUBMATRIX(SS3, J2,J2-1,J2-2,J2-3,J2-4,J2-5,J2-6,J2-7,J2-8,J2-9,
                 J2-10,J2-11,J2-12,J2-13,J2-14,J2-15,J2-16,J2-17),
SUBIS4:SUBMATRIX(SS4, I2,I2-1,I2-2,I2-3,I2-4,I2-5,I2-6,I2-7,I2-8,I2-9,
                 I2-10,I2-11,I2-12,I2-13,I2-14,I2-15,I2-16,I2-17),
SUBJS4:SUBMATRIX(SS4, J2,J2-1,J2-2,J2-3,J2-4,J2-5,J2-6,J2-7,J2-8,J2-9,
                 J2-10,J2-11,J2-12,J2-13,J2-14,J2-15,J2-16,J2-17),
SUBIS5:SUBMATRIX(SS5, I2,I2-1,I2-2,I2-3,I2-4,I2-5,I2-6,I2-7,I2-8,I2-9,
                 I2-10,I2-11,I2-12,I2-13,I2-14,I2-15,I2-16,I2-17),
SUBJS5:SUBMATRIX(SS5, J2,J2-1,J2-2,J2-3,J2-4,J2-5,J2-6,J2-7,J2-8,J2-9,
                 J2-10,J2-11,J2-12,J2-13,J2-14,J2-15,J2-16,J2-17),
SUBIS6:SUBMATRIX(SS6, I2,I2-1,I2-2,I2-3,I2-4,I2-5,I2-6,I2-7,I2-8,I2-9,
                 I2-10,I2-11,I2-12,I2-13,I2-14,I2-15,I2-16,I2-17),
SUBJS6:SUBMATRIX(SS6, J2,J2-1,J2-2,J2-3,J2-4,J2-5,J2-6,J2-7,J2-8,J2-9,
                 J2-10,J2-11,J2-12,J2-13,J2-14,J2-15,J2-16,J2-17),
SUBIS7:SUBMATRIX(SS7, I2,I2-1,I2-2,I2-3,I2-4,I2-5,I2-6,I2-7,I2-8,I2-9,
                 I2-10,I2-11,I2-12,I2-13,I2-14,I2-15,I2-16,I2-17),
SUBJS7:SUBMATRIX(SS7, J2,J2-1,J2-2,J2-3,J2-4,J2-5,J2-6,J2-7,J2-8,J2-9,
                 J2-10,J2-11,J2-12,J2-13,J2-14,J2-15,J2-16,J2-17),
SUBIS8:SUBMATRIX(SS8, I2,I2-1,I2-2,I2-3,I2-4,I2-5,I2-6,I2-7,I2-8,I2-9,
```

```
                    I2-10,I2-11,I2-12,I2-13,I2-14,I2-15,I2-16,I2-17),
SUBJS8:SUBMATRIX(SS8, J2,J2-1,J2-2,J2-3,J2-4,J2-5,J2-6,J2-7,J2-8,J2-9,
                    J2-10,J2-11,J2-12,J2-13,J2-14,J2-15,J2-16,J2-17),
SUBIS9:SUBMATRIX(SS9, I2,I2-1,I2-2,I2-3,I2-4,I2-5,I2-6,I2-7,I2-8,I2-9,
                    I2-10,I2-11,I2-12,I2-13,I2-14,I2-15,I2-16,I2-17),
SUBJS9:SUBMATRIX(SS9, J2,J2-1,J2-2,J2-3,J2-4,J2-5,J2-6,J2-7,J2-8,J2-9,
                    J2-10,J2-11,J2-12,J2-13,J2-14,J2-15,J2-16,J2-17),
SUBIS10:SUBMATRIX(SS10, I2,I2-1,I2-2,I2-3,I2-4,I2-5,I2-6,I2-7,I2-8,I2-9,
                    I2-10,I2-11,I2-12,I2-13,I2-14,I2-15,I2-16,I2-17),
SUBJS10:SUBMATRIX(SS10, J2,J2-1,J2-2,J2-3,J2-4,J2-5,J2-6,J2-7,J2-8,J2-9,
                    J2-10,J2-11,J2-12,J2-13,J2-14,J2-15,J2-16,J2-17),
SUBIS11:SUBMATRIX(SS11, I2,I2-1,I2-2,I2-3,I2-4,I2-5,I2-6,I2-7,I2-8,I2-9,
                    I2-10,I2-11,I2-12,I2-13,I2-14,I2-15,I2-16,I2-17),
SUBJS11:SUBMATRIX(SS11, J2,J2-1,J2-2,J2-3,J2-4,J2-5,J2-6,J2-7,J2-8,J2-9,
                    J2-10,J2-11,J2-12,J2-13,J2-14,J2-15,J2-16,J2-17),
SUBIS12:SUBMATRIX(SS12, I2,I2-1,I2-2,I2-3,I2-4,I2-5,I2-6,I2-7,I2-8,I2-9,
                    I2-10,I2-11,I2-12,I2-13,I2-14,I2-15,I2-16,I2-17),
SUBJS12:SUBMATRIX(SS12, J2,J2-1,J2-2,J2-3,J2-4,J2-5,J2-6,J2-7,J2-8,J2-9,
                    J2-10,J2-11,J2-12,J2-13,J2-14,J2-15,J2-16,J2-17),

CA:0.5$ CB:1./3.$ CC:2./3.$

N2S:N2S+AS[II,JJ]*( SUBIS0.Q.TQ.SUBJS0+CA*(TQ.SUBJS0.Q)*SUBIS0 ),
N2S:N2S+DS[II,JJ]*( CB*(SUBIS0.Q.TQ.SUBJS2+CA*(TQ.SUBIS0.Q)*SUBJS2+
                     SUBIS2.Q.TQ.SUBJS0+CA*(TQ.SUBIS2.Q)*SUBJS0)+
                       SUBIS1.Q.TQ.SUBJS1+CA*(TQ.SUBJS1.Q)*SUBIS1 ),
N2S:N2S+FS[II,JJ]*( CB*(SUBIS0.Q.TQ.SUBJS4+CA*(TQ.SUBIS0.Q)*SUBJS4+
                     SUBIS4.Q.TQ.SUBJS0+CA*(TQ.SUBIS4.Q)*SUBJS0)+
                   CC*(SUBIS1.Q.TQ.SUBJS3+CA*(TQ.SUBIS1.Q)*SUBJS3+
                     SUBIS3.Q.TQ.SUBJS1+CA*(TQ.SUBIS3.Q)*SUBJS1)+
                       SUBIS2.Q.TQ.SUBJS2+CA*(TQ.SUBJS2.Q)*SUBIS2 ),
N2S:N2S+HS[II,JJ]*( CB*(SUBIS0.Q.TQ.SUBJS6+CA*(TQ.SUBIS0.Q)*SUBJS6+
                     SUBIS6.Q.TQ.SUBJS0+CA*(TQ.SUBIS6.Q)*SUBJS0)+
                   CC*(SUBIS1.Q.TQ.SUBJS5+CA*(TQ.SUBIS1.Q)*SUBJS5+
                     SUBIS5.Q.TQ.SUBJS1+CA*(TQ.SUBIS5.Q)*SUBJS1)+
                   CC*(SUBIS2.Q.TQ.SUBJS4+CA*(TQ.SUBIS2.Q)*SUBJS4+
                     SUBIS4.Q.TQ.SUBJS2+CA*(TQ.SUBIS4.Q)*SUBJS2)+
                       SUBIS3.Q.TQ.SUBJS3+CA*(TQ.SUBJS3.Q)*SUBIS3 ),
N2S:N2S+JS[II,JJ]*( CB*(SUBIS0.Q.TQ.SUBJS8+CA*(TQ.SUBIS0.Q)*SUBJS8+
                     SUBIS8.Q.TQ.SUBJS0+CA*(TQ.SUBIS8.Q)*SUBJS0)+
                   CC*(SUBIS1.Q.TQ.SUBJS7+CA*(TQ.SUBIS1.Q)*SUBJS7+
                     SUBIS7.Q.TQ.SUBJS1+CA*(TQ.SUBIS7.Q)*SUBJS1)+
                   CC*(SUBIS2.Q.TQ.SUBJS6+CA*(TQ.SUBIS2.Q)*SUBJS6+
                     SUBIS6.Q.TQ.SUBJS2+CA*(TQ.SUBIS6.Q)*SUBJS2)+
                   CC*(SUBIS3.Q.TQ.SUBJS5+CA*(TQ.SUBIS3.Q)*SUBJS5+
                     SUBIS5.Q.TQ.SUBJS3+CA*(TQ.SUBIS5.Q)*SUBJS3)+
                       SUBIS4.Q.TQ.SUBJS4+CA*(TQ.SUBJS4.Q)*SUBIS4 ),
N2S:N2S+LS[II,JJ]*(CB*(SUBIS0.Q.TQ.SUBJS10+CA*(TQ.SUBIS0.Q)*SUBJS10+
                     SUBIS10.Q.TQ.SUBJS0+CA*(TQ.SUBIS10.Q)*SUBJS0)+
                   CC*(SUBIS1.Q.TQ.SUBJS9+CA*(TQ.SUBIS1.Q)*SUBJS9+
                     SUBIS9.Q.TQ.SUBJS1+CA*(TQ.SUBIS9.Q)*SUBJS1)+
```

```
                    CC*(SUBIS2.Q.TQ.SUBJS8+CA*(TQ.SUBIS2.Q)*SUBJS8+
                      SUBIS8.Q.TQ.SUBJS2+CA*(TQ.SUBIS8.Q)*SUBJS2)+
                    CC*(SUBIS3.Q.TQ.SUBJS7+CA*(TQ.SUBIS3.Q)*SUBJS7+
                      SUBIS7.Q.TQ.SUBJS3+CA*(TQ.SUBIS7.Q)*SUBJS3)+
                    CC*(SUBIS4.Q.TQ.SUBJS6+CA*(TQ.SUBIS4.Q)*SUBJS6+
                      SUBIS6.Q.TQ.SUBJS4+CA*(TQ.SUBIS6.Q)*SUBJS4)+
                        SUBIS5.Q.TQ.SUBJS5+CA*(TQ.SUBJS5.Q)*SUBIS5 ),
N2S:N2S+RS[II,JJ]*(CB*(SUBIS0.Q.TQ.SUBJS12+CA*(TQ.SUBIS0.Q)*SUBJS12+
                      SUBIS12.Q.TQ.SUBJS0+CA*(TQ.SUBIS12.Q)*SUBJS0)+
                     CC*(SUBIS1.Q.TQ.SUBJS11+CA*(TQ.SUBIS1.Q)*SUBJS11+
                      SUBIS11.Q.TQ.SUBJS1+CA*(TQ.SUBIS11.Q)*SUBJS1)+
                     CC*(SUBIS2.Q.TQ.SUBJS10+CA*(TQ.SUBIS2.Q)*SUBJS10+
                      SUBIS10.Q.TQ.SUBJS2+CA*(TQ.SUBIS10.Q)*SUBJS2)+
                    CC*(SUBIS3.Q.TQ.SUBJS9+CA*(TQ.SUBIS3.Q)*SUBJS9+
                      SUBIS9.Q.TQ.SUBJS3+CA*(TQ.SUBIS9.Q)*SUBJS3)+
                    CC*(SUBIS4.Q.TQ.SUBJS8+CA*(TQ.SUBIS4.Q)*SUBJS8+
                      SUBIS8.Q.TQ.SUBJS4+CA*(TQ.SUBIS8.Q)*SUBJS4)+
                    CC*(SUBIS5.Q.TQ.SUBJS7+CA*(TQ.SUBIS5.Q)*SUBJS7+
                      SUBIS7.Q.TQ.SUBJS5+CA*(TQ.SUBIS7.Q)*SUBJS5)+
                        SUBIS6.Q.TQ.SUBJS6+CA*(TQ.SUBJS6.Q)*SUBIS6 ),
N2S:N2S+TS[II,JJ]*(CC*(SUBIS2.Q.TQ.SUBJS12+CA*(TQ.SUBIS2.Q)*SUBJS12+
                      SUBIS12.Q.TQ.SUBJS2+CA*(TQ.SUBIS12.Q)*SUBJS2)+
                     CC*(SUBIS3.Q.TQ.SUBJS11+CA*(TQ.SUBIS3.Q)*SUBJS11+
                      SUBIS11.Q.TQ.SUBJS3+CA*(TQ.SUBIS11.Q)*SUBJS3)+
                    CC*(SUBIS4.Q.TQ.SUBJS10+CA*(TQ.SUBIS4.Q)*SUBJS10+
                      SUBIS10.Q.TQ.SUBJS4+CA*(TQ.SUBIS10.Q)*SUBJS4)+
                    CC*(SUBIS5.Q.TQ.SUBJS9+CA*(TQ.SUBIS5.Q)*SUBJS9+
                      SUBIS9.Q.TQ.SUBJS5+CA*(TQ.SUBIS9.Q)*SUBJS5)+
                    CC*(SUBIS6.Q.TQ.SUBJS8+CA*(TQ.SUBIS6.Q)*SUBJS8+
                      SUBIS8.Q.TQ.SUBJS6+CA*(TQ.SUBIS8.Q)*SUBJS6)+
                        SUBIS7.Q.TQ.SUBJS7+CA*(TQ.SUBJS7.Q)*SUBIS7 ),
N2S:N2S+XHS[II,JJ]*(CC*(SUBIS4.Q.TQ.SUBJS12+CA*(TQ.SUBIS4.Q)*SUBJS12+
                      SUBIS12.Q.TQ.SUBJS4+CA*(TQ.SUBIS12.Q)*SUBJS4)+
                     CC*(SUBIS5.Q.TQ.SUBJS11+CA*(TQ.SUBIS5.Q)*SUBJS11+
                      SUBIS11.Q.TQ.SUBJS5+CA*(TQ.SUBIS11.Q)*SUBJS5)+
                    CC*(SUBIS6.Q.TQ.SUBJS10+CA*(TQ.SUBIS6.Q)*SUBJS10+
                      SUBIS10.Q.TQ.SUBJS6+CA*(TQ.SUBIS10.Q)*SUBJS6)+
                    CC*(SUBIS7.Q.TQ.SUBJS9+CA*(TQ.SUBIS7.Q)*SUBJS9+
                      SUBIS9.Q.TQ.SUBJS7+CA*(TQ.SUBIS9.Q)*SUBJS7)+
                        SUBIS8.Q.TQ.SUBJS8+CA*(TQ.SUBJS8.Q)*SUBIS8 ),
N2S:N2S+XJS[II,JJ]*(CC*(SUBIS6.Q.TQ.SUBJS12+CA*(TQ.SUBIS6.Q)*SUBJS12+
                      SUBIS12.Q.TQ.SUBJS6+CA*(TQ.SUBIS12.Q)*SUBJS6)+
                     CC*(SUBIS7.Q.TQ.SUBJS11+CA*(TQ.SUBIS7.Q)*SUBJS11+
                      SUBIS11.Q.TQ.SUBJS7+CA*(TQ.SUBIS11.Q)*SUBJS7)+
                     CC*(SUBIS8.Q.TQ.SUBJS10+CA*(TQ.SUBIS8.Q)*SUBJS10+
                      SUBIS10.Q.TQ.SUBJS8+CA*(TQ.SUBIS10.Q)*SUBJS8)+
                        SUBIS9.Q.TQ.SUBJS9+CA*(TQ.SUBJS9.Q)*SUBIS9 ),
N2S:N2S+XLS[II,JJ]*(CC*(SUBIS8.Q.TQ.SUBJS12+CA*(TQ.SUBIS8.Q)*SUBJS12+
                      SUBIS12.Q.TQ.SUBJS8+CA*(TQ.SUBIS12.Q)*SUBJS8)+
                     CC*(SUBIS9.Q.TQ.SUBJS11+CA*(TQ.SUBIS9.Q)*SUBJS11+
                      SUBIS11.Q.TQ.SUBJS9+CA*(TQ.SUBIS11.Q)*SUBJS9)+
```

```
                    SUBIS10.Q.TQ.SUBJS10+CA*(TQ.SUBJS10.Q)*SUBIS10 ),
N2S:N2S+XRS[II,JJ]*(CC*(SUBIS10.Q.TQ.SUBJS12+CA*(TQ.SUBIS10.Q)*SUBJS12+
                    SUBIS12.Q.TQ.SUBJS10+CA*(TQ.SUBIS12.Q)*SUBJS10)+
                    SUBIS11.Q.TQ.SUBJS11+CA*(TQ.SUBJS11.Q)*SUBIS11 ),
N2S:N2S+XTS[II,JJ]*( SUBIS12.Q.TQ.SUBJS12+CA*(TQ.SUBJS12.Q)*SUBIS12 ),

KILL(SUBJS12,SUBIS12,SUBJS11,SUBIS11),
KILL(SUBJS0,SUBJS1,SUBJS2,SUBJS3,SUBJS4,SUBJS5,
     SUBJS6,SUBJS7,SUBJS8,SUBJS9,SUBJS10),
KILL(SUBIS0,SUBIS1,SUBIS2,SUBIS3,SUBIS4,SUBIS5,
     SUBIS6,SUBIS7,SUBIS8,SUBIS9,SUBIS10)))$

KILL(SS0,SS1,SS2,SS3,SS4,SS5,SS6,SS7,SS8,SS9,SS10,SS11,SS12)$
N2SYM:ZEROMATRIX(18,18)$
FOR II THRU 18 DO FOR JJ:II THRU 18 DO N2SYM[II,JJ]:N2S[II,JJ]$
PRINT("SYMMETRIC N2 FORMED")$
KILL(N2S)$
N2:ZEROMATRIX(18,18)$
KILL(Q,TQ)$
FOR II THRU 18 DO FOR JJ:II THRU 18 DO
N2[II,JJ]:FACTOROUT(N2SYM[II,JJ],Q(1),Q(2),Q(3),Q(4),Q(5),Q(6),
Q(7),Q(8),Q(9),Q(10),Q(11),Q(12),Q(13),Q(14),Q(15),Q(16),Q(17),Q(18))$
FRAME(I,J):=CONCAT(TT,EV(18*(I-1)+J+1000))$
FOR I THRU 18 DO FOR J:I THRU 18 DO
(IF N2[I,J]#0 THEN (PT:1,GENTRAN(SN2S[EVAL(I),EVAL(J)]:EVAL(N2[I,J]),
[EVAL(FRAME(I,J))]))))$
IF PT#1 THEN GENTRAN(PT:EVAL(PT),[TT2000])$
```

Bibliography

1. Almroth, B. O., F. A. Brogan and G. M. Stanley. *Structural Analysis of General Shells, Volume II. User Instructions for STAGSC-1.* Palo Alto, California: Lockheed Palo Alto Research Laboratory, LSMC-D633873, December 1982.
2. Ashton, J. E., J. C. Halpin and P. H. Petit. *Primer on Composite Material Analysis.* Stamford, Connecticut: Technomic, 1969.
3. Axelrad, E. L. and F. A. Emmerling. "Intrinsic Shell Theory Relevant for Realizable Large Displacements," *International Journal of Non-Linear Mechanics, 22:* No. 2, 139–150, (1987).
4. Axelrad, E. L. and F. A. Emmerling. "Vector and Tensor Form of Intrinsic Shell-Theory Relations," *International Journal of Non-Linear Mechanics, 23:* No. 1, 9–23, (1988).
5. Bathe, Klaus-Jürgen and Eduardo N. Dvorkin. "A Formulation of General Shell Elements—The Use of Mixed Interpolation of Tensorial Components," *International Journal of Numerical Methods in Engineering, 22:* 697–722, (1986).
6. Becker, Marvin L., Anthony N. Palazotto and Narendra S. Khot. "Experimental Investigation of the Instability of Composite Cylindrical Panels," *Experimental Mechanics, 22:* No. 10, 372–376, (October 1982).
7. Beltzer, Abraham I. *Variational and Finite Element Methods A Symbolic Computation Approach.* New York: Springer-Verlag, 1990.
8. Belytschko, Ted, and L. Gaum. "Application of Higher Order Corrotational Stretch Theories to Nonlinear Finite Element Analysis," *Computers & Structures, 10:* 175–182, (1979).
9. Bhimaraddi, A., A. J. Carr and P. J. Moss. "A Shear Deformable Finite Element for the Analysis of General Shells of Revolution," *Computers & Structures, 31:* No. 3, 299–308, (1989).
10. Bhimaraddi, A., A. J. Carr and P. J. Moss. "Generalized Finite Element Analysis of Laminated Curved Beams with Constant Curvature," *Computers & Structures, 31:* No. 3, 309–317, (1989).
11. Briassoulis, Demetres. "The Zero Energy Modes Problem of the Nine-Noded Lagrangian Degenerated Shell Element," *Computers & Structures, 30:* No. 6, 1389–1402, (1988).
12. Bushnell, D. "Computerized Analysis of Shells — Governing Equations," *Computers & Structures, 18:* No. 3, 471–536, (1984).
13. Calcote, Lee R. *The Analysis of Laminated Composite Structures.* Cincinnati, Ohio: Van Nostrand Reinhold Co., 1969.
14. Chang, T. Y., A. F. Saleeb and W. Graf. "On the Mixed Formulation of a 9-Node Lagrange Shell Element," *Computer Methods in Applied Mechanics and Engineering, 73:* 259–281, (1989).

15. Chaudhuri, Reaz A. "An Equilibrium Method for Prediction of Transverse Shear Stresses in a Thick Laminated Plate," *Computers & Structures, 23:* No. 2, 139–146, (1986).

16. Cook, Robert D., David S. Malkus, and Michael E. Plesha. *Concepts and Applications of Finite Element Analysis* (Third Edition). New York: John Wiley & Sons, 1989.

17. DaDeppo, D. A. and R. Schmidt. "Instability of Clamped Hinged Circular Arches Subjected to a Point Load," *Journal of Applied Mechanics:* 894–896, (1975)

18. Dennis, Capt Scott T. *Large Displacement and Rotational Formulation for Laminated Cylindrical Shells including Parabolic Transverse Shear.* PhD Dissertation, AFIT/DS/AA/88-1. School of Engineering, Air Force Institute of Technology (AU), Wright-Patterson AFB, OH, May 1988 (AD-A194 871).

19. Dennis, Scott T. and Anthony N. Palazotto. "The Effects of Large Movement on a Composite Cylindrical Shell with Cutouts," *31st Structures, Structural dynamics and Materials Conference:* 2080–2088. AIAA Paper No. 89–1398. New York: American Institute of Aeronautics and Astronautics, April 1989.

20. Dennis, Scott T. and Anthony N. Palazotto. "Transverse Shear Deformation in Orthotropic Cylindrical Pressure Vessels Using a Higher-Order Shear Theory," *AIAA Journal, 27:* No. 10, 1441–1447, (October 1989).

21. Dennis, Scott T. and Anthony N. Palazotto. "Static Response of a Cylindrical Composite Panel with Cutouts Using a Geometrically Nonlinear Theory," *AIAA Journal, 28:* No. 6, 1082–1088, (June 1990).

22. Dennis, Scott T. and Anthony N. Palazotto. "Large Displacement and Rotational Formulation for Laminated Shells Including Parabolic Transverse Shear," *International Journal of Non-Linear Mechanics, 25:* No. 1, 67–85, (1990).

23. Donnell, L. H. *Stability of Thin Walled Tubes under Torsion,* NACA TR 479. Washington: National Advisory Committee for Aeronautics, 1934.

24. Engblom, John J. and O. O. Ochoa. "Finite Element Formulation Including Interlaminar Stress Calculations," *Computers & Structures, 23:* No. 2, 241–249, (1986).

25. Fuehne, Joseph P. and John J. Engblom. "A Shear-Deformable, Doubly-Curved Finite Element for the Analysis of Laminated Composite Structures," *Composite Structures, 12:* 81–95, (1989).

26. Hildebrand, F. B., E. Reissner, and G. B. Thomas. *Notes on the Foundations of the Theory of Small Displacements of Orthotropic Shells,* NACA TN 1833. Washington: National Advisory Committee for Aeronautics, 1949.

27. Hsiao, Kuo-Mo and Yeh-Ren Chen. "Nonlinear Analysis of hell Structures by Degenerated Isoparametric Shell Element," *Computers & Structures, 31:* No. 3, 427–438, (1989).

28. Hsiao, Kuo-Mo and Hung-Chan Hung. "Large Deflection Analysis of Shell Structure by Using Corotational Total LaGrangian Formulation," *Computer Methods in Applied Mechanics and Engineering, 73:* 209–225, (1989).

29. Huddleston, J. V. "Finite Deflections and Snap-Through of High Circular Arches," *Journal of Applied Mechanics:* 763–769, (December 1968).

30. Hughes, Thomas J. R. and W. K. Liu. "Nonlinear Finite Element Analysis of Shells I — Three-Dimensional Shells," *Computer Methods in Applied Mechanics and Engineering, 26:* 331–362, (1981).

31. Hughes, Thomas J. R. and W. K. Liu. "Nonlinear Finite Element Analysis of Shells II — Two-Dimensional Shells," *Computer Methods in Applied Mechanics and Engineering, 27:* 167–181, (1981).

32. Irons, Bruce M. and S. Ahmad *Techniques of Finite Elements.* Chichester, U. K.: Ellis Horwood, 1980.

33. Janisse, T. C. and Anthony N. Palazotto. "Collapse Analysis of Cylindrical Composite Panel with Cutouts," *Journal of Aircraft AIAA, 21:* No. 9, 731–733, (September 1984).

34. Jemielita, G. "Techniczna Teoria Plyt Sredniej Grubbosci (Technical Theory of Plates with Moderate Thickness)," *Rozprawy Inzynierskie (English Translation, Polska Akademia Nauk),23:* 483–499, (1975).

35. John, Fritz. "Estimates for the Derivatives of the Stresses in a Thin Shell and Interior Shell Equations," *Communications on Pure and Applied Mathematics, 18:* 235–267, (1965).

36. Jones, Robert M. *Mechanics of Composite Materials.* Washington, D.C.: Scripta Book Co., 1975.

37. Kant, T. and M. P. Menon. "Higher-Order Theories for Composite and Sandwich Cylindrical Shells with C^0 Finite Element," *Computers & Structures, 33:* No. 5, 1191–1204, (1989).

38. Kapania, Rakesh K. and Stefano Raciti. "Recent Advances in Analysis of Laminated Beams and Plates, Part I: Shear Effects and Buckling," *AIAA Journal, 27:* No. 7, 923–934, (July 1989).

39. Knight, Norman F., Jr., James H. Starnes, Jr. and William Allen Walters, Jr. "Postbuckling Behavior of Selected Graphite-Epoxy Cylindrical Panels Loaded in Axial Compression," *27th Structures, Structural dynamics and Materials Conference:* 142–158. AIAA Paper No. 86-0881. New York: American Institute of Aeronautics and Astronautics, May 1986.

40. Koiter, W. T. "A Consistent First Approximation in the General Theory of Thin Elastic Shells," *The Theory of Thin Elastic Shells:* 12–33. Amsterdam: North Holland, 1960.

41. Kwon, Y. K. and J. E. Akin. "Analysis of Layered Composite Plates Using a Higher-Order Deformation Theory," *Computers & Structures, 27:* No. 5, 619–623, (1987).

42. Liao, C. L. and J. N. Reddy. "Continuum-Based Stiffened Composite Shell Element for Geometrically Nonlinear Analysis," *AIAA Journal, 27:* No. 1, 95–101, (January 1989).

43. Libai, A. and J. G. Simmonds. "Nonlinear Elastic Shell Theory," *Advances in Applied Mechanics, 23:* 273-371, (1983).

44. Libai, A. and J. G. Simmonds. *The Nonlinear Theory of Shells.* New York: Academic Press, 1989.

45. Librescu, Liviu. "Refined Geometrically Nonlinear Theories of Anisotropic Shells," *Quarterly of Applied Mathematics, 45:* 1-22, (April 1987).

46. Librescu, Liviu and Rudiger Schmidt. "Refined Theories of Elastic Anisotropic Shells Accounting for Small Strains and Moderate Rotations," *International Journal of Non-Linear Mechanics, 23:* No. 3, 217-229, (1988).

47. Love, A. E. H. *A Treatise on the Mathematical Theory of Shells,* (Fourth Edition). New York: Dover Publications, 1944.

48. *MACSYMA Reference Manual.* Symbolics, Inc., 1988.

49. Mindlin, R. D. "Influence of Rotatory Inertia and Shear on Flexural Motions of Isotropic, Elastic Plates," *Journal of Apllied Mechanics, 18:* 336-343, (1951).

50. Mollmann, H. *Introduction to the Theory of Thin Shells.* New York: John Wiley & Sons, 1981.

51. Morley, L. S. D. "Approximation to Bending Trial Functions for Shell Triangular Finite Elements in Quadratic Parametric Representation," *Computers & Structures, 16:* No. 5, 657-668, (1983).

52. Naganarayana, B. P. and G. Prathap. "Consistency Aspects of Out-of-Plane Torsion and Shear in a Quadratic Curved Beam Element," *International Journal of Numerical Methods for Engineering, 30:* 431-443, (1990).

53. Nolte, L. -P., J. Makowski and H. Stumpf. "On the Derivation and Comparative Analysis of Large Rotation Shell Theories," *Ingenieur-Archiv, 56:* 145-160, (1986).

54. Noor, Ahmed K. and C. M. Andersen. "Computerized Symbolic Manipulation in Structural Mechanics — Progress and Potential," *Computers & Structures, 10:* 95-118, (1979).

55. Noor, Ahmed K., Jeanne M. Peters, and Carl M. Andersen. "Mixed Models and Reduction Techniques for Large-Rotation Nonlinear Problems" *Computer Methods in Applied Mechanics and Engineering, 44:* 67-89, (1984).

56. Noor, Ahmed K. and W. Scott Burton. "Assessment of Computational Models for Multilayered Composite Shells," *Applied Mechanics Review, 43:* No. 4, 67-97, (April 1990).

57. Novozhilov, V. V. *Foundations of the Nonlinear Theory of Elasticity.* Gaylock, 1953.

58. Palazotto, Anthony N. "An Experimental Study of a Curved Composite Panel with a Cutout," *Composite Materials: Testing and Design (Eighth Conference):* 191-202, ASTM STP 972. Edited by J. D. Whitcomb. Philadelphia: American Society for Testing and Materials, 1988.

59. Palazotto, Anthony N. and Scott T. Dennis. *Nonlinear Analysis of Shells.* AIAA Education Series, J. S. Przemieniecki, Series Editor-in-Chief. New York: American Institute of Aeronautics and Astronautics, Inc. (to be published in early 1992).

60. Palazotto, Anthony N. and Thomas W. Tisler, Jr. "Insight into the Collapse Analysis of Composite Cylindrical Panels with Cutouts: Analysis and Experimentation," *Recent Advances in Structural Dynamics — PVP, 24:* 55-61, (1987)

61. Palazotto, Anthony N. and Thomas W. Tisler, Jr. "Considerations of Cutouts in Composite Cylindrical Panels," *Computers & Structures, 29:* No. 6, 1101–1110, (1988).

62. Palazotto, Anthony N. and Thomas W. Tisler, Jr. "Experimental Collapse Determination of Cylindrical Composite Panels with Large Cutouts Under Axial Load," *Composite Structures, 12:* 61–78, (1989).

63. Palazotto, Anthony N., Scott T. Dennis and Chi-Tay Tsai. "Snapping Characteristics of Laminated Cylindrical Panels Under Transverse Loading," *31st Structures, Structural dynamics and Materials Conference:* 669–705. AIAA Paper No. 90-0924-CP. New York: American Institute of Aeronautics and Astronautics, April 1990.

64. Palazotto, Anthony N., L. S. Chien and W. W. Taylor. "Stability Characteristics of Laminated Cylindrical Panels Under Transverse Loading," *32nd Structures, Structural dynamics and Materials Conference:* 926–932. AIAA Paper No. 91-0914. New York: American Institute of Aeronautics and Astronautics, April 1991.

65. Palmerio, A. F., J. N. Reddy and R. Schmidt. "On a Moderate Rotation Theory of Laminated Anisotropic Shells — Part 1. Theory," *International Journal of Non-Linear Mechanics, 25:* No. 6, 687–700, (1990).

66. Palmerio, A. F., J. N. Reddy and R. Schmidt. "On a Moderate Rotation Theory of Laminated Anisotropic Shells — Part 2. Finite-Element Analysis," *International Journal of Non-Linear Mechanics, 25:* No. 6, 701–714, (1990).

67. Pandya, B. N. and T. Kant. "A Consistent Refined Theory for Flexure of a Symmetric Laminate," *Mechanics Research Communication, 14:* 107–113, (1987).

68. Pandya, B. N. and T. Kant. "Finite Element Analysis of Laminated Composite Plates using a Higher-Order Displacement Model," *Composites Science and Technology, 32:* 137–155, (1988).

69. Parisch, H. "Large Displacements of Shells Including Material Nonlinearities," *Computer Methods in Applied Mechanics and Engineering, 27:* 183–214, (1981).

70. Pietraszkiewicz, W. "Lagrangian Description and Incremental Formulation in the Nonlinear Theory of Thin Shells," *International Journal of Non-Linear Mechanics, 19:* 115–140, (1984).

71. Pietraszkiewicz, W. and M. L. Szabowicz. "Entirely Lagrangian Nonlinear Theory of Thin Shells," *Archives of Mechanics, 33:* 273–288, (1981).

72. Popov, Egor P. *Introduction to Mechanics of Solids.* Englewood Cliffs, New Jersey: Prentice-Hall, 1968.

73. Prathap G. and B. P. Naganarayana. "Analysis of Locking and Stress Oscillations in a General Curved Beam Element," *International Journal of Numerical Methods for Engineering, 30:* 177–200, (1990).

74. Putcha, N. S. and J. N. Reddy. "A refined Mixed Shear Flexible Finite Element for Nonlinear Analysis of Laminated Plates," *Computers & Structures, 22:* No. 4, 529–538, (1986).

75. Rajasekaran, Sundaramoorthy and David W. Murray. "Incremental Finite Element Matrices," *Journal of the Structures Division ASCE:* 2423–2437, (December 1973).

76. Rankin, C. C. and F. A. Brogan. "An Element Independent Corotational Procedure for the Treatment of Large Rotations," *Journal of Pressure Vessel Technology ASME, 108:* 165–174, (1986).

77. Reddy, J. N. *A Refined Nonlinear Analysis of Laminated Composite Plates and Shells,* Final Technical Report ARO 21203.7–MA. US Army Research Office, 1987. (AD–A184 436)

78. _____. "On Refined Computational Models of Composite Laminates," *International Journal of Numerical Methods for Engineering, 27:* 361–382, (1989).

79. _____. "A General Non-Linear Third-Order Theory of Plates with Moderate Thickness," *International Journal of Non-Linear Mechanics, 25:* No. 6, 677–686, (1990).

80. Reddy, J. N., and C. F. Liu. "A Higher-Order Shear Deformation Theory of Laminated Elastic Shells," *International Journal of Engineering Sciences, 23:* No. 3, 319–330, (1985).

81. Reddy, J. N. and A. K. Pandey. "A First Ply Failure Analysis of Composite Laminates," *Computers & Structures, 25:* No. 3, 371–393, (1987).

82. Reissner, E. "The Effect of Transverse Shear Deformation on the Bending of Elastic Plates," *Journal of Applied Mechanics, 12:* 69–77, (1945).

83. _____. "On Finite Symmetrical Deflections of Thin Shells of Revolution," *Transactions of the ASME, 91:* Series E, 267–270, (1969).

84. _____. "On the Equations of Nonlinear Shell Theory," *Studies in Applied Mathematics, 48:* 171–175, (1969).

85. Ren, J. G. "Exact Solutions for Laminated Cylindrical Shells in Cylindrical Bending," *Composites Science and Technology, 29:* (1987).

86. Saada, Adel S. *Elasticity Theory and Applications.* Pergamon Press Inc. New York, (1974).

87. Sabir, A. B. and A. C. Lock. "The Application of Finite Elements to the Large Deflection Geometrically Non-Linear Behavior of Cylindrical Shells," *Variational Methods in Engineering.* 7/66–7/75. Edited by C. A. Brebbia and H. Tottenham. London: Southhampton Press, 1972.

88. Schimmels, Capt Scott A. *Investigation of Collapse Characteristics of Cylindrical Composite Panels with Large Cutouts.* Masters thesis, AFIT/GAE/ENY/89D-33.

School of Engineering, Air Force Institute of Technology (AU), Wright-Patterson AFB, OH, December 1989. (AD-A216 378)

89. Schimmels, Scott and Anthony Palazotto. "Collapse Characteristics of Free Edged Cylindrical Composite Panels under Axial Loads," *31th Structures, Structural dynamics and Materials Conference:* 689-698. AIAA Paper No. 90-0923. New York: American Institute of Aeronautics and Astronautics, April 1990. Technology, Wright-Patterson AFB, Ohio. 3-7 June 1991.

90. Schmidt, R. "On Geometrically Non-Linear Theories for Thin Elastic Shells," *Flexible Shells Theory and Applications:* 76-90. Edited by E. L. Axelrad and F. A. Emmerling. New York: Springer-Verlag, 1984.

91. Schmidt, R. and D. A. DaDeppo. "A Survey of Literature on Large Deflections of Non Shallow Arches," *Journal of Industrial Math Soc, 42:* (1975).

92. Schmidt, R. and J. N. Reddy. "A Refined Small Strain and Moderate Rotation Theory of Elastic Anisotropic Shells," *Journal of Applied Mechanics, 55:* 611-617, (September 1988).

93. Silva, Capt Kevin. *Finite Element Investigation of a Composite Cylindrical Shell under Transverse Load with Through Thickness Shear and Snapping.* Masters thesis, AFIT/GAE/ENY/89D-35. School of Engineering, Air Force Institute of Technology (AU), Wright-Patterson AFB, OH, December 1989. (AD-A216 377)

94. Simmonds, James G. "The Nonlinear Thermodynamical Theory of Shells: Descent from 3-Dimensions without Thickness Expansions," *Flexible Shells Theory and Applications:* 1-11. Edited by E. L. Axelrad and F. A. Emmerling. New York: Springer-Verlag, 1984.

95. Simmonds, J. G. and D. A. Danielson. "Nonlinear Shell Theory with Finite Rotation and Stress-Function Vectors," *Journal of Applied Mechanics:* 1085-1090, (December 1972).

96. Simo, J. C., D. D. Fox and M. S. Rifai. "On a Stress Resultant Geometrically Exact Shell Model, Part III: Computational Aspects of the Nonlinear Theory," *Computer Methods in Applied Mechanics and Engineering, 79:* 21-70, (1990).

97. Singh, Gajbir, Y. V. K. Sadasiva Rao and N. G. R. Iyengar. "Buckling of Thick Layered Composite Plates under In-Plane Moment Loading," *Composite Structures, 13:* 35-48, (1989).

98. Surana, Karan S. "Geometrically Nonlinear Formulation for the Curved Shell Elements." *International Journal of Numerical Methods for Engineering, 19:* 581-615, (1983).

99. _____. "A Generalized Geometrically Nonlinear Formulation with Large Rotations for Finite Elements with Rotational Degrees of Freedoms," *Computers & Structures, 24:* No. 1, 47-55, (1986).

100. Taylor, Major Walter W. *Finite Element Investigation into the Dynamic Instability Characteristics of Laminated Composite Panels.* Masters thesis, School of Engineering, Air Force Institute of Technology (AU), Wright-Patterson AFB, OH, December 1990.

101. Tisler, Second Lieutenant Thomas W. Jr. *Collapse Analysis of Cylindrical Composite Panels with Large Cutouts Under Axial Load.* Masters thesis, AFIT/GAE/AA/86D-18. School of Engineering, Air Force Institute of Technology (AU), Wright-Patterson AFB, OH, December 1986. (AD-A179 112)

102. Tsai, Chi-Tay and Anthony N. Palazotto. "A Modified Riks Approach to Composite Shell Snapping Using a High-Order Shear Deformation Theory," *Computers & Structures,35:* No. 3, 221-226, (1990).

103. Tsai, Chi-Tay and Anthony N. Palazotto. "Large-Rotation Snap-Through Buckling in Laminated Cylindrical Panels," *Finite Elements in Analysis and Design, 9:* 65-75, (1991).

104. Vlasov, V. Z. *General Theory of Shells and its Application in Engineering,* Washington D.C.: National Aeronautics and Space Administration, 1964.

105. Washizu, Kyuichiro. *Variational Methods in Elasticity and Plasticity* (Third Edition). New York: Pergamon Press, 1982.

106. Wempner, Gerald. "Mechanics and Finite Elements of Shells," *Applied Mechanics Review, 42:* No. 5, 129-142, (May 1989).

107. Whitney, J. M. *Structural Analysis of Laminated Anisotropic Plates.* Lancaster, Pennsylvania: Technomic, 1987.

108. Yang, T. Y. H. and Y. C. Wu. "A Geometrically Non-Linear Tensorial Formulation of a Skewed Quadrilateral Thin Shell Finite Element," *International Journal of Numerical Methods for Engineering, 28:* 2855-2875, (1989).

109. Yuan, K. Y. and C. C. Liang. "Nonlinear Analysis of an Axisymmetric Shell Using Three Noded Degenerated Isoparametric Shell Elements," *Computers & Structures: 32,* No. 6, 1225-1239, (1989).